AGRICULTURAL WATER DEMAND ASSESSMENT IN THE SOUTHEAST U.S. UNDER CLIMATE CHANGE

A Dissertation
Presented to
The Academic Faculty

By

Christian V. Braneon

In Partial Fulfillment
Of the Requirements for the Degree
Doctor of Philosophy in the
School of Civil and Environmental Engineering

Georgia Institute of Technology
January 2014

AGRICULTURAL WATER DEMAND ASSESSMENT IN THE SOUTHEAST U.S. UNDER CLIMATE CHANGE

Approved by:

Dr. Aris Georgakakos, Advisor
School of Civil and Environmental Engineering
Georgia Institute of Technology

Dr. Huaming Yao
School of Civil and Environmental Engineering
Georgia Institute of Technology

Dr. Terry Sturm
School of Civil and Environmental Engineering
Georgia Institute of Technology

Dr. Heinrich Matzinger
School of Mathematics
Georgia Institute of Technology

Dr. Jian Luo
School of Civil and Environmental Engineering
Georgia Institute of Technology

Dr. Gerrit Hoogenboom
Department of Biological Systems Engineering
Washington State University

Date Approved: January 10, 2014

ACKNOWLEDGEMENTS

There are numerous people and organizations that directly and indirectly contributed to the successful completion of my PhD studies and research. This work would not have been possible without the generous support of the School of Civil and Environmental Engineering, the Office of Student Affairs, the National Aeronautics and Space Administration, the MacArthur Foundation, the National Science Foundation, and the Georgia Space Grant Consortium.

This thesis would not have been possible without the advice and support of my academic advisor, Dr. Aris Georgakakos. I am very thankful for the time and energy that he has dedicated towards my intellectual and professional development. He has been a pillar for me as I have progressed through my graduate studies and he has always encouraged me to pursue excellence as opposed to mediocrity.

I must thank Drs. Huaming Yao, Gerrit Hoogenboom, Jian Luo, Heinrich Matzinger, Terry Sturm, Ridgely Muhammad, Joel Paz, and Axel Garcia for their expert advice and technical support as I completed this research. In addition, I am thankful for the support of Rad Yager, Calvin Perry, as well as all of the farmers and agricultural extension staff I consulted in order to complete this work.

I want to thank my friends at Georgia Tech, my peers in the Environmental Fluid Mechanics and Water Resources Group, as well as my colleagues at the Georgia Water

Resources Institute for all of the meaningful experiences, conversations, and memories that have made my time as a graduate student so valuable.

Finally, I must thank my ancestors and my mother for their sacrifices on my behalf.

TABLE OF CONTENTS

LIST OF TABLES

LIST OF FIGURES

SUMMARY

This study utilized (a) actual measured agricultural water use along with (b) geostatistical techniques, (c) crop simulation models, and (d) general circulation models (GCMs) to assess irrigation demand and the uncertainty associated with demand projections at spatial scales relevant to water resources management. In the first part of the study, crop production systems in Southwest Georgia are characterized and the crop simulation model error that may be associated with aggregated model inputs is estimated for multiple spatial scales.

In the second portion of this study, a methodology is presented for characterizing regional irrigation strategies in the Lower Flint River basin and estimating regional water demand. Regional irrigation strategies are shown to be well represented with the moisture stress threshold (MST) algorithm, metered annual agricultural water use, and crop management data. Crop coefficient approaches applied at the regional scale to estimate agricultural water demand are shown to lack the interannual variability observed with this novel approach.

In the third portion of this study, projections of regional agricultural demand under climate change in the Lower Flint River basin are presented. GCMs indicate a range of possible futures that include the possibility of relatively small changes in irrigation demand in the Lower Flint River basin. However, most of the GCMs utilized in this work project significant increases in median water demand towards the end of this century. In

particular, results suggest that peak agricultural water demands in July and August may increase significantly.

Overall, crop simulation models are shown to be useful tools for representing the intra-annual and interannual variability of regional irrigation demand. The novel approach developed may be applied to other locations in the world as agricultural water metering programs become more common.

Chapter 1: Introduction

Agricultural water use dominates consumptive use of water in many parts of the world, but reliable estimates of historical and future agricultural water demand are lacking. Individual farmers generally do not monitor or record their water applications in a systematic manner and often existing statutes do not require them to explicitly report their water use to any governing body. This presents significant challenges for retrospective analysis of interannual and seasonal water demand and has resulted in climate change impact assessments based on assumptions about historical and future irrigation practices that are not supported with data at the scales relevant to water resources management. While global climate models provide plausible scenarios of future climate associated with increasing greenhouse gas concentration, water resources stakeholders lack tools to translate these climate scenarios into useful assessments of agricultural water demand.

Crop simulation models are playing an increasing role in utilizing past and future climate data to provide useful information for a range of stakeholders. These models overcome the 'black box' nature of less mechanistic, empirical models by integrating current knowledge from disciplines such as agrometeorology, soil physics, and agronomy into a set of mathematical equations that represent the dynamic, nonlinear interactions between weather, soil water and nutrient dynamics, crop characteristics, and management practices. In addition, crop simulation models serve as surrogate laboratories that allow for rapid and inexpensive experimentation that compliments traditional field experiments

(Brumbelow et al., 2003; Challinor et al., 2009). Typical environmental inputs include daily weather data, soil properties, and crop management factors.

While crop simulation models are developed and tested at the spatial scale of a homogenous plot or field, stakeholders are often interested in climate impacts at the district, watershed or broader scales where significant spatial variability in environmental inputs may exist (Hansen and Jones, 2000; Kersebaum et al., 2007). The outputs from these models are intensive variables (e.g. 'crop yield' or the amount of a crop harvested per unit area) expressed as spatial averages that must be scaled up to the scales relevant to water resources management and regional crop production.

Crop simulation models have been used in studies all over the world and have the potential to become vital components of interdisciplinary research on climate change impacts. However, upscaling their outputs to obtain meaningful information is not straightforward. Questions that influence the development of assessments include: what spatial scales relevant to water resources managers and planners allow for comparison of model outputs with available agricultural data sets; how can the variability in weather, soil, and management conditions be represented in the modeling framework; can approaches be developed to take advantage of local expert knowledge of management practices; can irrigation demand be simulated with a consistent approach to represent current as well as future conditions?

1.1 Research Objective

This research aims to develop and demonstrate a novel approach for applying crop simulation models to assess the impacts of climate change on agricultural water demand. Some relevant questions addressed in this work include:

- What are realistic and consistent approaches for mimicking the farmer's decision to irrigate historically and in the future;
- How does simulation error change as spatial scale increases;
- What conclusions can be drawn about the benefit of crop models in comparison to simpler empirical models when conducting agricultural water demand assessments;
- Can crop models be utilized to translate historical climate data and scenarios of future climate into useful information for water resources stakeholders?

The research scope of this work includes (1) a quantitative assessment of a crop simulation model's ability to represent the relationship between atmospheric forcing, soils, irrigation input, and yield at different spatial scales; (2) scale dependent model calibration guidelines and characterization of uncertainty associated with calibration parameters; (3) a comparison with existing approaches; and (4) an assessment of climate change impacts on agricultural water demand.

1.2 Case Study System

The agriculture industry plays a huge role in Georgia's economy, contributing billions of dollars annually. In addition, the state's water resources are intrinsically tied to the agricultural sector since both surface water and groundwater are used by farmers to irrigate crops throughout the state. Although Georgia is typically considered to be a state with plentiful water resources due to average annual rainfall exceeding that of many other parts of the United States, the competing demands placed on water resources by the municipal, industrial, agricultural, and ecological sectors make water resources management and planning a significant challenge for stakeholders and policy makers. This is complicated further by the uncertainty surrounding agricultural water use due to a lack of observed data associated with seasonal irrigation volumes or the timing of water applications during the crop season. Furthermore, climate change has the potential to decrease the availability of water resources due to probable changes in rainfall distribution and increases in potential evaporative demand (Hatch et al., 1999; Xu and Singh, 2004; Zhang and Georgakakos, 2011).

1.3 Thesis Organization

Following a review of the relevant literature on empirical crop response models, crop simulation models, and agricultural water demand assessments, Chapters 3 through 6 consist of the methods and results of this research. In Chapter 3, the uncertainty associated with upscaling crop simulation model outputs is characterized. In Chapter 4, a methodology is presented for estimating irrigation demand with regional irrigation strategies and measured agricultural water use data. In Chapter 5, projections of

agricultural water demand under climate change are presented. Finally, Chapter 6 consists of conclusions and recommendations for future work.

Chapter 2: Literature Review

2.1 Introduction to empirical crop response models

The positive response of agricultural crops to well timed water applications (i.e. irrigation) has been acknowledged by humanity for millennia. Some of the earliest engineering projects involved drainage and irrigation of fields to improve crop production and provide an adequate supply of food and fiber. Human reliance on a sufficient and timely supply of water for crop production continues (Eash et al., 2008).

Quantifying the relationship between management factors (such as irrigation and applied nutrients) and crop response has been of interest to farmers and scientists for a long time. As a result, farmers and scientists have dedicated significant amounts of time and resources to the study and improvement of agricultural production. For example, John Bennet Lawes devoted his family estate in England to the study of agricultural production and conducted chemical experiments in a laboratory in his house. He patented a process for manufacturing superphosphate in 1842 and his subsequent research on various crops in field plots led to many publications in scientific journals (Overman and Scholtz, 2002).

One of the earliest approaches for determining crop water "requirements" is still popular and is known as the Blaney-Criddle (1950)equation (Banerjee et al., 2007). By disregarding many relevant factors, the original form of the method determines seasonal consumptive use of water as a function of empirical crop coefficients, monthly temperature and monthly percentage of annual daytime hours. The equation is

$$U = Kf$$

where U is the consumptive use in inches; K is a monthly crop coefficient; $f = (t \times p)/100$ is the monthly consumptive use factor; t is the mean monthly temperature in degrees Farenheit; p is the monthly percentage of daytime hours (as a percentage of the annual total).

On a seasonal basis, the equation is given by

$$U = \sum_{i=1}^{m} K_i f_i = K_s \sum_{i=1}^{m} (t_i \times p_i)/100$$

where K_s is a seasonal crop coefficient and m is the number of months in a season.

Although the Blaney-Criddle (1950)equation has been modified for use at shorter time scales and to incorporate wind speed and humidity (Allen and Pruitt, 1986; Doorenbos and Pruitt, 1977; USDA, 1970), it still is based on crop coefficients that may not be applicable at locations other than where the coefficients were determined. Furthermore, this approach disregards many significant factors (e.g. soil moisture, timing of water applications, management practices, water logging, etc.) and does not provide information about crop yield. Rather it assumes that crop growth and yield is not limited by inadequate soil moisture at any time during the growing season. Thus, the Blaney-Criddle equation can be classified as a "full irrigation" method.

2.2 Evapotranspiration driven crop water use methods

Soil water can evaporate directly from the soil or it can be absorbed by the roots of a plant and evaporate from small openings on the leaves of plants referred to as stomata. The latter process is called transpiration and the combination of evaporation from the soil

and the leaves of plants is known as evapotranspiration. Potential evapotranspiration is the rate of evapotranspiration that would occur in an area of dense vegetation cover when soil moisture supply is not limiting. The amount of water evaporated from leaf surfaces and consequently discharged to the atmosphere is far greater than the amount of water consumed in the formation of plant matter. The actual rate of transpiration depends on the species and growth stage of a plant, as well as the soil and weather conditions. Thus, actual evapotranspiration drops below its potential level as the soil becomes unsaturated (Bras, 1990; Chow et al., 1988; J.E.Pallas et al., 1979).

2.2.1 Reference crop methods

Many approaches have been developed to determine crop water requirements that are based on methods for calculating open water evaporation with adjustments to account for the condition of the vegetation and soil (Bras, 1990; Monteith, 1980; Van Bavel, 1966). While these methods are typically considered easy to use and understand, (1) they do not express a relationship between applied water and yield in absolute terms and (2) parameters (i.e. coefficients) may vary by location and crop.

A fundamental assumption when reference crop methods are applied is that water supply does not limit evapotranspiration (ET). Thus, there is a fundamental assumption that no water stress is experienced by the crop of interest. A common approach is to assume the basic rate of ET is the "reference crop ET", i.e. "the rate of evapotranspiration from an extensive surface of 8 cm to 15 cm tall green grass cover of uniform height, actively growing, completely shading the ground and not short of water" (Doorenbos and Pruitt,

1977). A relationship between the calculated ET for the reference crop and the ET of the crop of interest is utilized and applied to determine crop water needs.

Two common approaches for estimating reference crop ET are the Penman-Monteith equation and a method based on field experiments by Priestley and Taylor (1972). Monteith (1965) showed how the Penman (1948)equation for evaporation from a free-water surface can be modified to calculate ET from a vegetated surface by incorporating resistance to vapor flux through leaf stomata and unsaturated soil. Priestly and Taylor (1972) demonstrated with experimental evidence that ET could be approximated as the product of a constant and the term in the Penman (1948)equation that represents the evaporation rate due to net radiation (Dingman, 2002).

The potential evapotranspiration (ET_c) of the crop of interest may be calculated by multiplying the reference crop evapotranspiration (ET_{ref}) by an empirical crop coefficient (K_c). Crop coefficients vary with crop phenology, i.e. stage of growth of the crop. As crops develop, K_c increases to a maximum value and then decreases as the crop approaches maturity. A procedure for irrigation scheduling(Brumbelow et al., 2003), the decision of when and how much to irrigate, with crop coefficients can be expressed as

$$ET_{ref,t} = f_{ETref}(T_{\max,t}, T_{\min,t}, RH_t, R_{n,t}, u_t, etc.)\forall t$$
$$ET_{c,t} = K_{c,t} \cdot ET_{ref,t}\forall t$$
$$I_t = 0, \text{if } P_t \geq ET_{c,t}\forall t$$
$$I_t = ET_{c,t} - P_t, \text{if } P_t < ET_{c,t}\forall t$$

where t is an index indicating the time increment, $T_{\max}$ is maximum temperature, $T_{\min}$ is minimum temperature, RH is relative humidity, R_n is net solar radiation, u is wind speed, I is irrigation, and P is precipitation.

Reference crop methods have limited value for estimating agricultural water use because many production situations do not allow for full irrigation, i.e. irrigation scheduling that prevents the crop from experiencing any significant degree of water stress. Although full irrigation methods are intended to maximize yield, competing demands on water supplies in many river basins necessitate a more sustainable demand management strategy that allows for deficit irrigation, i.e. situations where total applied water is less than potential ET (Brumbelow, 2001; Farahani et al., 2009; Kijne et al., 2003).

2.2.2 Deficit irrigation methods

Empirical production functions that relate harvestable yield to ET are commonly used in agricultural yield and water demand assessments (Cai et al., 2003). By far, the most influential method based on this approach is FAO Irrigation and Drainage Paper no. 33, *Yield Response to Water* (Doorenbos and Kassam, 1979).The basis of this approach is a relationship between relative yield and relative ET given by

$$\left(\frac{Y_m - Y_a}{Y_m}\right) = K_y \left(\frac{ET_m - ET_a}{ET_m}\right)$$

where Y_m and Y_a are the maximum and actual yield; ET_m and ET_a are the maximum and actual evapotranspiration, and K_y is a yield response factor that varies with species, variety, irrigation method and management under deficit evapotranspiration.

While equation (2.4) may be applied for an entire season (Kirda, 2002), Doorenbos and Kassam (1979) also specified a model that allowed K_y to vary with growth stage. Rao et al. (1988)proposed a multiplicative form that is given by

$$\frac{Y_a}{Y_m} = \prod_{i=1}^{n} \left[1 - K_{y,i} \left(1 - \frac{ET_{a,i}}{ET_{m,i}} \right) \right]$$

where *i* is an index for growth stage and *n* is total number of crop growth stages. An additive form was also supported by Rao et al. (1988)and is given by

$$\frac{Y_a}{Y_m} = 1 - \sum_{i=1}^{n} K_{y,i} \left(1 - \frac{ET_{a,i}}{ET_{m,i}} \right)$$

While the Doorenbos and Kassam (1979)equation and similar equations are still quite popular today (Cai et al., 2009), using the K_y values that the authors reported in *Yield Response to Water* may lead to significant errors (Kaboosi and Kaveh, 2011). For example, Dehghanisanij et al. (2009) reported the seasonal K_y for winter wheat as 1.03 and 1.23 for two different locations in Iran, while Doorenbos and Kassam (1979) presented it as one. In another study, Moutonnet (2002) presented K_y for the vegetative stage of cotton in Argentina and Pakistan as 0.75 and 0.8 respectively while it was given as equal to 0.2 by Doorenbos and Kassam (1979).

Thus, determining the coefficients in the Doorenbos and Kassam equation and similar equations may require lengthy and expensive local experiments (Fourcard et al., 2008; Tsuji et al., 1998). In addition, the coefficients derived at a given site from experiments

may not be valid at locations with different soil properties, climate, crop varieties, or management practices. Furthermore, yield is not expressed in absolute terms.

Although these empirical approaches are widely accepted and allow for analytical methods of parameter estimation and error propagation, there are significant limitations to their application and factors other than evapotranspiration that influence agricultural yield and water demand are not taken into account (Brumbelow, 2001). Furthermore, plant water stress is dictated by a combination of potential ET, plant extractable soil moisture, root distribution, canopy size as well as other plant and environmental factors (Hoogenboom, 2000). For the representation of spatially aggregated response to the interactive effects of climate and management, the physiological detail in crop simulation models is required (Hansen and Jones, 2000).

2.3 Introduction to crop simulation models

From the mid-1960s through the 1990s, crop physiologists contributed a great deal to the understanding of plant physiology (Boote and Sinclair, 2006). After these scientists' discoveries improved the understanding of photosynthesis in different plant species in the 1960s (Hesketh, 1963; Hesketh and Moss, 1963), the mechanistic basis of crop-water relations was revealed in the 1970s and 1980s (Boyer, 1969; Hsiao, 1973). By the 1990s, the work of researchers investigating crop response to elevated CO_2 and temperature allowed for scientific discussion on the impacts of global climate change on agricultural production (Allen, 1990; Kimball, 1983; Rogers et al., 1983).

In the late 1960s, computers had evolved enough to allow for crop growth modeling to emerge as a means of integrating knowledge about plant physiological processes in order to explain whole-plant response, i.e. the functioning of a plant as a whole (Bouman et al., 1996). Over the next few decades, new insights into the underlying mechanisms and processes associated with crop growth and development were expressed using mathematical equations and integrated in simulation models. As a result of the interaction between biologists, mathematicians and computer scientists, plant growth modeling and simulation has progressed significantly (Fourcard et al., 2008).

2.3.1 Dynamic system models

Crop growth models are considered 'process based' or 'physiologically based' because they take into account the physiological processes involved in growth and development such as water and nutrient dynamics, photosynthesis, and carbon partitioning (Gifford and Evans, 1981). The term 'crop simulation model' refers to a dynamic system of differential or difference equations, which describe the interaction of a crop with the soil by calculating both rate and state variables over time (Hoogenboom, 2000). Thus, a crop simulation model is a mathematical representation (Wallach et al., 2006) of the soil-plant-atmosphere system (SPA system) given by

$$X_1(t+\Delta t) = X_1(t) + g_1\left[X(t), w(t); \theta\right]$$
$$\vdots$$
$$X_n(t+\Delta t) = X_n(t) + g_n\left[X(t), w(t); \theta\right]$$

where t is time; Δt is some time increment that is often one day; $X(t) = \left[X_i(t), \ldots, X_n(t) \right]^{\mathrm{T}}$ is the vector of state variables at time t; n is the number of state variables; $w(t)$ is the vector of input variables at time t; θ is the vector of parameters; and g is some function.

Environmental conditions (such as climate variables and soil characteristics) and crop management practices (e.g. irrigation amounts and dates) are typical inputs, while state variables could include leaf area index (i.e. leaf area per unit land area), grain weight, root density in each soil layer, soil water content in each soil layer, etc. Crop simulation models typically operate on a daily time step and aspatial scale of a homogenous plot or field (Hansen et al., 2006). When one integrates the equations of the crop simulation model, this is commonly referred to as "running" the model (Wallach et al., 2006). These equations contain parameters that remain unchanged from one simulation to another after the model is calibrated. For the purposes of agricultural and water resources management, the model results or outputs of interest are typically state variables at the end of the season (e.g. irrigation depth) or at particular times during the season (e.g. daily water stress and irrigation applications). Crop models can be considered deterministic in that differences in outputs are only due to variations in input data (Lichtfouse et al., 2009).

2.3.2 Primary modules

For more than a decade, many in the agricultural system modeling community have made a concerted effort to promote more effective model development and documentation approaches (Porter et al., 1999). Although models have become more complex in a sense as new components have been added or modified, many modeling groups have implemented a modular structure and modular programming techniques that allow for

more cooperation amongst experimentalists, model developers, and model users (Hunt et al., 2001; Jones et al., 2001). As a result, three main modules are common in most crop simulation models: the soil module, the plant module, and the soil-plant-atmosphere module which links the soil and plant modules (Jones et al., 2003).

The soil module computes water infiltration, drainage, and redistribution within the soil profile. Water inputs such as precipitation and irrigation are the source of water that infiltrates into the soil. Crop simulation models may compute soil nitrogen and carbon processes due to fertilizer applications and crop residue as well (Lichtfouse et al., 2009).

The plant module computes growth of the plant (i.e. the accumulation of biomass) and the development of the crop. The crop grows and develops by expanding its canopy and deepening its root system as it progresses through its growth stages (Steduto et al., 2009).Canopy growth is driven by assimilation of carbon through photosynthesis, while the development of the crop is driven by temperature and photoperiod, i.e. the duration of the plant's daily exposure to light.

The soil-plant-atmosphere module allows interactions between the plant and soil modules. In particular, when potential root water uptake is limited by soil water content, physiological processes such as photosynthesis and cell expansion are reduced depending on the level of water stress (Lichtfouse et al., 2009).

2.3.3 Production situation classification

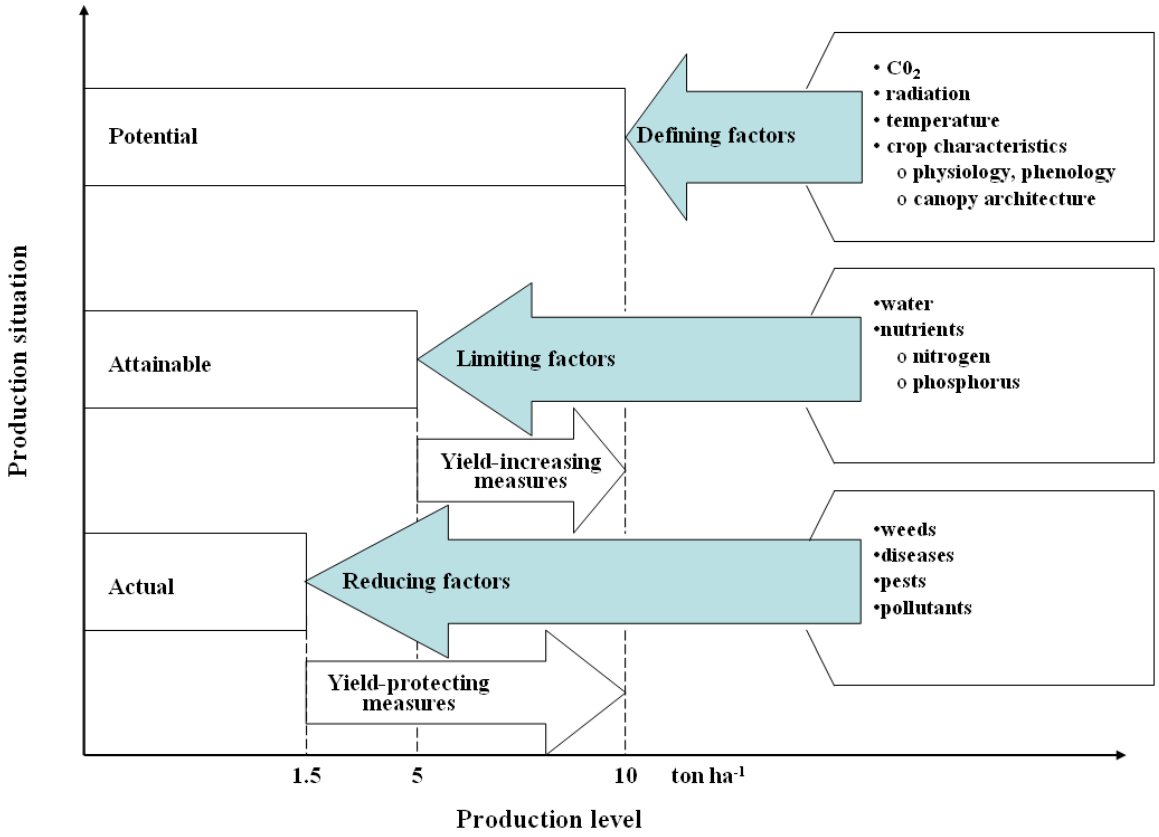

Figure 2.1. Classification of agricultural production systems proposed by the C.T. de Wit Graduate School of Production Ecology (Rabbinge, 1993).

At the start of any research study with crop simulation models, classifying the agricultural system allows for progress to be made although this is an obvious simplified representation of reality (Bouman et al., 1996).A popular classification of crop production systems was introduced by the C.T. de Wit Graduate School of Production Ecology (see Figure 1.1). Potential yield is defined by the concentration of atmospheric CO_2, solar irradiance, temperature, and characteristics of the crop. Attainable yield is limited by the availability of water and nutrients. Actual yield is reduced from attainable

yield by factors such as weeds, pests, diseases, and pollutants (Hoogenboom, 2000; Rabbinge, 1993). Crop simulation models capable of simulating potential production processes (i.e. photosynthesis, respiration, partitioning, phenology) were the first developed. These models were modified to allow for simulation of soil water dynamics, and later nitrogen dynamics and use. Ongoing efforts attempt to incorporate additional determinants of actual crop production such as models of phosphorous dynamics, pests, diseases and other factors (Delonge, 2007; Hansen and Jones, 2000; Willocquet et al., 1998).

2.4 Spatially aggregated response applications

The availability of input data presents significant challenges to the application of crop simulation models at regional and larger scales. The environment of the agricultural system modeled is defined by the inputs which typically consist of daily weather observations, soil properties, and crop management practices. Due to data and cost constraints, in many studies regional crop response is often based on one or a few "representative" locations. However, outputs simulated with data from representative locations may not necessarily represent the spatial average or the interannual variability of regional values due to aggregation error (Hansen and Jones, 2000; Lichtfouse et al., 2009).

When historical data is available at the scale of model development and application, calibration of model parameters and inputs can correct for sources of error (Rastetter et al., 1992). This can be achieved by utilizing a nonlinear optimization algorithm to

determine representative parameters and environmental inputs. For applications involving climate variability, several years of observed data at multiple sites in the region of interest is desirable for calibration but often not available (Hansen and Jones, 2000; Persson et al., 2008).

Temporal trends in historical water demand and yield data can be attributed to changes in technology or land-use patterns if weather is regarded as stationary (Garcia et al., 2006; Xu and Singh, 2004). This can be accounted for by calibration of model outputs since crop models simulate the current range of agricultural technologies (Hatch et al., 1999). For example, the difference or ratio of mean observed yields and yields simulated with fixed management may provide an adequate technology trend adjustment. The lower frequency tend may be attributed to technology while higher frequency deviations are primarily associated with weather variability (Bell and Fischer, 1994; Hansen and Jones, 2000; Jagtap and Jones, 2002).

2.5 Linking global climate and crop simulation models

As decision makers begin to integrate climate change into ongoing and new programs and policies, the climate change impacts, adaptations and vulnerability (IAV) research community needs to "sharpen the rigor of its analyses in regard to clarity of its mental constructs, data, and standards of evidence" (Rosenzweig and Wilbanks, 2010). The benefit of using general circulation (global climate) models (GCMs) for climate change impact assessments is that they allow one to account for mean change in temperature and precipitation as well as change in variability in a climatically consistent manner

(Brumbelow and Georgakakos, 2007). These models allow for scenarios of future climate to be generated that are based on our current understanding of the coupled atmospheric and oceanic processes that govern the Earth's climate (Zhang and Georgakakos, 2011). Due to the mismatch in spatial scale between outputs from GCMs and inputs for crop simulation models, simulation of climate change impacts includes the use of downscaling techniques to link climate models and crop simulation models (Xu and Singh, 2004). However, one should spatially and temporally downscale climate model outputs in a manner that preserves both the meaningful features of the climate scenarios as well as the relevant properties of the historical daily sequences (Hansen and Jones, 2000).

2.5.1 Raw daily climate model output

The simplest option for calibrating daily GCM output to match observed mean local climate is to apply an additive or multiplicative shift (Hansen et al., 2006). An additive shift is appropriate for temperature and solar irradiance. However, for precipitation, a multiplicative shift is more appropriate and given by

$$P_i' = P_{i,GCM} \overline{P}_{obs} / \overline{P}_{GCM}$$

where $P_{i,GCM}$ and P_i' refer to raw and calibrated GCM rainfall on day i, respectively; $\overline{P}_{obs}$ and $\overline{P}_{GCM}$ are long-term mean observed and simulated rainfall, respectively, for a given time of year.

There are other methods proposed that allow for calibrating both the frequency and intensity distributions of GCM rainfall (Baron et al., 2005; Schmidli et al., 2006). However, the value of daily GCM outputs may be limited more by the model's ability to

simulate rainfall with a realistic time structure (Hansen et al., 2006; Ines and Hansen, 2006).

2.5.2 Synthetic weather conditioned on monthly GCM output

An alternative approach is to constrain stochastically generated daily sequences to match the monthly values of GCM outputs. A simple additive shift may be adequate for temperature. Rainfall sequences are generated and tested until monthly totals are within some percentage (e.g. 5%) of monthly GCM targets. Then, the generated sequence is corrected with a multiplicative shift to match the target value (Hansen and Indeje, 2004; Kittel et al., 2004). Hansen and Ines (2005) found that this approach performed better than adjusting the parameters of the weather generator to reproduce statistical properties of monthly rainfall targets (Hansen et al., 2006; Hoogenboom, 2000).

2.5.3 Constructed analogues

Hidalgo et al. (2008) developed a new method for statistically downscaling daily temperature and precipitation from GCMs to determine the effects of climate change. The method utilizes a library of previously observed daily weather patterns to construct an analogue for a course scale GCM output of interest. The weather patterns for several days serve as predictors that are combined to construct the analogues. The method is used to downscale GCM output to obtain daily temperature and precipitation on a 1/8 x 1/8 degree resolution grid for the contiguous U.S. The authors found that the number of wet days is overestimated producing a very light “drizzle” on some days. Overall, the

downscaling method was found to skillfully reproduce the variability of daily average temperature and precipitation as well as seasonal cycles.

2.6 Agricultural assessments and farmer behavior

Crop simulation models are often called upon to reproduce past production situations and assess future scenarios where management decisions by farmers are needed as inputs. Consequently, decision rules are useful ways to relate a decision variable (e.g. water application depth and date) to other input variables (e.g. rainfall) or state variables (e.g. plant stress or soil moisture content at a user-specific soil depth) in a manner that is consistent from the past to the present or the future. When the goal is modeling water demand for irrigation in a region, the criteria for judging a decision rule is how closely it imitates farmer behavior (Cros et al., 2003; Wallach et al., 2006).

When investigating historical irrigation at numerous fields, it is more reasonable to try to characterize "irrigation strategies" than to determine irrigation dates and amounts for every field in the study region. An irrigation strategy corresponds to a set of rules that relate irrigation decisions to relevant factors such as soil moisture, climate, and state of crop development (Jones et al., 2003). It is useful for mimicking farmer behavior because the irrigation strategy of a farmer may be assumed to be relatively stable, while irrigation depths and dates may exhibit significant interannual variability. Thus, simulating a representative irrigation strategy for a region is a useful alternative to approximating total irrigation for many discrete irrigated fields. Furthermore, it is a reasonable approach for future or hypothetical situations as well (Wallach et al., 2006).

Most historical yield and water demand assessments utilize irrigation strategies that are not developed with monitored agricultural water use data in the region of interest. This is due to the fact that recorded measurements of agricultural water use by individual farmers are not common. For example, only in recent years have measurements of agricultural water use in Georgia become available as a result of the research conducted by the Agricultural Water Pumping Program and the Soil Water Conservation Commission. The most common irrigation strategy encountered in the literature is to suppose that irrigation is applied to fully satisfy crop water "needs". A number of studies utilizing either empirical models or crop simulation models are based on this approach. The latter typically involves simulating irrigation so that yield in maximized or is some arbitrary percentage of potential yield. These approaches avoid the more difficult challenge of modeling actual farmer behavior and consequently agricultural water demand (Cros et al., 2003; Wallach et al., 2006).

Few studies have evaluated irrigation strategies over a region. A transparent and defensible approach is interviewing a sample of farmers and deducing a regional irrigation strategy from their responses. This strategy is determined by comparing simulated results with observed water consumption data for the whole region (Leenhardt et al., 2004). Alternatively, Maton et al. (2005) interviewed farmers and developed a typology of irrigation strategies (Wallach et al., 2006).

2.7 Assessments of agricultural water demand in the Southeast U.S.

J.R. Bramblett (1995) provides an overview of the agricultural water demand study conducted by the U.S. Department of Agriculture's Natural Resources Conservation Service in 1994 as part of a broader Comprehensive Study of water resources in the Alabama-Coosa-Tallapoosa (ACT) and Apalachicola-Chattahoochee-Flint (ACF) River Basins in Alabama, Georgia, and Florida. This study relies on historical data from 1970-1992 and makes projections of water demand for crop and orchard irrigation, aquaculture, livestock, and poultry through 2050. However, projected future water demands were developed through a consensus of expert opinion. In addition, the author notes that a complete record of county commodity data for the 1970-1992 time period is not available for every county in all years. Furthermore, many individuals and groups questioned the "static" nature of the study's annual distribution of withdrawals and annual totals (Hook et al., 1999).

Blood et al. (1999) evaluate several methods for deriving irrigated acreage, water application rates, and annual irrigation water volume for four counties in SW Georgia, and compare these results with the ACT/ACF River Basins Comprehensive Study 1995 projected irrigated acres and irrigation withdrawals. The authors present the scope of data sources (UGA-CES, NASS, USDA NRCS-NRI, GA DNR-EPD, SPOT satellite images) available and the trends in the resulting estimates. The authors suggest that regardless of the method for calculating the volume, the differences among counties were largely determined by the acreage under irrigation. However, only an average water application rate and volume were calculated for the four approaches for comparative purposes.

Hook et al. (1999) use crop growth and water use models to determine potential water withdrawals by month for Georgia's primary irrigated crops during dry, normal, and wet years. The authors suggest that permitted pump capacity is not very useful for determining agricultural water use since the permitted pump capacity of the irrigation systems exceeds 8 billion gallons per day. However, they agree with Blood et al. (1999) in their conclusion that previous estimates of irrigated acreage by UGA-CES are certainly more reliable than their estimates of irrigation amounts. In this study, records from 1961-1990 were utilized from four to six meteorological stations in or near each basin that were located above selected gauging stations. However, for each region and crop, the crop model made 100 simulations in which a weather station, weather year, soil type, and crop variety were chosen by random selection with replacement. Planting dates were selected from a "random-normal distribution of dates centered on the optimal planting date". Irrigation to keep yield within 93-97% of optimal no water stress yields were ranked and the average quartile values were used to determine irrigation amounts needed for dry, normal , and wet years. The results were compared with actual farmer irrigation records for 7 to 11 years from the Southwest Georgia Agribusiness Association and the USDA National Peanut Laboratory (Dawson, GA). Farmer data showed wider spread of irrigation application than the models.

Martin et al., 1999 show a simplistic methodology for estimation of agricultural water uses in the Cape Fear River Basin of North Carolina to aid the NC Division of Water Resources (NCDWR) in current and future water resources management issues such as

water conservation measures, water supply allocations, and inter-basin transfers. Due to time and budgetary constraints, detailed interviews with farmers and irrigation equipment dealers were not feasible. A procedure was ultimately developed that was intended to be easily updated and allowed for sensitivity analyses. This procedure utilized readily available published agricultural data (42 years of crop acreage data from 1940-1998) and interviews with selected agricultural extension agents and irrigation experts. Simulation of sub-county scale agricultural water use for the 1930-1998 time period is demonstrated, but the crop water demand curves utilized were developed for optimal conditions and rely on static season lengths. However, expert knowledge of the pumps, irrigation systems, and irrigation practices currently utilized by farmers suggest that the methodology produced reasonable estimates of crop irrigation within the basin.

Hatch et al. (1999) conducted an analysis to determine potential effects of climate change on field crops in Georgia. Simulations with CROPGRO and CERES crop models were forced with historical (1975-1993) and projected (1975-1995, 2021-2040 and 2080-2099) daily weather data from the VEMAP project (Kittel et al, 1997) and consequently, the United Kingdom Meteorological Office, Hadley Center for Climate Prediction and Research model (Hadley). Planting dates in simulations occurred on the first date with one representative range of adequate soil moisture and soil temperature. Average values of yield, water use, mean growing season temperature, precipitation, and days to maturity were determined for the three 20-year time periods considered by averaging one to nine variety - planting date combinations for the five crops (peanut, corn, soybean, wheat, and sorghum) evaluated. The U.S. Department of Agriculture, Agriculture Research Service

economic model, PNTPLAN, was used to assess potential crop mix adjustments and management changes associated with economic optimization of a representative 200-acre farm for each county. In addition, sensitivity analysis was used to assess how water use might be affected as non-irrigated land is converted to irrigated agricultural land. The results show increased water efficiency in future yield due to increased atmospheric CO_2 concentration that results in lower agricultural water use despite increased irrigated acreage.

Salazar et al. (2012) evaluate the CSM-CERES-Maize crop simulation model with observed irrigation data from the Ag Water Pumping program from 2000 to 2004. The authors estimate historical irrigation requirements from 1950 to 2007 in 88 counties in Georgia with an approach that allows irrigation to be triggered on days when the available water holding capacity of the simulated soil profile falls below approximately 60% of field capacity. Comparison between annual simulated and observed irrigation for five counties suggest that the CSM-CERES-Maize model has potential as a tool for estimating supplementary irrigation requirements and agricultural water demand.

Chapter 3: Characterization of System Model Response

A "cropping system" may be defined as the crops, their succession order and the crop production systems associated with each crop (Leenhardt et al., 2010). In this chapter, crop production systems in Southwest Georgia are characterized and the crop simulation model error that may be associated with aggregated model inputs is estimated for multiple spatial scales. The estimated aggregation error associated with projections of agricultural water demand in subsequent chapters is presented in this chapter.

3.1 Introduction

A "system model" is an abstraction of the system of interest that is often indispensable when exploring the effect of alternative policies (Walker et al., 2003). For assessments of agricultural water demand, the system model encompasses the crop simulation model as well as the assumptions associated with model development and application to regional water demand projections. The crop production systems in the Southeast U.S. that utilize irrigation are the motivation for this work and the data, policies, and context associated with them have consequently influenced how crop simulation models are utilized to assess irrigation demand.

While crop simulation models allow for a simplified mathematical representation of the real-world agricultural systems investigated, it is impossible to include all the interactions between the environment and the crop production systems of interest in a computer model (Hoogenboom, 2000). When information describing the system model and its

interactions are limited, not available or do not exist, modeling assumptions must be made that are consonant with the crop production systems and environment of interest. Crop simulation models have considerable potential for the exploration of management and policy decisions. However, an important limitation to broader, more transparent use of these models is our relatively limited knowledge of the uncertainty in the models' outputs (Bert et al., 2007; Boote et al., 1996).

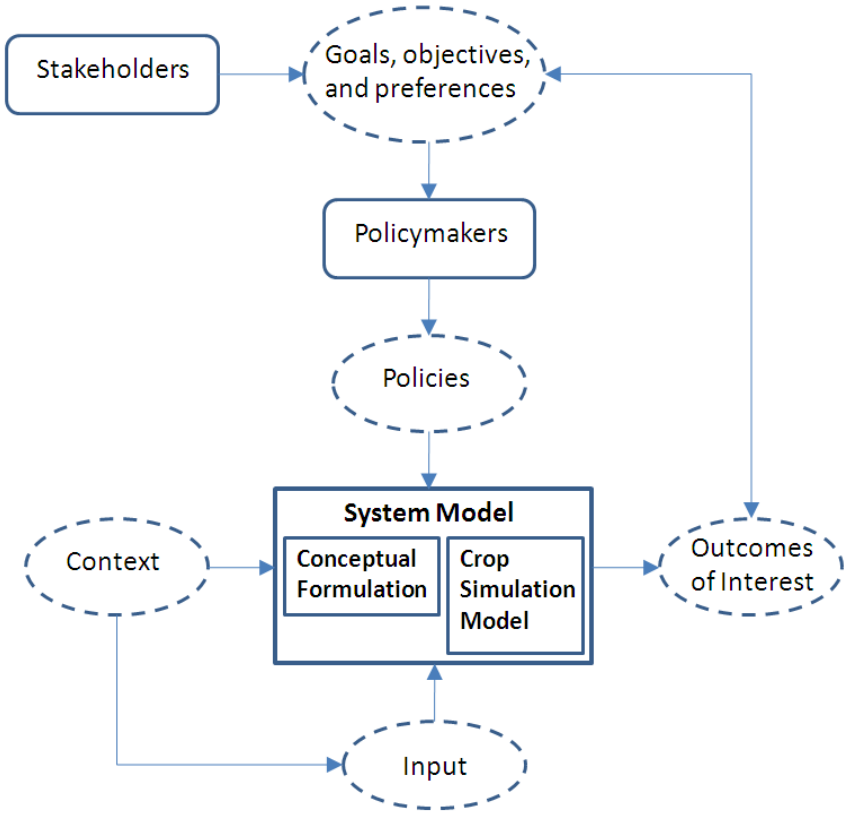

Figure 3.1. The system model as part of the policymaking process (adapted from Walker et al., 2003).

Uncertainty implies that error, unreliability, and imperfection affect our knowledge and understanding of the agricultural systems of interest (Li and Wu, 2006). Uncertainty can

directly affect policy in cases where the actions by decision makers when 'best estimates' are provided do not align with the decisions made when quantitative expressions of uncertainty are considered as well (Katz, 2002). Due to the different dimensions of uncertainty, a conceptual framework for the systematic treatment of uncertainty allows for a better understanding of model outputs and their implications for decision support (Walker et al., 2003).

3.2 Systematic Uncertainty Characterization

Uncertainty is often not given the attention it deserves even though it affects every aspect of modeling. It can be caused by incomplete data, limitations of models, and lack of understanding of the underlying processes. Incomplete data are a common problem in crop simulation modeling at scales broader than a field. Often the data necessary to evaluate the crop simulation model are not available and the techniques for evaluating models have not been perfected (Aggarwal, 1995).

Typically crop simulation models suppose that the simulated plot or field is homogenous with respect to input data. Thus, regardless of the size of the simulated field there exists only one soil type, uniform weather conditions, and the same agricultural management practices (i.e. fertilizer applications, irrigation, etc). Since agricultural observations, experiments, and crop simulation model evaluation are typically performed at small spatial scales (i.e. several square meters to hectares) over relatively short time spans (a few weeks to years), the challenge for modelers is to find bounds to the application of

crop simulation models developed from studies conducted under a limited range of conditions (Luxmoore et al., 1991; Schulze, 2000).

If simulation results are to be useful for water resources planning and other purposes, analysts must provide information about crop simulation model adequacy and limitations (Li and Wu, 2006). This is particularly relevant when decision makers need to consider the risk of extreme weather events such as droughts or heat waves (e.g. Horton et al, 2011). These events can have a significant impact on agricultural water demand and their frequency of occurrence is influenced by variability as well as mean values of model input variables (Mearns et al., 1997; Semenov and Porter, 1995).

3.2.1 Nature

The nature of uncertainty may be described by two basic kinds of uncertainty with fundamental differences: ontological (*variability*) and *epistemic* uncertainty. Ontological uncertainty is associated with phenomena that are inherently variable over time, space, or populations. It originates from variability in the underlying stochastic process. For example, variability exists in the annual precipitation amount at a given location over consecutive years or the soil properties across a field and a probabilistic model may be adopted for their description. On the other hand, epistemic uncertainty is dictated by our ability to measure, understand, and describe the system of interest. It arises from incomplete knowledge about the system under study (Merz and Thieken, 2005). For example, seasonal irrigated acreage is rarely known for every farm in a given county for a

given crop and, yet, approaches have developed for estimating irrigated acreage at the county scale.

Within a given crop simulation model, input variables, parameters, and the model structure (system dynamics) are all subject to uncertainty. Rarely does one encounter only one type of uncertainty in practical applications (Merz and Thieken, 2005). A case with only natural uncertainty or 'pure variability' would suggest that all relationships and their parameters which describe the system are exactly known. On the other hand, 'pure epistemic uncertainty' suggests that a deterministic process is considered but the relevant information describing the system is not available (Helton et al., 2004).

Crop simulation model based decision support exercises must characterize the different dimensions of uncertainty in order to truly add value to the policymaking process. Walker et al., 2003 distinguish three dimensions of uncertainty that allow for a better understanding of uncertainty and better communication amongst analysts.

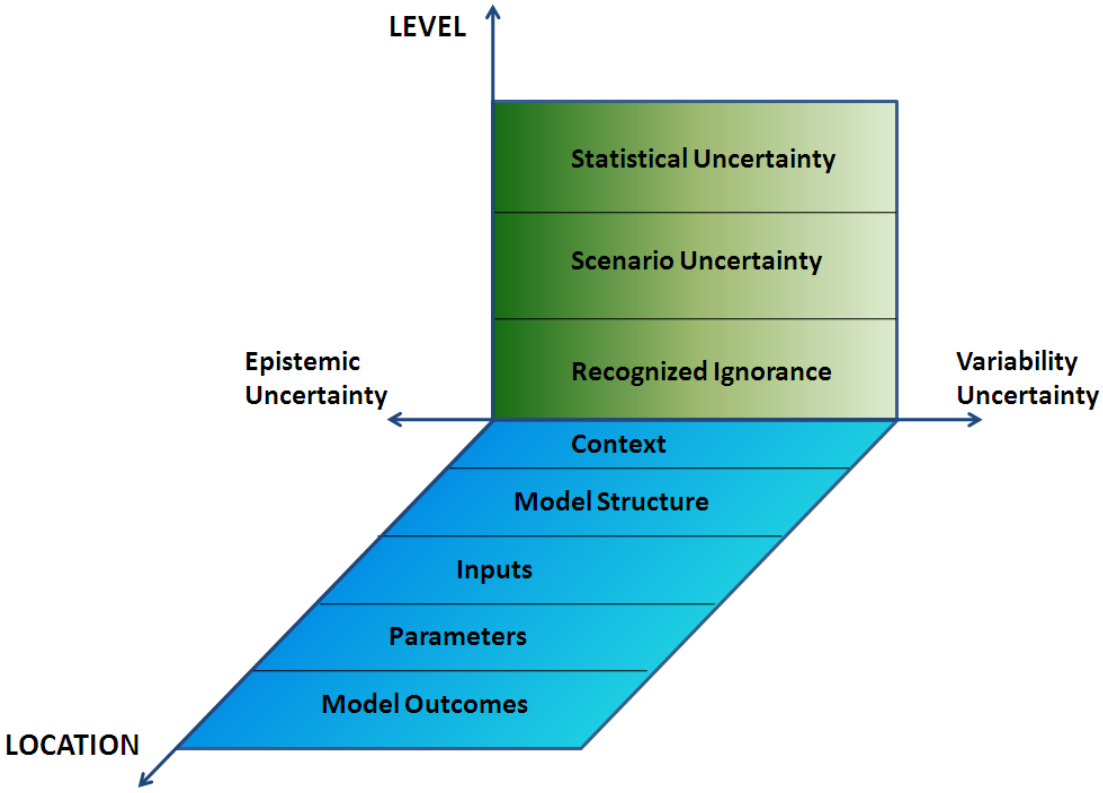

Figure 3.2. Uncertainty depicted in three dimensions characterized by *nature* (epistemic uncertainty and variability), *location*, and *level* (adapted from Walker et al., 2003).

3.2.2 Location

The system model locations are unique to the conceptual formulation and crop simulation model that compose the system model in question. In this work, the Decision Support System for Agrotechnology Transfer (DSSAT) suite of crop models is utilized. DSSAT was originally developed by an international network of scientists, cooperating in the International Benchmarks Sites Network for Agrotechnology project (IBSNAT, 1993) to facilitate the application of crop models in a systems approach to agronomic research. It has been in use for more than 20 years by researchers in over 100 countries worldwide (Jones et al., 1998).

3.2.2.1 Context

Irrigation accounts for the largest consumptive use of freshwater (i.e. approximately 60%) in the United States where over 55 million acres of cropland are irrigated (Howell, 2001; Minchenkov, 2009). In the Flint River Basin agricultural water use accounts for the majority of consumptive water use between May and September and exhibits marked interannual variability, depending on the prevailing climate during the growing season. While Georgia is typically considered to be a state with plentiful water resources due to average annual rainfall exceeding that of many other parts of the United States, the competing demands placed on water resources by the municipal, industrial, agricultural, and ecological sectors make water resources management and planning a significant challenge for stakeholders and policy makers.

River basin management requires projecting irrigation demand under uncertain climate even though observed data related to irrigation volumes and application timing is often sparse, unreliable, or only available for a few continuous years. Climate change has the potential to decrease the availability of water resources due to probable changes in rainfall distribution and increases in potential evaporative demand. Physiologically based crop simulation models are regarded as embodying our current understanding of crop environmental response (Saarikko, 2000). As a result, crop simulation models are playing an increasing role in translating information about climate variability into predictions tailored to the needs of stakeholders and policymakers (Hansen et al., 2006).

3.2.2.2 Model Structure

The equations used in crop simulation models are a representation of the elementary processes in the soil-plant-atmosphere (SPA) system. The Decision Support System for Agrotechnology Transfer (DSSAT) suite of crop models are a group of physiologically based models that simulate important processes in crop growth and development including daily meteorological forcing, soil water transport, plant water uptake, phenological development, and agricultural management inputs (Tsuji et al., 1998). The DSSAT cropping system model (DSSAT-CSM) simulates the growth, development and yield of a crop growing on a uniform area of land under prescribed or simulated management as well as the changes in soil water, carbon, and nitrogen that take place under the cropping system over time. More than 28 different crops can be simulated with DSSAT-CSM, including maize, wheat, rice, barley, sorghum, millet, soybean, peanut, dry bean, chickpea, cowpea, faba bean, velvet bean, potato, tomato, bell pepper, cabbage, bahia and brachiaria and bare fallow (Hoogenboom et al., 2010; Jones et al., 2003).

The DSSAT-CSM simulates monocrop production systems considering weather, genetics, soil water, soil carbon and nitrogen, and management in single or multiple seasons and in crop rotations at any location where minimum inputs are provided. The DSSAT-CSM has a main driver program, a land unit module, and modules for the primary components that make up a land unit in a cropping system. The primary modules are for weather, soil, plant, soil-plant-atmosphere interface, and management components. The modular structure of the DSSAT-CSM incorporates all crops as modules using a single soil model (Jones et al., 2003).

3.2.2.2.1 Soil Water Balance

The functional soil water balance model used in DSSAT requires parameters for establishing how much water the soil will hold by capillarity, how much will drain out due to gravity, and how much is available for root water uptake. Soil water content (volumetric fraction) inputs for each soil layer required for calculation procedures include the lower limit of plant water availability (*LL*), the drained upper limit (*DUL*), and soil water content at field saturation (*SAT*). The *LL* water content corresponds to the limit where capillary forces exceed gravitational force (wilting point) and water potentials of -15 bar. The *DUL* corresponds closely to field capacity concepts and to water potentials in the range of - 0.1 to - 0.33 bar. Other parameters needed for soil water balance include a single value of soil surface albedo, the limit of first stage soil evaporation, the runoff curve number, and a drainage coefficient (Ritchie, 1998).

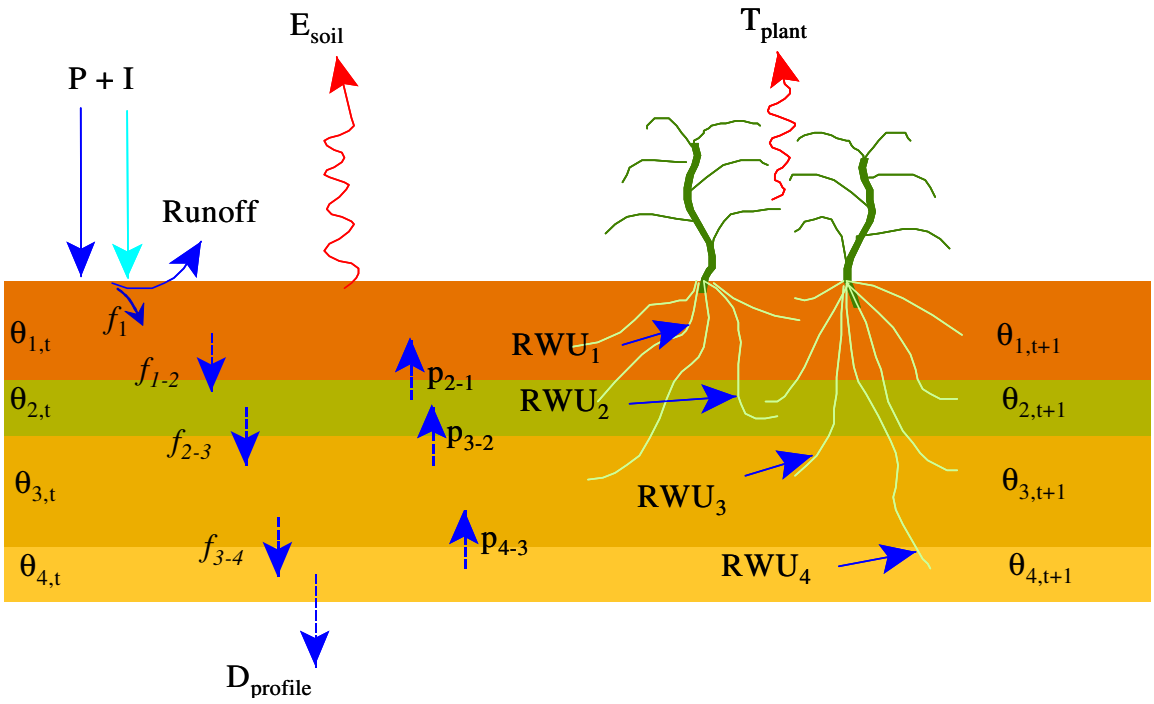

Figure 3.3. Water balance within a hypothetical soil profile (Brumbelow, 2001; Ritchie, 1998).

The soil water balance model computes the daily changes in soil water content by soil layer due to infiltration of rainfall and irrigation, vertical drainage, unsaturated upward flow, soil evaporation, and root water uptake processes (see Fig. 2). This one-dimensional model uses a 'tipping bucket' approach for computing soil water drainage when a layer's water content is above a drained upper limit parameter. Thus, for soil water redistribution during infiltration, water is moved downward from the top soil layer to lower layers in a cascading approach. Drainage from a layer takes place only when the soil water content (*SW*) in a given layer is between field saturation (*SAT*) and the drained upper limit (*DUL*) for that layer. The drainage at the bottom of the soil profile is the drainage flux of the bottom layer. Upward flow can be caused by root water uptake due to transpiration and

soil evaporation. It is computed using a conservative estimate of the soil water diffusivity and differences in volumetric soil water content of adjacent layers (Ritchie, 1998).

Daily water balance calculations begin with the soil water content ($\theta_{j,\,t}$) of each soil layer from the previous day. If precipitation (P) and/or irrigation (I) occurs on a given day, the amount of runoff is determined, and the remainder (f_1) infiltrates into the top soil layer. In addition, soil evaporation (E_{soil}) and plant transpiration (T_{plant}) are determined and subtracted from the top soil layer's moisture content. Drainage ($f_{j\text{-}k}$; $D_{profile}$), upward flow ($p_{j\text{-}k}$), and root water uptake (RWU_j) are determined before soil water content ($\theta_{j,\,t+1}$) for each layer is found to be referenced the next day (Brumbelow, 2001).

Actual soil evaporation is based on a two- stage process (Ritchie 1972). After the soil surface is first wetted due to either rainfall or irrigation, evaporation occurs at the potential rate until a cumulative soil evaporation amount since wetting is reached. Then, a soil-limiting daily soil evaporation amount is computed as a square root function of time since stage one ended. Potential evapotranspiration (ET) and soil water availability govern evaporation from the top soil layer and transpiration from the root zone. Potential ET is partitioned into soil evaporation and plant transpiration, assuming that evaporation depends on the energy that reaches the soil surface and transpiration is proportional to the energy intercepted by the crop canopy. Actual transpiration is the minimum between potential transpiration and total root water uptake (Ritchie, 1972).

This method for computing evapotranspiration is a functional approach for determining water stress in the plant without explicitly modeling water status in the plant component. The ratio of actual ET to potential ET, if less than 1.0, indicates that stomatal conductance would decrease some time during the day to prevent plant desiccation. This ratio is typically used in the plant modules to reduce photosynthesis in proportion to relative decreases in transpiration. Similarly, a ratio of potential root water uptake and potential transpiration is used to reduce plant turgor and expansive growth of crops.

3.2.2.2.2 CROPGRO

CROPGRO was developed as a generic approach for modeling crops in the sense that it has one common source code, yet it can predict the growth of a number of different crops (Boote et al., 1998). Currently, the CROPGRO plant growth and development model simulates cotton; seven grain legumes (soybean; peanut; dry bean*;* chickpea; cowpea; velvet bean and faba bean), and non-legumes such as tomato, cabbage, bell pepper, and two grasses: bahia and brachiaria. CROPGRO is process oriented and considers crop carbon balance, crop and soil N balance, and soil water balance. In this approach, state variables are the amounts, masses, and numbers of tissues whereas rate variables are the rates of inputs, transformations, and losses from state variable pools.

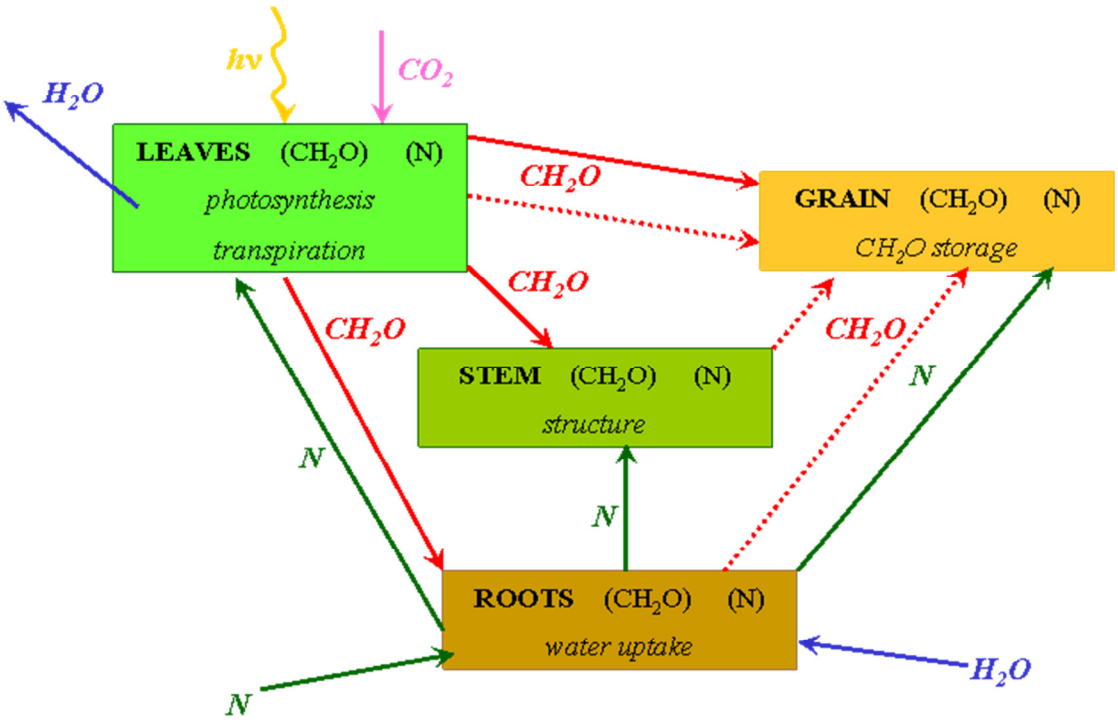

Figure 3.4. Sources and sinks of C and N as modeled in CROPGRO (Boote et al., 1998; Brumbelow, 2001).

The crop carbon balance includes daily inputs from photosynthesis conversion and condensation of C into crop tissues, C losses due to abscised parts, and C losses due to growth and maintenance respiration (see Fig. 3). Supply of C is from the current day's photosynthesis process and from mobilized C from reserves (C in leaves and/or stems). Mobilized C depends on the availability of C stored in vegetative tissue as well as the availability of N for growing new tissue and the potential growth rates of the tissue. The crop N balance processes include daily N uptake, N_2-fixation, mobilization from vegetative tissues, rate of N use for new tissue growth, and rate of N loss in abscised parts (Boote et al., 1998). Nitrogen may be taken up from the soil, mobilized from plant tissue, and assimilated through symbiotic N_2-fixation. The daily allocation of C and N in

the model is based on source-sink concepts. In the model, N mobilization is computed first, followed by root uptake of N. N uptake from the soil can replenish the N mined from vegetative tissue up to a seasonally varying maximum concentration. If these sources of N satisfy the demand for N, then growth proceeds at its potential rate, using all of the day's available C, and no N_2-fixation occurs. If there is a shortage of N, relative to that needed for potential growth, then some C is made available to nodules for N_2-fixation.

Crop development in CROPGRO uses a flexible approach that allows development during various growth phases to be differentially sensitive to temperature, photoperiod, water deficit, and N stresses. Crops like soybean are sensitive to day length, whereas other crops such as peanut are not. There are up to thirteen phases, each having its own unique developmental calculator starting at a unique phenological stage. The physiological time development rate during any one day in a phase is typically a function of temperature, photoperiod, and water deficit. If conditions are optimal, one physiological day is accumulated per calendar day. The number of physiological days required for a phase to be completed is equal to calendar days if temperature, photoperiod, and water status are optimal (Boote et al., 1998).

3.2.2.2.3 CERES

The CERES models include simulation procedures for wheat (*Triticumaestivum L.*), maize (*Zea mays L.*), rice (*Oryza sativa L.*), barley (*Hordeumvulgare L.*), grain sorghum (*Sorghum bicolor L.*), and pearl millet (*Pennisetumamericanum L.*). The CERES-Maize, Wheat and Barley models were modified for integration into the modular DSSAT

cropping system model. For these CERES models, the plant life cycle is divided into several phases, which are similar among the crops. Rate of development is governed by thermal time, or growing degree-days (GDD), which is computed based on the daily maximum and minimum temperatures. The number of GDD occurring on a calendar day is a function of a triangular or trapezoidal function defined by a base temperature, one or two optimum temperatures, and a maximum temperature above which development does not occur.

The potential biomass of a crop can be thought of as the product of the rate of biomass accumulation times the duration of growth. The rate of biomass accumulation is principally influenced by the amount of light intercepted over an optimum temperature range. Daylength may affect the total number of leaves formed by altering the duration of the floral induction phase, and thus, floral initiation. Currently, only temperature and, in some cases, daylength, drive the accumulation of growing degree-days (GDD); drought and nutrient stresses currently have no effect. During the vegetative phase, emergence of new leaves is used to limit leaf area development until after a species-dependent number of leaves have appeared. Thereafter, vegetative branching can occur, and leaf area development depends on the availability of assimilates and specific leaf area. Leaf area expansion is modified by daily temperature (GDD), and water and nitrogen stress.

Daily plant growth is computed by converting daily intercepted photosynthetically active radiation (PAR) into plant dry matter using a crop specific radiation use efficiency parameter. Light interception is computed as a function of leaf area index, plant population, and row spacing. The amount of new dry matter available for growth each

day may also be modified by the most limiting of water or nitrogen stress, and temperature, and is sensitive to atmospheric CO_2 concentration. Above ground biomass has priority for carbohydrate, and at the end of each day, carbohydrate not used for above ground biomass is allocated to roots. Roots must receive, however, a specified stage dependent minimum of the daily carbohydrate available for growth. Leaf area is converted into new leaf weight using empirical functions. If the daily pool of carbon is insufficient to allow growth at the potential rate, a fraction of carbon can be remobilized from the vegetative to reproductive sinks each day. Kernels are allowed to grow until physiological maturity is reached (Jones et al., 2003).

3.2.2.3 Inputs and Parameters

Input data are required to run crop simulation models for decision support applications. Input variables (also sometimes referred to as explanatory variables) consist of data that is measured or observed for each situation where the model is applied (or based on measured or observed values). The simplest source of uncertainty comes from measuring an unknown physical variable (e.g. daily rainfall, temperature, or solar irradiance). While it is generally considered straightforward to estimate the precision of the instruments on which measurements are based, the detection of systematic error can be more difficult and this component of measurement error is commonly ignored (Katz, 2002; Li and Wu, 2006). It is common for researchers to derive input values for crop simulation models from indirect measurements or relationships with other variables in some cases. In addition, measurements or estimations at locations other than the simulation site may be used to fill data gaps or considered to be representative (Bert et al., 2007).

A major portion of the uncertainty in model outputs may be ascribed to incomplete information associated with crop, soil, weather, and management input values (Aggarwal, 1995). The availability of input data of adequate quality and spatial coverage presents challenges to the application of crop models at regional or larger scales (Hansen and Jones, 2000). This is due in part to the fact that the outputs from crop simulation models are typically non-linearly related to their inputs due to model complexity. As a result, the outputs are affected by the spatial aggregation of input variables and parameters that may occur when models are applied in practice to a region of interest (Lorite et al., 2005). In many cases, soil and weather data are approximated using spatial interpolation, geographic information systems (GIS) and/or stochastic weather generators (e.g. WGEN) (Aggarwal, 1995). Alternatively, many studies utilize representative input values based on available data and consultation with local experts (e.g. Bouman 1994) that account for the spatial variation associated with input variables and parameters. However, outputs simulated with data from representative locations may not necessarily represent the spatial average or the interannual variability of regional values (Hansen and Jones, 2000). As a result, when making long term decisions under uncertainty, many stakeholders often prefer projection ranges as opposed to a single 'most likely' value (Horton et al., 2011).

While input variables can differ depending on the situation, a parameter is by definition constant across similar situations of interest. For example, in some cases parameters may change in space but are constant in time. However, crop parameter values could be significantly uncertain due to random errors related to the size and number of

observations when experimental data is utilized to determine parameters. In addition, there may be systematic errors related to bias in the experimental, measurement, observation and calibration procedures used to derive them. Alternatively, parameter values may be derived from bibliographic reviews or expert opinion.

3.2.2.4 Model Outcomes

Model outcomes contain all errors that result from the various assumptions and simplifications that occur over the course of model development. While the structure of crop simulation models is generally considered to be adequate, the results may be uncertain depending on the assumptions made (Aggarwal, 1995). The uncertainty associated with the assumed form of the model is problematic because it is rarely easy to quantify the model outcome error. One important reason is that model error may vary for different applications. For example, when model development involves calibration of model parameters, model error may increase when the model is applied to another area or another time period. In addition, a fundamental choice is made during model development about which state variables, input variables, and parameters are to be included in the model. In this case a basic decision is made about what is important in determining the dynamics of the system. Furthermore, the functional form of relationships in the model may be specified incorrectly. However, any model can only be viewed as an approximation at best. Thus, some simplifications are inevitable so that the model is manageable (Katz, 2002).

3.2.3 Level

Geophysical processes may exhibit real systematic differences over space and time as well as inherent randomness (Katz, 2002).While crop simulation models are developed and tested at the spatial scale of a homogenous plot or field, water resources stakeholders are often interested in climate impacts at the county, watershed or broader scales where significant spatial variability may exist (Hansen and Jones, 2000; Kersebaum et al., 2007). Typical input variables include soil properties (e.g. wilting point, field capacity, saturation water content, slope, bulk density, saturated hydraulic conductivity, etc.) , daily weather data (e.g. solar irradiance, minimum and maximum temperature, precipitation, etc.), and management conditions (e.g. crop variety, planting density, row spacing, nutrient applications, irrigation, etc).

3.2.3.1 Recognized Ignorance

Ideally, there would be multi-horizon soil property data, daily weather data, and crop management information for every agricultural field in a region of interest when water demand for agriculture is being assessed with crop simulation models. However, this information is rarely (if ever) available and, as a result, simulation studies have often inferred regional crop response to soil and climate variability based on a limited number of sites or "representative locations" within the study area (Hansen and Jones, 2000). It is not uncommon for researchers to derive input values for crop simulation models from indirect measurements or relationships with other variables in some cases due to data constraints. In addition, measurements or estimates at locations other than the simulation site may be used to fill data gaps or considered to be representative (Bert et al., 2007). Regional crop management parameters such as planting depth, crop variety, and row

spacing may be assessed by consulting local experts (i.e. farmers, agricultural extension agents, and agricultural researchers), but reliable estimates of irrigation demand benefit from comparison with observed water application data in addition to consultation with a sample of farmers about their decisions regarding when to irrigate and how much water to apply (i.e. an irrigation strategy). In Chapter 4, there is additional discussion about characterizing regional irrigation strategies.

3.2.3.2 Scenario Uncertainty

Scenarios allow all inputs to evolve in time in a contextually consistent manner so that model outcomes of interest can be evaluated that correspond to plausible manifestations of reality. Scenarios are postulated sequences of events that help policymakers focus attention on causality, impacts, and tradeoffs. While scenarios alone are not an adequate means of addressing model outcome uncertainty, scenario analysis is quite popular in the climate change impacts, adaptations, and vulnerability (IAV) research community (Katz, 2002).

Climate change impact studies typically identify a baseline scenario associated with current or recent conditions that allows for the projection of future impact. The model outcomes of interest from the baseline scenario are compared with outcomes derived from scenarios of future climate in order to assess climate change impacts. There is recognized ignorance underlying long range projections of irrigation demand due to volatility in agricultural markets, technological innovations, and genetic development that increases water use efficiency (Bramblett, 1995). As opposed to the impossible task of

identifying a “most likely” climate scenario, exploring a range of plausible future conditions with multiple climate scenarios allows for system resilience (Daniels et al., 2012) .

To obtain daily data for future scenarios, many studies that utilize crop simulation models have simply adjusted historical data by doubling ambient CO_2 concentrations and/or modifying observed local temperature, solar radiation, and precipitation with rather arbitrary relationships (Saarikko, 2000). However, global climate models (GCMs) used in conjunction with weather generators (e.g. WGEN) provide stochastic sequences of daily weather that are intended to be statistically representative of future climate conditions. Alternatively, monthly mean GCM averages are often projected onto historical data with a simple and low-cost downscaling technique known as the delta approach (Horton et al., 2011). Dynamic downscaling uses a regional climate model (RCM) nested within a GCM in an attempt to better represent regional climate (Daniels et al., 2012).Both statistical and dynamic downscaling approaches are frequently utilized in the climate change IAV research community. There is no consensus on the best method for downscaling GCM outputs. While these techniques assist in providing greater spatial and temporal detail than GCM outputs at courser scales, the assumptions associated with the downscaling approaches introduce another aspect of uncertainty. There is no individual downscaling approach that has yet to be identified as the most appropriate for climate change studies (Southworth et al., 2002).

3.2.3.3 Statistical Uncertainty

There are different methods for evaluating the impacts of uncertainty in model inputs with varied degrees of complexity, effort, and data requirements. Notably Aggarwal (1995) assesses the implications of uncertainties in crop, soil, and weather inputs in the spring wheat WTGROWS crop simulation model by representing the uncertainty of each input with a statistical distribution of values based on literature review, measurements, and expert judgment. Monte Carlo simulation was utilized to assess total uncertainty in simulated yield. One hundred combinations of random values were generated from the specified distributions and the uncertainty in simulated outputs was expressed as the percentage deviation in the output as compared to the deterministic output associated with fixed input values. The author evaluates potential, irrigated, and rainfed production environments for three contrasting crop seasons and concludes that deterministic model outputs have a larger bias in water and N limited environments in comparison to a potential production environment. However, non-linear crop simulation model response to variation in input variables and parameters was not taken into account. Furthermore, no significant spatial correlation existed amongst the randomly generated input variables and parameters.

Spatial interpolation methods are popular tools for estimating values of environmental variables at unsampled locations with data from point observations (Guerra et al., 2007). A recent review of comparative studies of spatial interpolation methods in environmental sciences by Li and Heap (2011) found that inverse distance weighting (IDW), ordinary kriging (OK), and ordinary co-kriging (OCK) are the most commonly used methods. In

general, kriging methods performed better than non-geostatistical methods when the statistics of the differences between measured and predicted values at sampled points are used to evaluate performance (Li and Heap, 2011).

3.3 Aggregation Error Assessment

Many problems associated with "scale transfer" or "scale change" occur due to scale differences between the model and observations on one hand and the model and policy makers on the other hand. The term "scale" has a colloquial sense (as opposed to the cartographic sense) that is used in this work, in which "large scale" refers to large areas. The "extent" is the area that is of interest for the study. The extent may be divided into smaller areas that are called "support units" and the "support" is the information available on some or all support units. The support units associated with crop simulation models typically correspond to the simulation units which are the spatial units considered to be homogeneous for the model application. In most cases, the crop simulation model is run independently for each simulation unit. Thus, the possible interactions between the simulations units are not taken into account. When the spatial interactions are important and need to be considered, the crop simulation model may be coupled with a different model for an integrated assessment. For example, the coupling of a crop model with a hydrological model allows one to obtain simulation results at the watershed outlet.

The *scaling* problem has been identified by Beven and Fisher (1996) as the pursuit of a set of concepts that allow information gathered, or a model developed, at one particular scale to be used in making predictions at another scale (Schulze, 2000). The terms

"upscaling" and "downscaling" refer to increasing and decreasing the support respectively in this work and are commonly referred to as "aggregation" and "disaggregation" respectively. While the characteristic scales of a crop simulation model are both spatial and temporal, this chapter will focus primarily on changes in spatial scale. In Chapter 5, there is additional discussion about challenges and solutions associated with changes in temporal scale.

When crop simulation models developed at the field scale are used to make decisions at a broader scale such as the county scale, the extent and the support unit of the study becomes larger than a field or individual cropping system. All input data inevitably will not be available for all fields in the county. Thus, a common assumption is that many fields have the same characteristics and, consequently, the crop simulation model can be run with same input data for all the fields considered. The support unit in this case is a set of fields although the units associated with the input data remain unchanged. In this case, upscaling (or aggregation) is accompanied by a change of support as well as a change in extent.

The integration of crop simulation model outputs across the range of variability of the environment within a region of interest results in a spatial average for an intensive variable (e.g. crop yield or irrigation depth). For example, the average irrigation demand over a two-dimensional region in a given year is given by

$$\bar{d}_t = A_t^{-1} \iint_{R_t} f\left(\boldsymbol{e}_t\left(x,z\right)\right) dxdz$$

where the function $d_t = f\left(\boldsymbol{e}_t\right)$ represents simulated irrigation demand in year t due to environmental inputs $\boldsymbol{e}_t$ (i.e. weather, soil, and management conditions), R_t is the region of interest, and A_t is the area of the region.

3.3.1 Background

Few studies have addressed the response of crop simulation models to variations in the level of input data and parameter aggregation. However, spatial averaging biases the variability of daily time-series weather data. This is particularly important for precipitation because of its influence crop water stress response which depends on soil water balance dynamics. Furthermore, soil heterogeneity has significant implications for crop simulation model applications (Hansen and Jones, 2000).This work aims to evaluate the aggregation error introduced by the aggregation of inputs in crop simulation modeling.

Lorite et al. (2005) assess the impacts of input parameter and data spatial and temporal aggregation on the assessment of irrigation scheme performance through the simulation of average irrigation schedules and the corresponding crop yields. This study is carried out using the Genil-Cabra irrigation scheme which covers an area of 6990 hectares in the province of Cordoba (Spain). Four irrigation seasons (1996/1997 – 1999/2000) are considered in analysis and the most frequent crops were winter cereals, sunflower, and cotton which occupy about 55% of the area. Daily meteorological data was obtained from a weather station in the irrigation area and information about irrigation application

methods, practices, and sowing dates was obtained by visiting each field during each irrigation season, consulting the scheme manager, and surveying farmers (about 10% of farmers responded). The water balance model relied on the USDA Soil Conservation Service (1972) curve number method and infiltrated water was distributed following a cascade approach along ten equal layers for a given soil profile. The Penman-Monteith formula was utilized to calculate reference evapotranspiration and subsequently maximum crop evapotranspiration. The ratio of seasonal actual evapotranspiration to seasonal maximum evapotranspiration allowed for a yield reduction estimate using a production function approach (Doorenbos and Kassam, 1979). Irrigation application efficiency and the depth of water necessary to refill the soil profile are utilized to determine gross irrigation requirements.

Three levels of aggregation (*aggregation level 1* ~ the entire area, *aggregation level 2* ~ 83 command areas, and *aggregation level 3* ~ approximately 800 parcels) were defined to evaluate the effects of input parameter aggregation on the estimation of scheme water requirements. To extend the validity of this analysis to situations where the variability in soil properties is different, four different soil scenarios were generated by varying the variance of the soil water holding capacity (i.e. the difference in soil water content between field capacity and wilting point) but keeping constant its average over the irrigation area. Five temporal aggregation levels (daily, weekly, monthly, quarterly, and annual) were defined for the temporal aggregation analysis that utilized the effective rainfall concept (as opposed to the curve number model) and a soil evaporation model lumped into a single crop coefficient (Allen et al., 1998; Doorenbos and Pruitt, 1977).

The authors found that irrigation requirements estimated with aggregation level 1 were about 0.5% and 1% less than those estimated with aggregation level II and III respectively. They argue that such differences are unexpectedly small and deserve closer analysis. However, soil variation was shown to influence the magnitude of the aggregation effect. Its impact was most marked for deep-rooted crops in rainy years (i.e. 20% error associated with highest soil variability evaluated for sunflower in 1997/1998).Temporal aggregation had little effect on the simulation of irrigation requirements up to monthly time steps. The authors did not observe interaction between temporal and spatial aggregation.

The full integration of crop simulation models and GCMs remains a challenging endeavor due to the different scales at which processes take place. In order to quantify the bias in yield simulation introduced by the spatial aggregation of precipitation inputs, Baron et al. (2005) conducted a case study in Senegal where 17 rain gauges were available inside a grid box with a size (i.e. 17° W to 14.2° W and 12.6° N to 15.4° N) similar to a GCM grid box. A smaller box approximately 1° square was also defined as an intermediate level of aggregation. The authors interpret GCM output as a spatial average as opposed to a point observation.

The SARRA-H crop modeling platform was utilized with daily weather records (1950-1980) to simulate millet production on a sandy soil with a water holding capacity of 100 mm m^{-1}. The water balance model consisted of two soil layers. Runoff and evaporation

was simulated daily and the remaining water was partitioned into storage, drainage, and transpiration. Plant transpiration and carbon assimilation are reduced as the soil water in the root zone decreases. Maximum evapotranspiration (ET) was determined by a crop factor while potential evapotranspiration (PET) is governed by FAO guidelines for different species (Doorenbos and Kassam, 1979; Doorenbos and Pruitt, 1977). Grain yield simulations were performed by averaging weather inputs or with individual weather station inputs (with subsequent averaging of simulated yields). Both grain yield and crop biomass were significantly overestimated as a result of aggregated rainfall input. The authors argue that the distortion of rainfall frequency and intensity caused overestimation of 'agronomically effective precipitation' or the fraction of rainfall that is ultimately transpired.

3.3.2 Study area

The Apalachicola – Chattahoochee – Flint (ACF) basin extends across 50 counties in Georgia, 10 counties in Alabama and 8 counties in Florida. The basin is drained by the Apalachicola, Chattahoochee and Flint rivers. The Flint River drains an area of 8,460 square miles and is characterized by humid, subtropical climate with long summers and mild winters (USGS, 2007). Agricultural irrigation represents the largest consumptive use of water in the Flint River basin (Hook et al., 1999).

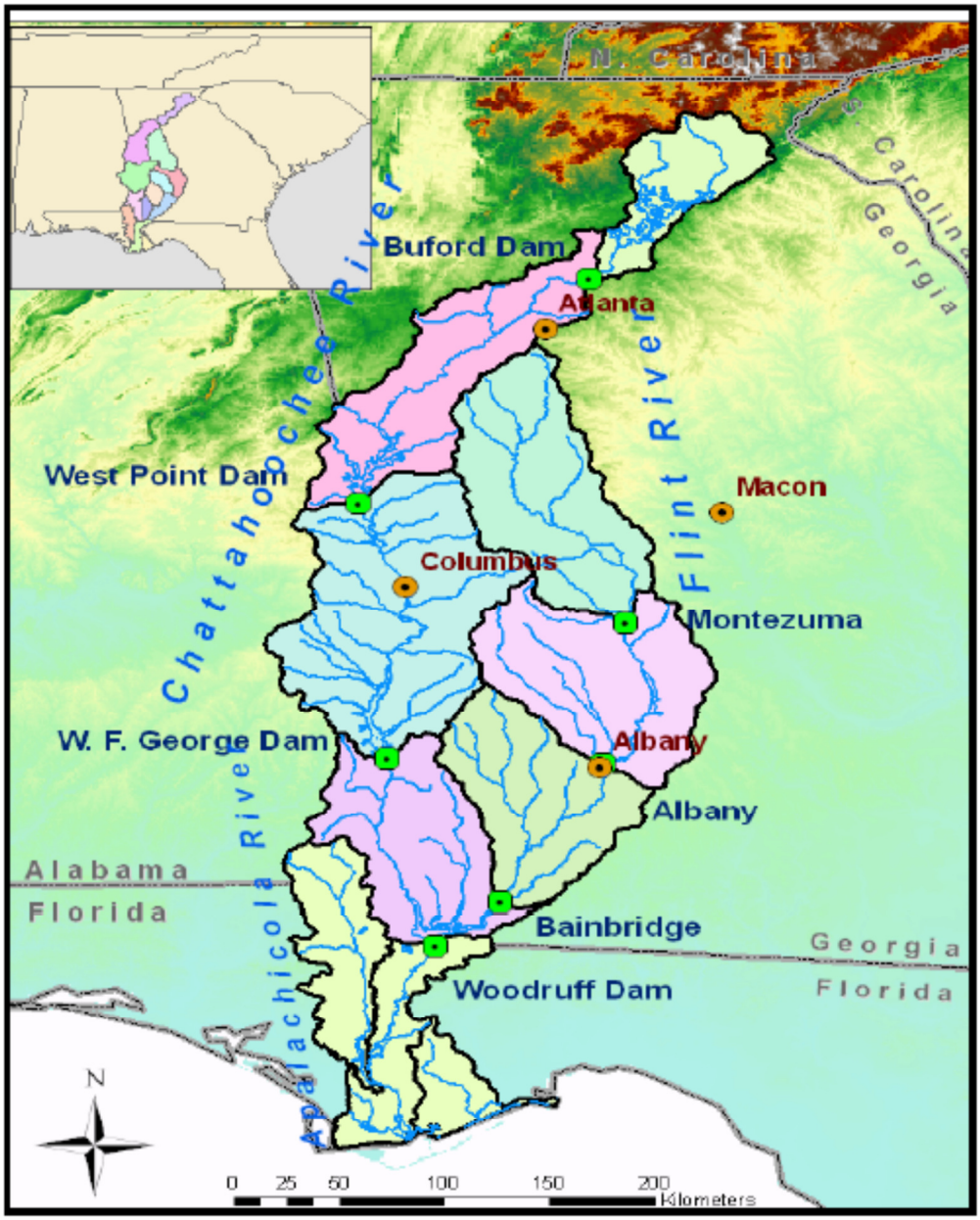

Figure 3.5. Map of Apalachicola – Chattahoochee – Flint Watersheds: Buford, West Point, George, Montezuma, Albany and Woodruff-Bainbridge (Kimaite, 2011).

The study area (31°32’ N, 84°31’W to 31°36’ N, 84°27’W) is approximately 10,000 acres and lies in Baker County, GA which has over 20,000 acres of irrigated acreage (USDA, 2007). Water withdrawals for agriculture in Baker County were estimated to

exceed 40 million gallons per day (MGD) in the year 2000 (USGS, 2009). This area lies in the Lower Flint – Ochlockonee water planning region (WPR) which is in the southern portion of the Flint River basin.

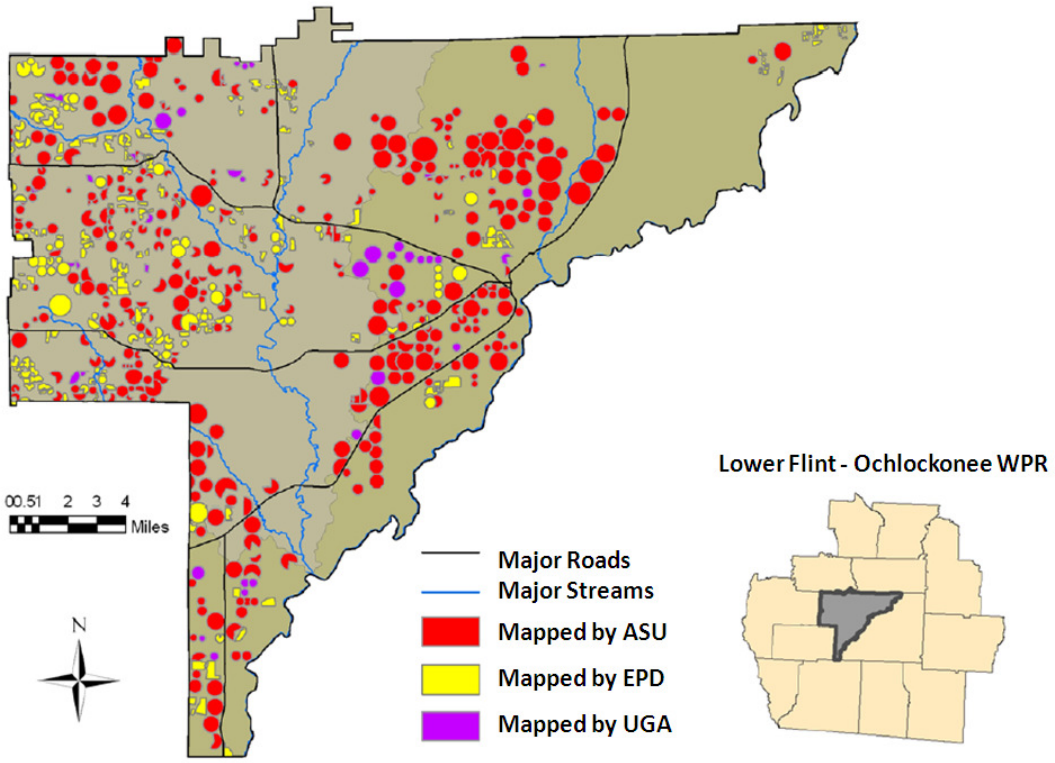

Figure 3.6. Irrigated acreage in Baker County, GA (adapted from Hook et al 2010).

Mean annual temperature ranges from 56 °F in the mountains to 69 °F near the coast in Georgia (Perkins, 1987). Annual precipitation ranges from 43 inches (1,100 mm) to 75 inches (1,900 mm) and is caused by two different processes (frontal and convective). While rainfall occurs mainly as a result of fronts during the fall and winter (i.e. October to March), the spring and summer (i.e. April to September) are characterized by convective processes, tropical storms, and small concentric patterns. Significant correlation in monthly rainfall exists at distances as large as 600 km in the ACF basin

during January. However, the range decreases to 200 km in the month of July due to the different atmospheric physics causing rainfall during the convective rainy season (Baigorria et al., 2007).

3.3.3 Weather Data

Daily historical weather records were obtained from the Georgia Environmental Monitoring Network (GAEMN) for 38 automated weather stations. The data consists of daily values of solar radiation (MJ/m^2), minimum/maximum temperature (°C), and precipitation (mm/day). The GAEMN is a valuable resource that is utilized frequently by farmers and agricultural researchers in the Southeast U.S.

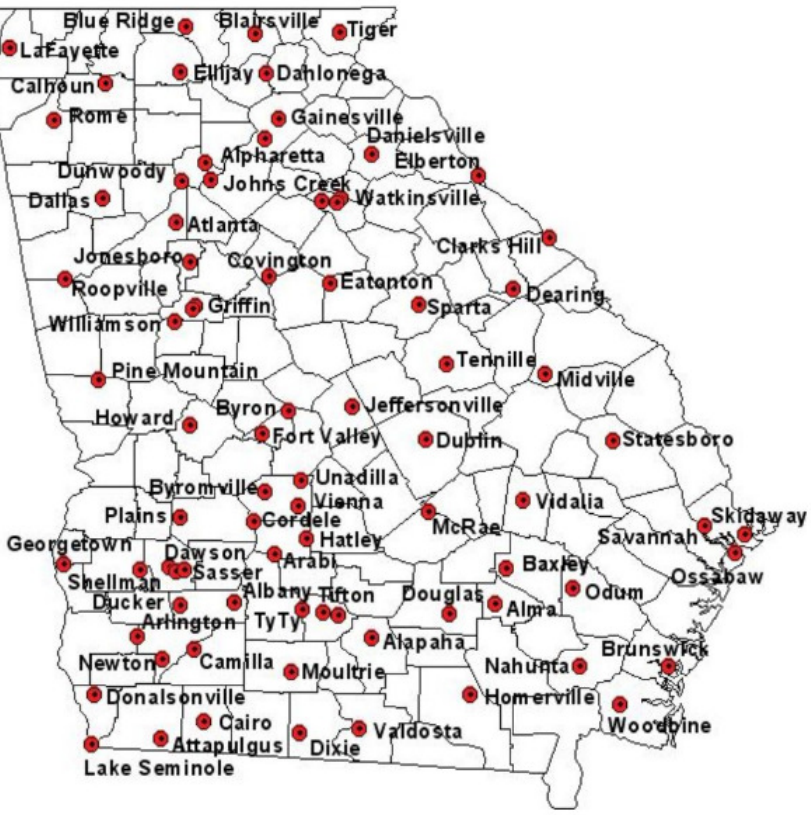

Figure 3.7. The Georgia Environmental Monitoring Network (GAEMN, 2011).

3.3.4 Soils Data

Soil profile data is derived from bulk and core soil samples collected for multiple soil horizons in fifty counties (Perkins, 1987). In addition, USDA – Natural Resources Conservation Service (NRCS) soil characterization database and soil maps were utilized to develop the data set. Soil properties are also derived using methods incorporated into the SBUILD software program that accompanies the DSSAT suite of crop models (Hoogenboom et al., 2010; Jones et al., 2003; Perkins, 1987; Salazar et al., 2012; Tsuji et al., 1998). The soil profile data selected to develop the variogram function presented in this chapter included drained lower limit, drained upper limit, as well a geographic coordinates for each soil profile.

3.3.5 Methodology

In order to assess the aggregation errors associated with spatially aggregated inputs, a hypothetical region is developed and partitioned into a grid of homogenous land units. Each land unit is assigned unique soil properties and weather data. Spatial fields of daily weather data and soil properties are generated with geostatistical techniques and described below. Land units are aggregated into blocks at various levels of aggregation and then CSM-CROPGRO-Peanut is forced with aggregated inputs. Comparison is made between model outcomes with "true" weather inputs (i.e. non-aggregated input data) as opposed to aggregated inputs.

3.3.5.1 Geostatistics

Consider the problem of estimating soil properties (e.g. field capacity) or daily rainfall at an unmeasured location. The available information consists of soil property data and measured daily precipitation data at point locations in space. To estimate values at any location other than the measured locations, a mathematical model of spatial variability is needed. The kriging systems allows for spatial random field analysis and the "best estimation" of a random field by utilizing point measurements (Luo, 2007). The structural distance between model estimates and true values is measured and the most accurate estimate is subsequently obtained (Kitanidis, 1997). Baigorria et al. (2007) utilized kriging to quantify spatial correlations of daily and monthly rainfall events in the Southeast U.S. and to produce realizations of daily weather that preserve spatial patterns associated with historical rainfall events.

Geostatistical techniques consider the set of unknown values as a set of spatially dependent random variables related to the same attribute (Nour et al., 2006). The *variogram* function is utilized to represent spatial variability when utilizing the most common geostatistical model, the *intrinsic isotropic model* (Kitanidis, 1997; Nour et al., 2006). The best linear unbiased estimation (BLUE) methodology is applied and the mean square error of estimation is considered a rational measure of prediction reliability (Luo, 2007). The assumptions associated with the intrinsic model are that (1) the mean is an unknown constant and (2) the variogram may be represented as a function of the distance. Consider that *n* measurements have been collected:

$$Z(\boldsymbol{x_1}), Z(\boldsymbol{x_2}),\ldots, Z(\boldsymbol{x_n})$$

where $Z(\boldsymbol{x_i})$ and $\boldsymbol{x_i}$ represent the spatial random function and the set of spatial coordinates under consideration respectively. For any location $\boldsymbol{x_0}$, a method called kriging can obtain the best estimate of $z(\boldsymbol{x_0})$ as well as the error associated with the estimate. The *semivariogram* (hereafter referred to as the variogram) is closely related to the covariance function which is given by

$$C(\boldsymbol{h}) = \sigma^2 - \gamma(\boldsymbol{h})$$

where $\sigma^2$is the stationary variance, $C(\boldsymbol{h})$ is the covariance, and $\gamma(\boldsymbol{h})$ is the variogram function at Euclidean distance $\boldsymbol{h}$.

3.3.5.2 Realizations

The best estimation of a random field is in fact just one realization of the random field. For this study, a number of realizations conditioned on the known measurements $Z(\boldsymbol{x_i})$ are needed that that allow for statistical analysis (Luo, 2007). The procedure utilized for generating a conditional realization is as follows:

1. An unconditional realization $Z_{uc}(\boldsymbol{x_i})$ is generated with a mean of zero and the covariance matrix for the attribute of interest (i.e. daily rainfall or available water holding capacity).
2. The n differences $Z(\boldsymbol{x_i})$ - $Z_{uc}(\boldsymbol{x_i})$ are used for kriging over the extent of the area of interest.
3. The unconditional realization is added to the kriged differences over the extent of the area of interest. The conditional realization is given by

$$Z_c(\boldsymbol{x}_0) = Z_{uc}(\boldsymbol{x}_0) + \sum_{i=1}^{n} \lambda_i [Z(\boldsymbol{x}_i) - Z_{uc}(\boldsymbol{x}_i)]^2$$

where $Z_{uc}(\boldsymbol{x_0})$ is the unconditional realization at the location of interest and λ_i are the kriging weights associated with each measurement $Z(\boldsymbol{x_i})$. The simple kriging system is utilized to generate unconditional realizations with mean zero and the covariance matrix developed with the known measurement values and locations. The linear equation system is given by

$$\mathbf{A}\boldsymbol{\lambda} = \boldsymbol{b}$$

with

$$\boldsymbol{\lambda} = \begin{bmatrix} \lambda_1 \\ \lambda_2 \\ \vdots \\ \lambda_n \end{bmatrix}$$

$$\boldsymbol{b} = \begin{bmatrix} \mathrm{C}(\boldsymbol{x}_1, \boldsymbol{x}_0) \\ \mathrm{C}(\boldsymbol{x}_2, \boldsymbol{x}_0) \\ \vdots \\ \mathrm{C}(\boldsymbol{x}_n, \boldsymbol{x}_0) \end{bmatrix}$$

$$\mathbf{A} = \begin{bmatrix} \sigma^2 & \cdots & \mathrm{C}(\boldsymbol{x}_1, \boldsymbol{x}_n) \\ \vdots & \ddots & \vdots \\ \mathrm{C}(\boldsymbol{x}_n, \boldsymbol{x}_1) & \cdots & \sigma^2 \end{bmatrix}$$

where the kriging weights associated with the minimum mean square error are chosen such that

$$\sum_{j=1}^{n} \lambda_j C(\boldsymbol{x}_i, \boldsymbol{x}_j) = C(\boldsymbol{x}_i, \boldsymbol{x}_0)$$

and the estimator is unbiased in that the expectation of the estimator and the actual value is zero, i.e.,

$$E\left[\hat{Z}(\boldsymbol{x}_0) - Z(\boldsymbol{x}_0)\right] = 0$$

The ordinary kriging system exactly reproduces known values $Z(\boldsymbol{x_i})$ at the measurement locations $\boldsymbol{x_i}$ utilized to develop the covariance matrix. However, the kriging weights become subject to the constraint

$$\sum_{i=1}^{n} \lambda_i = 1$$

where

$$-\sum_{j=1}^{n} \lambda_j \gamma(\boldsymbol{x}_i, \boldsymbol{x}_j) + \nu = -\gamma(\boldsymbol{x}_i, \boldsymbol{x}_0)$$

and υ is a Lagrange multiplier. While the simple kriging system is utilized to generate random spatial fields that have a mean of zero with the desired spatial correlation structure in step 1, ordinary kriging is utilized to ultimately develop random fields that honor the true observations at measurement locations in step 2.

3.3.5.3 Variogram

The *raw* and *experimental variograms* contains information about the scale of spatial variability. The raw variogram is the scatter plot of the square difference $[Z(\boldsymbol{x_i}) - Z(\boldsymbol{x_j})]^2/2$ and the separation distance for all n(n-1)/2 measurement pairs. The experimental variogram is a common tool used in applied geostatistics to visualize spatial interdependence and it allows for a means to infer the distribution of spatial variability (Kitanidis, 1997). Examination of the experimental variogram is often a preliminary step used to estimate the variogram function and it is given by

$$\hat{\gamma}(h_k) = \frac{1}{2N(k)} \sum_{j=1}^{N(k)} [z(\boldsymbol{x}_i) - z(\boldsymbol{x}_j)]^2$$

where the axis of the separation distance has been discretized into k consecutive intervals (spatial lag classes) h_k and $N(k)$ is the number of data pairs separated by distance h_k. The experimental variogram is formed graphically by connecting all the points given by the separation distance intervals h_k and the corresponding average square differences.

There are limitations to the experimental variogram that are important when fitting a variogram model. While the experimental variogram is a useful tool for exploratory analysis, it is often sensitive to the number of intervals used to discretize the separation distance range. Furthermore, fitting a variogram model data to the experimental variogram does not ensure that the model is adequate.

Alternatively, the concept of the stochastic process may be invoked and a probability distribution is established for the *residuals*. The actual error and the normalized error of the kriging estimate are given by

$$\delta_i = z(\boldsymbol{x}_i) - \hat{z}_i \text{ and}$$
$$\varepsilon_i = \frac{\delta_i}{\sigma_i}$$

where δ_i is the actual error, $\sigma_i = 2\gamma(\boldsymbol{x}_1,\boldsymbol{x}_2)$ is the standard error, and ε_i is the normalized (orthonormal) residual at the i-th measurement location. All ε_i are orthonormal in that they are uncorrelated with each other and normalized to have unit variance. In fact, the orthonormal residuals must be uncorrelated if kriging is a minimum variance unbiased estimator (Kitanidis, 1997).

The residuals may be thought of as random variables and consequently, their probability distributions may be calculated. The evaluation of the variogram is based on statistical tests (Q_1 and Q_2) involving the residuals. Under the null hypothesis, Q_1 is normally distributed with mean zero and variance 1/(n-1). Alternatively, Q_2 is normally distributed with mean one and variance 2/(n-1). In addition, (n-1)Q_2 follows the chi-square distribution with parameter (n-1).

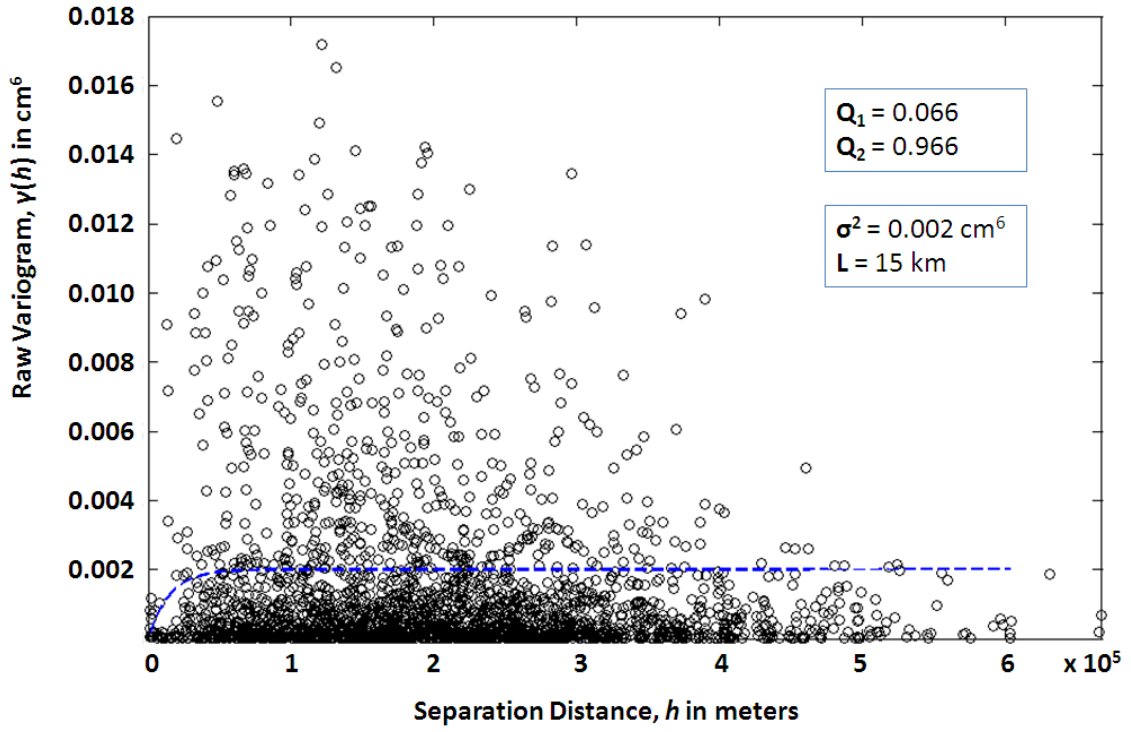

Figure 3.8. Raw variogram cloud (black circles) and fitted exponential variogram model (blue dashed line) associated with available water holding capacity (AWHC).

The exponential variogram model is given by

$$\gamma(\boldsymbol{h}) = \sigma^2[1-e^{-\boldsymbol{h}/l}]$$

where $\sigma^2 > 0$ and $l > 0$. While the spatial structure of the available water holding capacity (AWHC) may be described with one exponential variogram model (see Figure 3.6), daily rainfall is modeled as a collection of temporally correlated random spatial functions (Nour et al., 2006). Stochastic simulation of rainfall occurs on all days in which at least one weather station recorded rainfall.

Realizations or random spatial fields of the rainfall distribution are constructed for the days under consideration (Nour et al., 2006). In this work, a drought year (i.e. 2002) is considered and exponential variogram parameters are estimated for all the wet days of the crop season. The geographic coordinates (i.e. latitude and longitude) included with the soil profile data allowed for a variogram cloud to be developed and subsequently a variogram function to be evaluated.

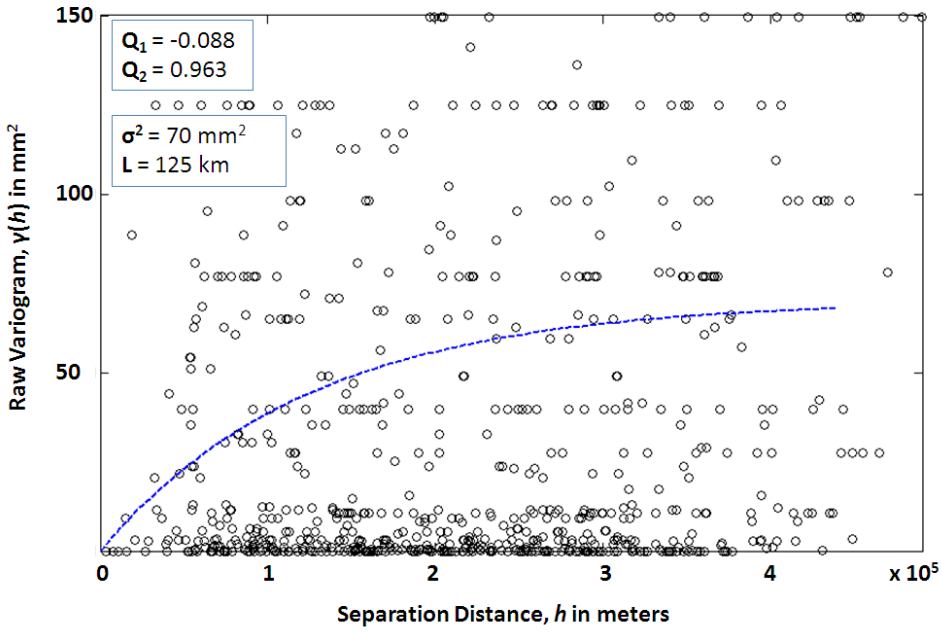

Figure 3.9. Example of raw variogram cloud (black circles) and fitted exponential variogram model (blue dashed line) associated with daily rainfall (May 17th, 2002).

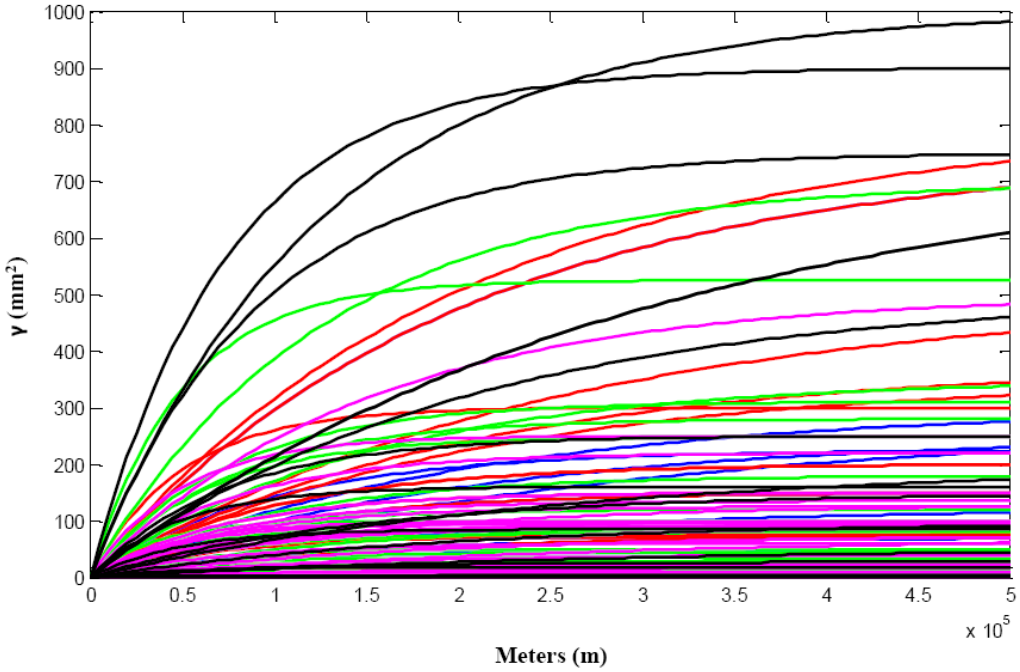

May wet days – Blue; **June wet days** – Red; **July wet days** – Green; **August wet days** – Magenta; **September wet days** - Black

Figure 3.10. Fitted variogram models associated with daily rainfall.

3.3.5.4 Spatial Aggregation

Stochastic simulation algorithms have become more common over the last two decades for uncertainty modeling in soil science although assessing uncertainty about soil attributes is rarely the goal. Rather it is typically a precursor to a more in depth in investigations concerning the propagation of errors through complex functions or models (Goovaerts, 2001). In this work, input sampling is employed by simulating crop response to stochastic realizations of soil and weather that are sampled in a manner that captures the spatial heterogeneity of the environment. While aggregation by stochastic input sampling and crop model simulation is data and computationally intensive, it allows for the characterization of uncertainty associated with applying the crop simulation model at a scale different from the one for which it was developed (Hansen and Jones, 2000).

Representative management practices consistent with the recommendations of agricultural extension agents and farmers in the Lower Flint River basin are employed. The CSM-CROPGRO-Peanut model was used to simulate irrigated peanut production. The popular Runner type variety "Georgia Green" is selected due to its widespread use over the last decade by farmers in the Flint River basin. One planting date (May 5th) was used and irrigation scheduling was automated with the *irrigation threshold* (IT) approach. This approach allows irrigation events (i.e. water applications of 25 mm, 100% efficiency) to be automatically simulated whenever soil moisture falls below a set threshold value (IT = 50%) at a given management depth (40 cm). The application of a fixed amount is consistent with irrigation systems commonly used by farmers in this region (see Fig. 3.11).

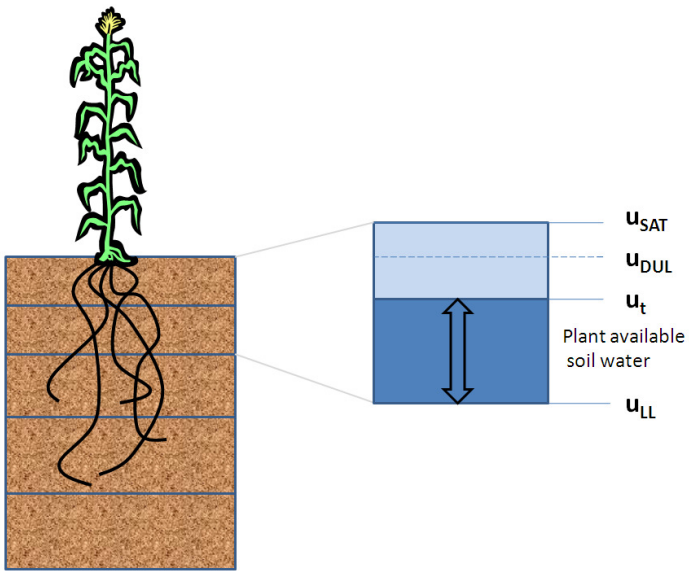

Figure 3.11. Plant water availability in the soil column (adapted from Ines et al., 2001).

One hundred realizations of daily precipitation inputs and soil properties (drained upper limit and lower limit) have been generated for each land unit and the crop simulation model was run to obtain crop water demand at each land unit. There are 2,304 land units that form the 48 cell by 48 cell grid that covers approximately 40 square kilometers. Rainfall at the boundaries of the conditional realizations exactly reproduced rainfall at the Arlington, GA and Camilla, GA weather stations adjacent to Baker County, GA.

Next, precipitation and soil inputs are averaged for blocks of land units and the crop simulation model is run utilizing these various levels of spatial aggregation. Statistical comparison between the model outputs generated using the "true" input data associated with individual land units and the outputs generated using spatially aggregated inputs will provide valuable insight into the effects of aggregation error on estimates of agricultural water demand.

Several preliminary analyses were conducted before assessing the full aggregation scenario (all 2,304 grid cells aggregated). The effects of aggregation on irrigation demand are shown in Figures 3.13 – 3.15 for blocks of 4 grid cells, 9 grid cells, and 16 grid cells for one stochastic realization of AWHC and precipitation. The smoothing of the irrigation demand surface is evident as a result of the aggregation of inputs.

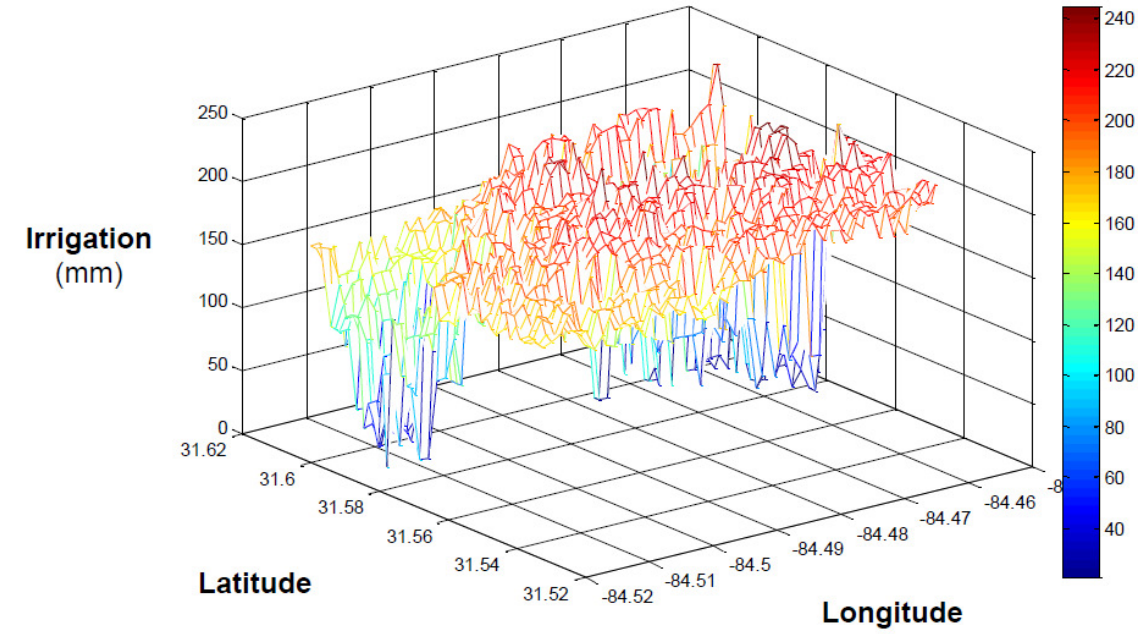

Figure 3.12. Simulated irrigation demand with no aggregation.

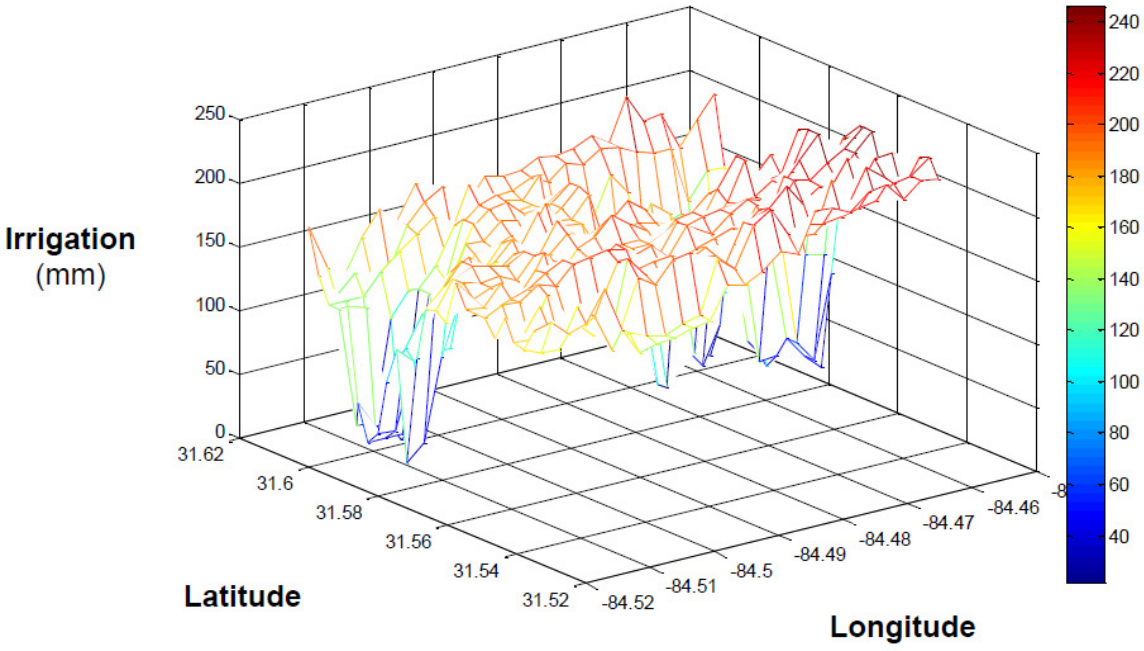

Figure 3.13. Simulated irrigation with aggregation of blocks of four grid cells.

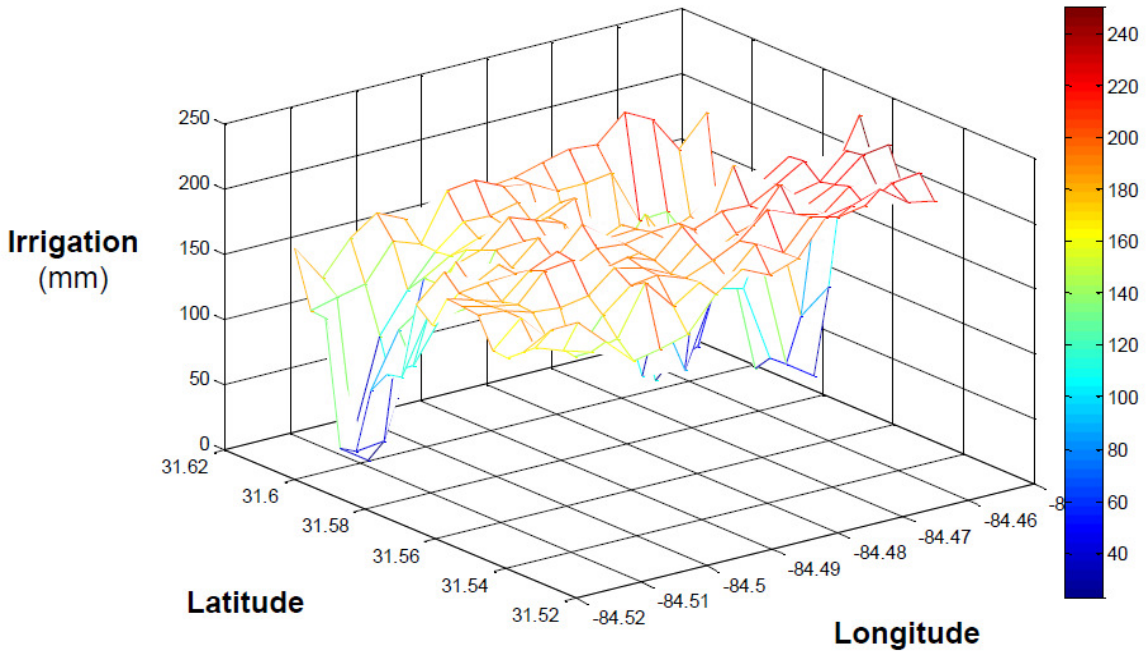

Figure 3.14. Simulated irrigation demand with aggregation of blocks of nine grid cells.

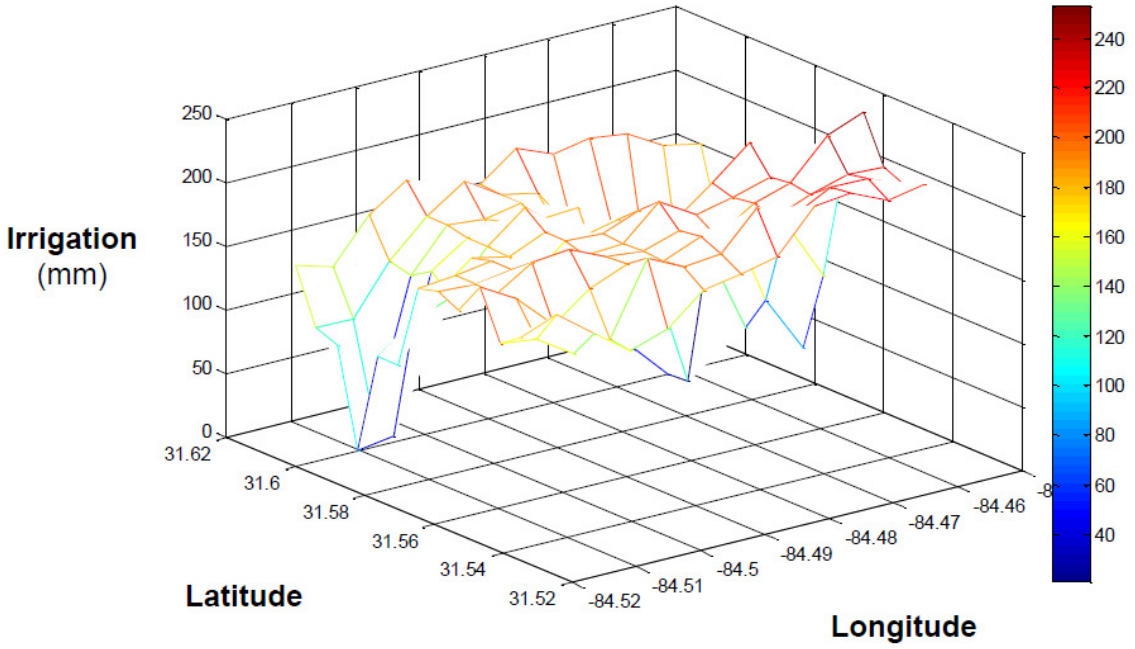

Figure 3.15. Simulated irrigation demand with aggregation of blocks of sixteen grid cells.

The model outcome (i.e. irrigation demand) errors resulting from the conditional realizations generated form an empirical cumulative distribution function (see Figure 3.16). As the level of aggregation increases, the results show that the distribution spreads and the magnitude of simulated errors increases. The box plot of aggregation errors associated with full aggregation (i.e. all 2,304 grids) in shown in Figure 3.17. The standard deviation of aggregation error is plotted against spatial scale in Figure 3.18.

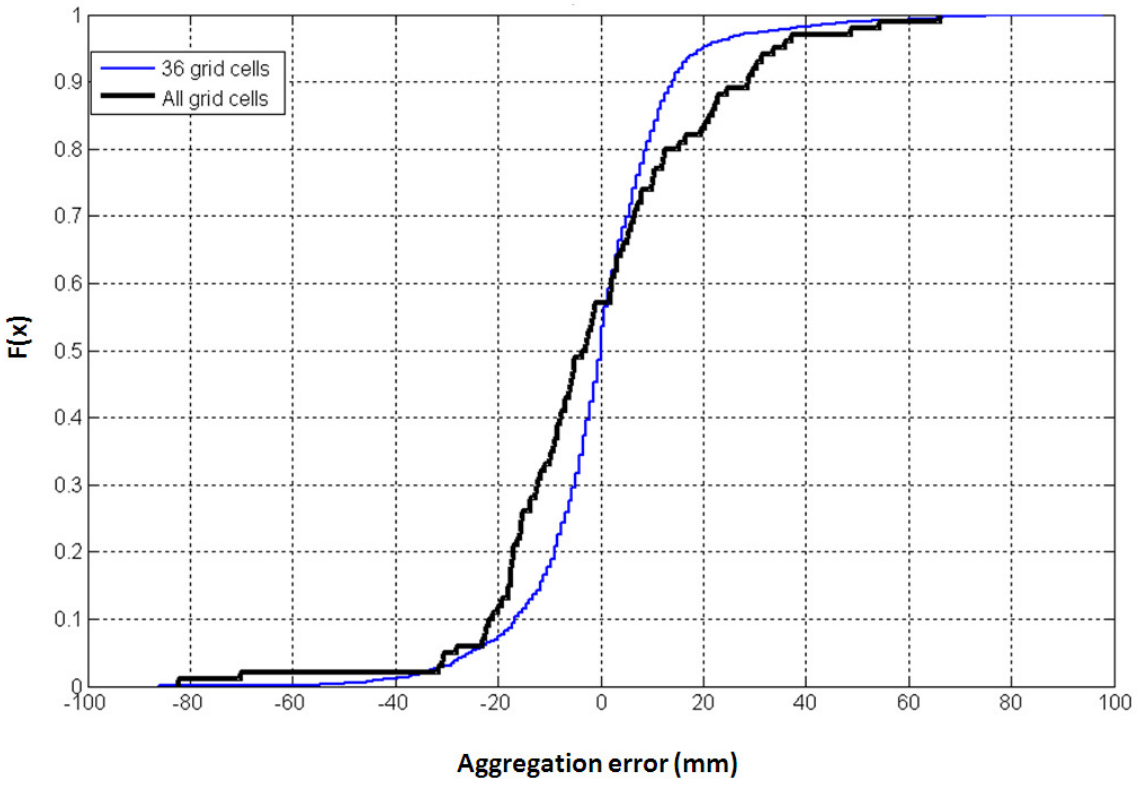

Figure 3.16. Empirical cumulative distribution functions of aggregation error.

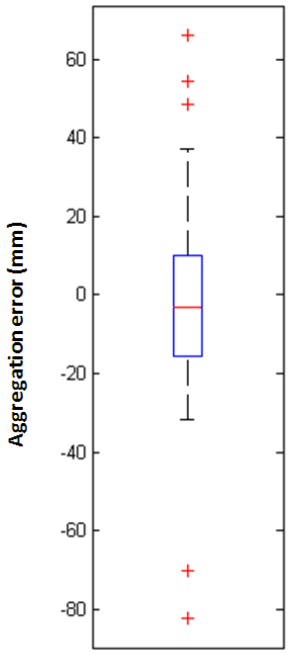

Figure 3.17. Box plot of crop water demand error associated with full aggregation.

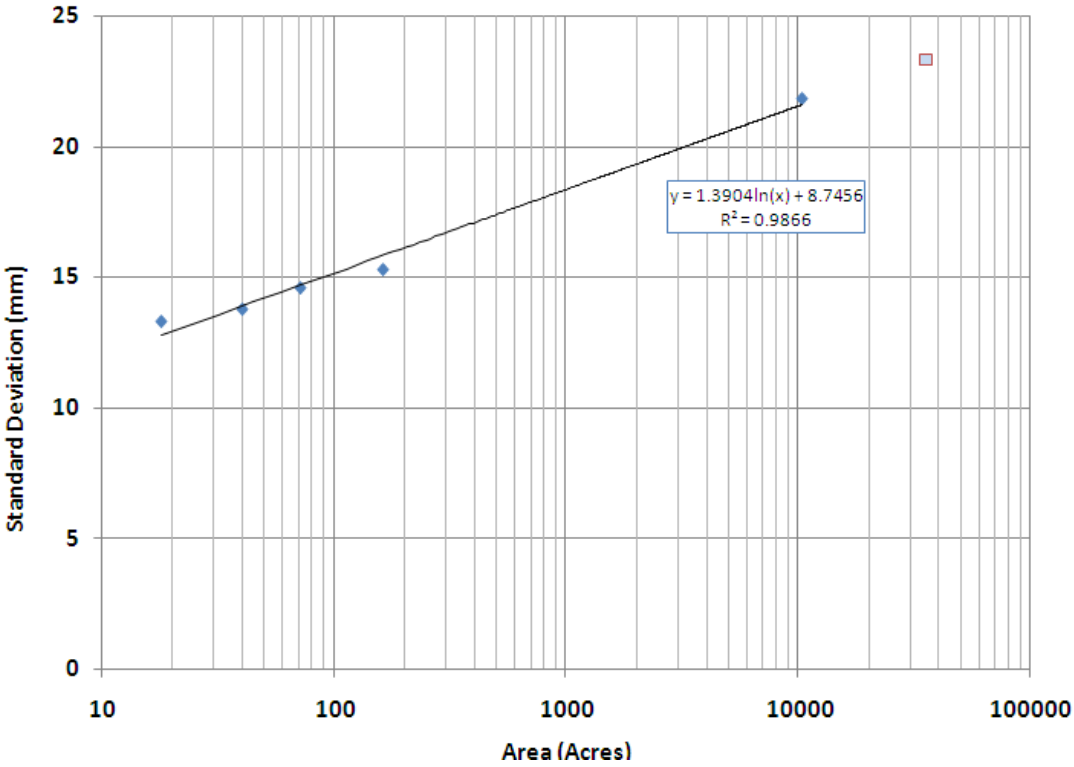

Figure 3.18. Standard deviation of aggregation error with increasing spatial scale.

3.3.6 Summary

The soil profile data selected to develop the variogram function presented in Chapter 3 included drained lower limit, drained upper limit, as well a geographic coordinates for each soil profile. The soil profiles were developed by agricultural researchers at the University of Georgia with USDA - Natural Resources Conservation Service (NRCS) soil maps, bulk and core soil samples collected for multiple soil horizons in fifty counties (Perkins, 1987), as well as the SBUILD software program that accompanies the DSSAT suite of crop models. The geographic coordinates (i.e. latitude and longitude) allowed for a variogram cloud to be developed and subsequently a variogram function to be evaluated. This is now described in more detail in the thesis.

Ideally a network of weather stations with an average distance between stations of about 0.4 square kilometers (i.e. 0.16 square miles or a spatial scale of 100 acres) would be utilized to develop the variogram functions of daily precipitation described in Chapter 4. However, there is no such weather station network in existence due to the high costs associated with the desired spatial density and consequently, consultants and planners typically use representative or aggregated weather inputs from the nearest weather station(s) for water resources planning applications. Thus, the precipitation data from the Georgia Environmental Monitoring Network is utilized and the geostatistical techniques described in Chapter 4 are employed for this research. The work presents a technique to evaluate the potential benefit of a denser weather network when utilizing aggregated weather inputs to assess agricultural water demand.

Radar-derived precipitation derived may present a useful means of evaluating real-time drought stress at a relatively high resolution (McNider et al., 2011). For planning applications and climate change projections, actual measured data from rain gauges is typically used. Furthermore, radar data must be used in conjunction with ground based measurements in order to characterize the uncertainty associated with radar-derived precipitation. Future work may evaluate the potential benefits of radar data for describing the spatial variability of daily rainfall and aggregated weather inputs for agricultural water demand assessments.

In this chapter, geostatistical techniques are utilized to represent the heterogeneous nature of soils, crop management, and climate at multiple scales. A methodology for estimating the aggregation error associated with forcing crop simulation models with aggregated inputs is presented. Results suggest that the standard deviation of model error is approximately 23 mm at a spatial scale of 1/8 degree. In chapter four, irrigation strategies are characterized by simulating observed irrigation depths. The results from this chapter inform model calibration guidelines for estimating parameters to represent regional irrigation strategies in the Lower Flint River basin.

Chapter 4: Agricultural Water Demand in the Southeast U.S.

In this chapter a methodology is presented for characterizing regional irrigation strategies in the Lower Flint River basin and estimating regional water demand. Previous research with the AWP data set has shown that the moisture stress threshold (MST) irrigation scheduling algorithm (Brumbelow, 2001) has the potential to represent regional irrigation demand under current climate conditions in the Flint River basin (Braneon and Georgakakos, 2011).County-scale irrigation strategies are determined with metered irrigation data from the GSWCC for 2007 and the MST irrigation scheduling algorithm. Historical assessments of agricultural water demand are subsequently conducted in the Lower Flint River basin that utilize the 2007 baseline irrigated acreage developed by Hook et al. (2009). In Chapter 5, agricultural water demand assessments under climate change are presented.

4.1 Introduction

In order to effectively develop water management plans and policies in the Southeast U.S., estimation of water demand in the agricultural sector is essential. Agricultural water use is the dominant form of consumptive water use in the Flint River basin and many river basins throughout the world. While measurements of municipal and industrial abstractions have been available for many years, comprehensive measurements of agricultural water demand remain scarce (GWRI, 2012). Furthermore, Georgia's significant population growth and expansion of irrigated agriculture over the last four

decades (see Fig. 4.1) has raised concerns about whether flows in the Flint River will be sufficient during periods of drought or below average rainfall.

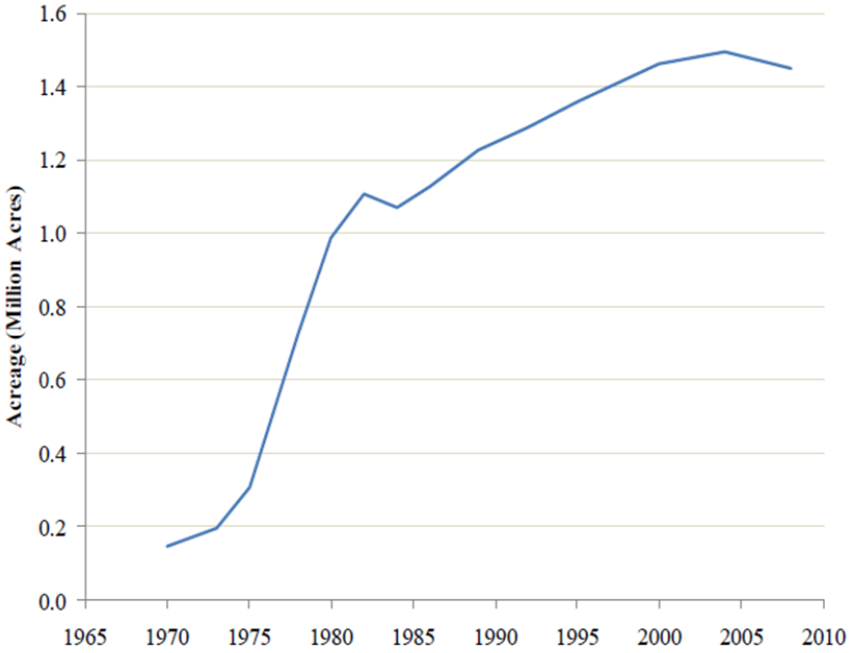

Figure 4.1. Georgia irrigated acreage trend (Kimaite, 2011).

The doctrine of "riparianism" forms the basis of Georgia's modern water rights and dictates that land ownership entitles the property owner to "reasonable use" of surface and ground water (Hodgson, 2006). These water rights are "usufructary" in that land owners have a right to the use and enjoyment of water within the state but no property right (Hodgson, 2006). Reasonable use of surface water suggests that a property owner adjacent to a waterway must leave enough water in the waterway so as not to inhibit reasonable use by downstream users. Amendments to Georgia's Groundwater Use Act of 1972 and Water Quality Control Act were made in 1988 to require agricultural water users to obtain permits from the Environmental Protection Division (EPD) of the Georgia Department of Natural Resources (DNR).

While agricultural irrigators that use more than 100,000 gallons per day on a monthly basis are required to obtain permits from the EPD (see Fig. 4.2), permit records do not include enough information to estimate actual water consumption by irrigators. Permit records identify permitted agricultural water users by (1) type of water source(s), (2) county of withdrawal, (3) pumping limit, and (4) total possible irrigated area(s). However, no information is provided in permitted records regarding which crops are irrigated or what types of irrigation systems are utilized.

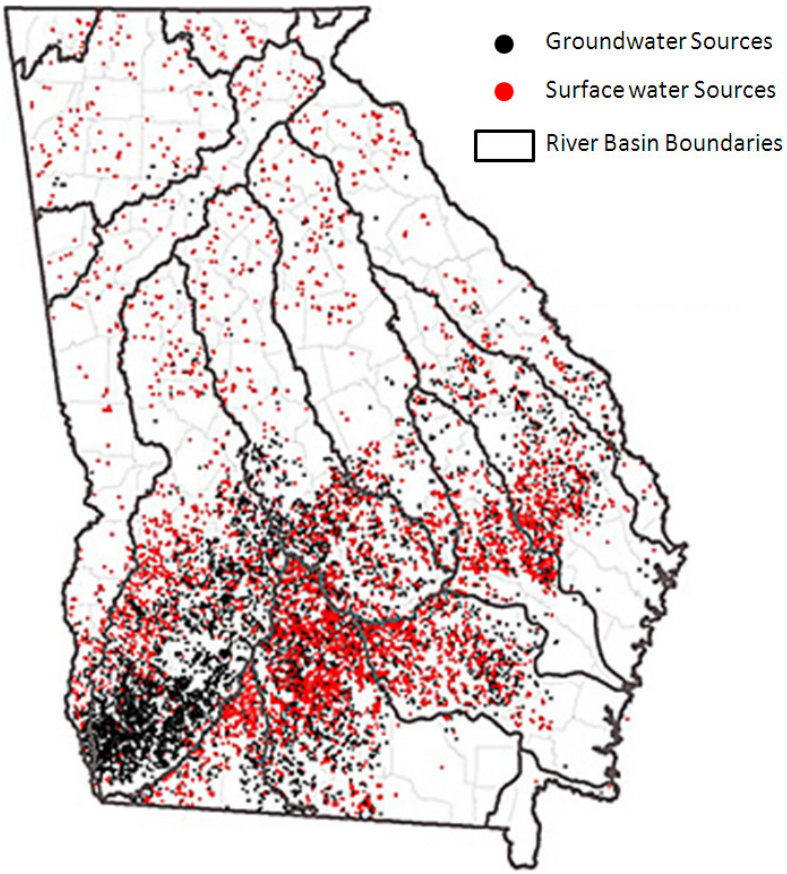

Figure 4.2. EPD permitted withdrawals for irrigation within the state of Georgia (adapted from GSWCC, 2013)

In the last fifteen years there have been significant efforts to strengthen the quality and spatial extent of agricultural water use data in Georgia. The Ag Water Pumping (AWP) monitoring program included monthly field visits to more than 800 irrigated fields from 1999 to 2004 (Hook et al., 2005). A stratified random sampling approach was developed when identifying potential participants in this voluntary irrigation monitoring program. While AWP contributed much needed information regarding irrigation depths applied during the 2000 to 2002 drought by agricultural producers in Georgia, uncertainty regarding the spatial distribution of irrigated acreage throughout the state remained a water planning challenge. As a result, a comprehensive map of irrigated area was developed by Hook et al., 2009 as part of EPD led research efforts to support regional water planning groups. The map formed a common irrigated area baseline that is representative of 2007 land use. Approximately 1,450,000 acres of irrigated cropping systems were mapped and water sources were identified for most irrigated fields by 2009.

The Georgia Soil and Water Conservation Commission (GSWCC) took on the challenge of reading and maintaining meters for all permitted water withdrawals for irrigation in 2003. However, it would be several years before the majority of irrigated fields in Georgia actually had meters installed on their irrigation systems. In 2011, an analysis of metered locations from 2007 to 2010 showed that groundwater users used about a third more irrigation volume than surface water users on average. However, normalization of applied irrigation by irrigated acreage nearly eliminates the disparity between groundwater and surface water irrigation demand. Evaluation of metered irrigation data

shows that more irrigation (water depth per acre) was applied in dry years with less rainfall such as 2007 and 2010. Over 10,000 meters were installed by the end of 2010 (Torak and Painter, 2011).

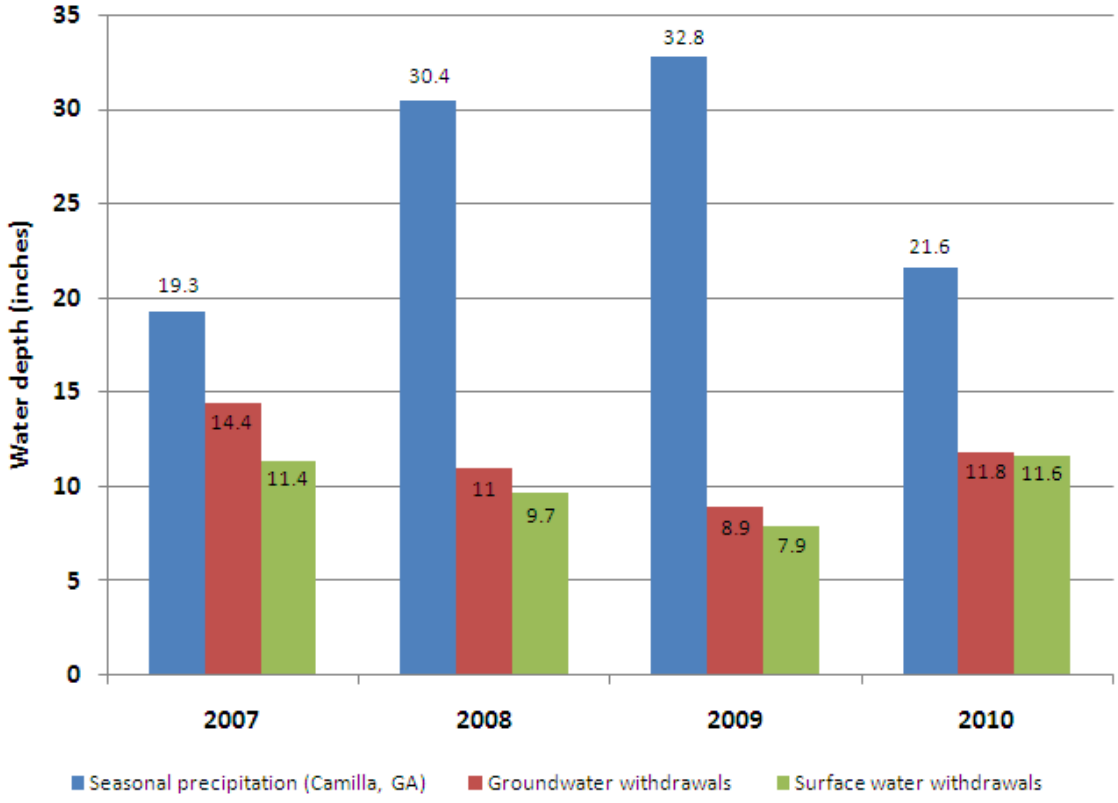

Figure 4.3. Precipitation depth (April to September) at GAEMN weather station in Mitchell County and metered irrigation depth in the Lower Chattahoochee-Flint River basin (Torak and Painter, 2011).

4.2 Methodology

While estimates of agricultural water demand were utilized to develop the Flint-Ochlockonee Regional Water Plan, the Council has indicated that there is a need for improved "quantification of agricultural water withdrawal permit limits, based on use over a number of years "(Georgia State-Wide Water Management Plan, 2011). A better understanding (i.e. "quantification") of actual agricultural water use "may provide for more predictable and fair management of agricultural water demand in drought periods" (Georgia State-Wide Water Management Plan, 2011).

4.2.1 GSWCC Metering Data

The GSWCC currently oversees Georgia's legally mandated Agricultural Water Use Measurement Program that began in 2004. Ultimately, all permitted agricultural irrigation wells and pumps must have a measurement device installed (see Fig. 4.13 and 4.14). Installation of annually reported meters progressed to completion in the Lower Flint River basin in time to monitor agricultural water use during the 2007 growing season (Torak and Painter, 2011).

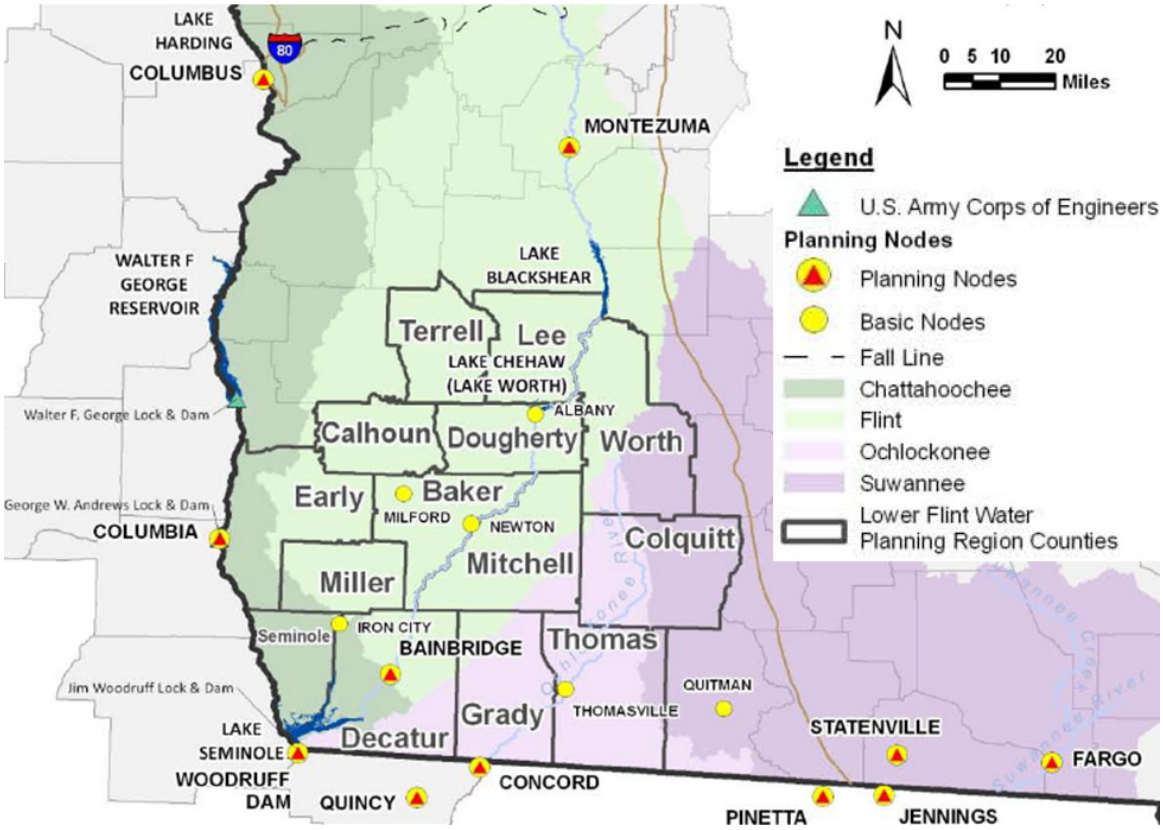

Figure 4.4. Map showing the counties that form the Lower Flint-Ochlockonee Region (adapted from Georgia State-Wide Water Management Plan, 2011).

Data from the GSWCC that is presented in this dissertation is used solely in a manner consistent with the intent of Georgia General Assembly House Bill 579 (Georgia General Assembly, 2003) and the Privacy Act of 1974 (U.S. Department of Justice, 2010). The right to privacy of each farmer is protected as only aggregated data and analyses are presented without reference to specific water use by individual farmers.

A thorough quality-assurance program was developed by GSWCC to ensure internal consistency of metered agricultural water use data. Annually reported meter data from the Chattahoochee-Flint River basin was assessed to determine if "roll-back" or "roll-

forward" may have occurred (Torak and Painter, 2011). Roll-back occurs when the impeller of the water meter rotates in reverse and consequently, measured water use is reduced. Roll-back may be attributed to (A) suction in the supply pipe containing the meter after the pump is turned off or (B) negative air pressure in a well due to a water level drop in the aquifer. Roll-forward may be caused by rising water levels in wells but this phenomenon is more difficult to detect.

4.2.2 Data Sampling Procedure

Metered sites are randomly sampled from the population of sites associated with a given county within the Lower Flint River basin (see Fig. 4.15). Approximately 75% of irrigated acreage in the Lower Flint River basin is associated with maize, peanut, and cotton (see Fig. 4.16). Furthermore, these field crops have been shown to be well represented with the DSSAT suite of crop models by several researchers in the Southeast U.S**.** (e.g. Hook et al., 1994; Brumbelow and Georgakakos, 2001; Salazar et al., 2012) Thus, only metered sites that could be identified as growing one of the three primary irrigated field crops in isolation were allowed to comprise the county populations utilized for random selection. These sites are assumed to rotate crops in order to reduce the prevalence of plant disease and achieve higher yields (see Fig. 4.17). The sampled sites were further reduced to sites that did not utilize well-to-pond systems and sites that applied less than thirty-five inches during the year.

The decision to irrigate is mimicked by utilizing the moisture stress threshold (MST) algorithm to represent regional irrigation strategies. Consultation with farmers,

agricultural extension agents, and agricultural researchers revealed that in some instances an inch or water may not be applied to large fields (e.g. a 250 acre field in one day). Furthermore, while many farmers have irrigation systems that are able to irrigate multiple fields with one source and minimal manpower, some farmers have irrigation systems that require manual adjustments that may result in situations in which an irrigation event occurs over a time period that exceeds one day. In order to focus on the farmer's decision to apply irrigation on a daily basis and the environmental heterogeneity associated with increasing the spatial scale, only permitted sites that included less than one hundred acres of irrigated area are selected to characterize irrigation strategies. This final constraint is imposed to reduce the likelihood of operational constraints that prevent water from being applied to the entire irrigated area in one day.

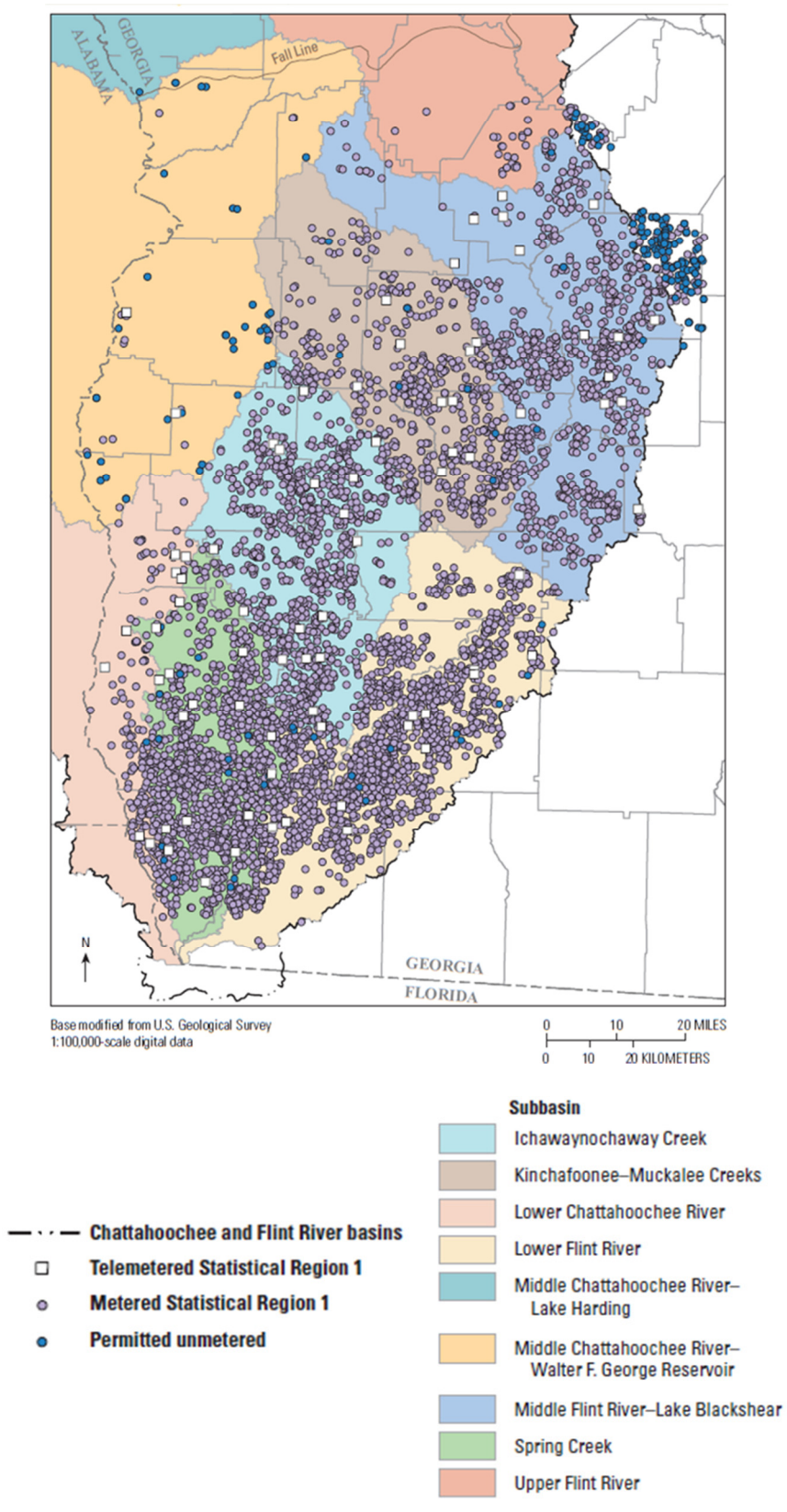

Figure 4.5. Sites in Statistical Region 1 (adapted from Torak and Painter, 2011).

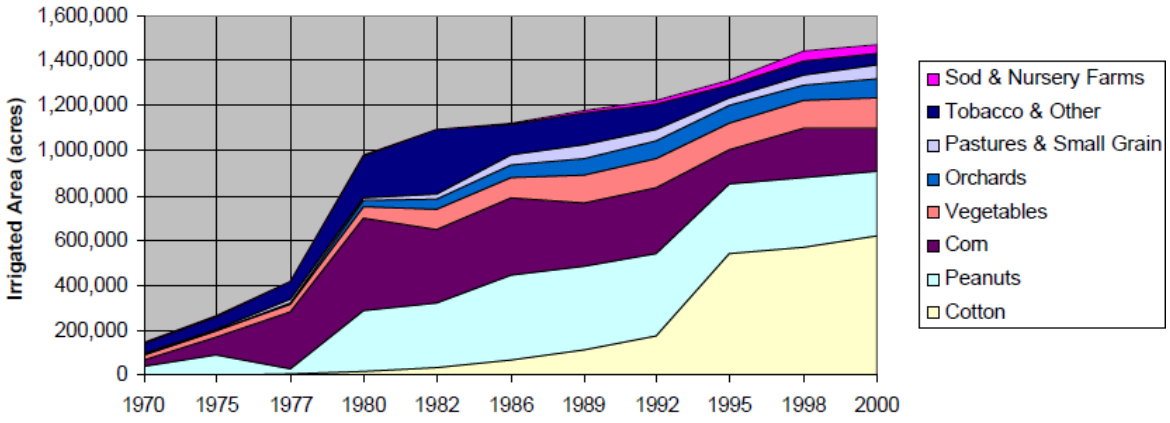

Figure 4.6. Historical crop acreage in Georgia (Lin et al., 2007)

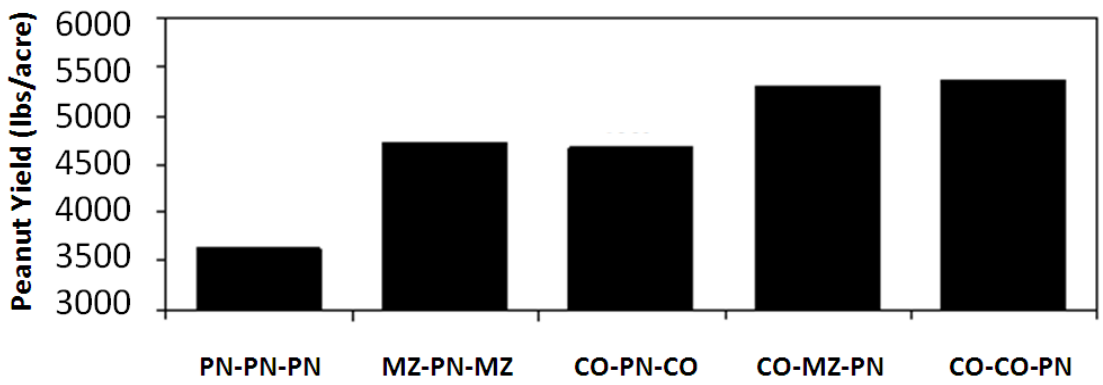

Figure 4.7. Peanut yield estimates for various maize (MZ), peanut (PN), and cotton (CO) rotations (USDA, 2008).

4.2.3 Irrigation Strategy Characterization

A random sample of twenty-one to thirty-two metered sites was selected from each county population. The MST algorithm (Brumbelow, 2001) is implemented with the DSSAT suite of crop models in order to quantify the irrigation strategy utilized at each metered site.

Irrigation demand is represented with a dynamic system model as

$$I\left(t+\Delta t\right)=I\left(t\right)+d_m\left[X\left(t\right),w\left(t\right);\theta\right]$$

where $I(t)$ = total applied irrigation at the end of day t, Δt is one day, d_m is a daily water demand function associated with the crop simulation model, $X(t)$ is the vector of state variables, $w(t)$ is the vector of daily climatic forcing, and θ is the vector of parameters.

Physiological moisture stress is a phenomenon that is observable at the field scale by farmers (Brumbelow, 2001). However, farmers are influenced by a variety of factors when scheduling irrigation. Many irrigators in the Flint River basin rely on "visual inspection of the plant" and "general experience" as a means to determine how much water to apply (Yu et al., 2005). The irrigation demand planning framework utilized in this work relies on a plant stress index (state variable) calculated by the DSSAT suite of physiologically-based crop models. Thus, plant water stress (or moisture stress) is assumed to be the primary cause for irrigation by agricultural producers in the Southeast U.S.

After numerous discussions and extensive correspondence with agricultural researchers and producers in the Lower Flint River basin, a regional irrigation scheduling approach was developed that allows approximately 33 mm of water to be applied at 75% efficiency when plant water stress exceeds a crop-specific moisture stress threshold (MST). The implementation of the irrigation scheduling approach follows:

1. The daily moisture stress index is determined form the daily plant stress factor as:

$$MST = TURFAC$$

   TURFAC (i.e. turgor factor) is the most sensitive of the plant stress factors determined daily for all crops in DSSAT. It directly affects the growth rates of most plant organs and ranges from zero (i.e. extreme plant stress) to one (i.e. no plant stress).

2. At each metered site, irrigation is scheduled in a dynamic approach so that an irrigation application is applied any time the MST exceeds the user defined MST target. The crop-MST combination that results in a seasonal irrigation depth that is closest to the observed irrigation at each metered site is retained as a plausible irrigation strategy.

Developing irrigation strategies based on maintaining soil moisture stress below a particular threshold is justified in that this approach implicitly incorporates crop development stage, precipitation, and soil moisture. Agricultural producers aim to prevent plant water stress because water is used by plants for temperature regulation, chemical transport, structural integrity, as well as photosynthetic processes (Brumbelow, 2001). TURFAC is a drought stress index affecting cell expansion that is a function of the ratio of potential plant water uptake to potential transpiration. The index is represented mathematically as:

$$TURFAC = \min\left(1, 0.67\frac{\sum_{1}^{n} \boldsymbol{RWU}_{l}}{\boldsymbol{T}_{pot}}\right)$$

where RWU_l is root water uptake in soil layer l, n is the number of soil layers, and T_{pot} is potential transpiration. Thus, when total potential root water uptake is 125% of potential transpiration, cell expansion is reduced to 83% of the potential transpiration rate.

4.2.4 Weather Data

Daily weather data is utilized from the Global Summary of the Day (GSOD) dataset (NCDC, 2010) as well as the Georgia Environmental Monitoring Network (GAEMN). The GSOD dataset is derived from hourly observations associated with the Integrated Surface Hourly (ISH) database. This database is composed of surface weather observations from about 20,000 stations worldwide (see Fig. 4.18). The data in the ISH database is collected and stored from sources such as the Automated Weather Network (AWN), the Global Telecommunications System (GTS), and the Automated Surface Observing System (ASOS). The GAEMN is described in section 3.3.3 and Figure 3.7 of chapter three.

Figure 4.8. NCDC weather stations in the Southeast U.S. (adapted from NCDC, 2010).

The daily temperature and precipitation inputs utilized for each metered site are spatially interpolated from GSOD weather stations in the Southeast U.S. The inverse distance weighting procedure applied is given by

$$w_j = \frac{\sum_{i=1}^{n} \frac{w_i}{d_{i,j}^2}}{\sum_{i=1}^{n} \frac{1}{d_{i,j}^2}}$$

Where w_j is the daily weather variable being estimated for metered site j, w_i is the value of the weather variable of interest at weather station i, $d_{i,j}$ is the distance between the metered site j and weather station i, and n is the number of weather stations utilized for the estimation procedure. Conversely, daily solar radiation inputs are utilized from the nearest GAEMN weather station as climatic forcing for crop simulations at metered sites.

4.2.5 Soils Data

Soil profile data is utilized that was developed as part of the Agricultural Irrigation Water Demand study completed by Hook et al, 2009 (see Table 4.1). The data set is described in section 3.3.4 of chapter three and includes several soil properties such as saturated hydraulic conductivity as well as soil water content of the drained upper limit (i.e. field capacity) and lower limit (i.e. wilting point) of plaint available soil water. Simulated irrigation water demand estimates that are utilized to assess irrigation strategies are weighted by the estimated proportion of each soil type associated with irrigated production within selected counties.

Table 4.1. Soil profiles utilized in crop model simulations (Hook et al., 2009).

County	Soil Association	Soil type
BAKER	ORANGEBURG-FACEVILLE-LUCY	Orangeburg Loamy Sand
BAKER	BONNEAU-BLANTON-TROUP	Troup Sand
BAKER	TIFTON-DOTHAN-GRADY	Tifton Loamy Sand
CALHOUN	ORANGEBURG-FACEVILLE-LUCY	Orangeburg Loamy Sand
CALHOUN	TIFTON-DOTHAN-GRADY	Dothan Loamy Sand
CRISP	TIFTON-ALAPAHA-DOTHAN	Tifton Loamy Sand
CRISP	TIFTON-ALAPAHA-DOTHAN	Dothan Loamy Sand
DECATUR	BONNEAU-BLANTON-TROUP	Troup Sand
DECATUR	ORANGEBURG-FACEVILLE-LUCY	Orangeburg Loamy Sand
DECATUR	TIFTON-DOTHAN-GRADY	Tifton Loamy Sand
DOOLY	TIFTON-DOTHAN-GRADY	Tifton Loamy Sand
DOOLY	ORANGEBURG-FACEVILLE-LUCY	Orangeburg Loamy Sand
DOOLY	TIFTON-ALAPAHA-DOTHAN	Dothan Loamy Sand
EARLY	TIFTON-DOTHAN-GRADY	Tifton Loamy Sand
EARLY	ORANGEBURG-FACEVILLE-LUCY	Orangeburg Loamy Sand
EARLY	ORANGEBURG-FACEVILLE-LUCY	Faceville Sandy Loam
LEE	TIFTON-ALAPAHA-DOTHAN	Tifton Loamy Sand
LEE	ORANGEBURG-FACEVILLE-LUCY	Orangeburg Loamy Sand
LEE	TROUP-FUQUAY-PELHAM	Fuquay Loamy Sand
MILLER	TIFTON-DOTHAN-GRADY	Tifton Loamy Sand
MILLER	BONNEAU-BLANTON-TROUP	Troup Sand
MILLER	GRADY-OCILLA-TIFTON	Ocilla Loamy Sand
MITCHELL	BONNEAU-BLANTON-TROUP	Troup Loamy Sand
MITCHELL	TIFTON-DOTHAN-GRADY	Tifton Loamy Sand
MITCHELL	ORANGEBURG-FACEVILLE-LUCY	Orangeburg Loamy Sand
SUMTER	ORANGEBURG-FACEVILLE-LUCY	Orangeburg Loamy Sand
SUMTER	ORANGEBURG-FACEVILLE-LUCY	Faceville Sandy Clay Loam
SUMTER	ORANGEBURG-FACEVILLE-LUCY	Lucy Loamy Sand
TERRELL	ORANGEBURG-FACEVILLE-LUCY	Orangeburg Loamy Sand
TERRELL	TIFTON-ALAPAHA-DOTHAN	Tifton Loamy Sand
WORTH	TIFTON-ALAPAHA-DOTHAN	Tifton Loamy Sand
WORTH	TIFTON-ALAPAHA-DOTHAN	Dothan Loamy Sand

4.2.6 Management Practices

The field management practices utilized as fixed parameters in crop model simulations were developed after consultation with agricultural specialists, researchers, and farmers

in the Lower Flint River basin. These practices are consistent with recommendations from agricultural extension agents in southwest Georgia.

Table 4.2. Field management practices utilized in crop simulations.

Crop	Cultivar	Planting Date (DOY)	Planting Density (plants/m^2)	Row Spacing (cm)	Planting Depth (cm)
Corn	PIO 31G98	74	7	90	5
Cotton	Deltapine 555 BG/RR	136	11	80	3
Peanut	Georgia Green	121	13	85	5

4.2.7 Regional Irrigation Strategies

The farmer's decision to irrigate is mimicked with the MST algorithm by simulating water applications during the crop season when daily plant water stress (i.e. [plant water uptake] / [potential transpiration]) exceeds a threshold MST value. While MST values may theoretically range from zero (i.e. high stress) to one (i.e. no stress), the box plot shown in Figure 4.20 reveals that the central tendency amongst randomly sampled irrigated fields in the Lower Flint River basin is approximately 0.77. MST values and irrigation demand are shown for several counties in Figures 4.21 - 4.44.

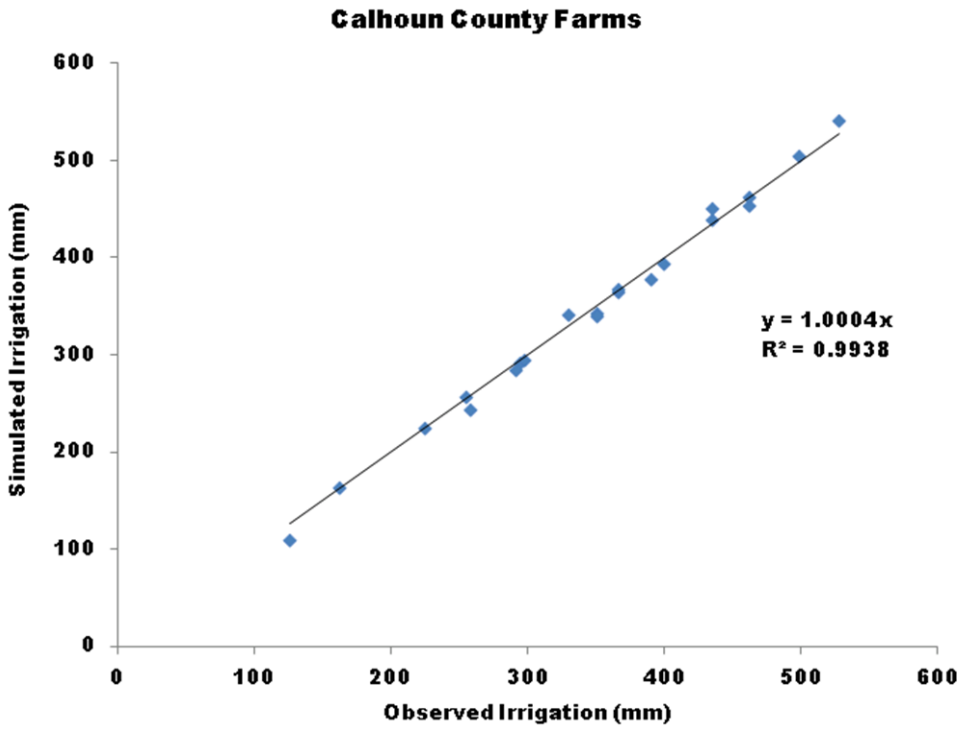

Figure 4.9. Simulated and measured irrigation demand at Calhoun County farms.

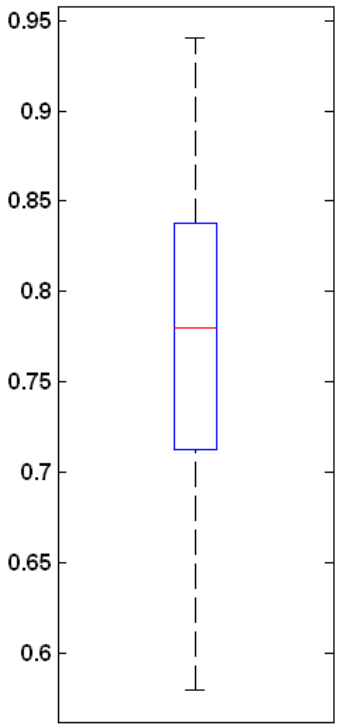

Figure 4.10. Box plot of MST values associated with Calhoun County.

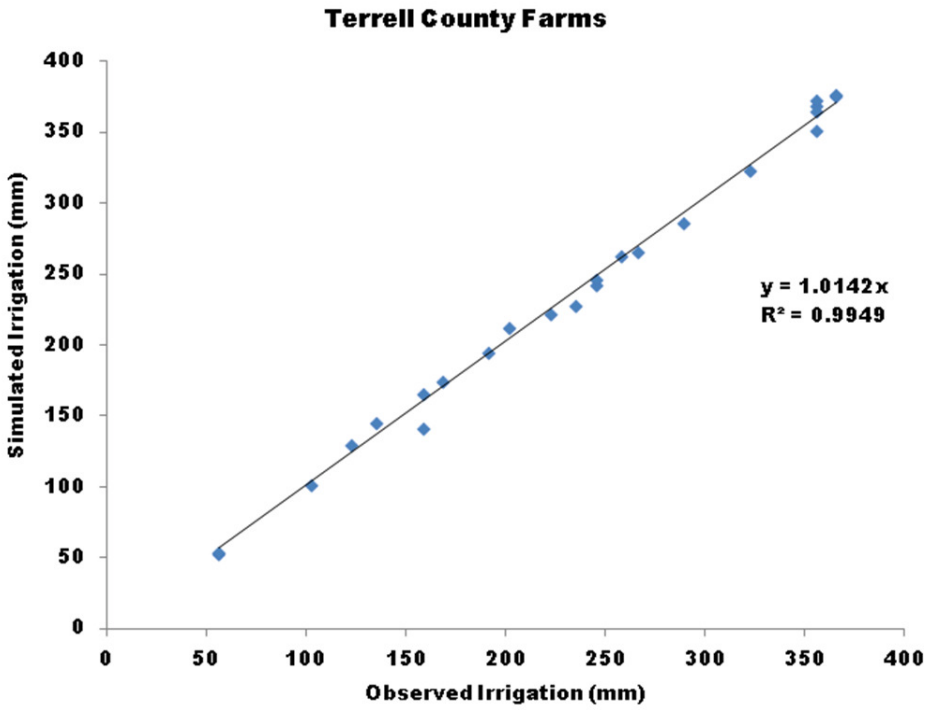

Figure 4.11. Simulated and measured irrigation demand at Terrell County farms.

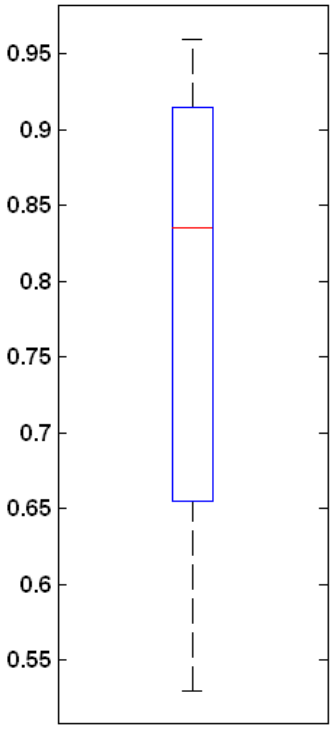

Figure 4.12. Box plot of MST values associated with Terrell County.

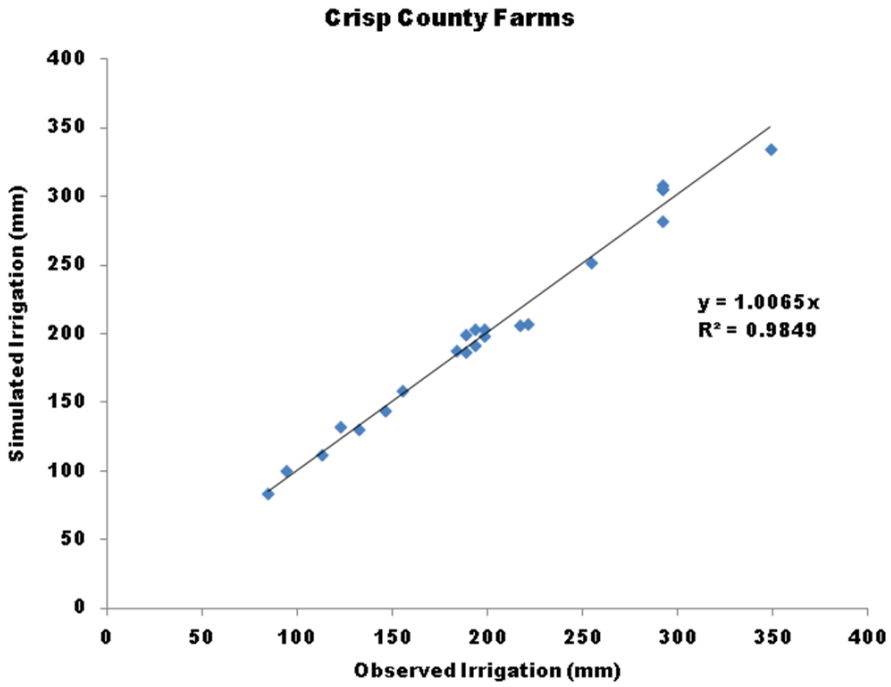

Figure 4.13. Simulated and measured irrigation demand at Crisp County farms.

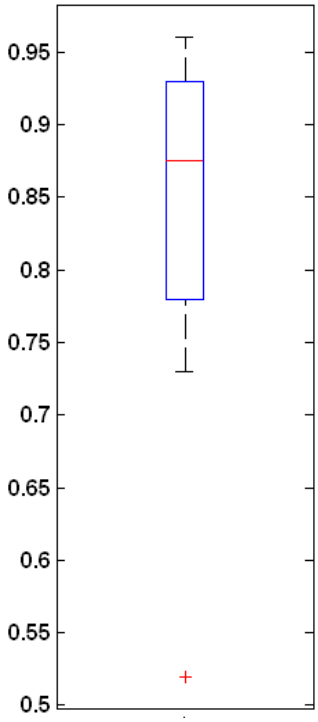

Figure 4.14. Box plot of MST values associated with Crisp County.

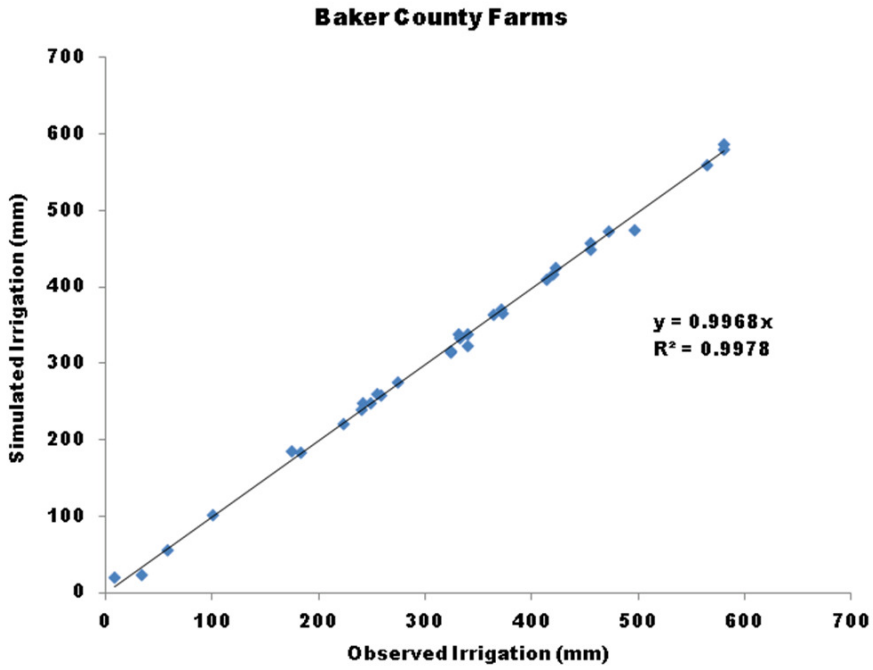

Figure 4.15. Simulated and measured irrigation demand at Baker County farms.

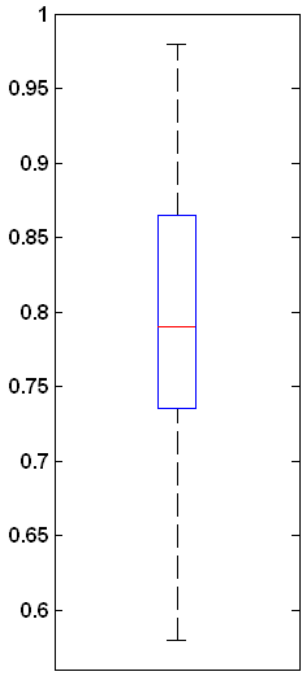

Figure 4.16. Box plot of MST values associated with Baker County.

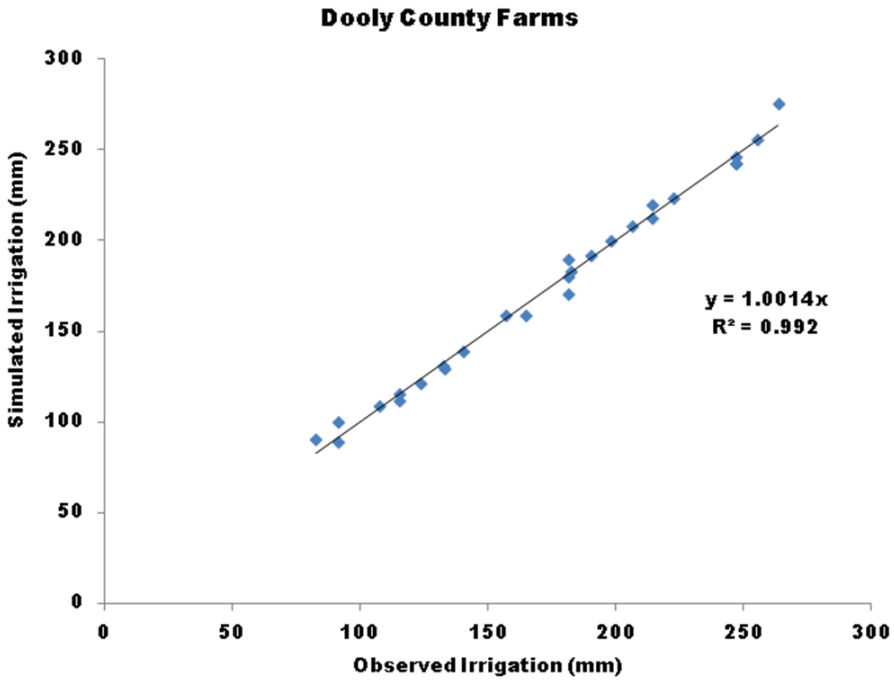

Figure 4.17. Simulated and measured irrigation demand at Dooly County farms.

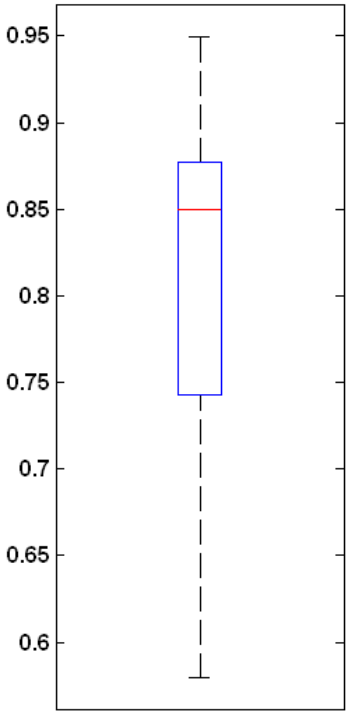

Figure 4.18. Box plot of MST values associated with Dooly County.

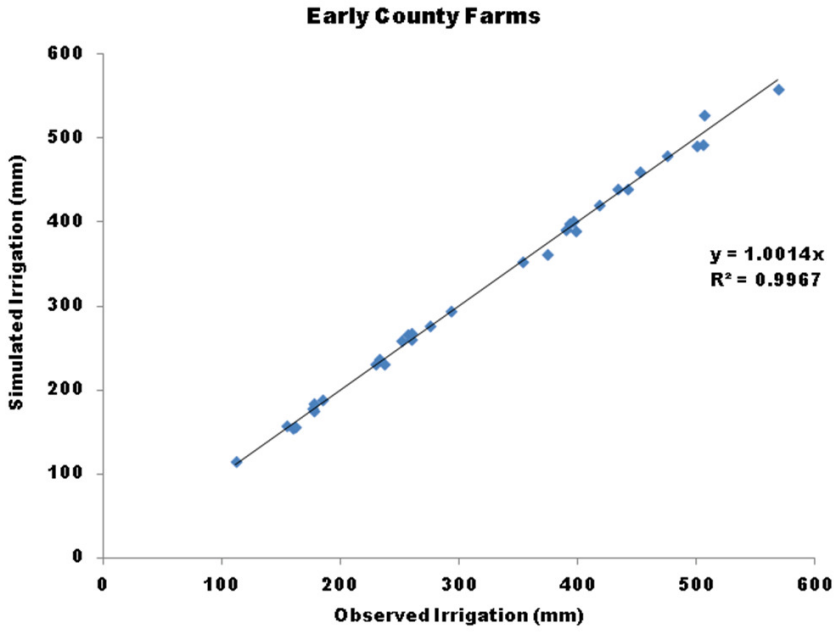

Figure 4.19. Simulated and measured irrigation demand at Early County farms.

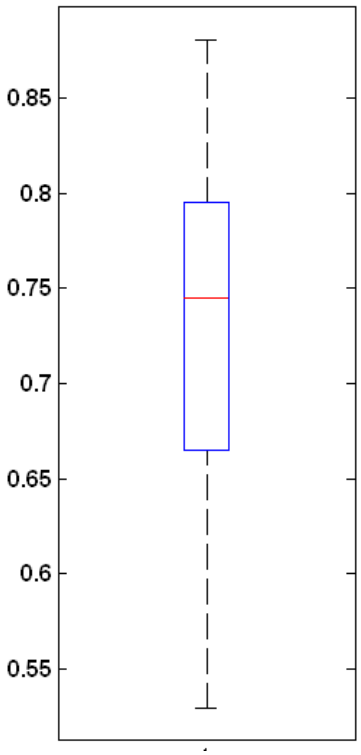

Figure 4.20. Box plot of MST values associated with Early County.

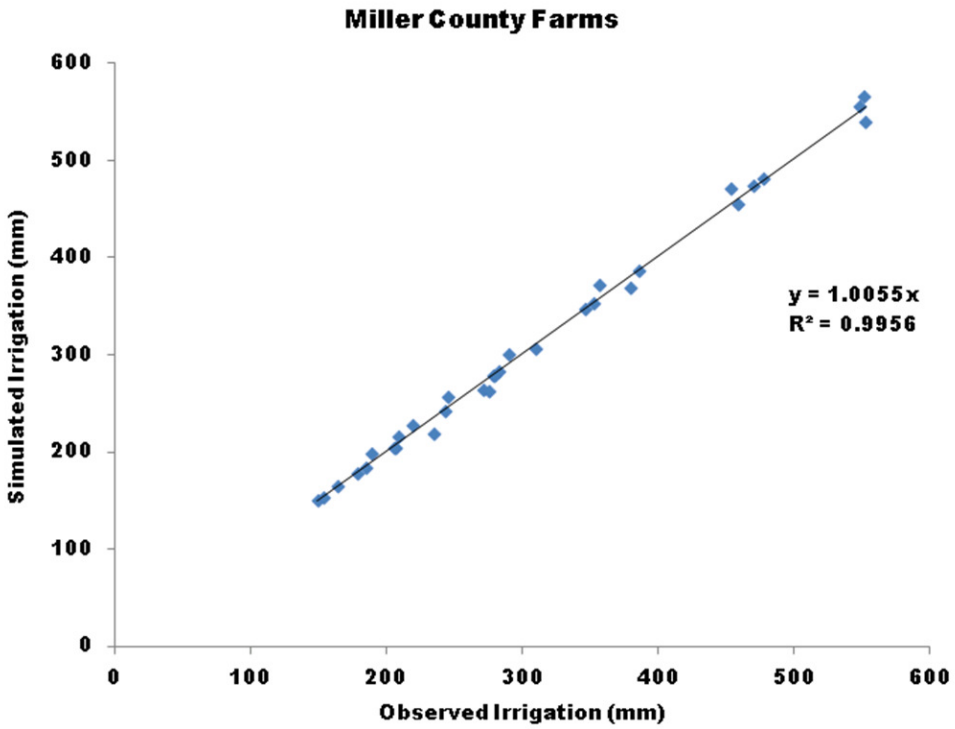

Figure 4.21. Simulated and measured irrigation demand at Miller County farms.

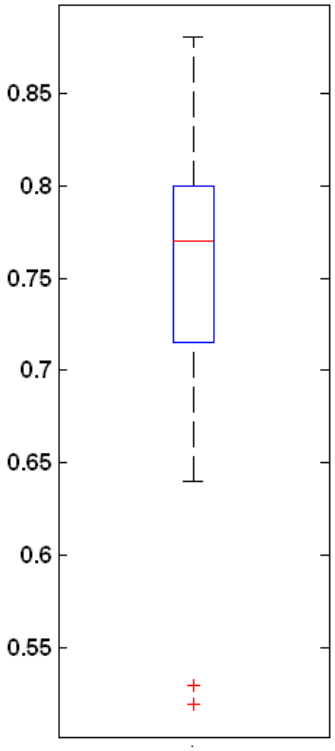

Figure 4.22. Box plot of MST values associated with Miller County.

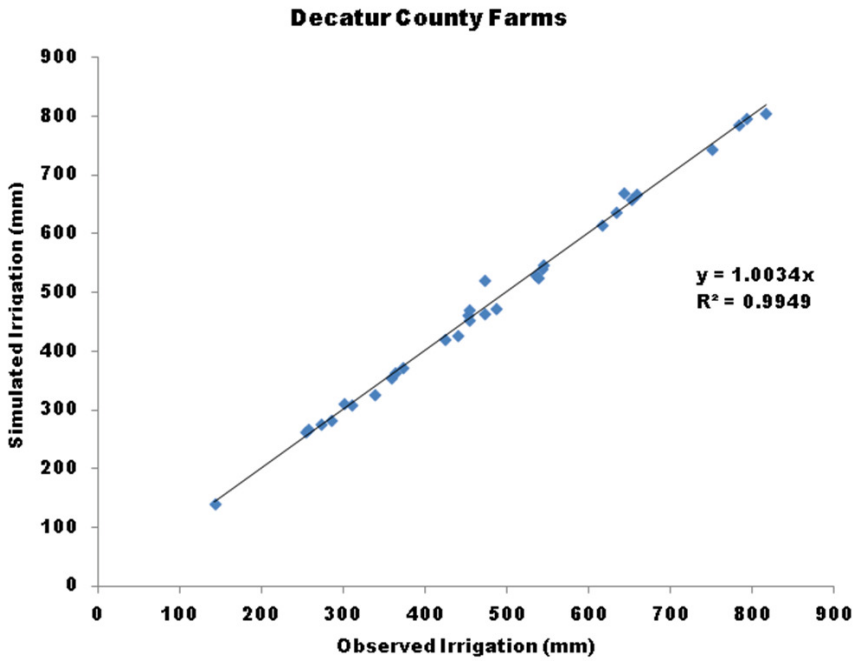

Figure 4.23. Simulated and measured irrigation demand at Decatur County farms.

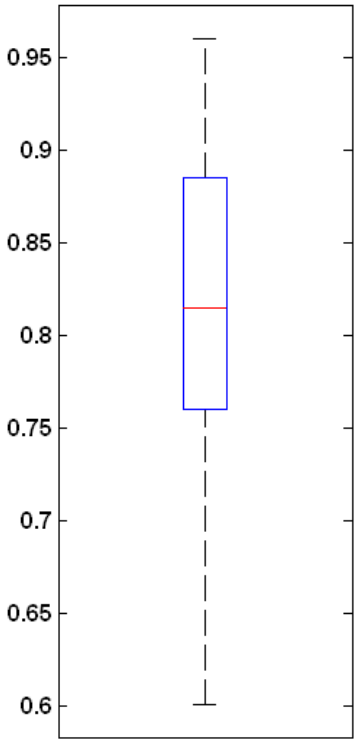

Figure 4.24. Box plot of MST values associated with Decatur County.

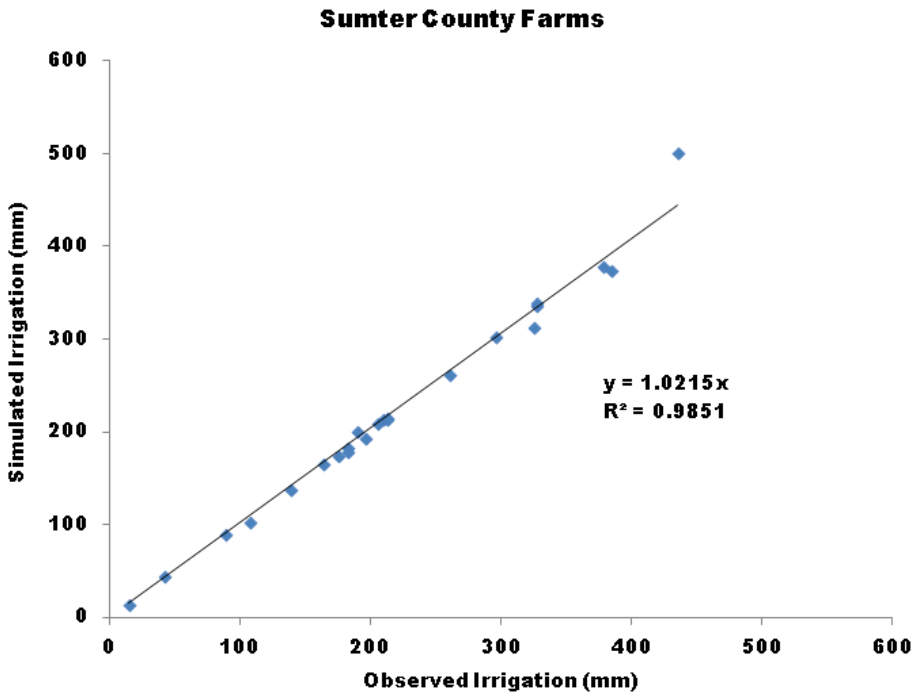

Figure 4.25. Simulated and measured irrigation demand at Sumter County farms.

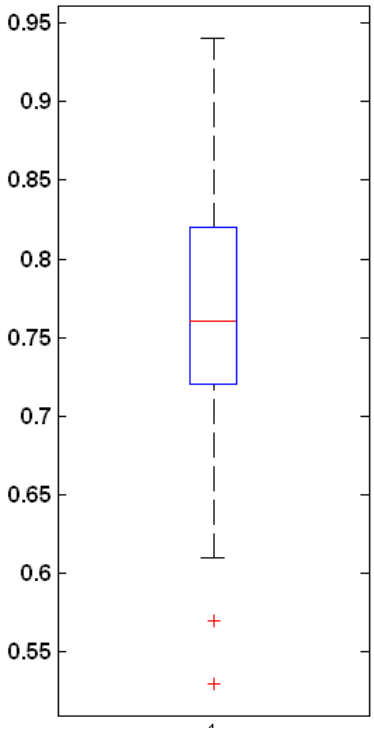

Figure 4.26. Box plot of MST values associated with Sumter County.

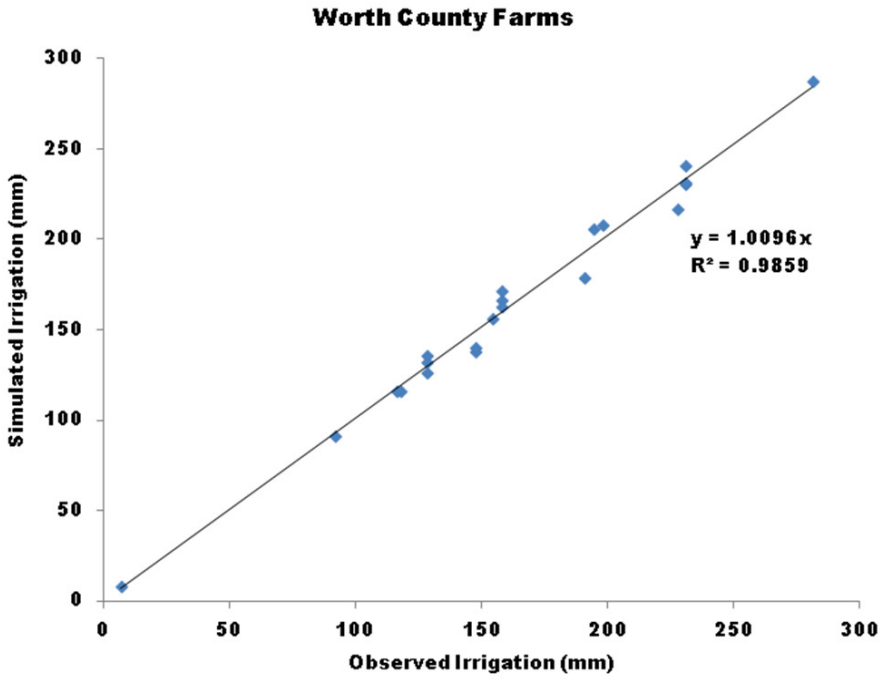

Figure 4.27. Simulated and measured irrigation demand at Worth County farms.

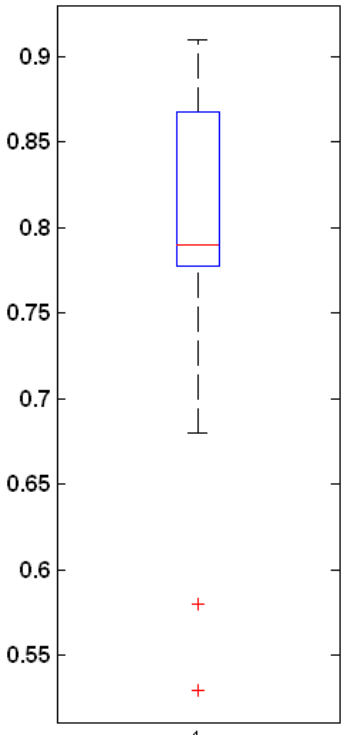

Figure 4.28. Box plot of MST values associated with Worth County.

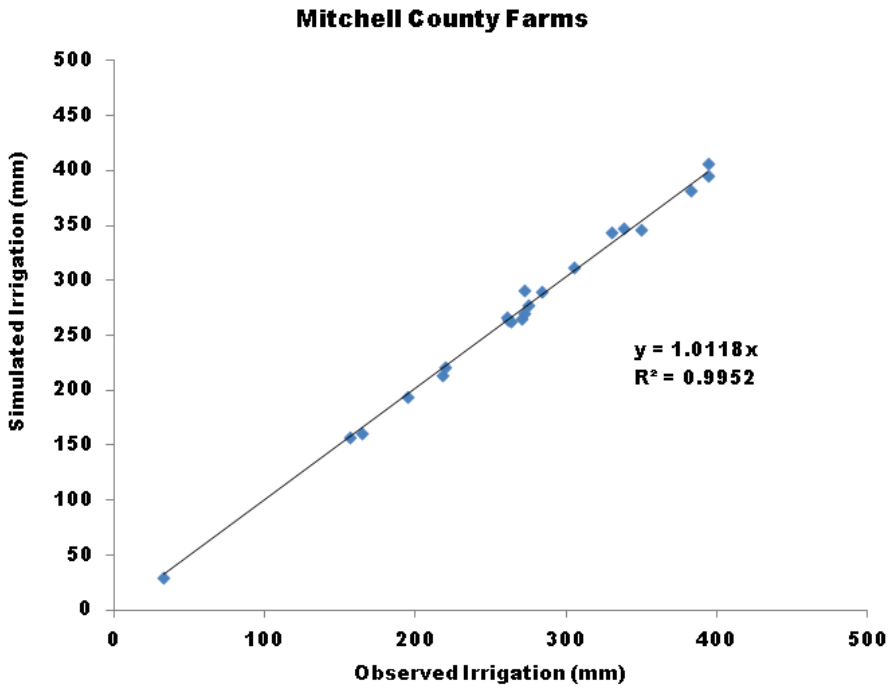

Figure 4.29. Simulated and measured irrigation demand at Mitchell County farms.

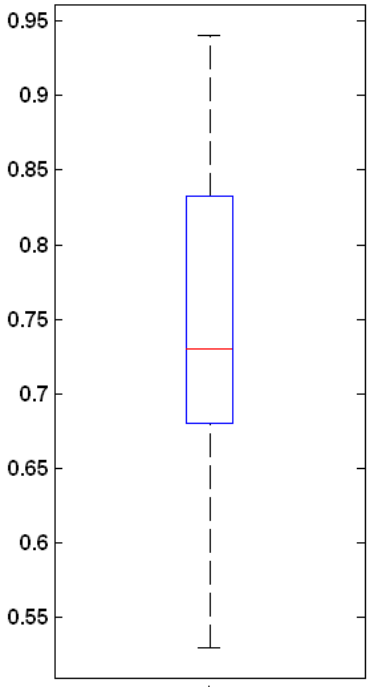

Figure 4.30. Box plot of MST values associated with Mitchell County.

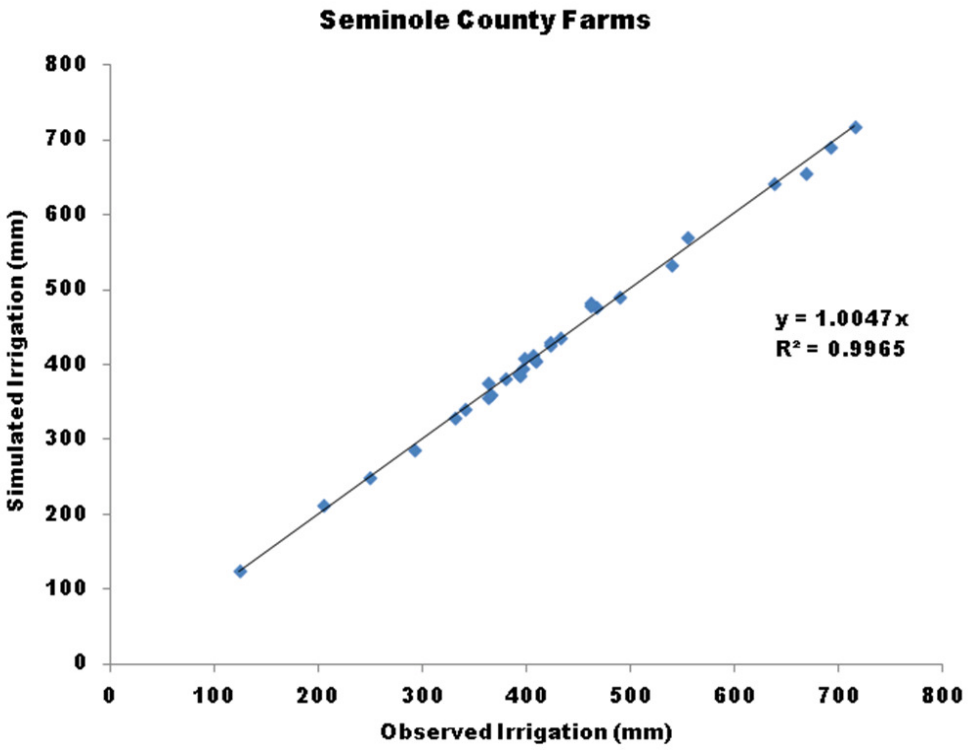

Figure 4.31. Simulated and measured irrigation demand at Seminole County farms.

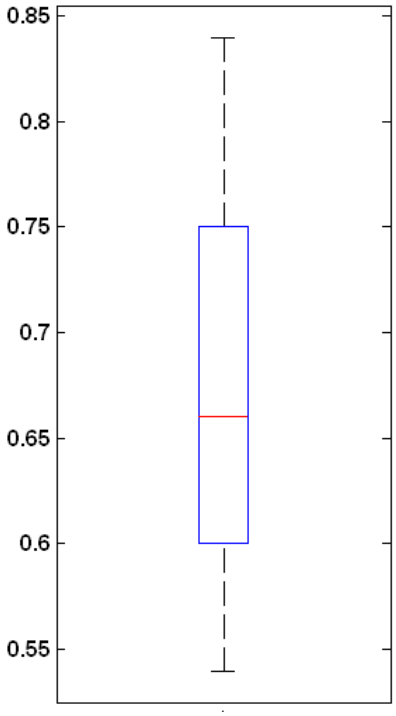

Figure 4.32. Box plot of MST values associated with Seminole County.

4.3 Historical Irrigation Water Demand Assessment

Historical assessments of agricultural water demand are prerequisite for the climate change assessments that will be discussed in chapter five. In the remaining sections, the approach utilized for characterizing regional frequency distributions of irrigation demand is presented as well as an evaluation of the irrigation strategies discussed in section 4.2.

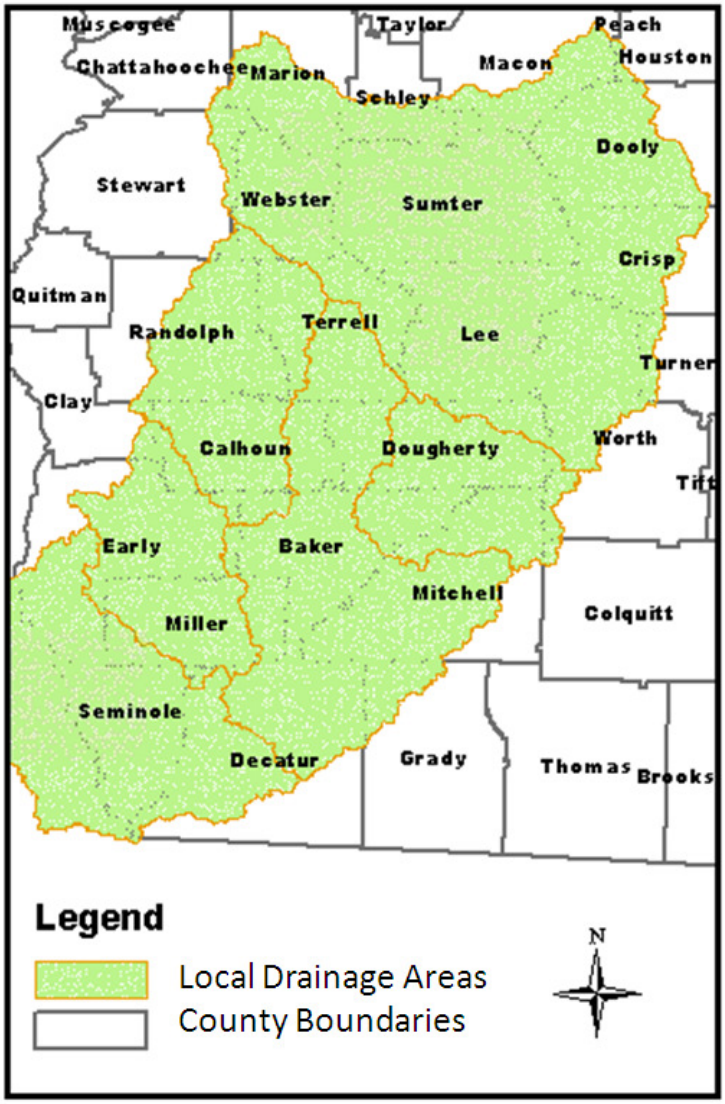

Figure 4.33. Local drainage areas and county boundaries in the Lower Flint River basin.

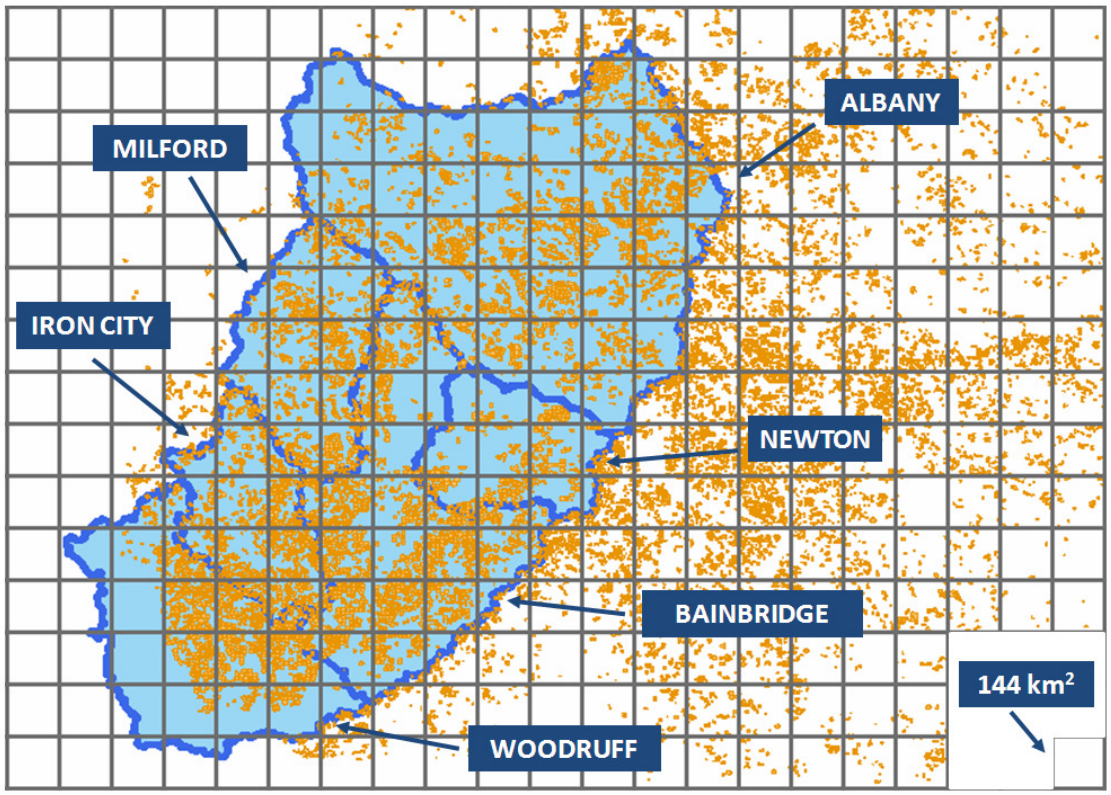

Figure 4.34. Schematic of irrigated acreage in Southwest Georgia and local drainage areas (LDAs) in the Lower Flint River basin: Albany, Bainbridge, Iron City, Milford, Newton, and Woodruff. The grid mesh associated with historical precipitation and temperature data is also shown (Hook et al., 2010).

4.3.1 Weather Data

The model-derived dataset of daily precipitation and temperature (minimum and maximum) developed by the University of Washington's Surface Water Modeling group is utilized for the historical assessment. The dataset spans the period (1950-2010) and has a 3-hr time step with a spatial resolution of 1/8 degree. The dataset was developed by forcing a macroscale (i.e. > 10 km) hydrological model, the variable infiltration capacity (VIC) model (Liang et al., 1994), with observed meteorological data. Data inputs for the

VIC model are derived from the National Oceanic and Atmospheric Administration (NOAA) Cooperative Observer (Co-op) network as well as the parameter-elevation regressions on independent slopes (PRISM) model (Daly et al., 1994). The VIC model balances both surface energy and water at each time step over all grid cells (Maurer et al., 2002). The grid mesh is shown along with local drainage areas and irrigated area in southwest Georgia in Figure 4.46.

Daily solar radiation data is utilized from the National Renewable Energy Laboratory (NREL, 2007) National Solar Radiation Database (NSRDB). The 1991–2005 NSRDB contains hourly solar radiation (including global, direct, and diffuse) and meteorological data for 1,454stations. This update builds on the1961–1990 NSRDB, which contains data for 239 stations.

Atmospheric carbon dioxide concentration data is obtained from NOAA. The data utilized is shown in Figure 4.47.

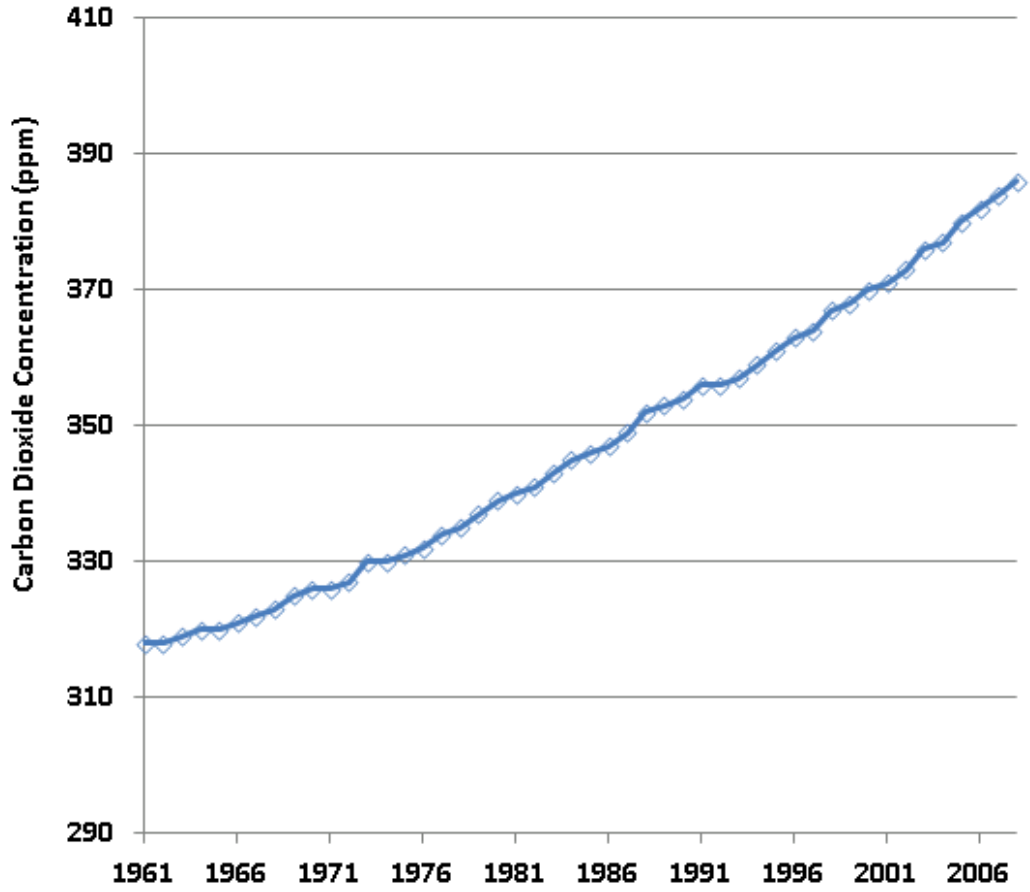

Figure 4.35. Historical atmospheric carbon dioxide concentration (NOAA, 2012).

4.3.2 Soils Data

The soils data has been previously described in section 4.2.5.

4.3.3 Assessment Approach

Historical assessments of agricultural water demand are conducted for local drainage areas in the Lower Flint River basin. The county-scale irrigation strategies discussed in section 4.2 are utilized along with scaling factors that were derived for each county. Metered sites utilized to develop the irrigation strategies are associated with row crops that may be less water intensive(i.e. applied water/acre) than other crops (e.g. vegetables)

that may contribute significant irrigation demand in some counties. Thus, county specific-factors were developed by taking the ratio of the irrigation depth of sampled sites and the irrigation depth of all metered sites within each county (see Table 4.2).

Table 4.3. County-specific scaling factors

County	Scaling Factor
Baker	0.95
Calhoun	0.86
Crisp	0.74
Decatur	0.95
Dooly	0.82
Early	0.97
Miller	0.76
Mitchell	0.6
Worth	0.49
Seminole	1
Sumter	0.82
Terrell	0.86

Each grid cell is associated with a county in the Lower Flint River basin. Each year a crop-MST combination is randomly sampled from the collection of irrigation strategies previously determined for the county of interest. This crop-MST combination is the irrigation strategy that drives irrigation scheduling when the DSSAT model is run. After weighting the crop simulation outputs based on the representative soil profiles, the scaling factor is applied to estimate irrigation depth for the grid cell. Finally, model outputs for all grid cells within a local drainage area are weighted equally to obtain historical irrigation demand estimates.

4.3.4 Model Evaluation

The results show that median historical irrigation demand varies between about six and ten inches. There is significant interannual variability in demand though. The highest demands are associated with the drought periods in the 1980s (see Figure 4.49)

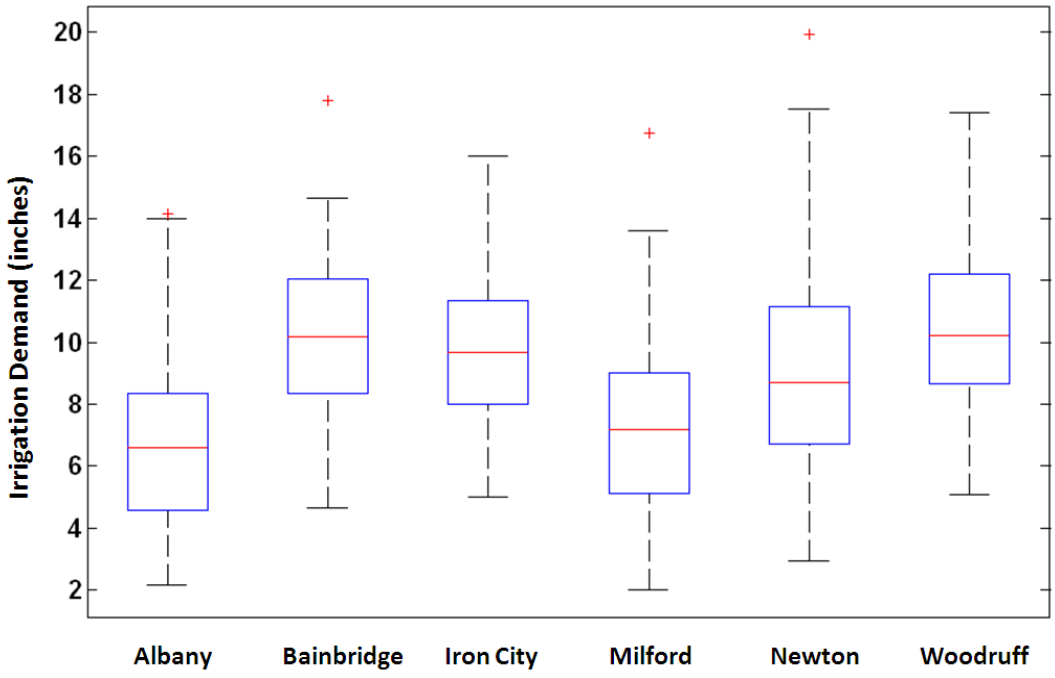

Figure 4.36. Box plots of historical irrigation demand for local drainage areas in the Lower Flint River basin.

A comparison with EPD estimates of agricultural water demand shows the value of estimating irrigation demand with this novel approach. While EPD estimated irrigation depth takes on only two values, the irrigation depths estimated with the approach described above display the interannual variability that is expected as weather and soil conditions vary from year to year.

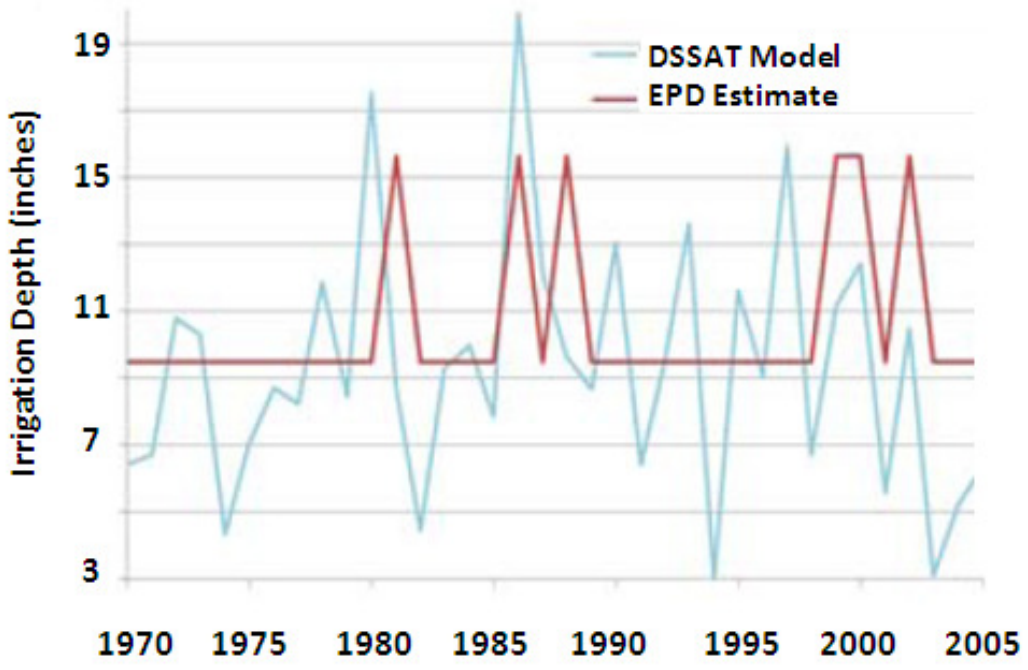

Figure 4.37. Comparison between different demand estimation approaches for the Newton local drainage area (GWRI, 2012).

A negative correlation may be observed between annual rainfall and irrigation depths. However, for all the drainage areas, the negative correlation increases when seasonal (i.e. May - Sept.) rainfall is considered instead of annual rainfall (see Table 4.3).

Table 4.4. Correlation between historical irrigation demand and precipitation.

Local Drainage Area	Annual Precipitation Correlation	Seasonal Precipitation Correlation
Albany	-0.5586	-0.729
Bainbridge	-0.5072	-0.7945
Iron City	-0.495	-0.7319
Milford	-0.6713	-0.7168
Newton	-0.4545	-0.5213
Woodruff	-0.411	-0.4578

4.3.5 Summary

In this chapter a methodology is developed for identifying irrigation strategies with field scale agricultural water use and management data. Historical projections of regional water demand in the Lower Flint River basin are presented that utilize these crop management strategies. This novel approach utilizes agricultural water use data as well crop simulation models to estimate irrigation strategies and subsequently, regional water demand. The irrigation demand projections are negatively correlated with seasonal precipitation as expected. Furthermore, simulated irrigation demands demonstrate greater interannual variability than methods relying on crop coefficient methods that are often used in practice. The uncertainty associated with the projections presented in this chapter is described in chapter three. In chapter five, the methodology presented in this chapter is applied to assessments of agricultural water demand under climate change.

There is some uncertainty that is not addressed regarding permitted sites that are greater than one hundred acres in area. These larger areas may have differing water use efficiency than sites with less acreage and this research does not fully address how water is delivered to large fields or multiple fields with one source of water. In order to evaluate the additional uncertainty associated with large irrigated fields and sites with multiple fields, an adaptive approach must be developed that relies on the distribution of field sizes and associated irrigation technologies. Future work may include an assessment of irrigated fields greater than one hundred acres and permitted sites that are associated with multiple fields.

While the FAO-56 approach and other crop coefficient techniques are still used by researchers to assess irrigation requirements, better results are generally expected by using crop models that operate on a daily time step for assessments of agricultural water demand. Physiological crop models account for the fact crops respond not only to monthly or seasonal conditions, but also to the dynamics of weather events (Allen et al., 1998; Suleiman et al., 2007).

For projections of irrigation demand under climate change, crop coefficients developed with historical data may not be appropriate for assessments under future climate conditions. The approach presented in this chapter utilizes actual regional irrigation data to develop irrigation strategies that are applied with crop simulation models under historical and future climate conditions. The crop simulation models also are advantageous in that they allow for varying irrigation practices to be taken into account in the modeling framework.

Chapter 5: Projections of Future Agricultural Water Demand

In Chapter 3, the aggregation error associated with simulated irrigation demand is characterized. In Chapter 4, regional irrigation strategies are presented and applied with crop simulation models to assess historical irrigation demand in six local drainage areas (LDAs) in Georgia. In this chapter, projections of regional agricultural demand in the Lower Flint River basin are presented.

5.1 Introduction

The United Nations Intergovernmental Panel on Climate Change (IPCC, 2007) has reported that "warming of the climate system in recent decades is unequivocal". Furthermore, the large-scale hydrological cycle may be linked to the observed warming during the 20th century. The area of land on Earth classified as "very dry" has more than doubled over the last four decades and the "proportion of land surface in extreme drought at any one time is projected to increase". Regionally, large scale changes in agricultural water demand are expected (IPCC, 2007).

The Apalachicola-Chattahoochee-Flint (ACF) River basin has historically been vulnerable to droughts that are associated with low lake levels and significant reductions in river flows. Thus, potential changes in the climate of the Southeast U.S. could have significant impacts on the agricultural sector and agricultural water demand (Hatch et al., 1999). Irrigation water use is estimated to account for 90% of water used during the April-September growing season in the Flint River basin (EPD, 2009). As a result, water

demand management is now recognized as a prudent compliment to water supply management for integrated and sustainable water resources management. Agricultural water use data and agricultural water demand projections are valuable resources as planners and policymakers seek to enhance conservation efforts and develop water management strategies that increase the ability of regional water resources systems to support society during periods of low water supply (Kimaite, 2011).

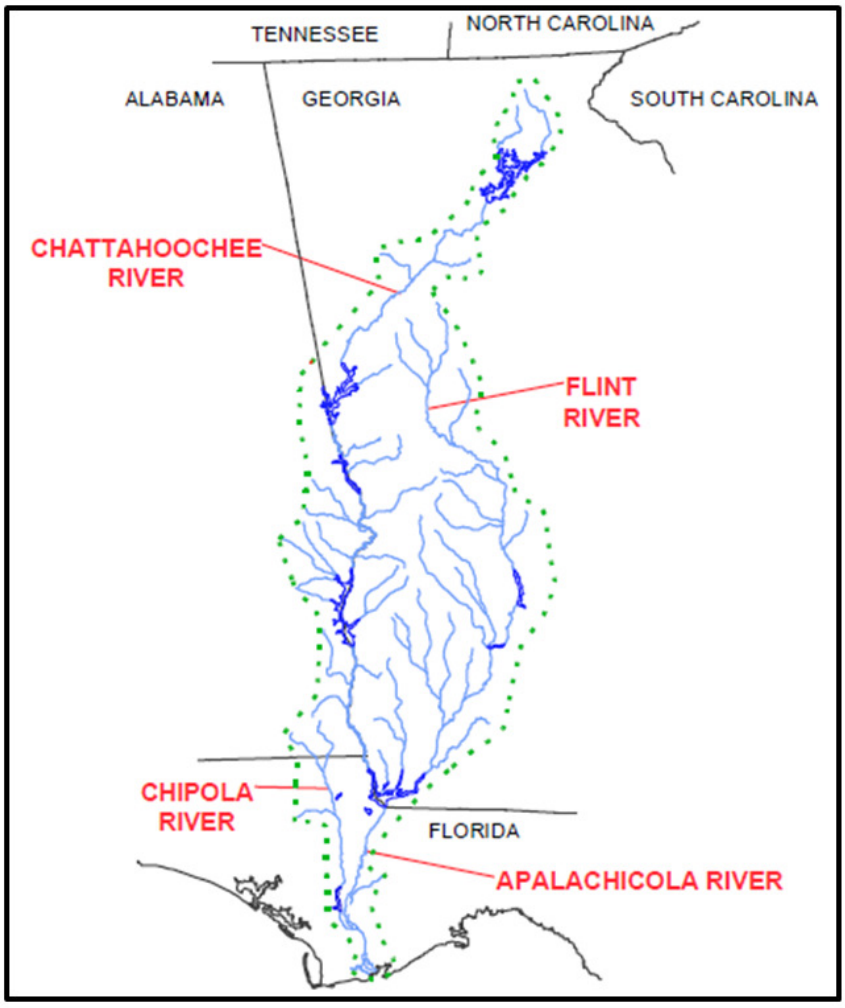

Figure 5.1. Map of the ACF basin (USACE, 1997).

5.2 Methodology

Climate change impact studies typically identify a baseline scenario associated with current or recent conditions that allows for the projection of future impact. The model outcomes of interest from the baseline scenario are compared with outcomes derived from scenarios of future climate in order to assess climate change impacts. There is recognized ignorance underlying long range projections of irrigation demand due to volatility in agricultural markets, technological innovations, and genetic development that increases water use efficiency (Bramblett, 1995). As opposed to the impossible task of identifying a "most likely" climate scenario, exploring a range of plausible future conditions with multiple climate scenarios allows for system resilience (Daniels et al., 2012).

Projections of future climate are uncertain due to (A) the uncertainty in forecasts of future anthropogenic and natural forcings, (B) the imperfection of climate models, and (C) the internal variability of the climate system. However, projections of future climate provide valuable information about the range of future conditions associated with a changing climate. In this work, a baseline period of 1986-2005 is utilized such that climate change is expressed as a change with respect to a recent period of history. The future conditions (i.e. "time slices") evaluated consist of twenty year time periods (2046-2065 and 2081-2100) that allow for some interannual-to-interdecadal variability and relatively monotonic anthropogenically induced forcing trends (Horton et al., 2011).

5.2.1 Historical conditions

The model-derived dataset of daily precipitation and temperature (minimum and maximum) developed by the University of Washington's Surface Water Modeling group is utilized for the historical assessment. The dataset spans the period (1950-2010) and has a 3-hr time step with a spatial resolution of 1/8 degree. Daily solar radiation data is utilized from the National Renewable Energy Laboratory (NREL, 2007) National Solar Radiation Database (NSRDB). These datasets are described in more detail in Chapter 4 (see Section 4.3.1).

5.2.2 Carbon emission scenarios

Scenarios allow all inputs to evolve in time in a contextually consistent manner so that model outcomes of interest can be evaluated that correspond to plausible manifestations of reality. Scenarios are postulated sequences of events that help policymakers focus attention on causality, impacts, and tradeoffs. While scenarios alone are not an adequate means of addressing model outcome uncertainty, scenario analysis is quite popular in the climate change impacts, adaptations, and vulnerability (IAV) research community (Katz, 2002).

There are four IPCC storylines (i.e. carbon emission scenarios) that form the basis of most studies on climate change impacts on water resources. The A1 and B1 scenarios assume that the world economy is dominated by global trade and alliances, while the A2 and B2 scenarios assume less globalization and cooperative agreements. In this work irrigation demand projections from two time slices (2046-2065 and 2081-2100) and two

emission scenarios (A1B and A2) are compared with historical demand projections (see Figure 5.2).

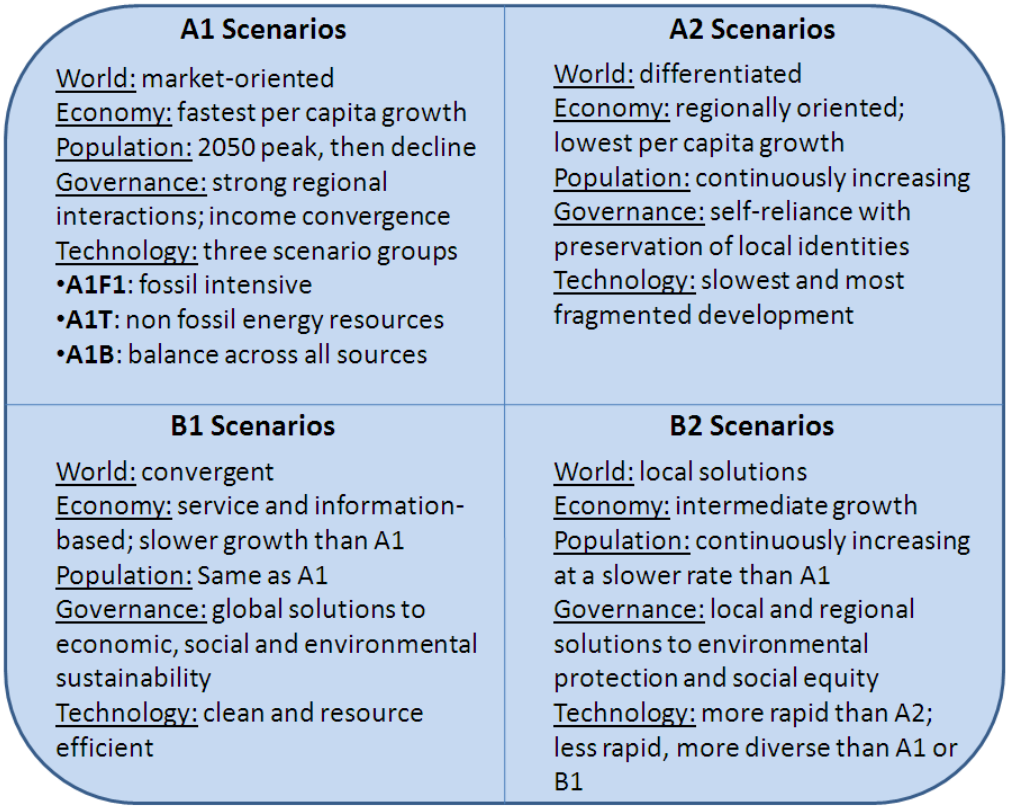

Figure 5.2. Summary characteristics of the four IPCC Special Report on Emissions Scenarios (SRES; adapted from IPCC, 2007).

5.2.3 Future conditions

Projections of future climate are based on six available GCM configurations with outputs available in the World Climate Research Programme (WRCP) Coupled Model Intercomparison Project, phase 3, (CMIP3) multimodel dataset (Meehl et al., 2007). The six GCMs and two emission scenarios (i.e. A1B and A2) considered combine to produce

12 output sets. These output sets are utilized as climatic forcing in order to evaluate impacts common to a range of possible future conditions.

Model Abbreviation	Modeling Group
CCCMA	Canadian Centre for Modeling & Analysis, Canada
CNRM	Centre National de Recherches Météorologiques, France
GFDL	Geophysical Fluid Dynamics Laboratory, USA
IPSL	Institut Pierre Simon Laplace, France
MIROC3	Center for Climate System Research, Japan
MIUB	Meteorological Institute of the University of Bonn, Germany

Figure 5.3. Description of GCMs (Jiang and Yang, 2012).

The bias correction and constructed analogues (BCCA) method is utilized to obtain daily climatic forcing of temperature and precipitation (Hidalgo et al., 2008). The method utilizes a library of previously observed daily weather patterns to construct an analogue for a course scale GCM output of interest. The weather patterns for several days serve as predictors that are combined to construct the analogues. The method is used to downscale GCM output to obtain daily temperature and precipitation on a 1/8 x 1/8 degree resolution grid. Daily solar radiation was derived from the downscaled daily air temperatures and rainfall using the Weather Generator for Solar Radiation (WGENR)

(Hodges et al., 1985), as modified and evaluated by Garcia y Garcia and Hoogenboom (2005) and Garcia y Garcia et al. (2008).

5.2.4 Demand projections

In this work, the Decision Support System for Agrotechnology Transfer (DSSAT) suite of crop models is utilized to estimate regional irrigation demand. Historical and future projections of agricultural water demand are informed by regional irrigation strategies that are represented with the moisture stress threshold (MST) algorithm (see Section 4.3.3). The farmer's decision to irrigate (i.e. the irrigation strategy) is represented with the MST algorithm by simulating water applications during the crop season when daily plant water stress (i.e. [plant water uptake] / [potential transpiration]) exceeds a threshold MST value (see Sections 4.2.2 and 4.2.3). Soils data and field management practices are described in sections 4.2.5 and 4.2.6 respectively.

5.3 Regional Water Demand Assessments

In the appendix, box plots of historical and future projections of agricultural water demand are presented for the six local drainage areas (see Figure 5.4) that compose the Lower Flint River basin. Annual and monthly irrigation demand projections are presented for two future time slices (i.e. 2046-2065 and 2081-2100), two emission scenarios (i.e. A1B and A2) and six GCMs. A discussion of key findings and conclusions is presented in Section 5.3.1.

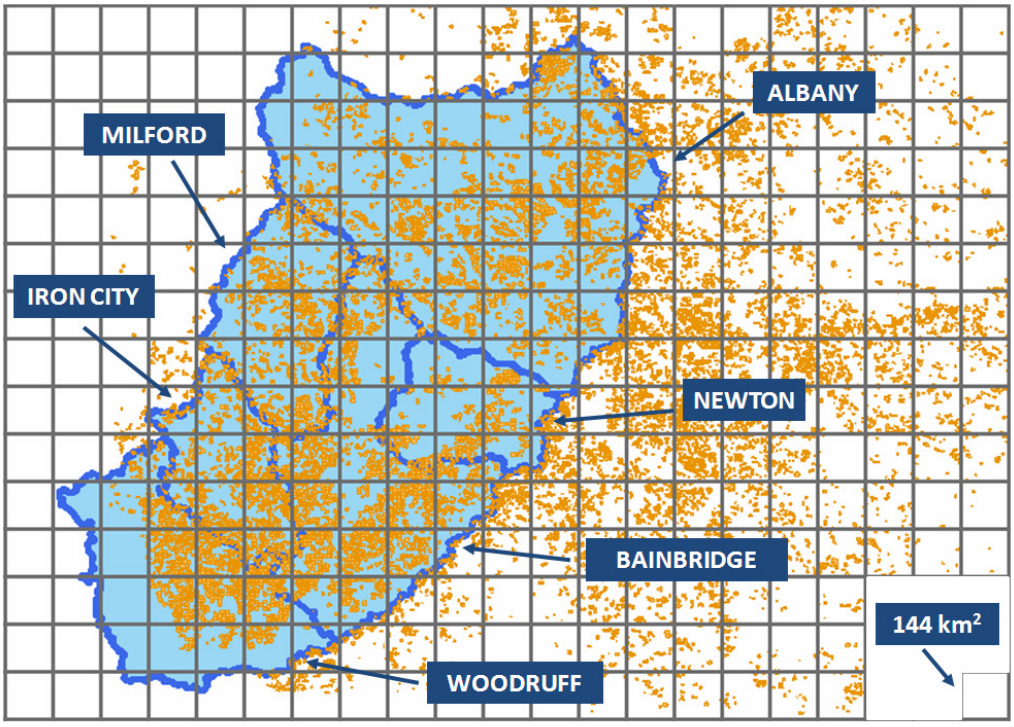

Figure 5.4. Schematic of irrigated acreage in Southwest Georgia and local drainage areas (LDAs) in the Lower Flint River basin: Albany, Bainbridge, Iron City, Milford, Newton, and Woodruff.

Table 5.1. Agricultural water demand expressed in inches (A1B Scenario, 2046-2065).

LDA	1986-2005 Historical	A1B Emission Scenario (2046 - 2065)							Relative Change
		GFDL	MIUB	IPSL	CCCMA	CNRM	MIROC3	GCM Avg	
Newton	8.99	11.16	4.42	8.45	8.96	8.49	16.61	9.68	7.7%
Milford	6.88	11.26	4.56	8.91	8.29	9.47	15.08	9.60	39.4%
Iron City	10.04	8.97	5.67	8.37	8.44	8.93	13.13	8.92	-11.2%
Bainbridge	10.07	11.88	5.48	9.17	8.68	9.15	15.49	9.98	-0.9%
Albany	6.27	10.47	4.58	8.70	8.91	9.47	15.43	9.59	53.0%
Woodruff	9.16	8.61	5.63	7.61	7.17	6.84	11.90	7.96	-13.1%

Table 5.2. Agricultural water demand expressed in inches (A1B Scenario, 2081-2100).

LDA	1986-2005 Historical	A1B Emission Scenario (2081 - 2100)							Relative Change
		GFDL	MIUB	IPSL	CCCMA	CNRM	MIROC3	GCM Avg	
Newton	8.99	9.00	5.76	9.20	7.53	9.92	17.48	9.81	9.2%
Milford	6.88	13.21	5.79	8.41	7.01	12.47	20.06	11.16	62.1%
Iron City	10.04	11.84	6.31	8.19	6.84	12.92	18.09	10.70	6.6%
Bainbridge	10.07	19.85	6.29	9.33	6.88	12.34	19.59	12.38	22.9%
Albany	6.27	13.84	5.73	8.85	7.16	12.94	20.06	11.43	82.3%
Woodruff	9.16	9.59	6.36	7.71	5.48	10.35	14.19	8.95	-2.3%

Table 5.3. Agricultural water demand expressed in inches (A2 Scenario, 2046-2065).

LDA	1986-2005 Historical	A2 Emission Scenario (2046 - 2065)							Relative Change
		GFDL	MIUB	IPSL	CCCMA	CNRM	MIROC3	GCM Avg	
Newton	8.99	14.05	5.02	8.53	6.89	12.86	20.68	11.34	26.2%
Milford	6.88	9.57	5.66	9.47	7.98	9.92	16.76	9.89	43.7%
Iron City	10.04	8.61	6.66	9.11	7.45	10.07	14.64	9.43	-6.1%
Bainbridge	10.07	9.84	6.37	9.72	8.45	9.81	16.71	10.15	0.8%
Albany	6.27	9.93	5.57	10.06	7.95	9.81	13.21	9.42	50.3%
Woodruff	9.16	7.76	5.80	8.09	6.28	8.01	11.75	7.95	-13.2%

Table 5.4. Agricultural water demand expressed in inches (A2 Scenario, 2081-2100).

LDA	1986-2005 Historical	A2 Emission Scenario (2081 - 2100)							Relative Change
		GFDL	MIUB	IPSL	CCCMA	CNRM	MIROC3	GCM Avg	
Newton	8.99	19.67	4.98	10.73	7.43	16.31	27.66	14.46	61.0%
Milford	6.88	17.40	5.10	11.09	8.17	15.98	24.40	13.69	98.9%
Iron City	10.04	16.24	6.42	10.19	8.35	15.12	22.46	13.13	30.8%
Bainbridge	10.07	18.09	6.03	10.73	8.69	16.22	25.26	14.17	40.7%
Albany	6.27	18.78	5.52	11.49	8.26	16.51	23.79	14.06	124.2%
Woodruff	9.16	13.09	5.66	7.88	6.46	11.94	18.31	10.56	15.3%

5.3.1 Discussion

There is an emphasis in this work on assessing the impacts of climate change on agricultural water demand with current irrigation technologies and management practices. The results of this work provide valuable information regarding the policy instruments, technological developments, and irrigation efficiency gains that are needed to address potential increases in agricultural water demand under climate change in the Southeast U.S.

The approach for estimating irrigation demand presented in this work is novel in that it utilizes actual metered irrigation data to develop irrigation strategies to estimate regional irrigation demand under historical and future climate conditions. The development of the irrigation strategies incorporated the errors associated with model structure and aggregated inputs at a spatial scale up to one hundred acres. However, it should be noted that GCM outputs have uncertainty at spatial scales greater than one hundred acres.

While results presented in section 5.3 suggest that annual irrigation demand will increase over the next century in the Lower Flint River basin, the magnitude and timing of demand increases varies depending on the climate change scenario. In general, the most significant climate change impacts may be associated with the A2 scenario and the 2081-2100 time slice. However, in some instances the annual irrigation demand associated with the 2046-2065 time slice doe not vary much between the two emission scenarios. The GFDL and MIROC3 models typically are associated with the largest projections of median agricultural demands. On the other hand, the MIUB model is often associated

with median demands that are less than or not significantly different than historical demands.

The monthly irrigation demands show the greatest increases during the peak crop water demand months of July and August. The largest changes in projected monthly irrigation demand are generally associated with the 2081-2100 time slices and the A2 emission scenarios. However, some significant increases in irrigation demand are also observed in June and September for some scenarios. Overall, there is minimal projected change in May irrigation demands.

Chapter 6: Conclusions and Recommendations

6.1 Summary of contributions and key findings

Although Georgia is typically considered to be a state with plentiful water resources due to average annual rainfall exceeding that of many other parts of the United States, population growth, rapid urbanization, and the competing demands placed on water resources by the municipal, industrial, agricultural, and ecological sectors make water resources management and planning a significant challenge for planners and policy makers. In addition, agricultural water use represents the primary consumptive use of water with over eighty percent of agricultural water demand occurring between the months of May and August. Furthermore, in dry years with rainfall totals significantly below average and reduced streamflow, agricultural water demands are higher. Thus, this research presents an important contribution towards improved water resources management and planning by presenting a new approach for estimating agricultural water demand under historical and future climate conditions.

This research uses a novel approach to estimate regional agricultural water demand with a consistent framework that may be applied to historic as well as future demand projections. The study utilizes (a) actual measured agricultural water use along with (b) geostatistical techniques, (c) crop simulation models, and (d) general circulation models (GCMs) to assess irrigation demand and the uncertainty associated with demand projections at spatial scales relevant to water resources management. The study has several important scientific contributions:

- Calibration of geostatistical models that describe the spatial variability of daily precipitation and soil water properties in the Lower Flint River basin (Chapter 3).
- Characterization of the uncertainty associated with crop simulation model outputs that utilize aggregated soil and climate data; development of a relationship between the standard deviation of model error and spatial scale (Chapter 3).
- Development and evaluation of procedures for representing regional irrigation strategies with the moisture stress threshold (MST) algorithm and metered irrigation data. (Chapter 4).
- Assessment of historical agricultural water demand in six local drainage areas (LDAs) in Southwest Georgia; comparison with existing approaches (Chapter 4).
- Assessment of future agricultural demand in the Lower Flint River basin under climate change with two emission scenarios and six GCMs (Chapter 5).

The main findings of the assessment are summarized below:

- The spatial variability of daily rainfall in Southwest Georgia may be represented with exponential variogram models with ranges that can exceed 200 km. On the other hand, available water holding capacity was found to have a range less than 20 km.
- The standard deviation of aggregation error is estimated to be approximately 23 mm or 10-15% of the spatial mean at a scale of 1/8 degree (i.e. 144 km^2). A logarithmic relationship is developed that is consistent with the exponential variogram models used to represent the spatial variability of soils and climate.

- Regional irrigation strategies are well represented with the MST algorithm, metered annual agricultural water use, and crop management data. The novel approach developed may be applied to other locations in the world as agricultural metering programs become more common.
- Crop coefficient approaches applied at the regional scale to estimate agricultural water demand lack the interannual variability observed with this novel approach. Crop simulation models are useful tools for representing the intra-annual and interannual variability of regional irrigation demand.
- GCMs indicate a range of possible futures that include the possibility of relatively small changes in irrigation demand in the Lower Flint River basin. However, most of the GCMs utilized in this work project significant increases in median water demand towards the end of this century. In particular, results suggest that peak agricultural water demands in July and August may increase significantly.

6.2 Recommendations for Future Work

The outcomes of this research create opportunities for future work related to (1) assessment of surface water and groundwater resources impacts, (2) evaluation of regional water demand in adjacent river basins, and (3) assessment of water management strategies during drought conditions. The following specific recommendations are made regarding future research areas to expand this work:

1. Consideration of farmer adaptation – This research focused on row crops (i.e. maize, peanut, and cotton) and held field management practices constant under future conditions. Although this approach allows for a transparent comparison between historical and future irrigation demands, farmers are likely to alter some crop management practices in a changing climate. This work may be improved by allowing planting dates to change based on soil moisture conditions and projected climatic trends.
2. Estimation of surface water and groundwater demand – Annual and monthly demand is assessed under current and future climates in this work. These assessments would be more valuable to water resources managers if demand was partitioned into surface water and groundwater demand. A significant amount of data regarding water sources utilized by irrigators has been collected in recent years and this information may allow for surface water and groundwater demand estimates.
3. Integration with river basin models – The demand projections developed in this work are estimated at spatial scales relevant to water resources management. This

work may be improved by simultaneously assessing integrated water resources impacts.

4. Further evaluation of aggregation error – A logarithmic function was developed to estimate the standard deviation of aggregation error as a function of spatial scale. The spatial variability of soils and climate in Southwest Georgia may not be representative of other regions in the world though. This work may be improved by characterizing aggregation error at larger spatial scales and in other regions.

Appendix

Figure A.1. Center pivot irrigation system in operation in the Lower Flint River basin (May, 2011).

Figure A.2. Center pivot irrigation system in operation in the Lower Flint River basin (May, 2011).

Figure A.3. Drip irrigation system (May, 2011).

Figure A.4. Hose-pull traveler type irrigation system (May, 2011).

Figure A.5. Well-to-pond system (May, 2011).

Figure A.6. Center pivot irrigation system in operation in the Lower Flint River basin (May, 2011).

Figure A.7. Linear irrigation system (SIRP, 2011).

Figure A.8. Richard Royal (left) discusses Flint-Ochlockonee Regional Water Planning Council activities with researchers and agricultural producers at Stripling Irrigation Research Park (SIRP, 2011).

Figure A.9. Schematic of propeller-style metering device (GSWCC, 2013).

Figure A.10. Example of propeller-style metering device (GSWCC, 2013).

Figure A.11. An agricultural extension agent examines an irrigated field in the Lower Flint River basin (June, 2011).

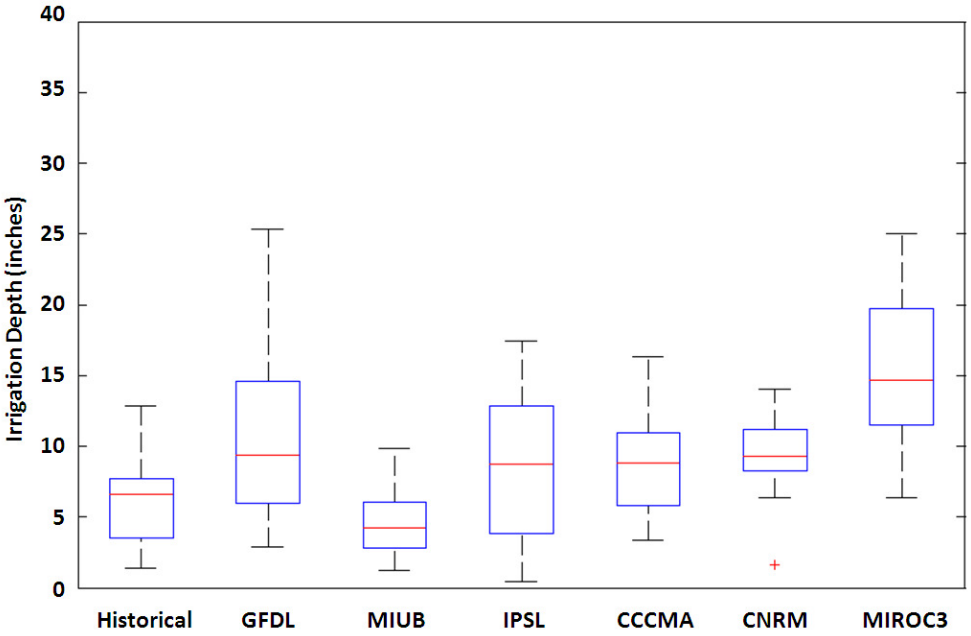

Figure A.12. Annual demand in Albany under A1B emissions scenario (2046-2065).

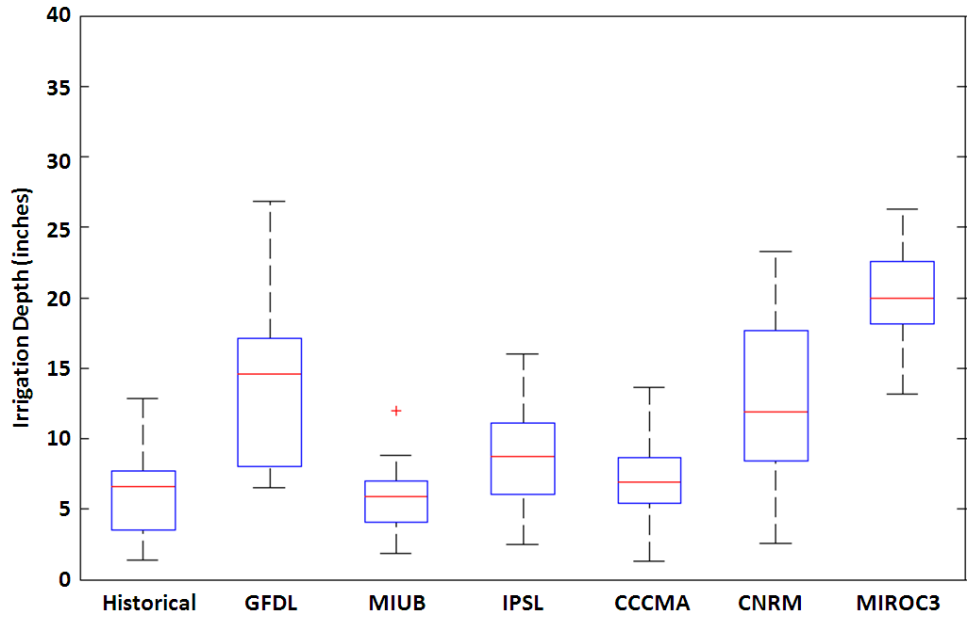

Figure A.13. Annual demand in Albany under A1B emissions scenario (2081-2100).

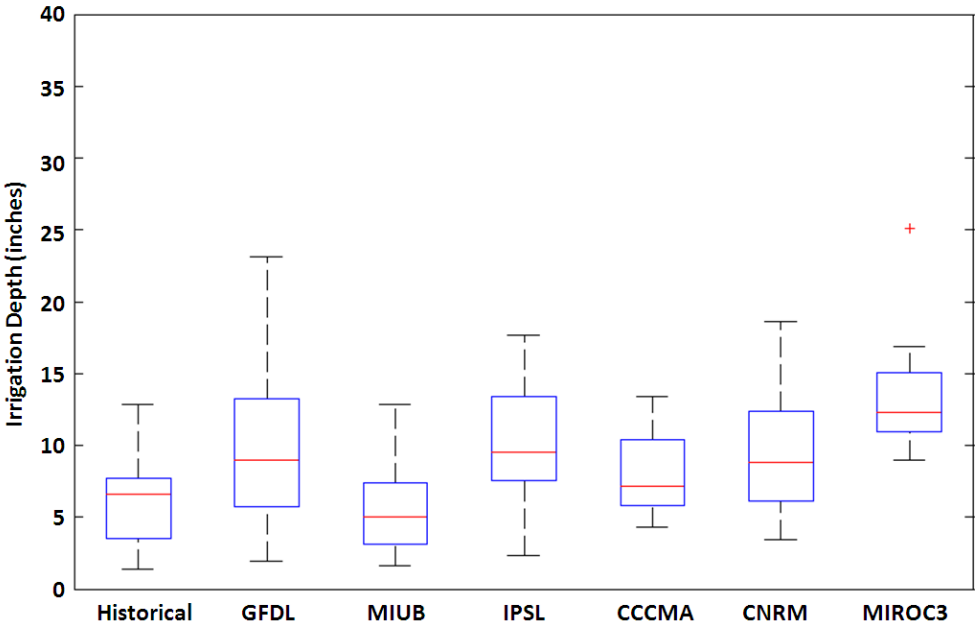

Figure A.14. Annual demand in Albany under A2 emissions scenario (2046-2065).

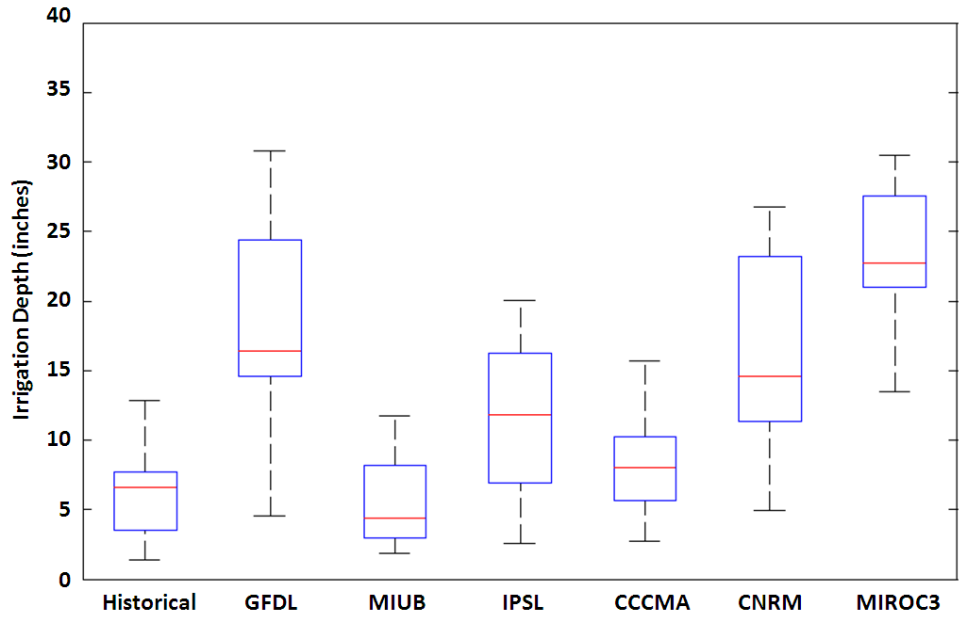

Figure A.15. Annual demand in Albany under A2 emissions scenario (2081-2100).

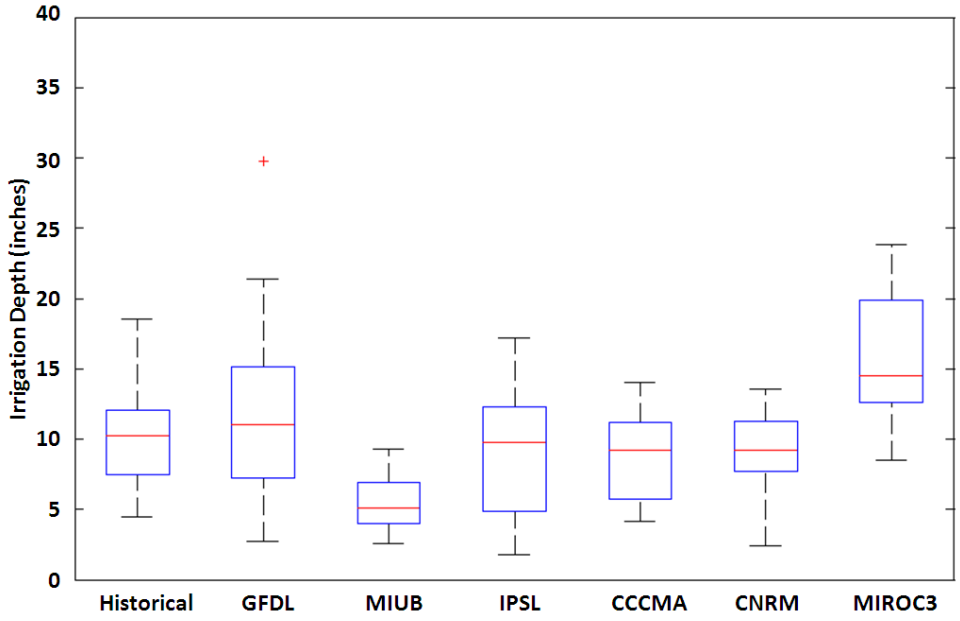

Figure A.16. Annual demand in Bainbridge under A1B emissions scenario (2046-2065).

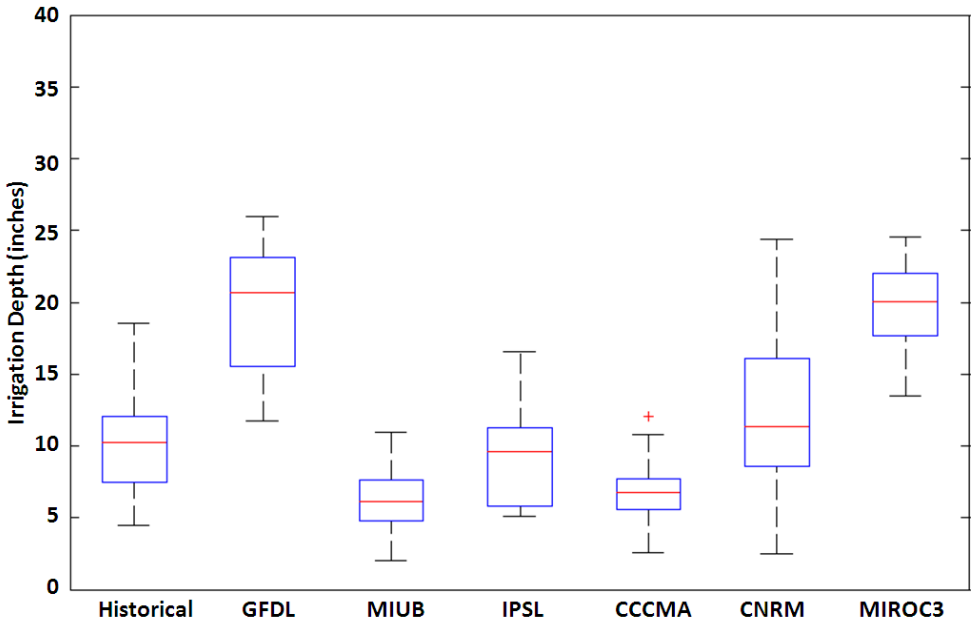

Figure A.17. Annual demand in Bainbridge under A1B emissions scenario (2081-2100).

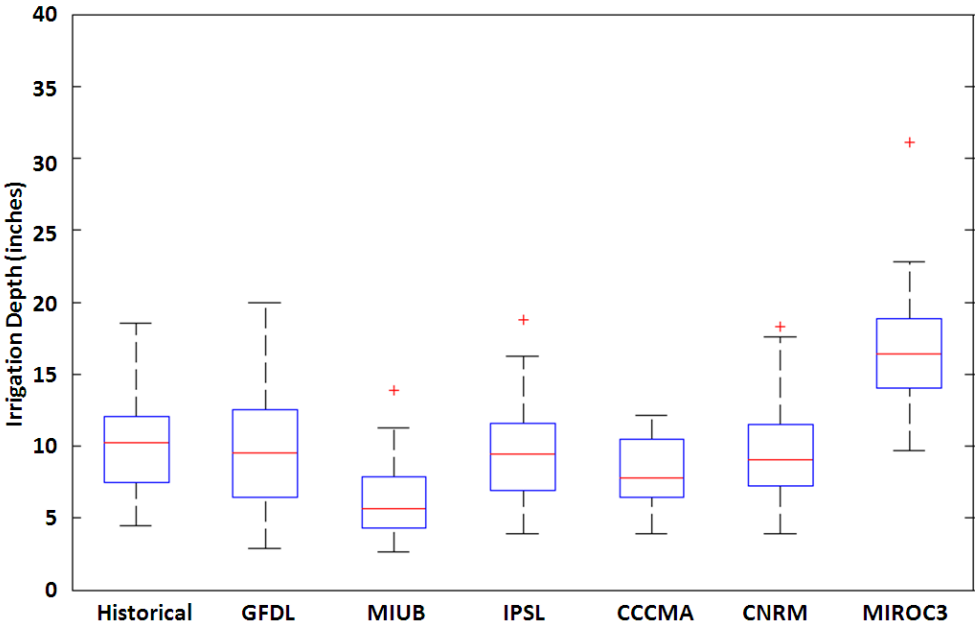

Figure A.18. Annual demand in Bainbridge under A2 emissions scenario (2046-2065).

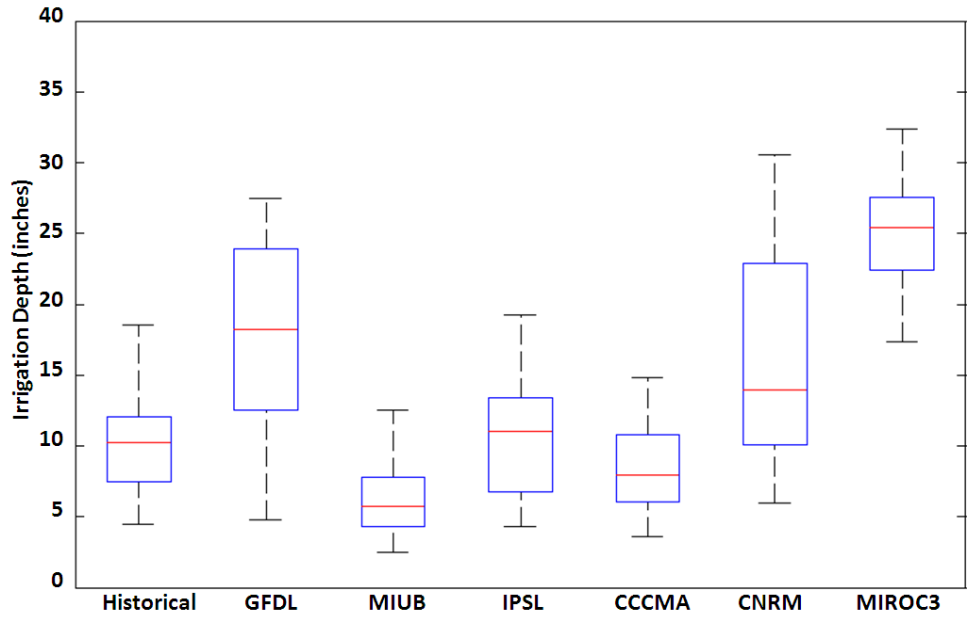

Figure A.19. Annual demand in Bainbridge under A2 emissions scenario (2081-2100).

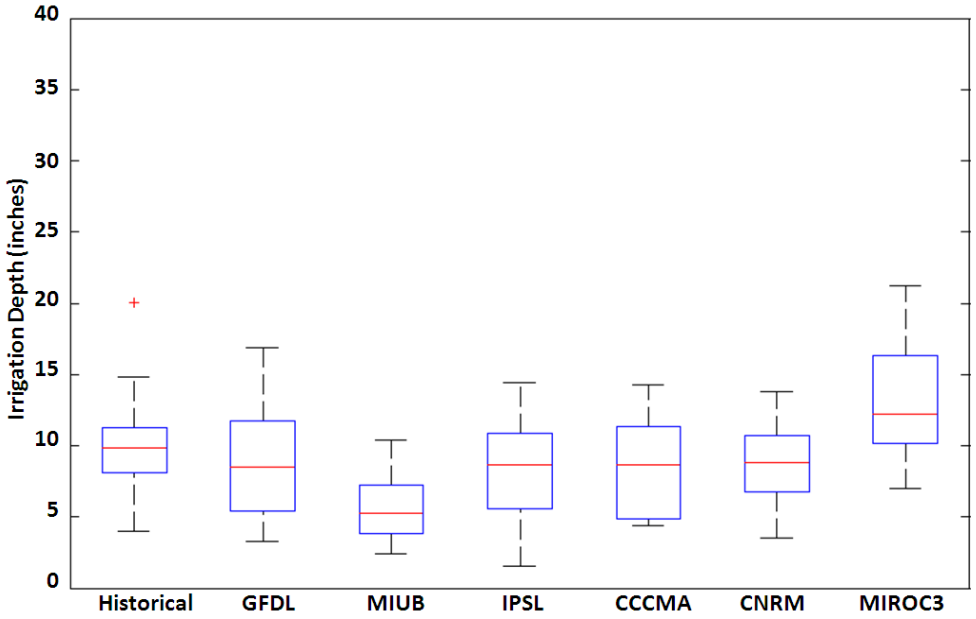

Figure A.20. Annual demand in Iron City under A1B emissions scenario (2046-2065).

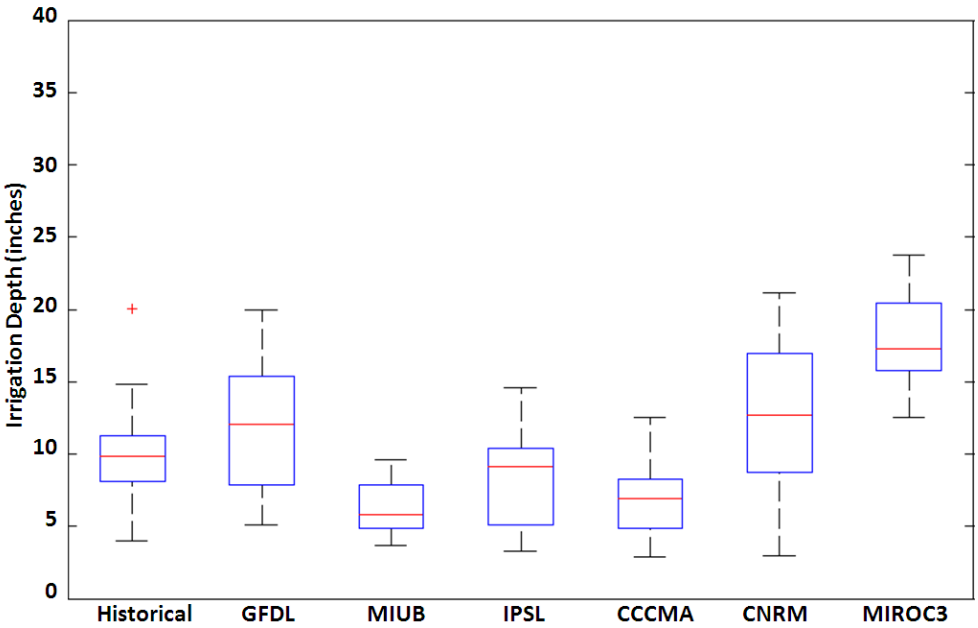

Figure A.21. Annual demand in Iron City under A1B emissions scenario (2081-2100).

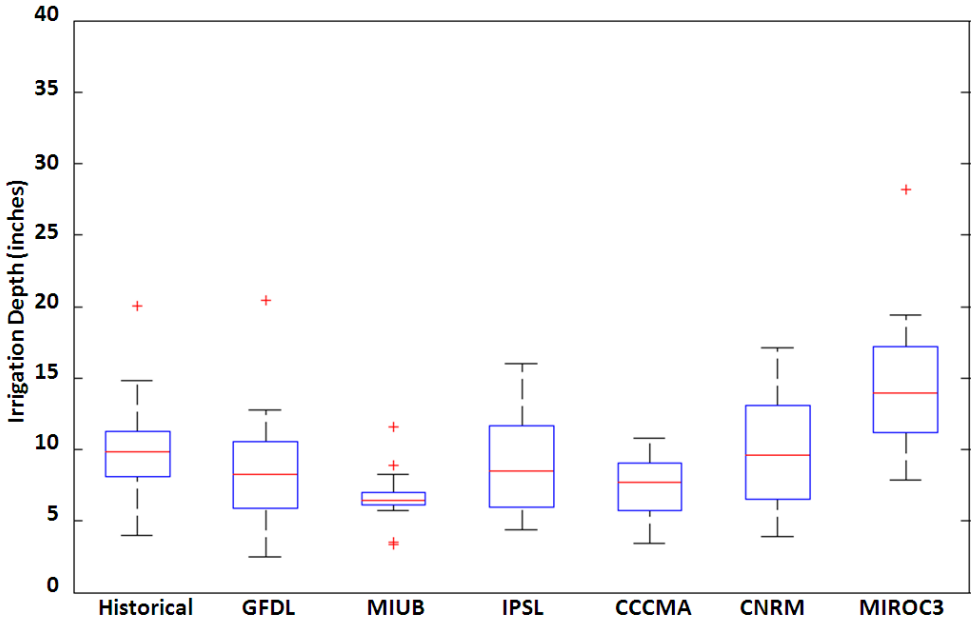

Figure A.22. Annual demand in Iron City under A2 emissions scenario (2046-2065).

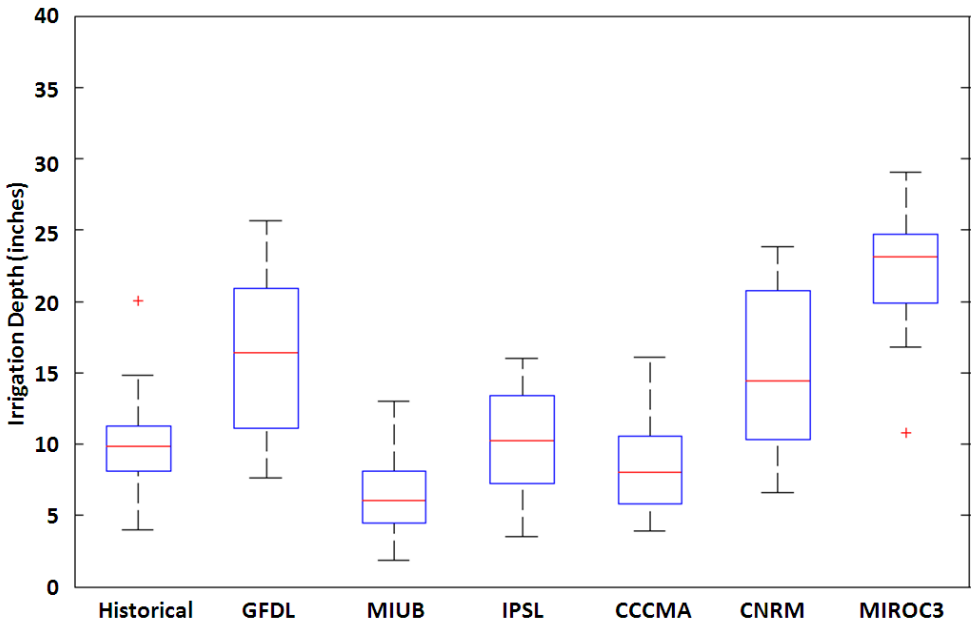

Figure A.23. Annual demand in Iron City under A2 emissions scenario (2081-2100).

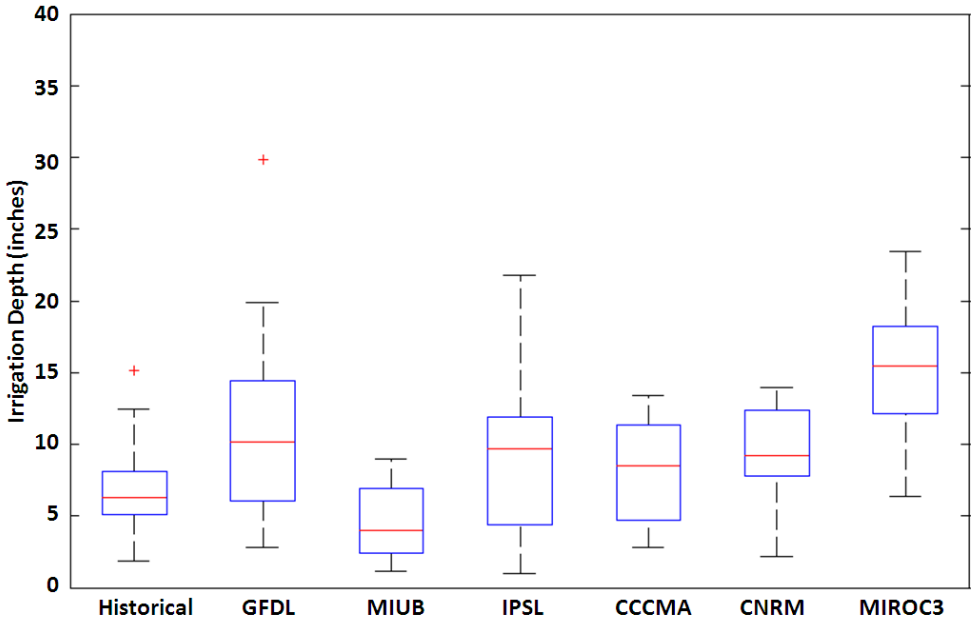

Figure A.24. Annual demand in Milford under A1B emissions scenario (2046-2065).

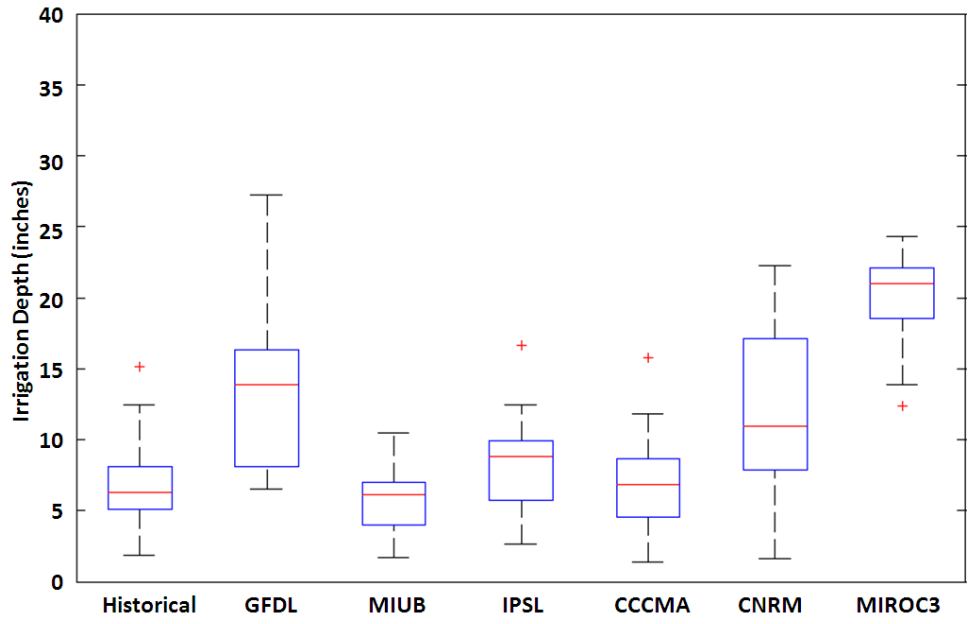

Figure A.25. Annual demand in Milford under A1B emissions scenario (2081-2100).

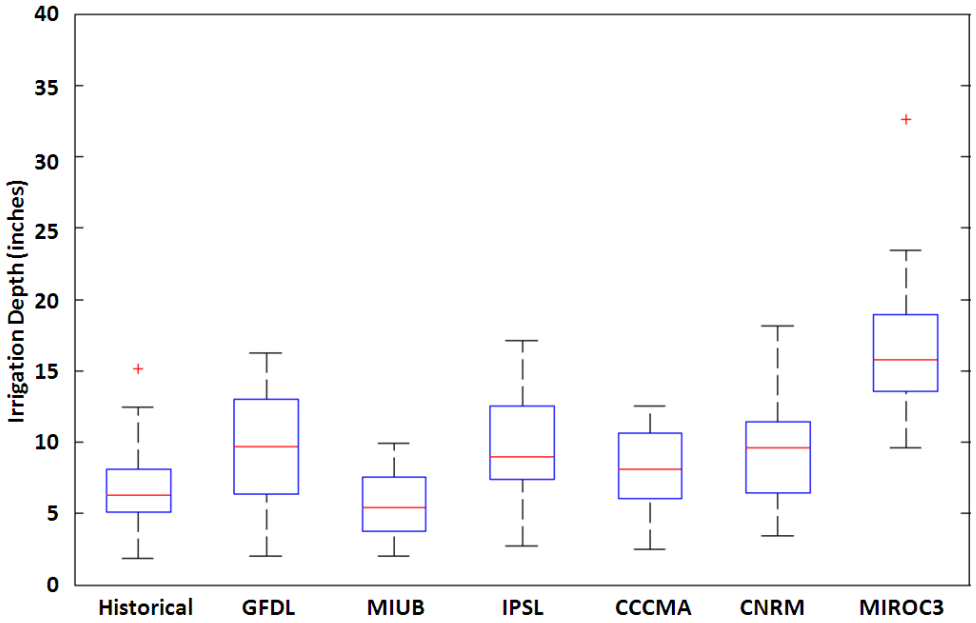

Figure A.26. Annual demand in Milford under A2 emissions scenario (2046-2065).

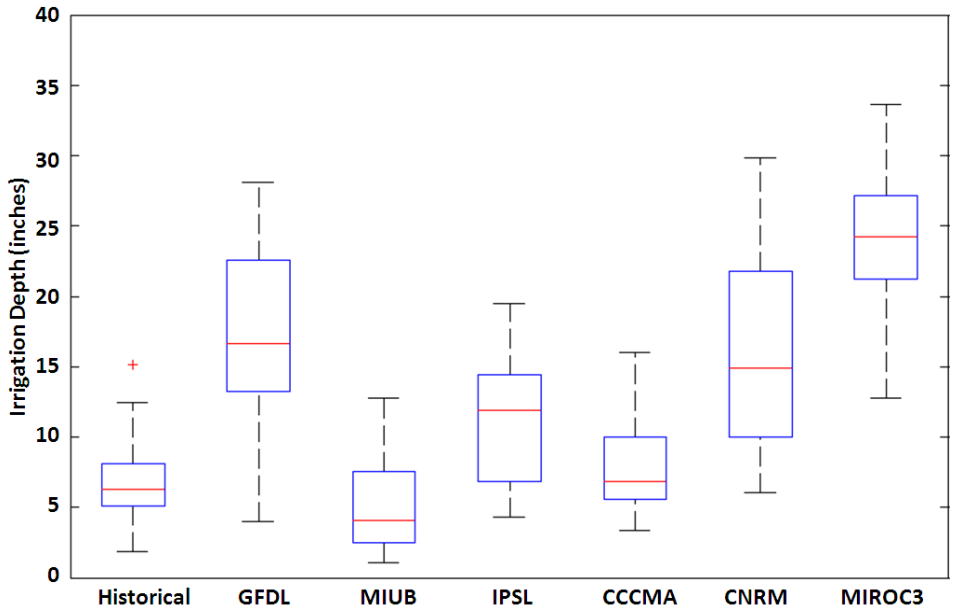

Figure A.27. Annual demand in Milford under A2 emissions scenario (2081-2100).

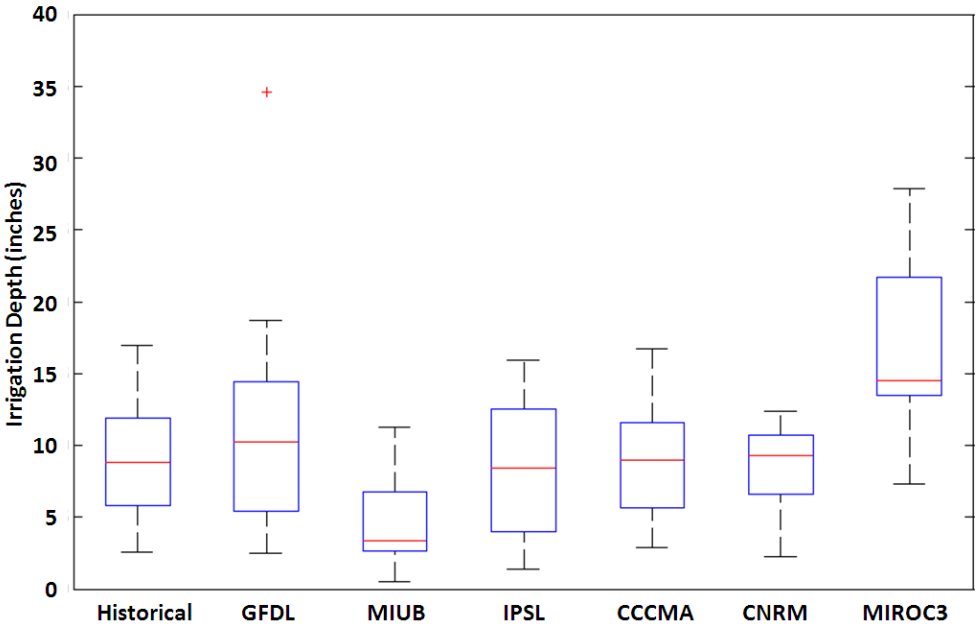

Figure A.28. Annual demand in Newton under A1B emissions scenario (2046-2065).

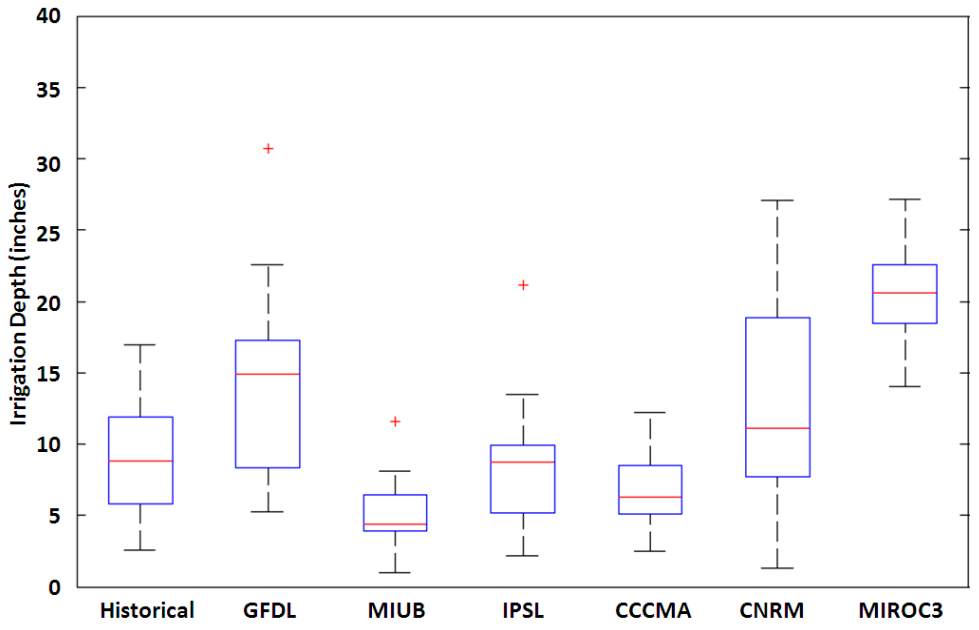

Figure A.29. Annual demand in Newton under A1B emissions scenario (2081-2100).

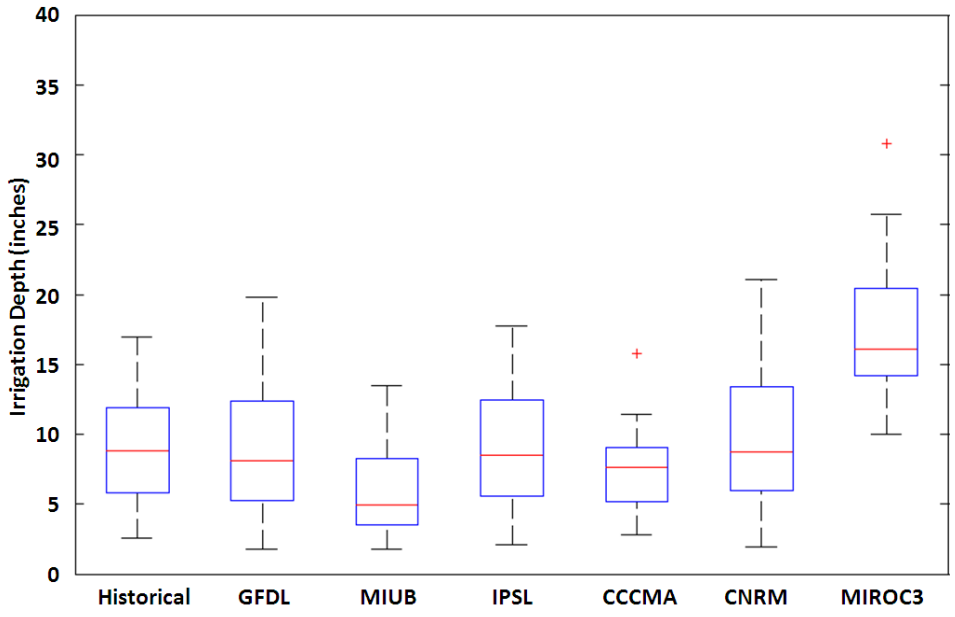

Figure A.30. Annual demand in Newton under A2 emissions scenario (2046-2065).

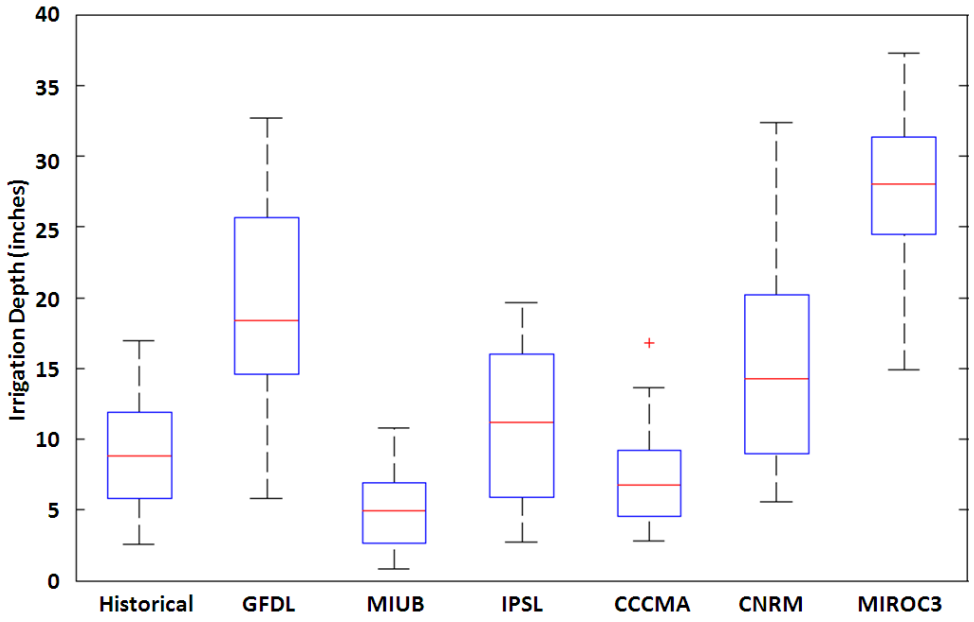

Figure A.31. Annual demand in Newton under A2 emissions scenario (2081-2100).

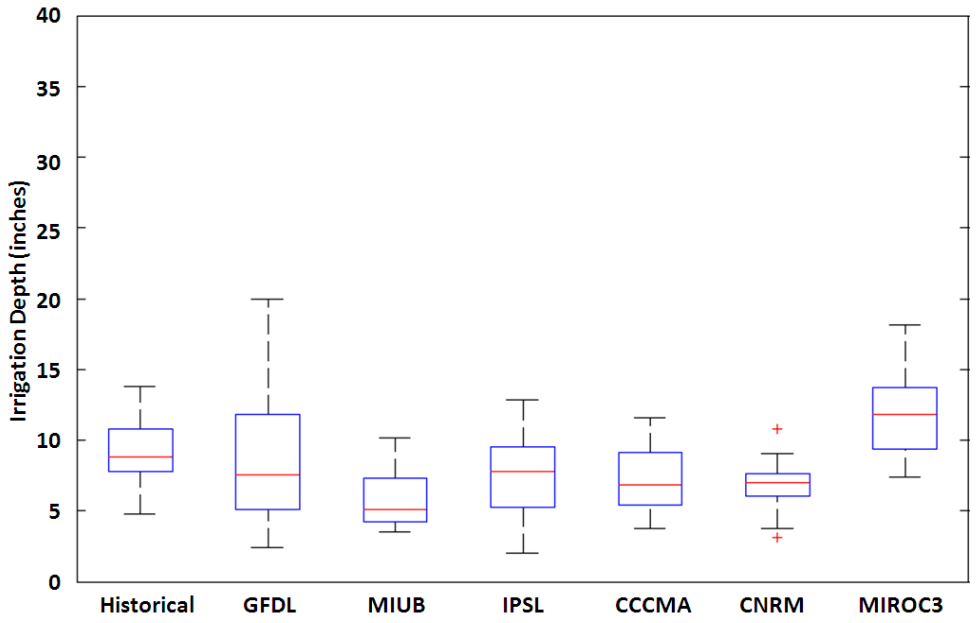

Figure A.32. Annual demand in Woodruff under A1B emissions scenario (2046-2065).

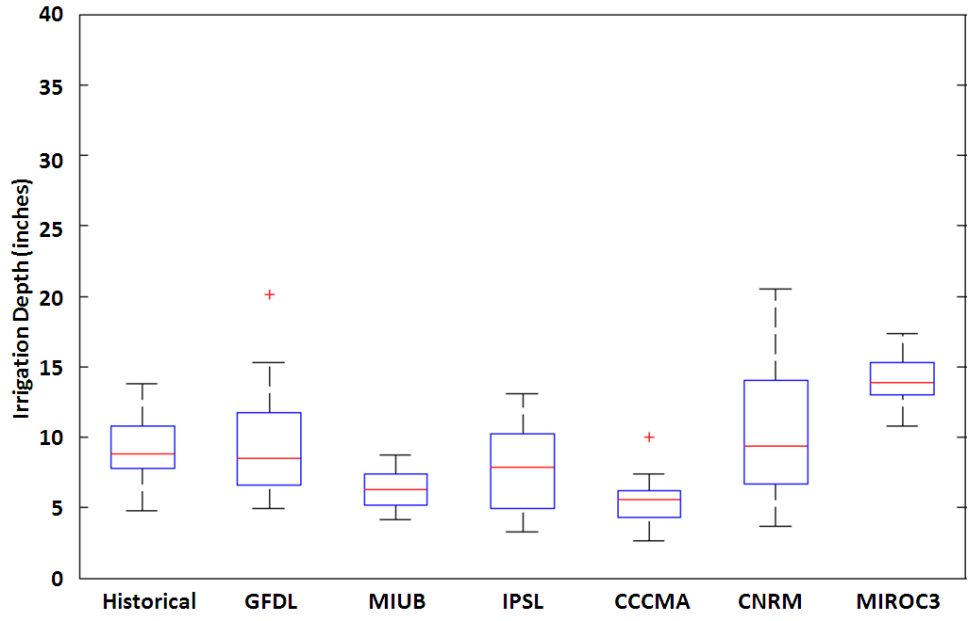

Figure A.33. Annual Demand in Woodruff under A1B emissions scenario (2081-2100).

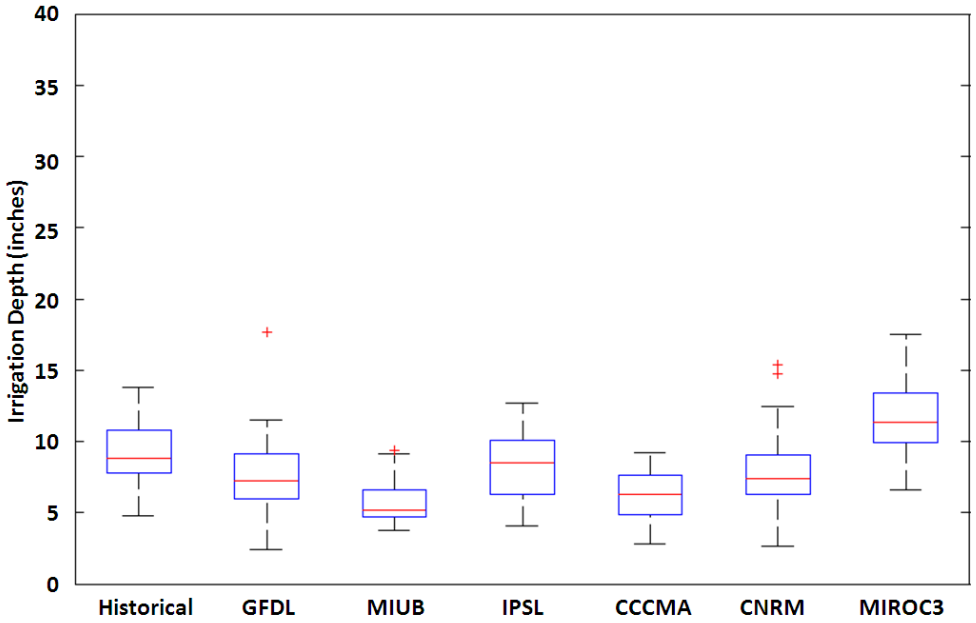

Figure A.34. Annual demand in Woodruff under A2 emissions scenario (2046-2065).

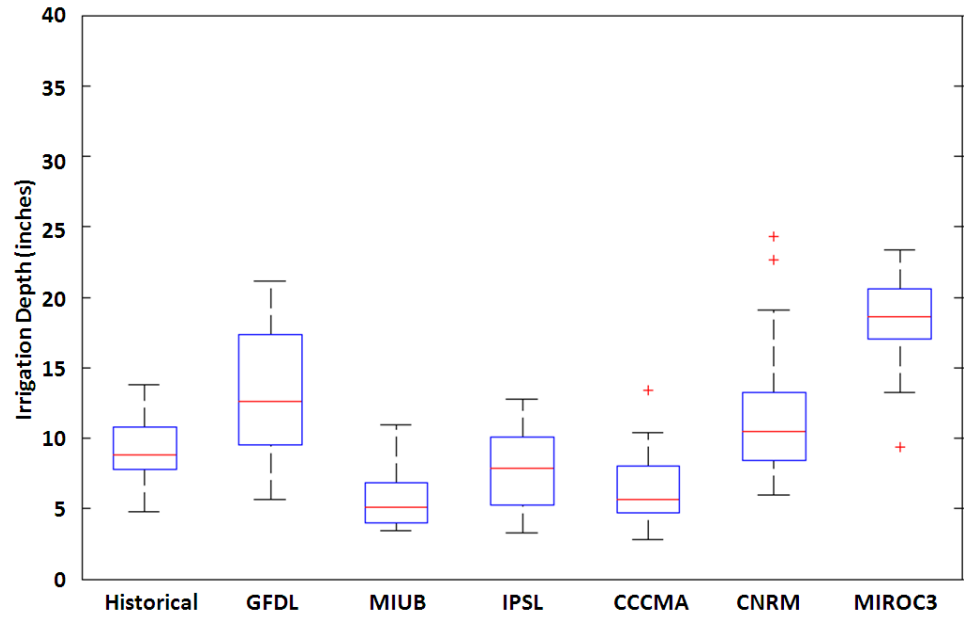

Figure A.35. Annual demand in Woodruff under A2 emissions scenario (2081-2100).

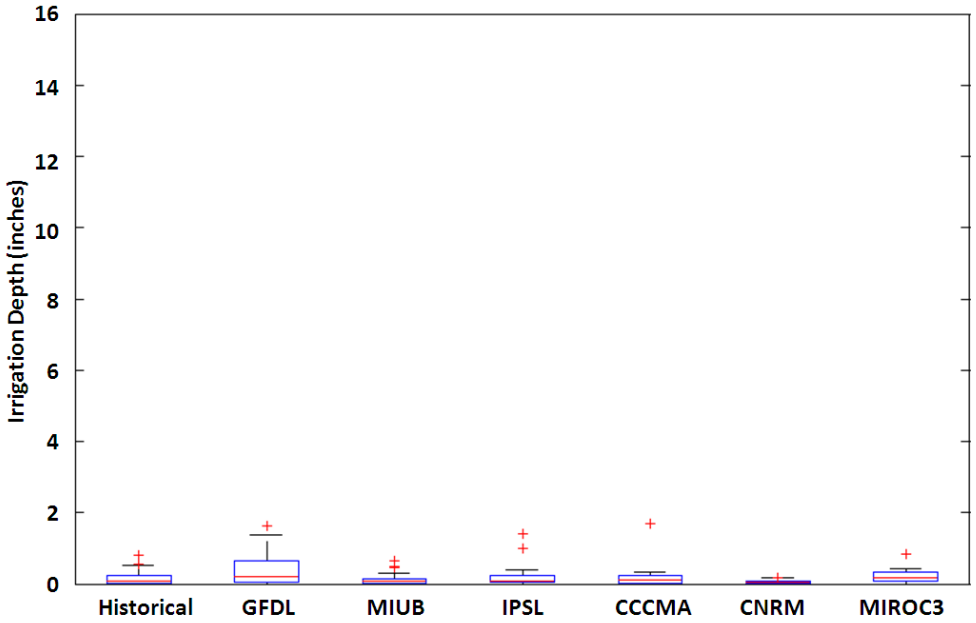

Figure A.36. May demand in Albany under A1B emissions scenario (2046-2065).

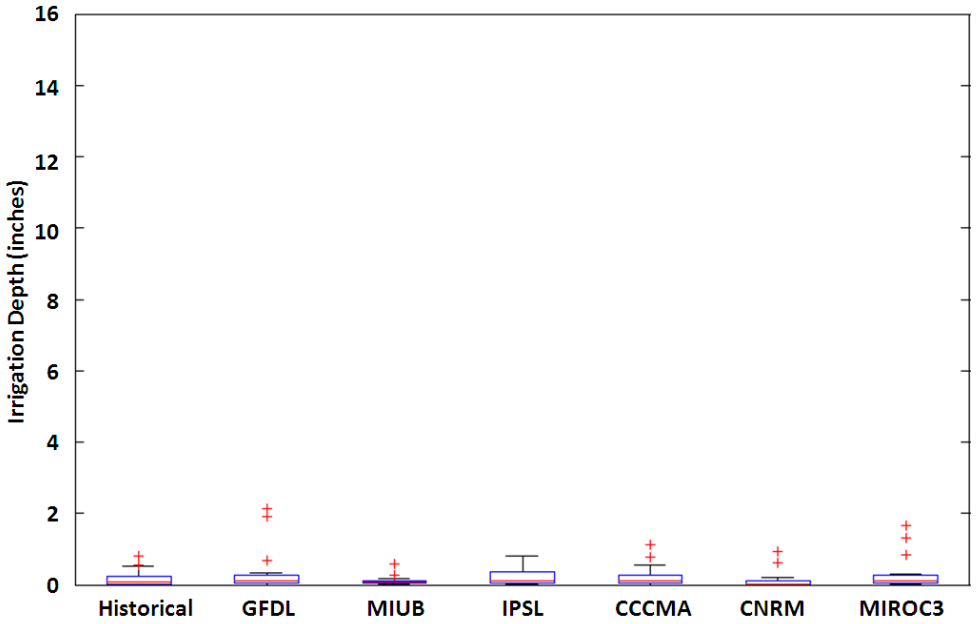

Figure A.37. May demand in Albany under A1B emissions scenario (2081-2100).

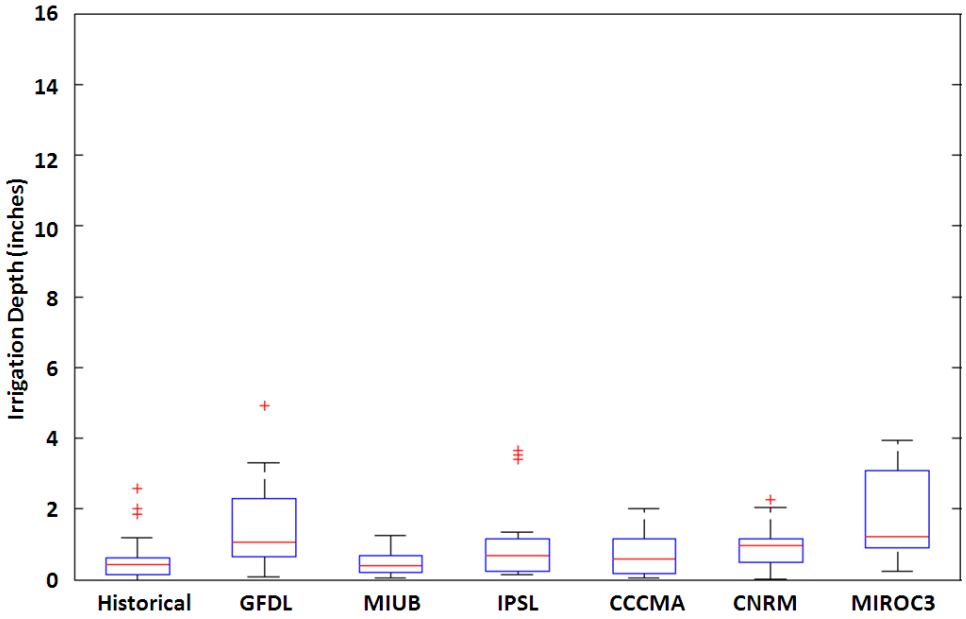

Figure A.38. June demand in Albany under A1B emissions scenario (2046-2065).

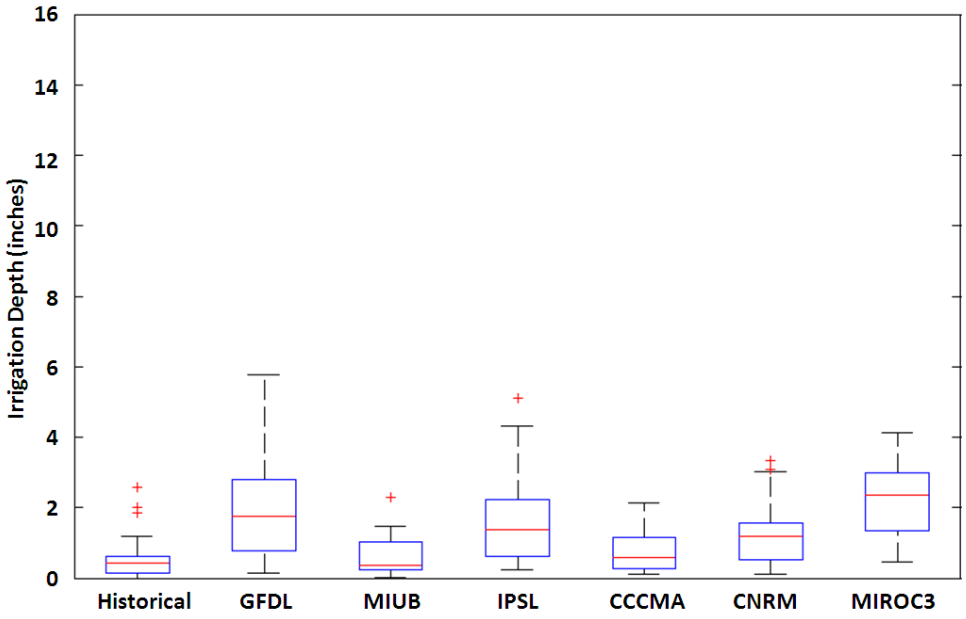

Figure A.39. June demand in Albany under A1B emissions scenario (2081-2100).

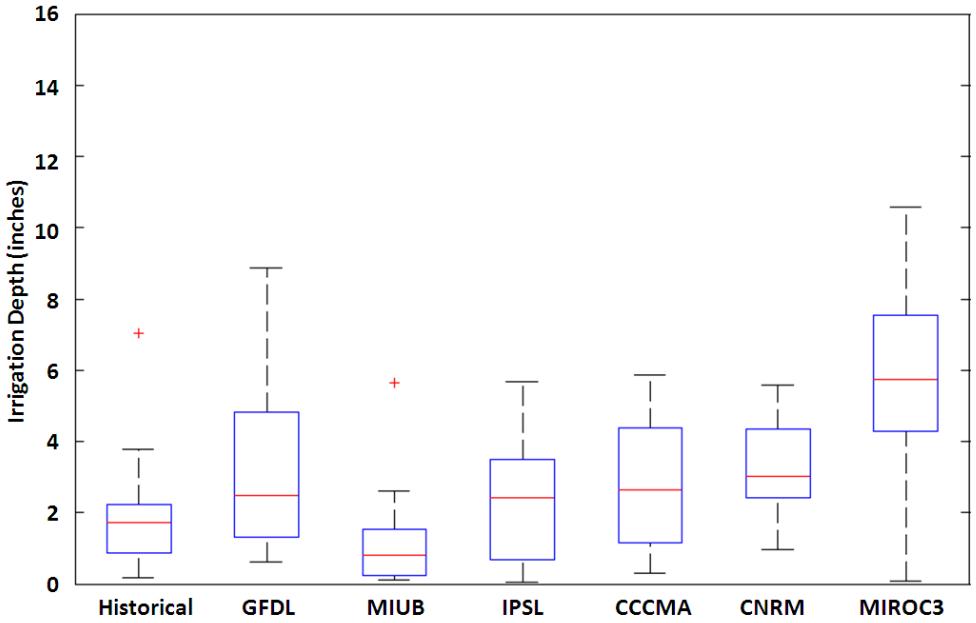

Figure A.40. July demand in Albany under A1B emissions scenario (2046-2065).

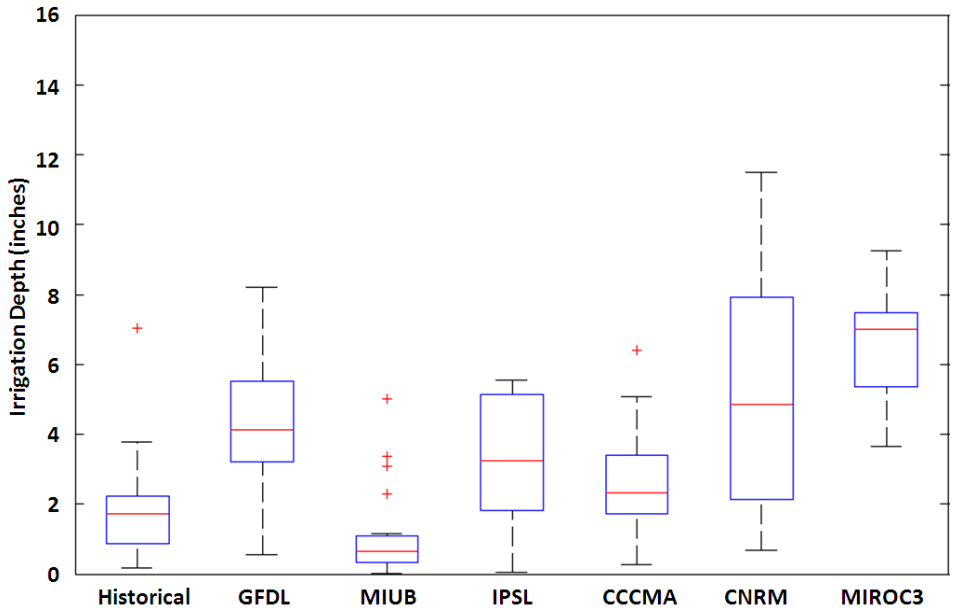

Figure A.41. July demand in Albany under A1B emissions scenario (2081-2100).

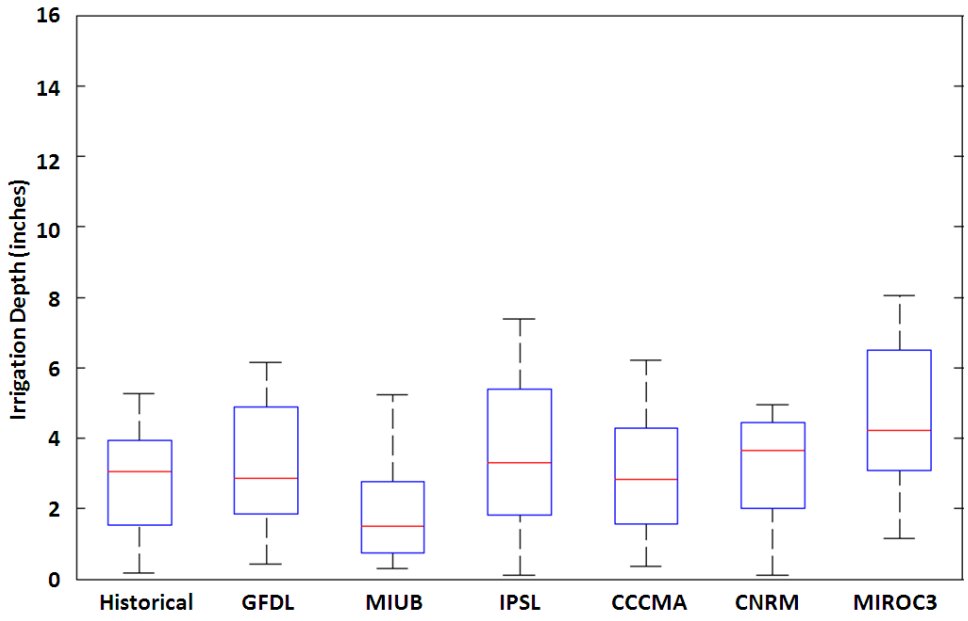

Figure A.42. August demand in Albany under A1B emissions scenario (2046-2065).

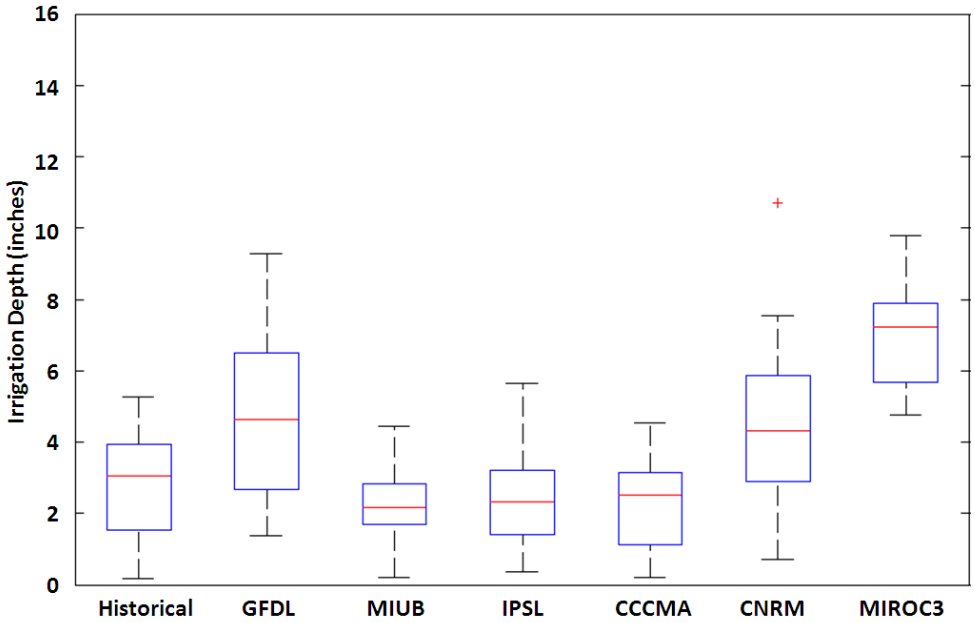

Figure A.43. August demand in Albany under A1B emissions scenario (2081-2100).

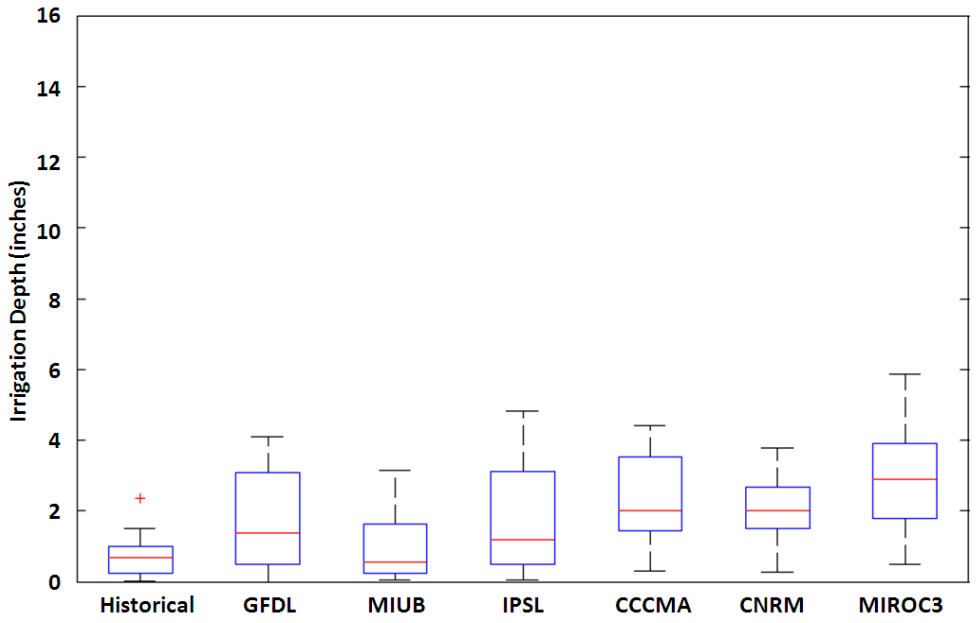

Figure A.44. Sept. demand in Albany under A1B emissions scenario (2046-2065).

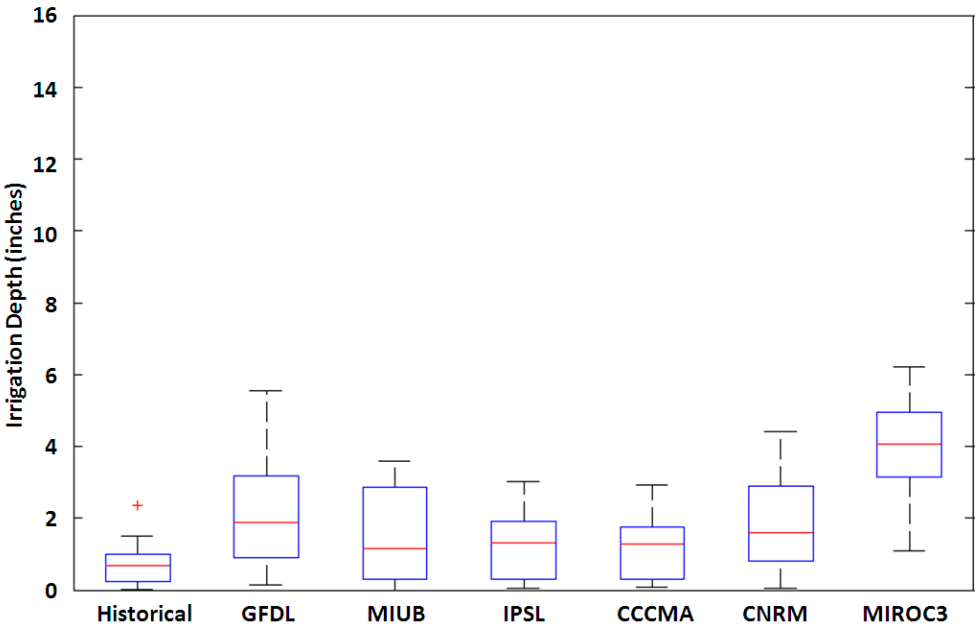

Figure A.45. Sept. demand in Albany under A1B emissions scenario (2081-2100).

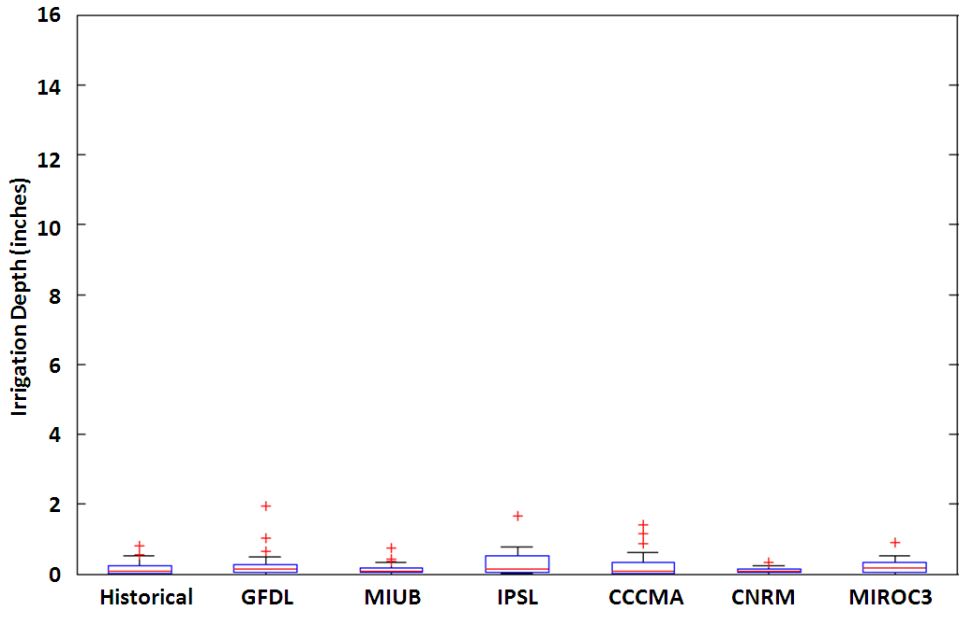

Figure A.46. May demand in Albany under A2 emissions scenario (2046-2065).

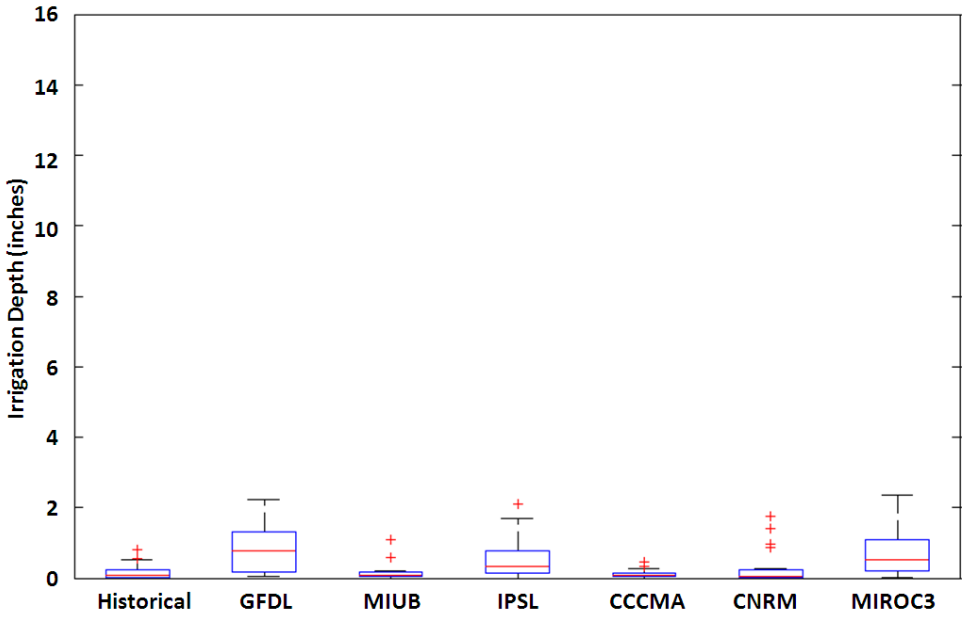

Figure A.47. May demand in Albany under A2 emissions scenario (2081-2100).

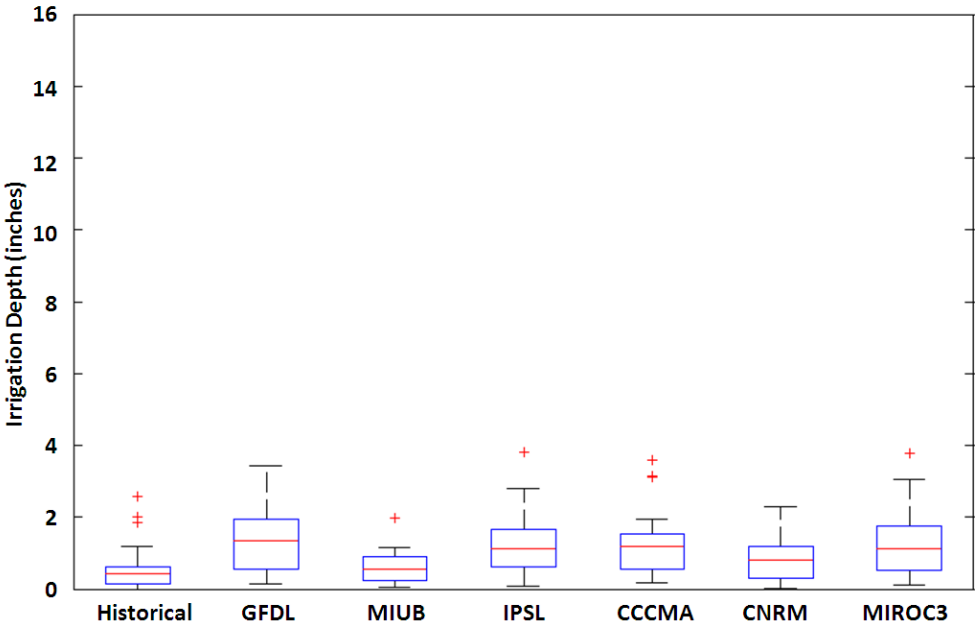

Figure A.48. June demand in Albany under A2 emissions scenario (2046-2065).

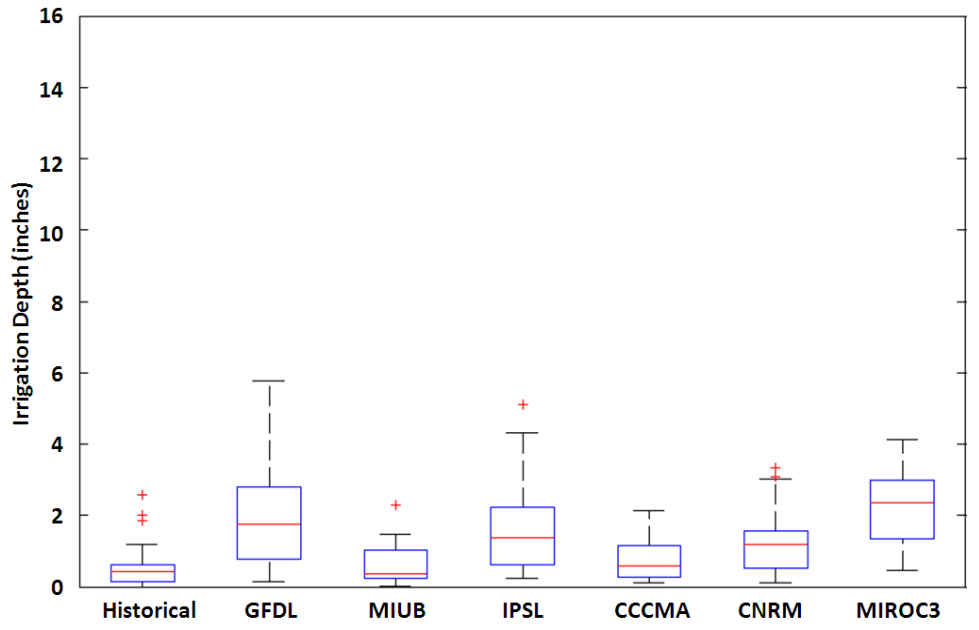

Figure A.49. June demand in Albany under A2 emissions scenario (2081-2100).

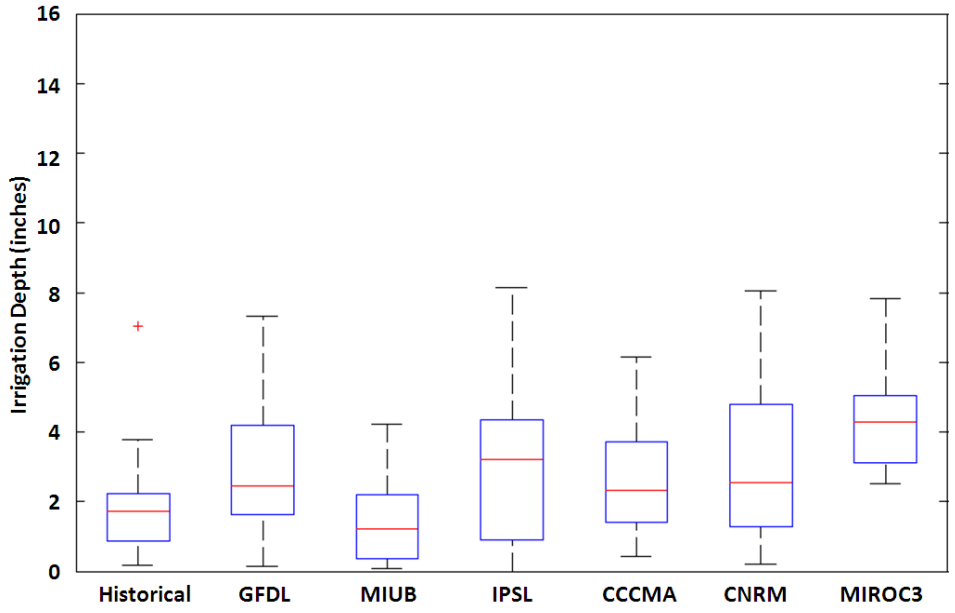

Figure A.50. July demand in Albany under A2 emissions scenario (2046-2065).

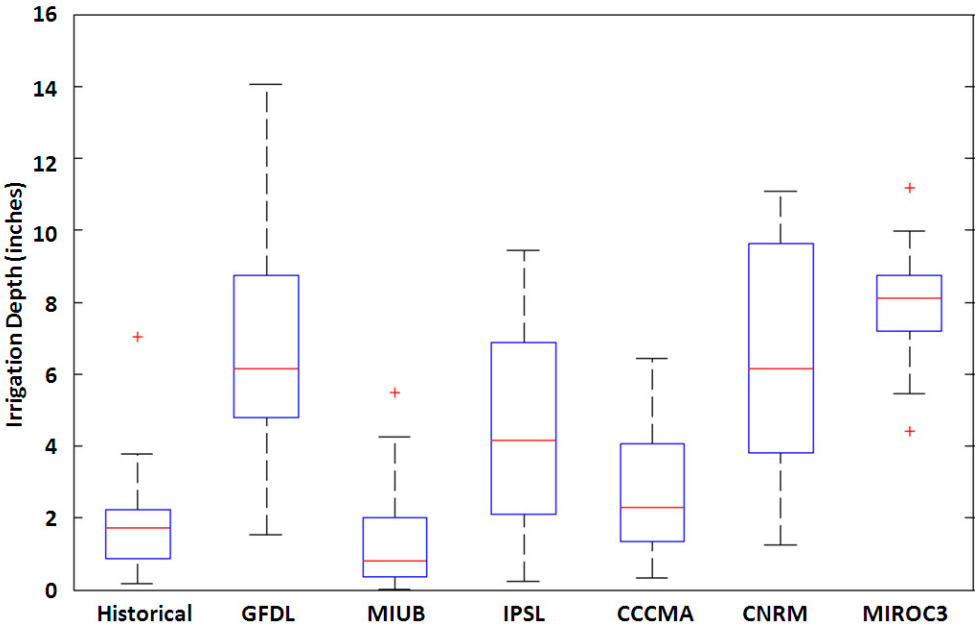

Figure A.51. July demand in Albany under A2 emissions scenario (2081-2100).

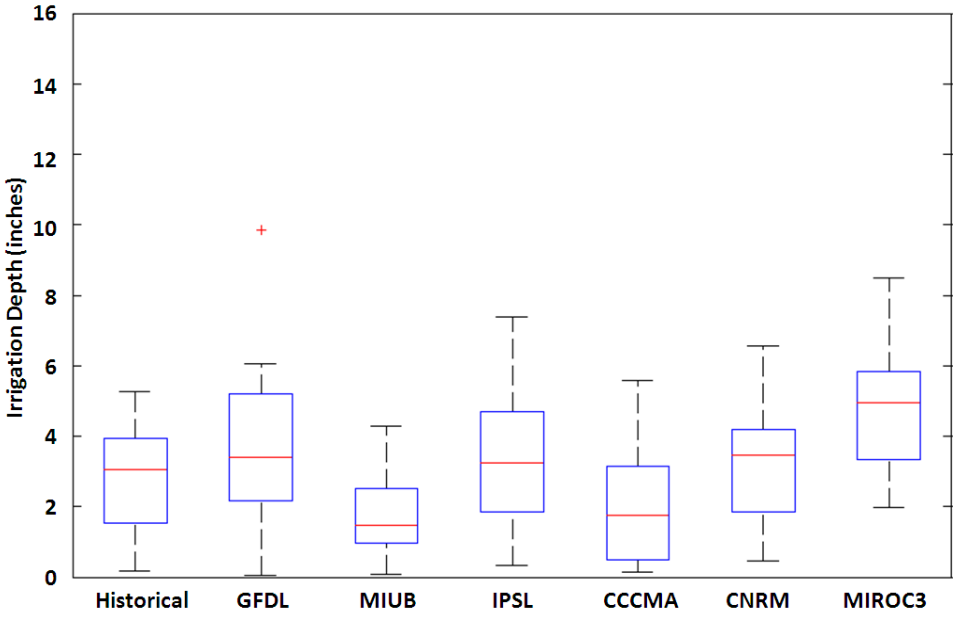

Figure A.52. August demand in Albany under A2 emissions scenario (2046-2065).

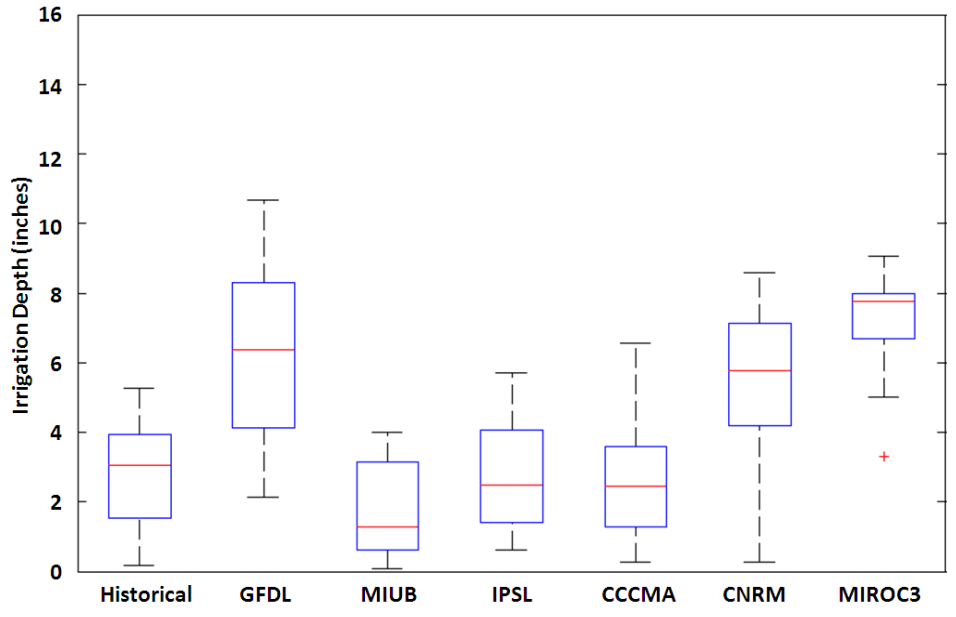

Figure A.53. August demand in Albany under A2 emissions scenario (2081-2100).

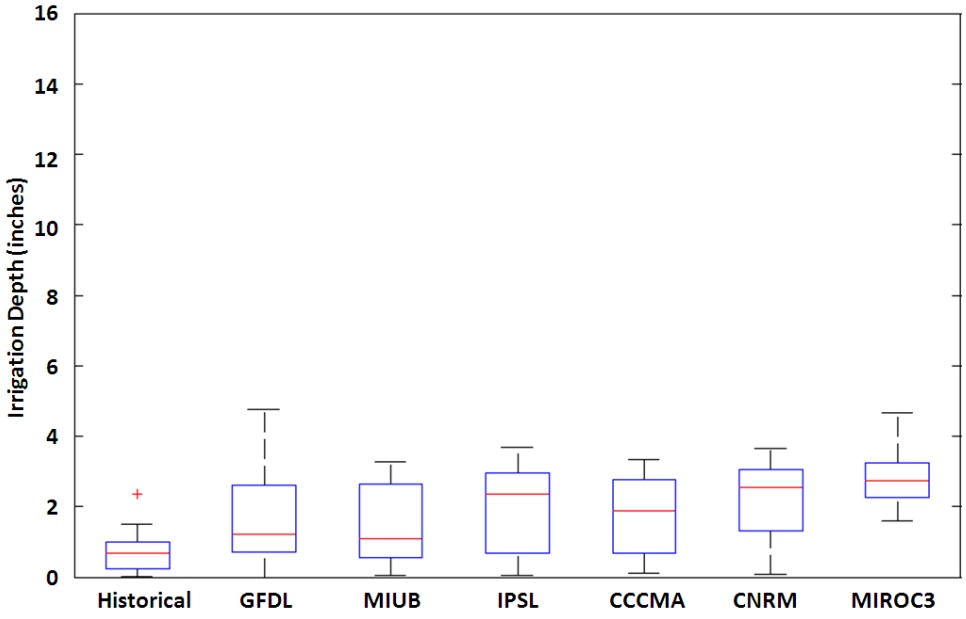

Figure A.54. Sept. demand in Albany under A2 emissions scenario (2046-2065).

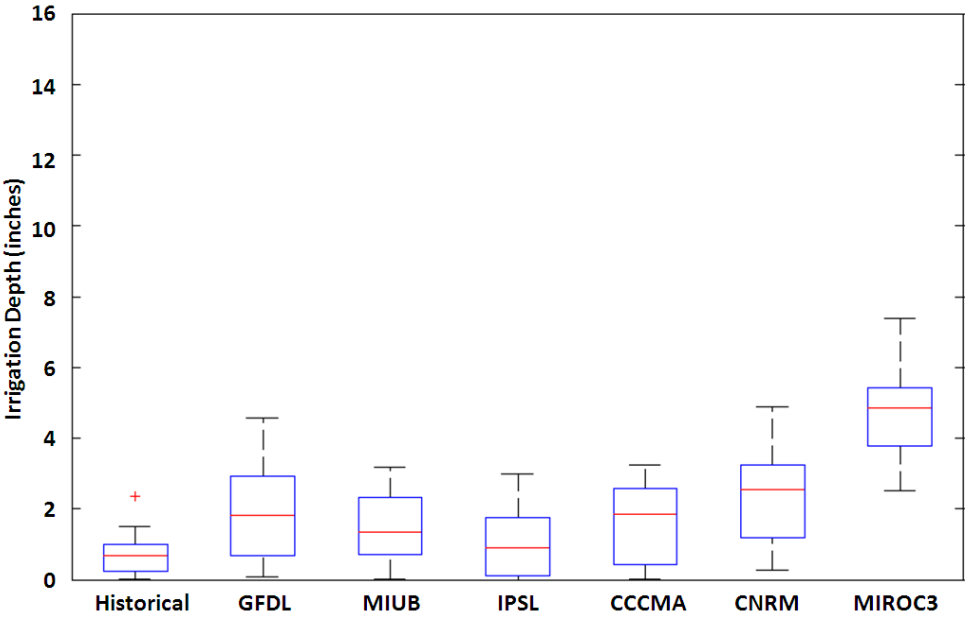

Figure A.55. Sept. demand in Albany under A2 emissions scenario (2081-2100).

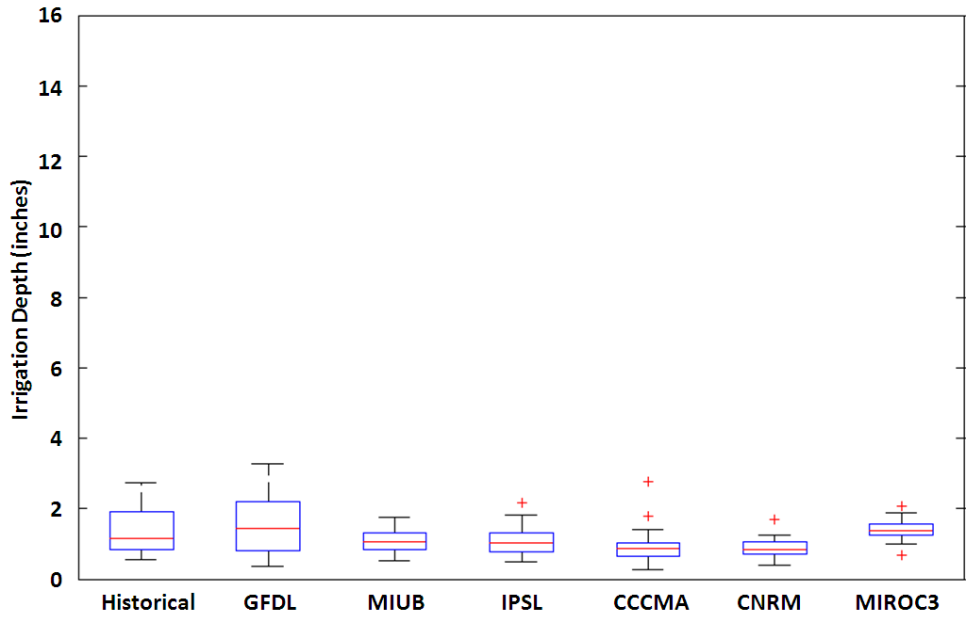

Figure A.56. May demand in Bainbridge under A1B emissions scenario (2046-2065).

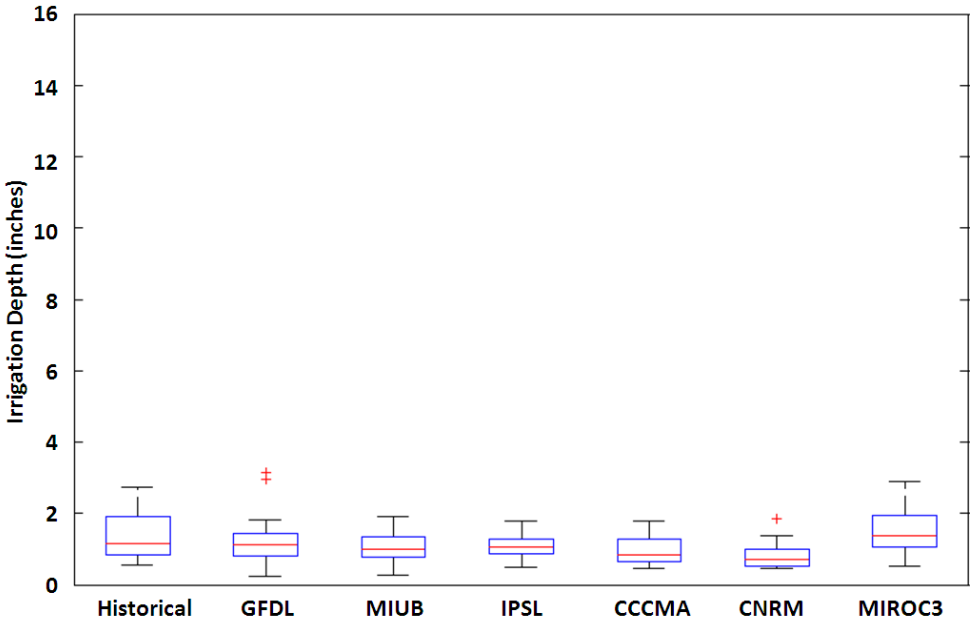

Figure A.57. May demand in Bainbridge under A1B emissions scenario (2081-2100).

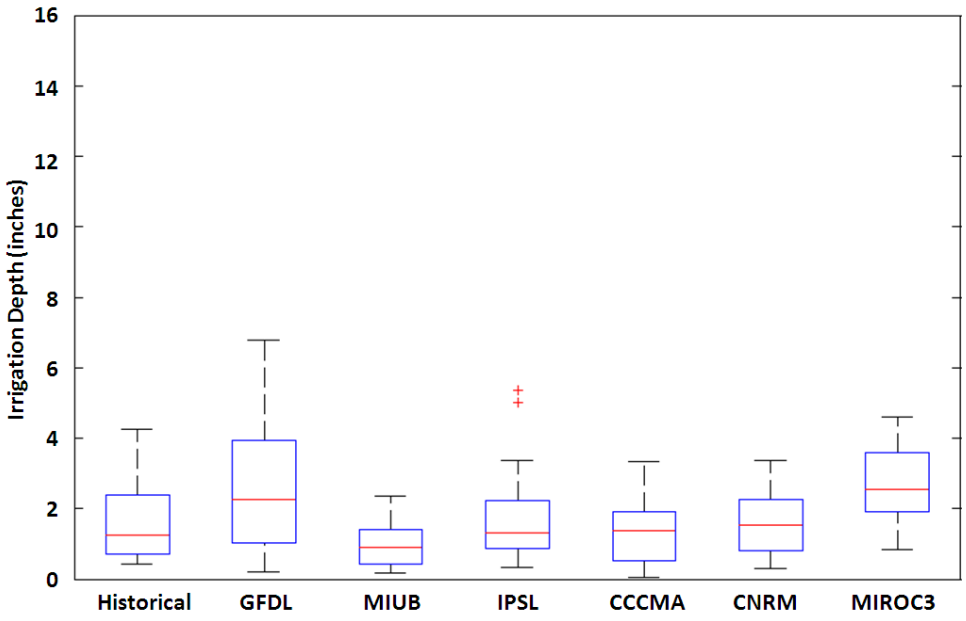

Figure A.58. June demand in Bainbridge under A1B emissions scenario (2046-2065).

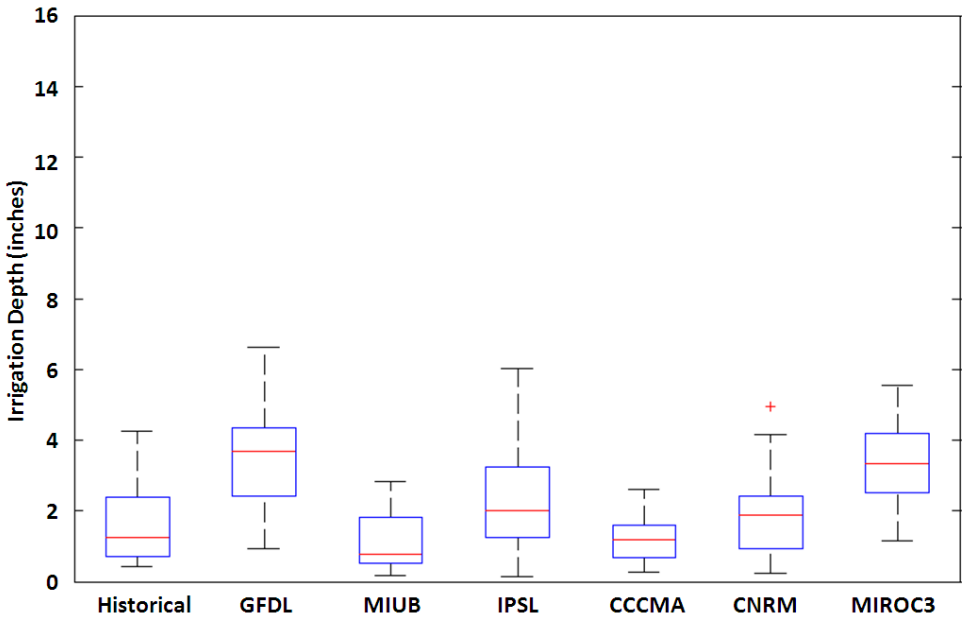

Figure A.59. June demand in Bainbridge under A1B emissions scenario (2081-2100).

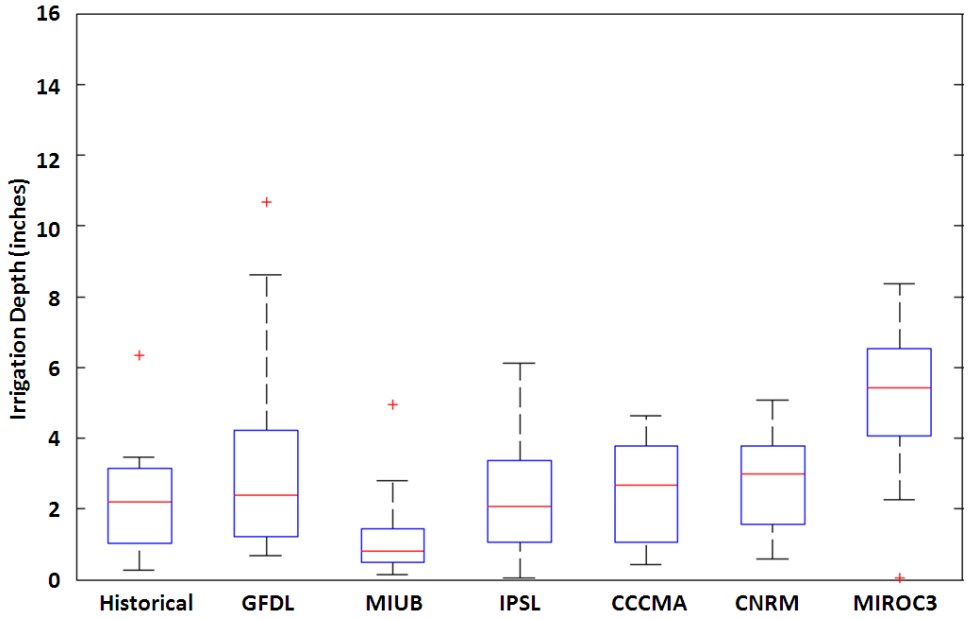

Figure A.60. July demand in Bainbridge under A1B emissions scenario (2046-2065).

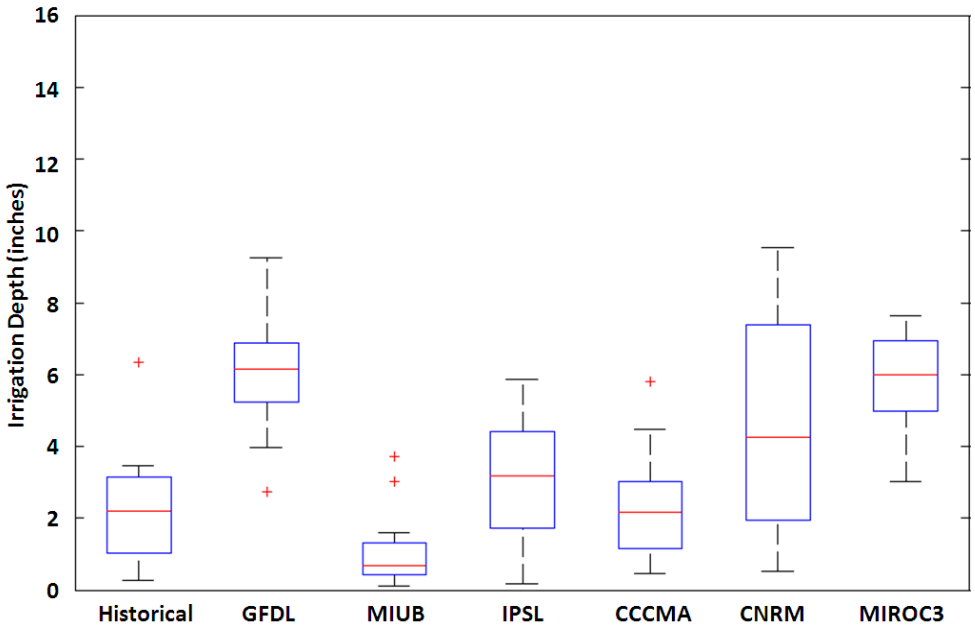

Figure A.61. July demand in Bainbridge under A1B emissions scenario (2081-2100).

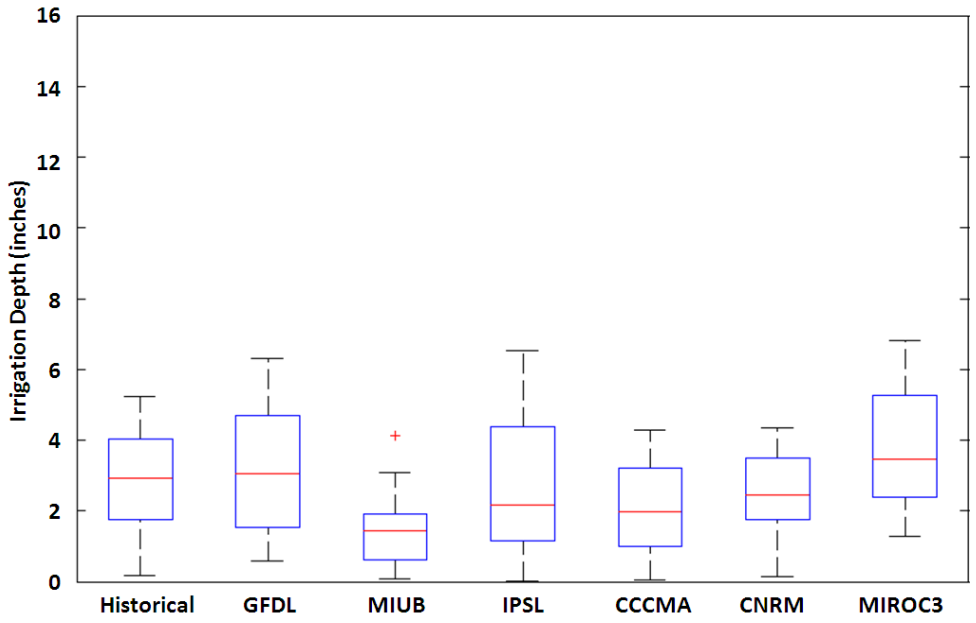

Figure A.62. August demand in Bainbridge under A1B emissions scenario (2046-2065).

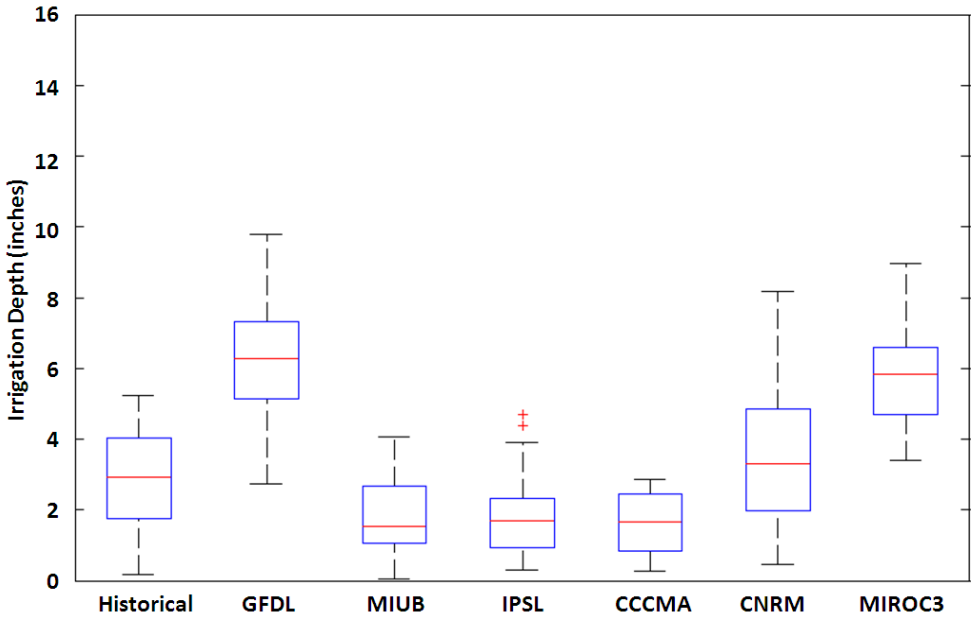

Figure A.63. August demand in Bainbridge under A1B emissions scenario (2081-2100).

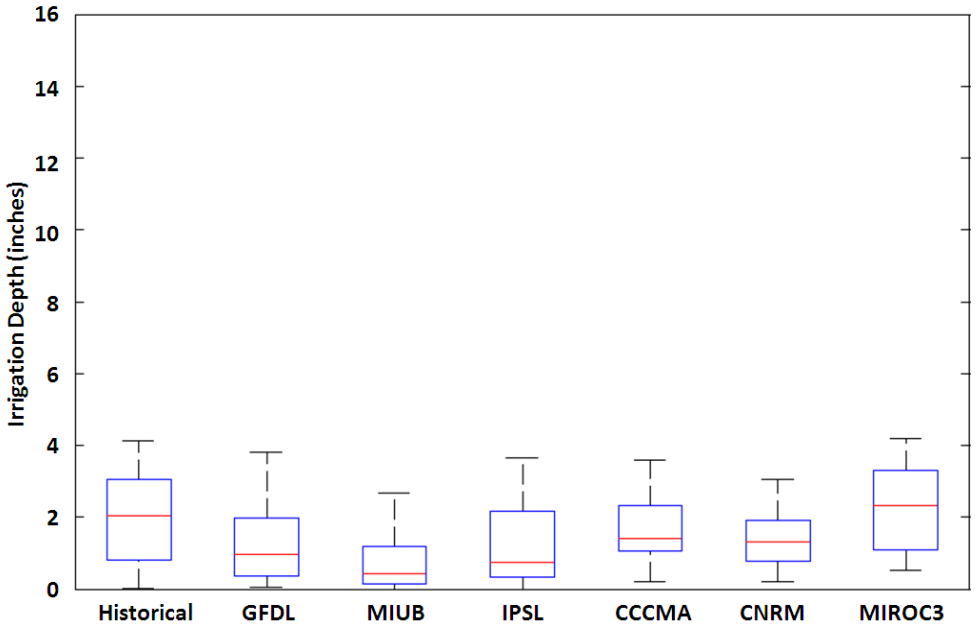

Figure A.64. Sept. demand in Bainbridge under A1B emissions scenario (2046-2065).

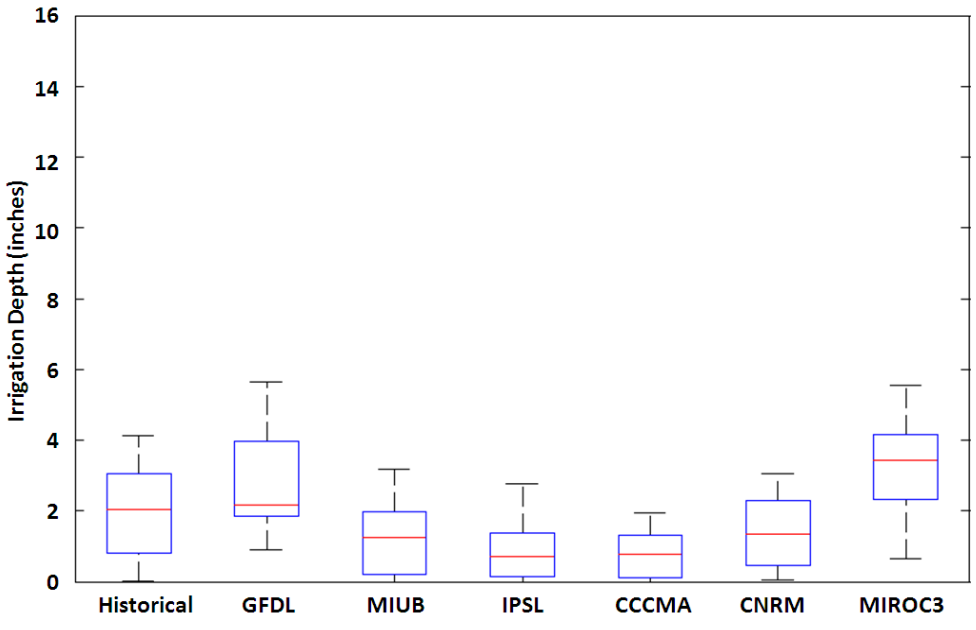

Figure A.65. Sept. demand in Bainbridge under A1B emissions scenario (2081-2100).

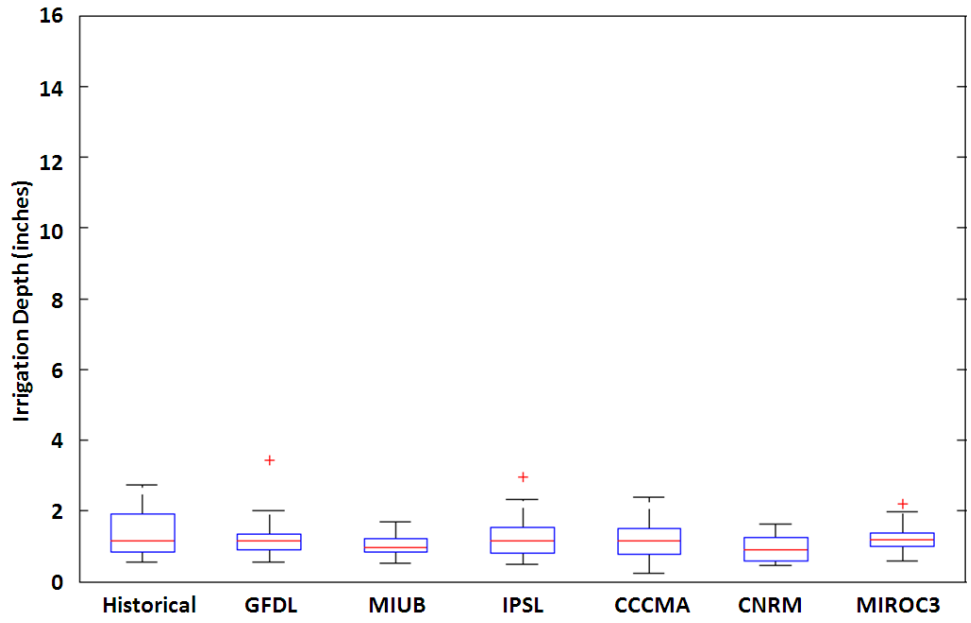

Figure A.66. May demand in Bainbridge under A2 emissions scenario (2046-2065).

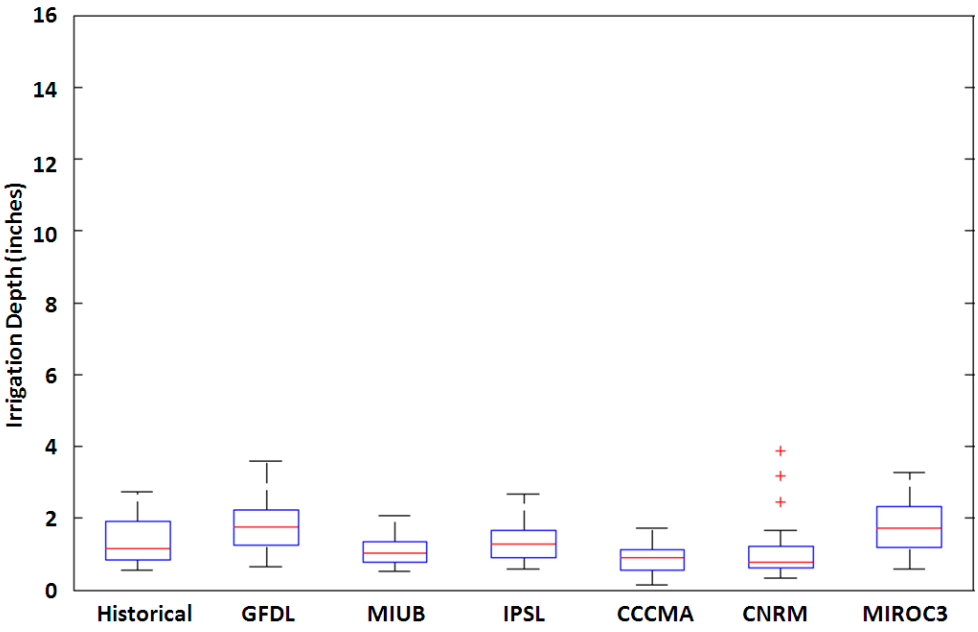

Figure A.67. May demand in Bainbridge under A2 emissions scenario (2081-2100).

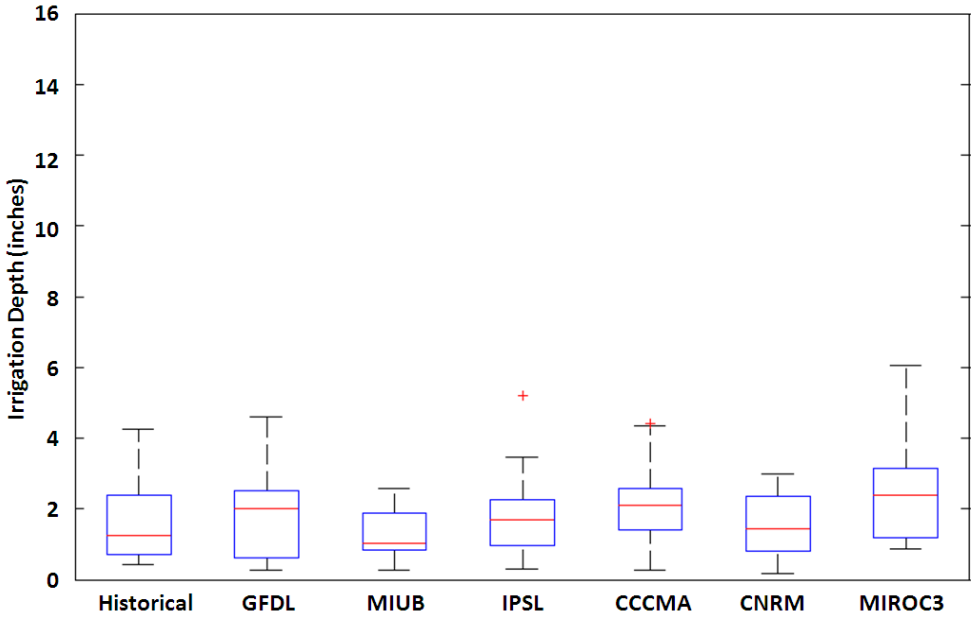

Figure A.68. June demand in Bainbridge under A2 emissions scenario (2046-2065).

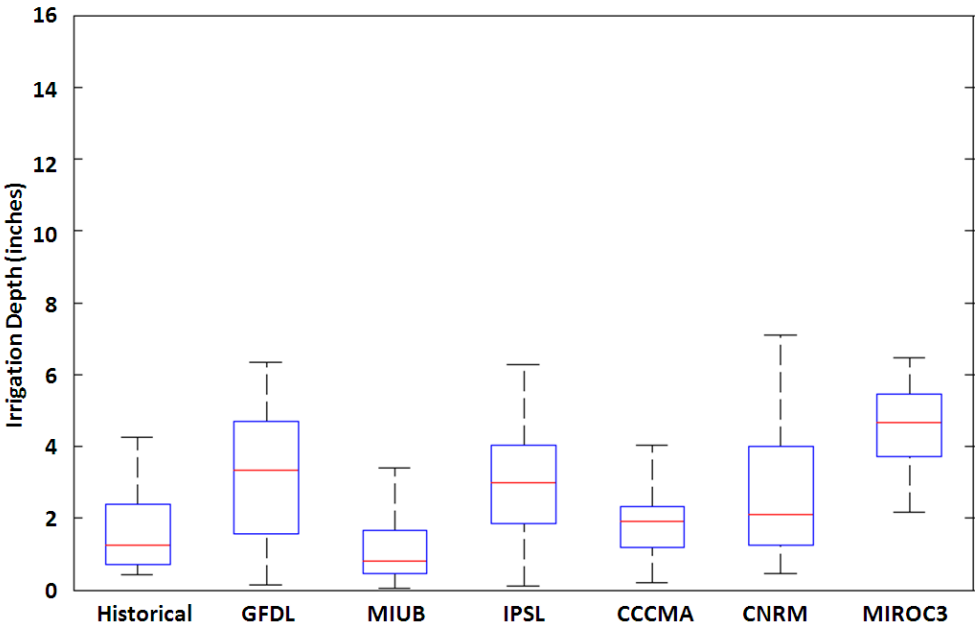

Figure A.69. June demand in Bainbridge under A2 emissions scenario (2081-2100).

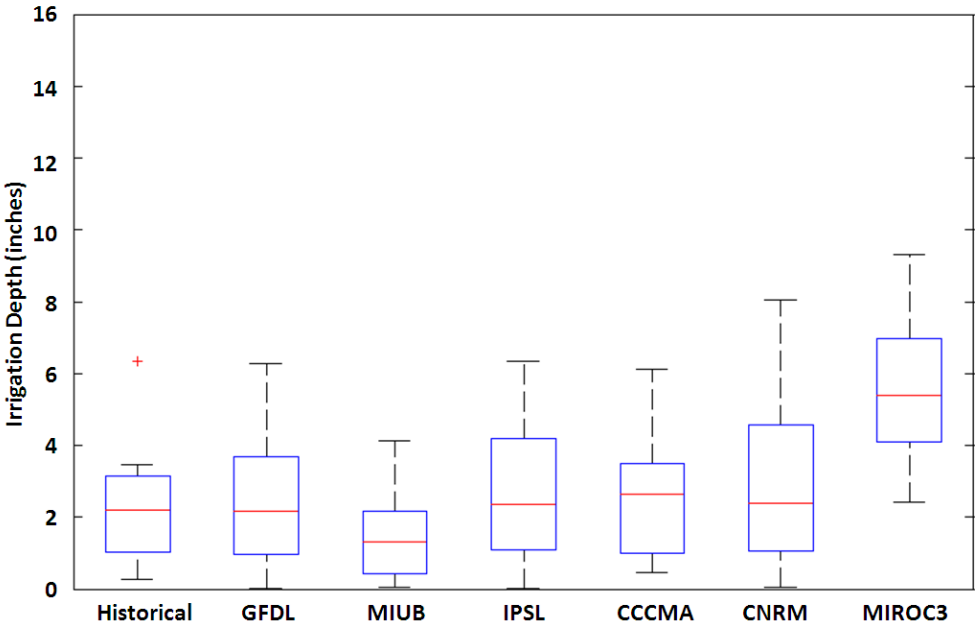

Figure A.70. July demand in Bainbridge under A2 emissions scenario (2046-2065).

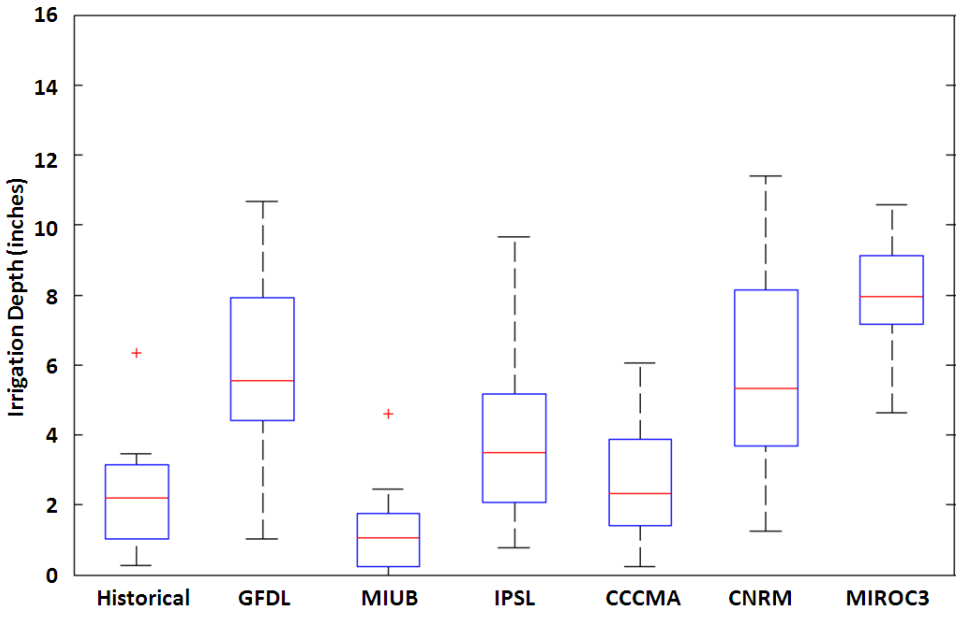

Figure A.71. July demand in Bainbridge under A2 emissions scenario (2081-2100).

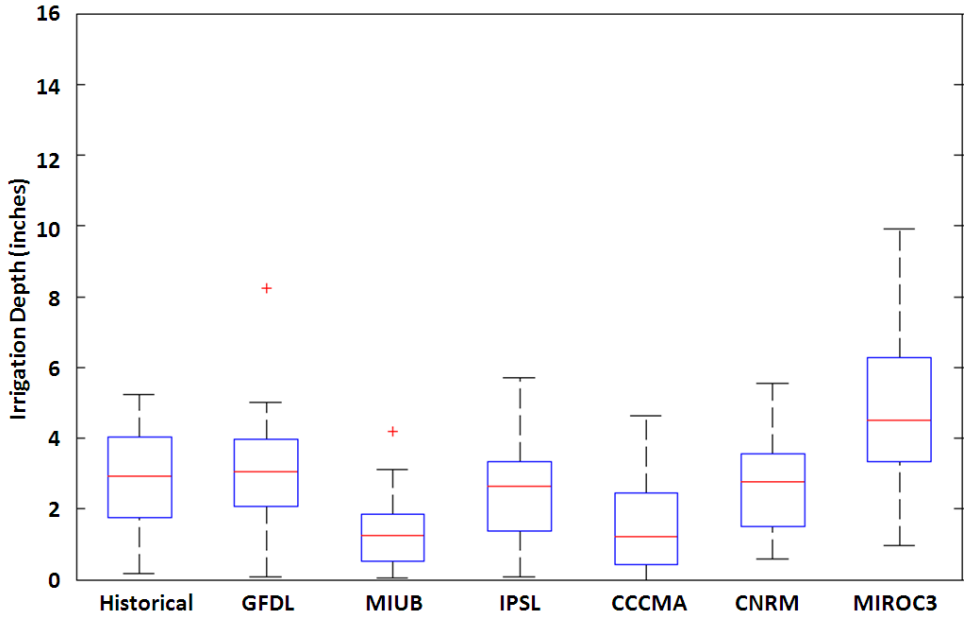

Figure A.72. August demand in Bainbridge under A2 emissions scenario (2046-2065).

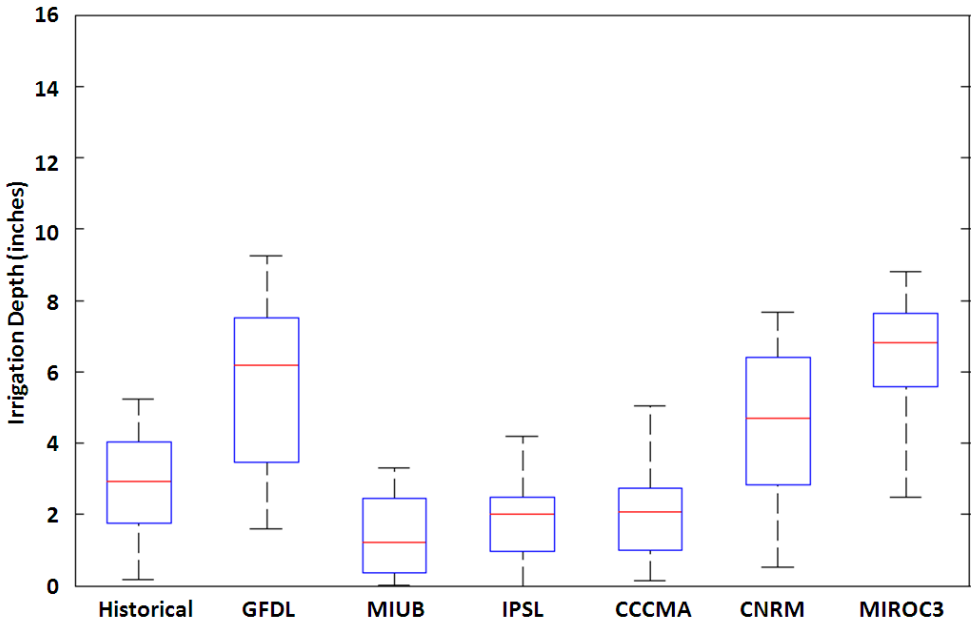

Figure A.73. August demand in Bainbridge under A2 emissions scenario (2081-2100).

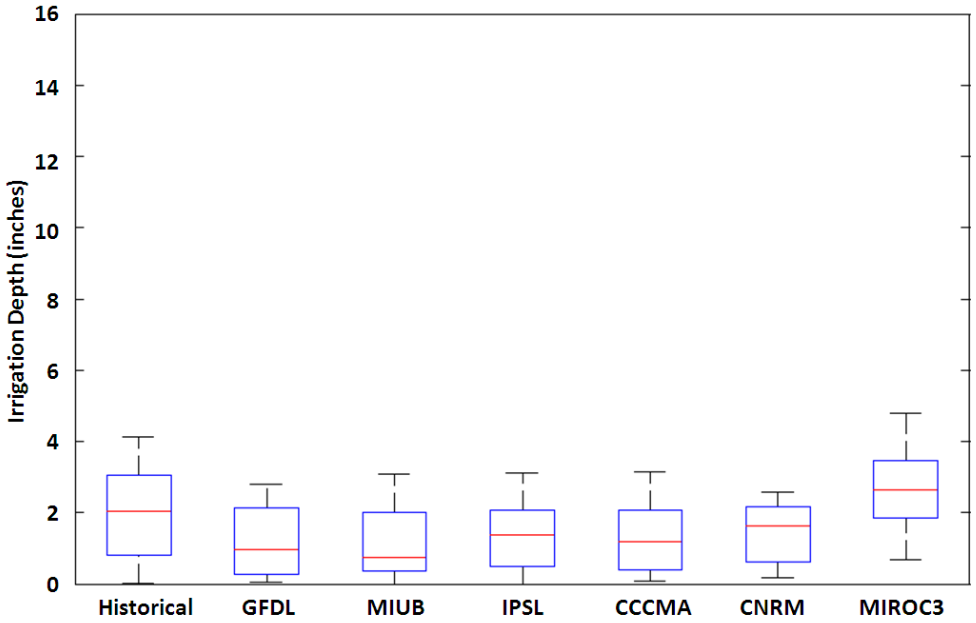

Figure A.74. Sept. demand in Bainbridge under A2 emissions scenario (2046-2065).

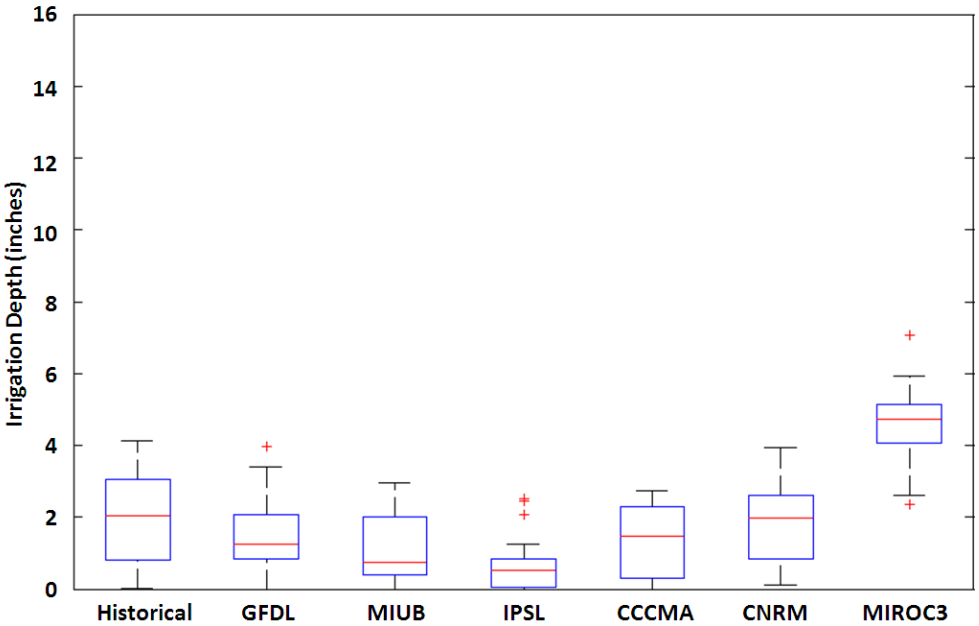

Figure A.75. Sept. demand in Bainbridge under A2 emissions scenario (2081-2100).

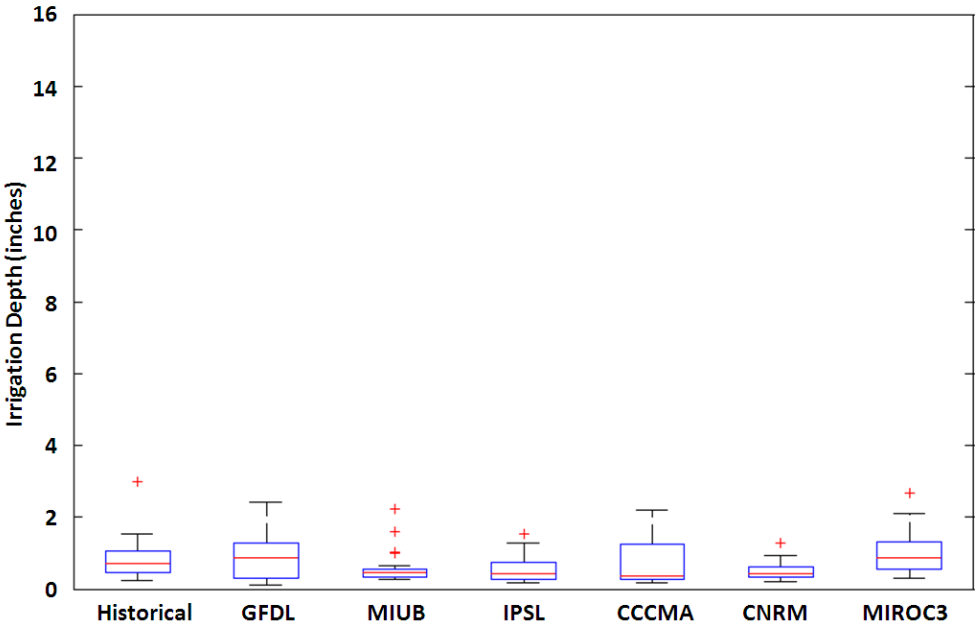

Figure A.76. May demand in Iron City under A1B emissions scenario (2046-2065).

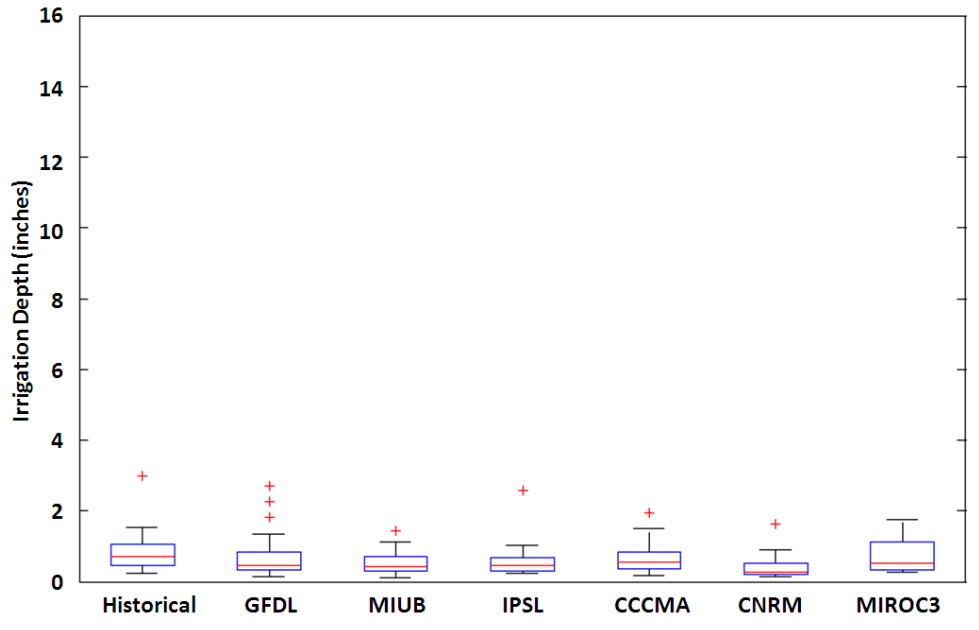

Figure A.77. May demand in Iron City under A1B emissions scenario (2081-2100).

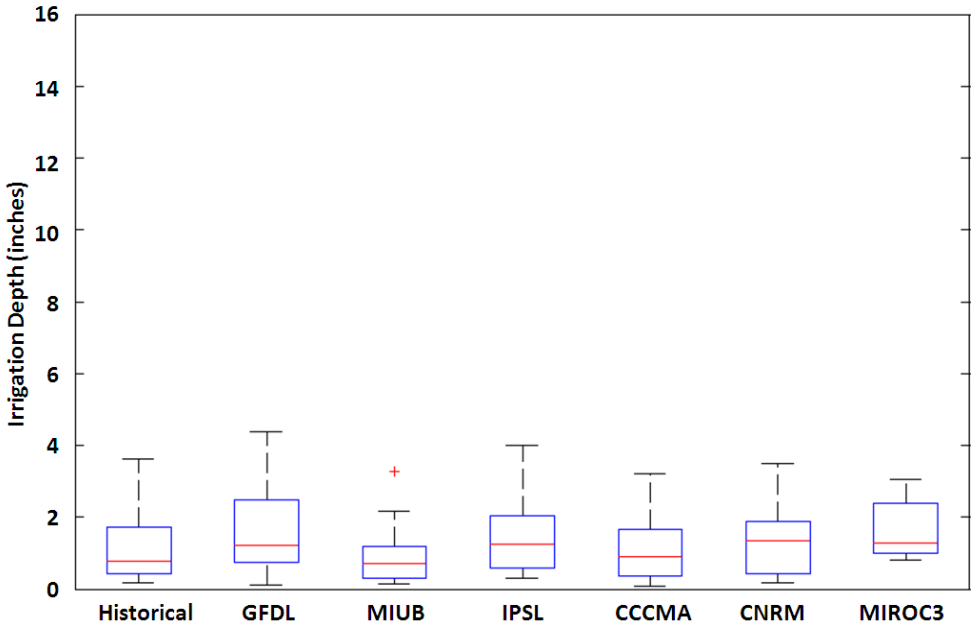

Figure A.78. June demand in Iron City under A1B emissions scenario (2046-2065).

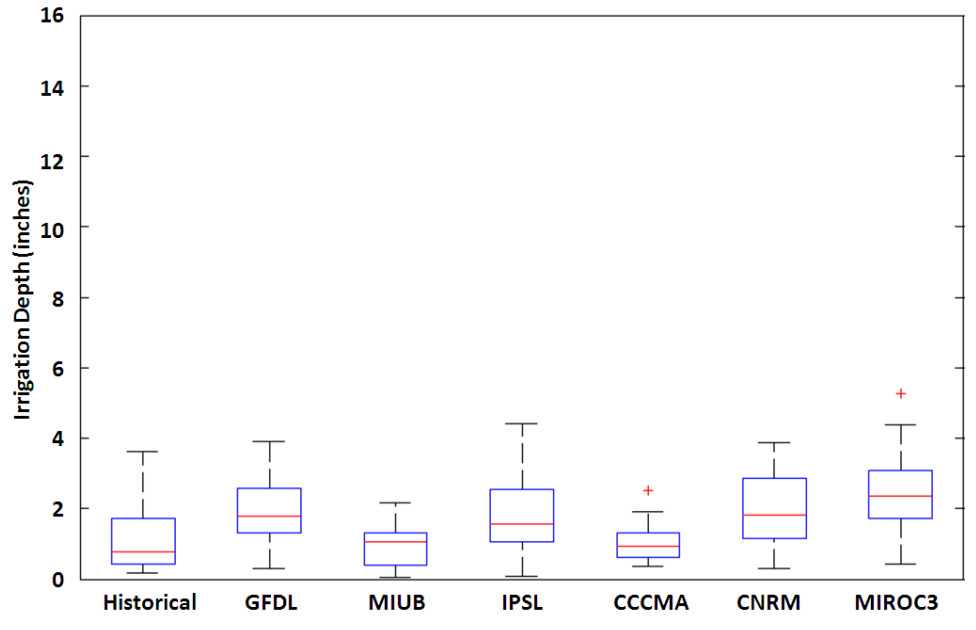

Figure A.79. June demand in Iron City under A1B emissions scenario (2081-2100).

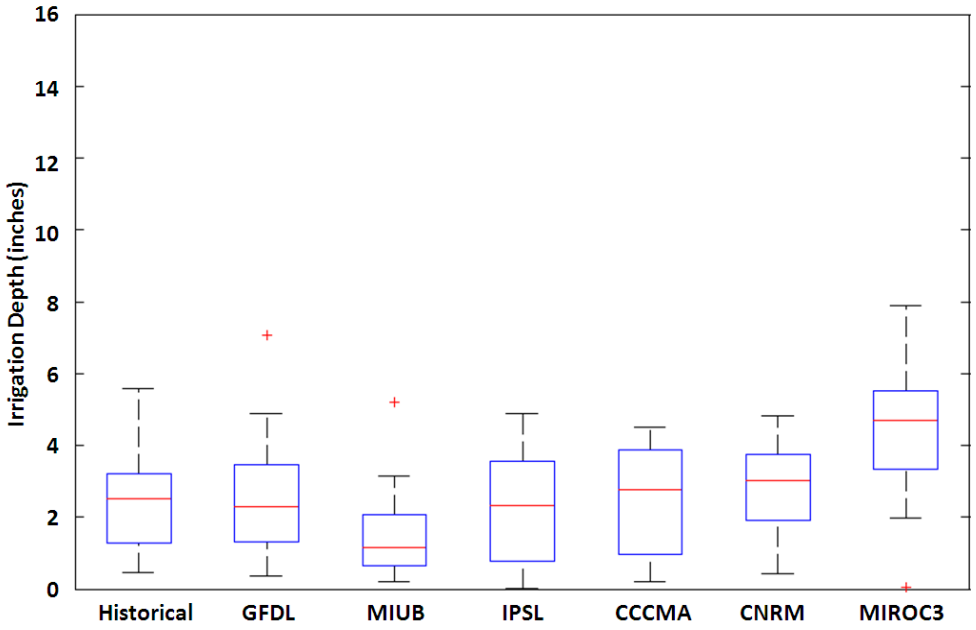

Figure A.80. July demand in Iron City under A1B emissions scenario (2046-2065).

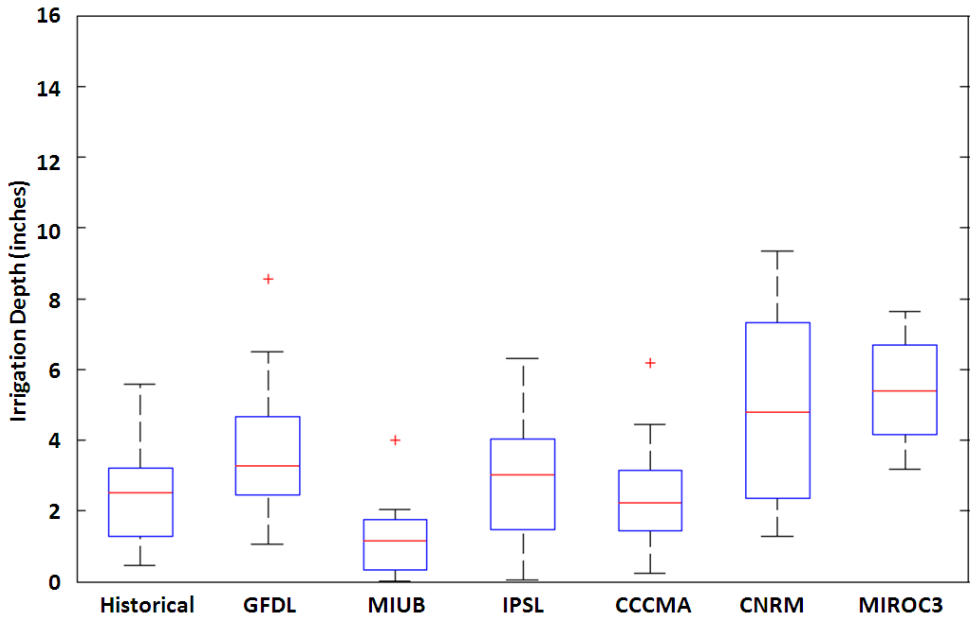

Figure A.81. July demand in Iron City under A1B emissions scenario (2081-2100).

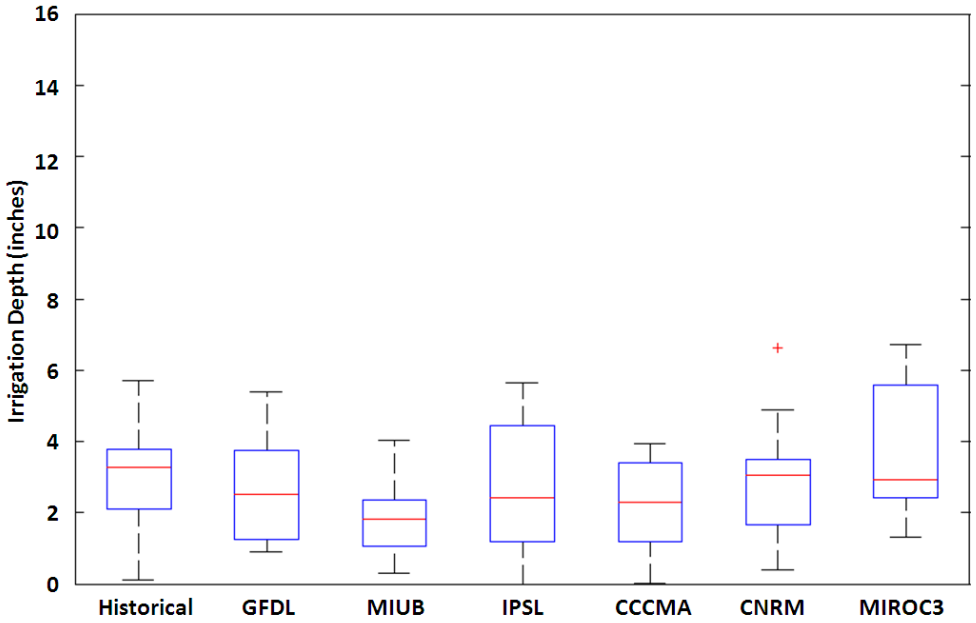

Figure A.82. August demand in Iron City under A1B emissions scenario (2046-2065).

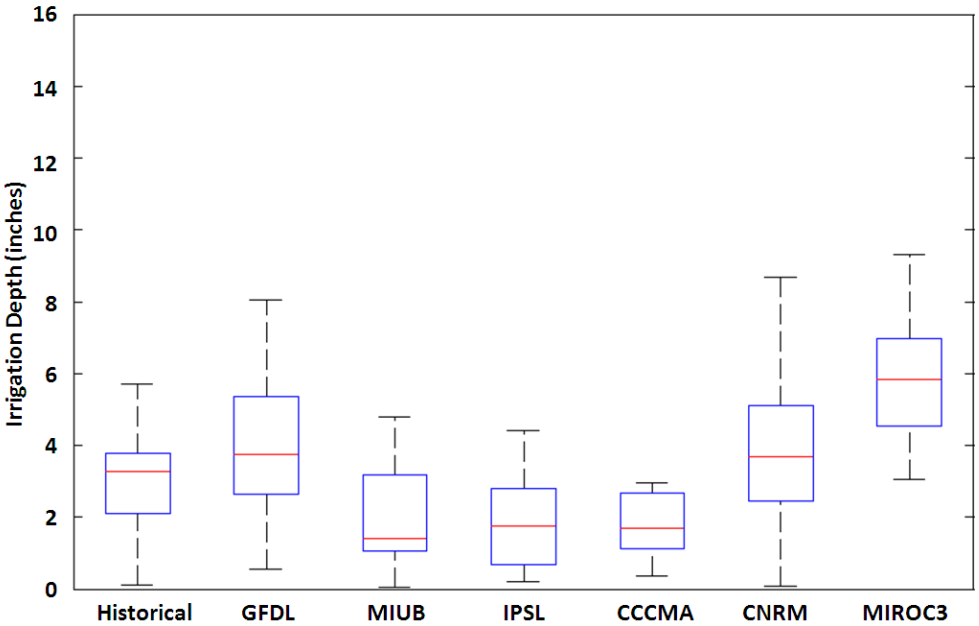

Figure A.83. August demand in Iron City under A1B emissions scenario (2081-2100).

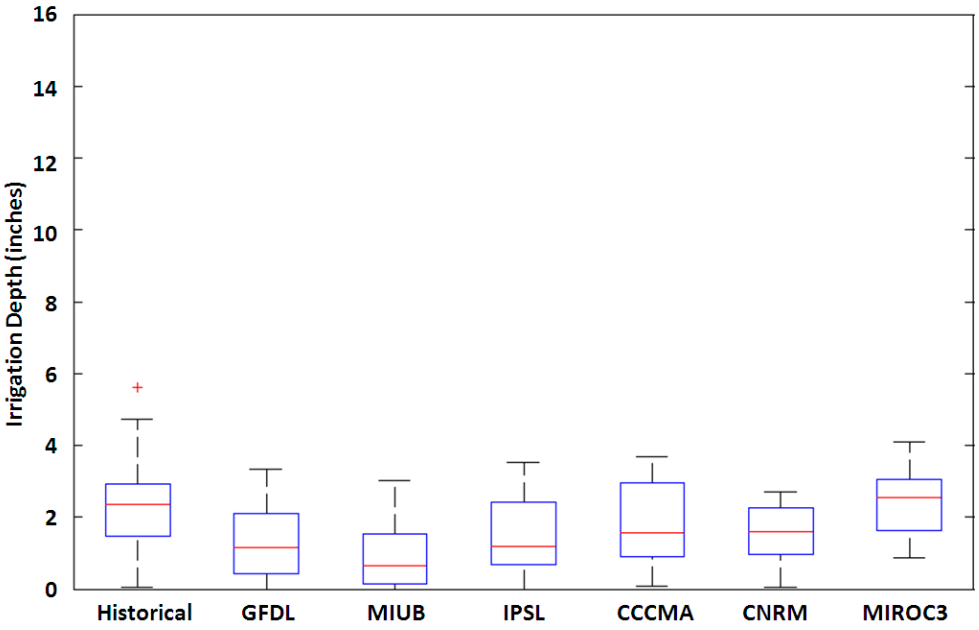

Figure A.84. Sept. demand in Iron City under A1B emissions scenario (2046-2065).

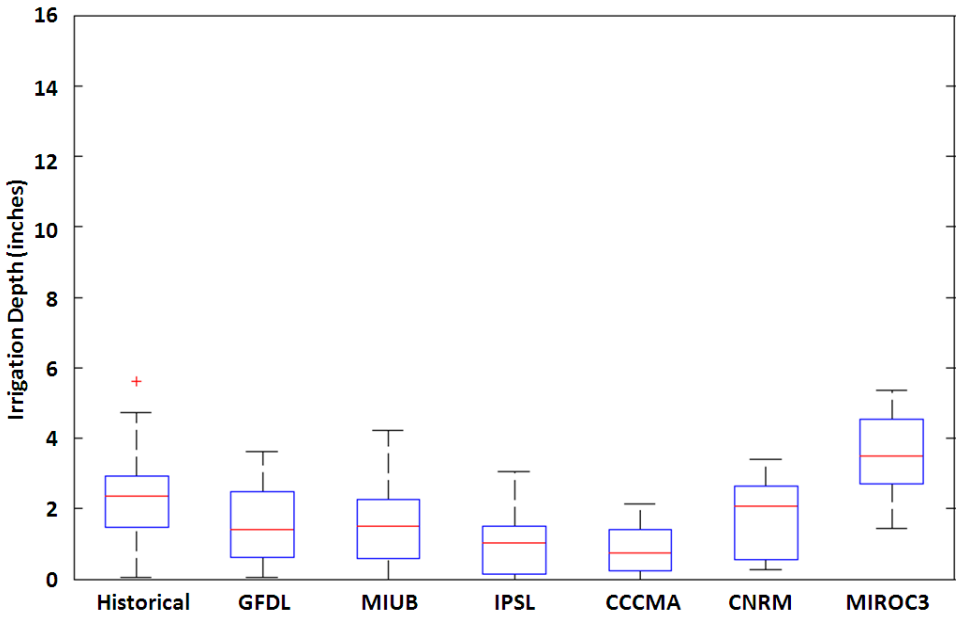

Figure A.85. Sept. demand in Iron City under A1B emissions scenario (2081-2100).

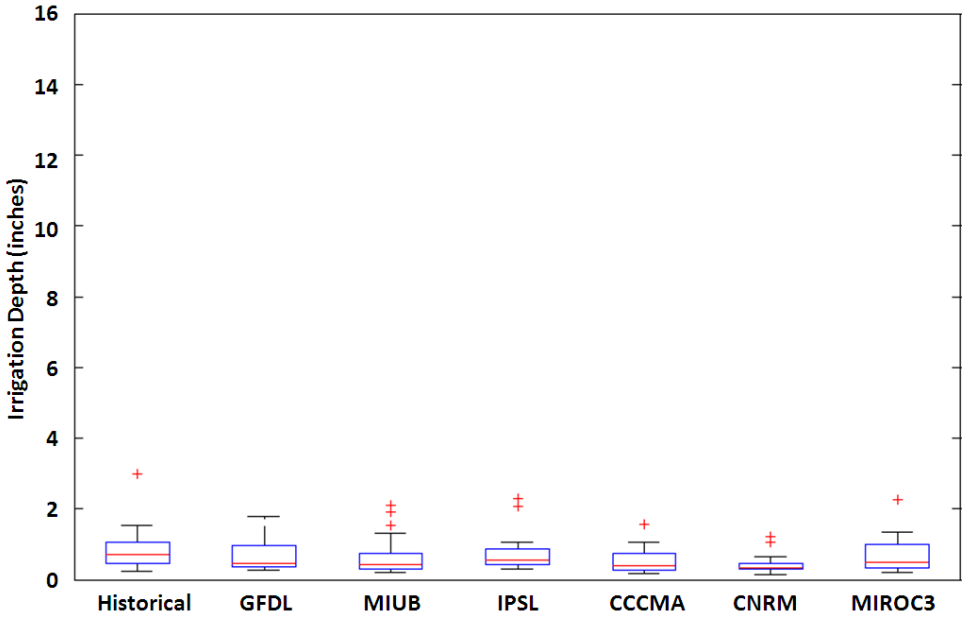

Figure A.86. May demand in Iron City under A2 emissions scenario (2046-2065).

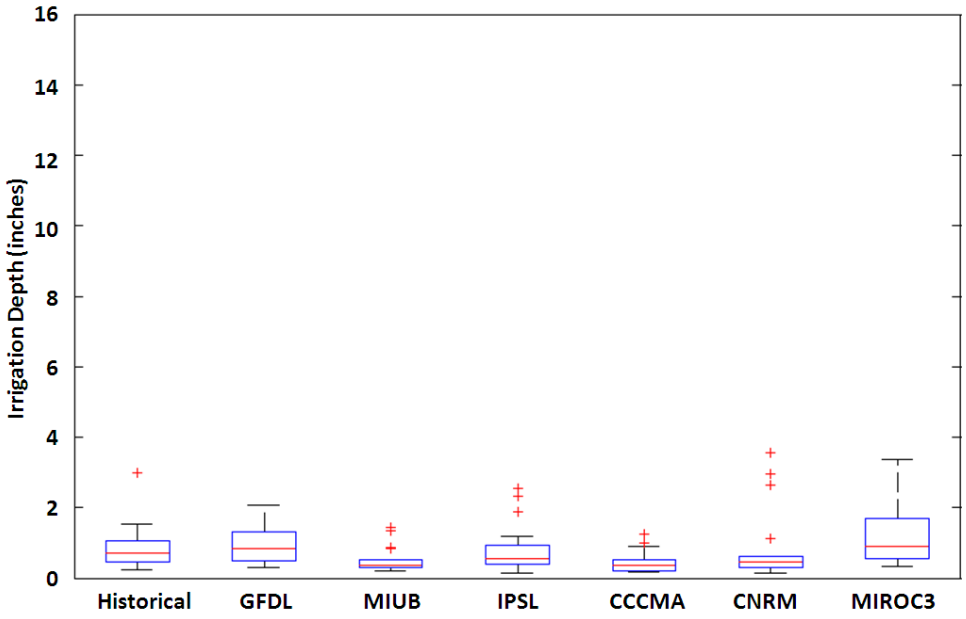

Figure A.87. May demand in Iron City under A2 emissions scenario (2081-2100).

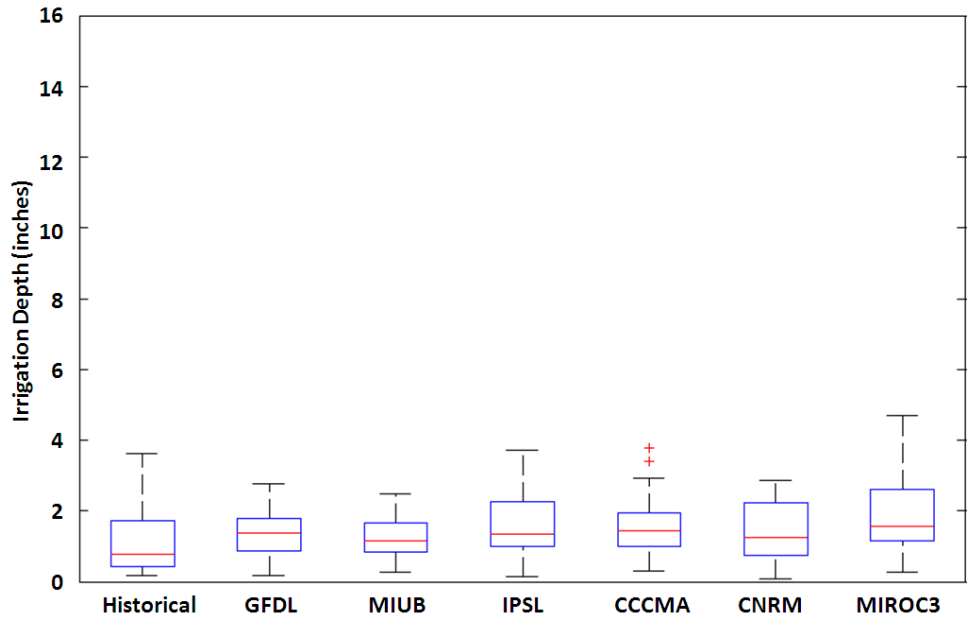

Figure A.88. June demand in Iron City under A2 emissions scenario (2046-2065).

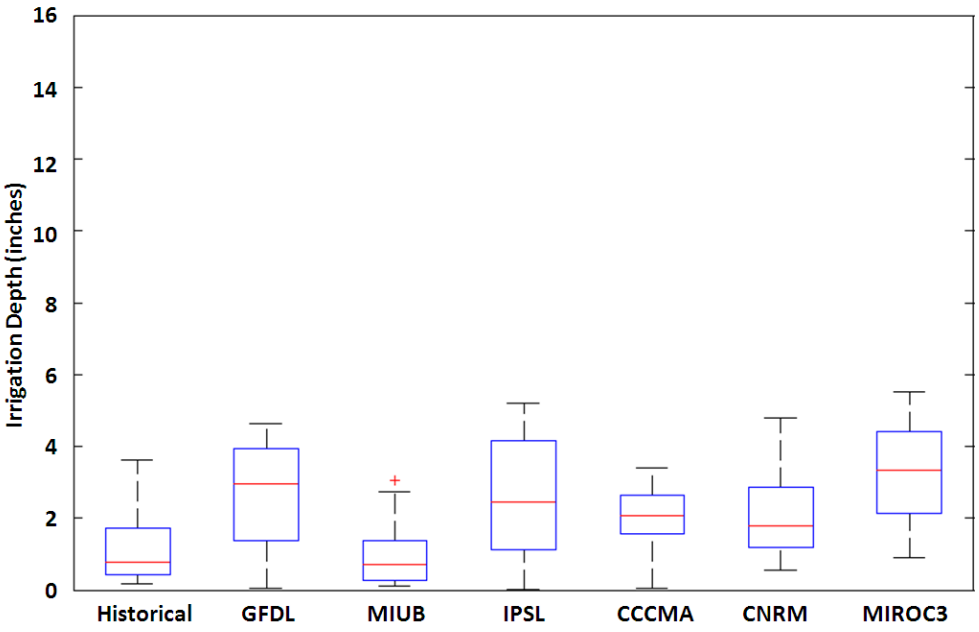

Figure A.89. June demand in Iron City under A2 emissions scenario (2081-2100).

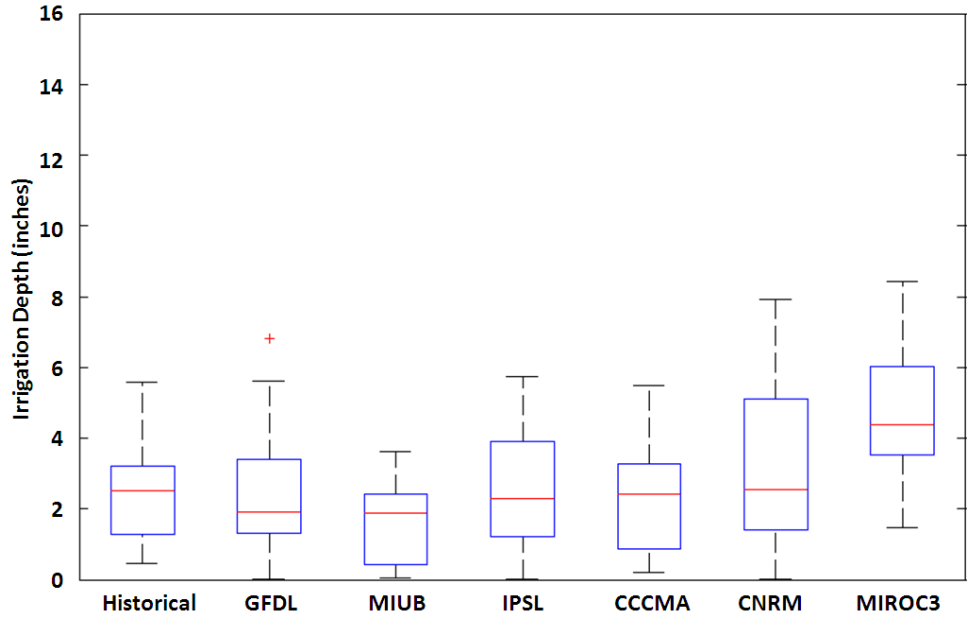

Figure A.90. July demand in Iron City under A2 emissions scenario (2046-2065).

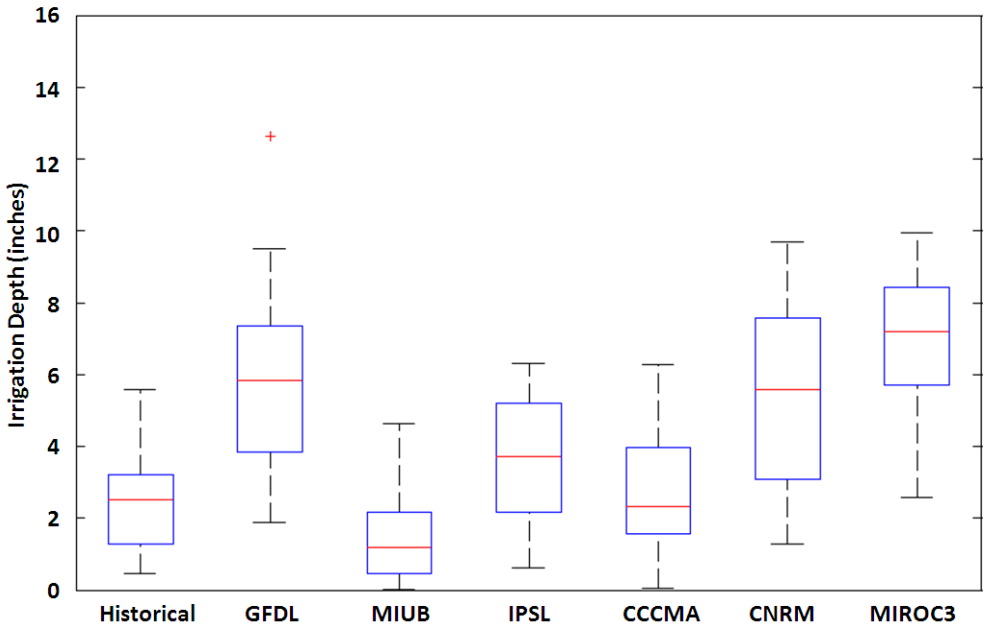

Figure A.91. July demand in Iron City under A2 emissions scenario (2081-2100).

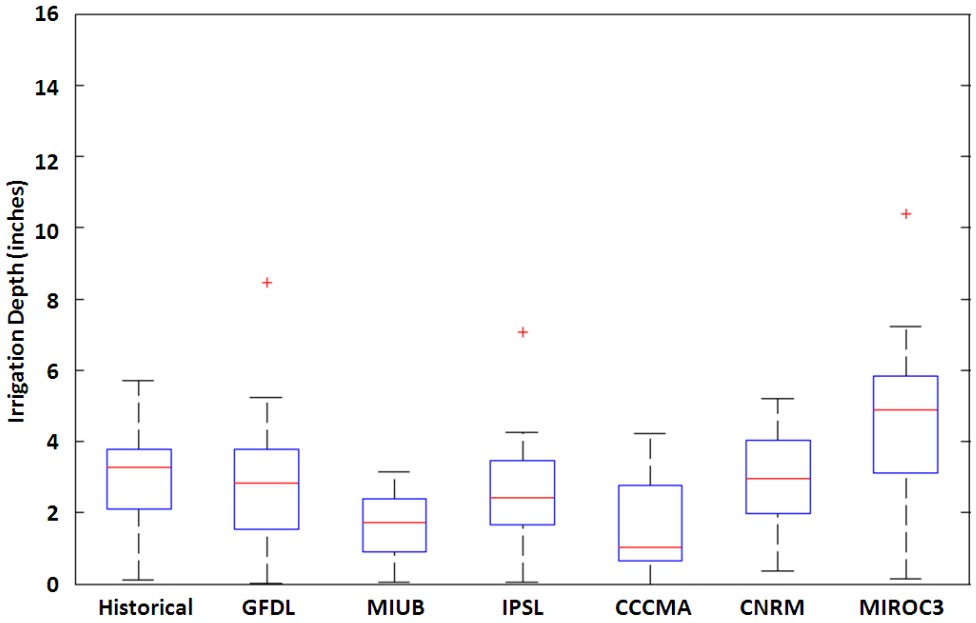

Figure A.92. August demand in Iron City under A2 emissions scenario (2046-2065).

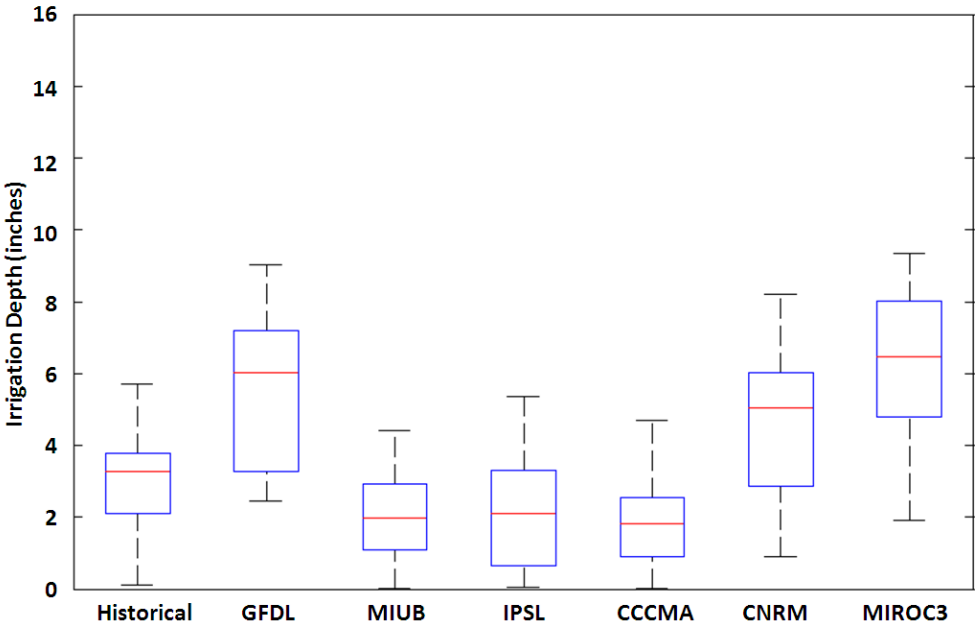

Figure A.93. August demand in Iron City under A2 emissions scenario (2081-2100).

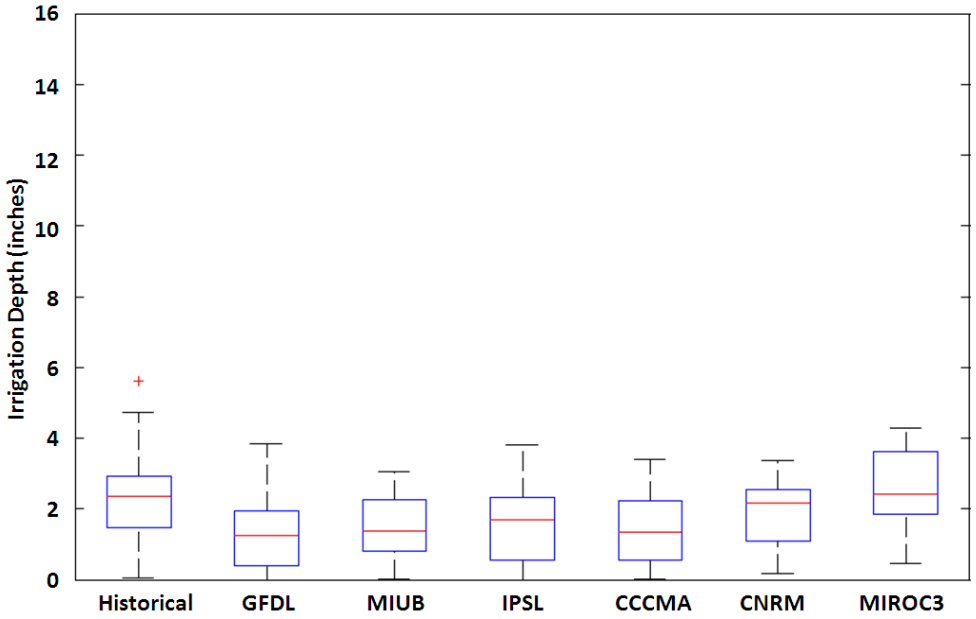

Figure A.94. Sept. demand in Iron City under A2 emissions scenario (2046-2065).

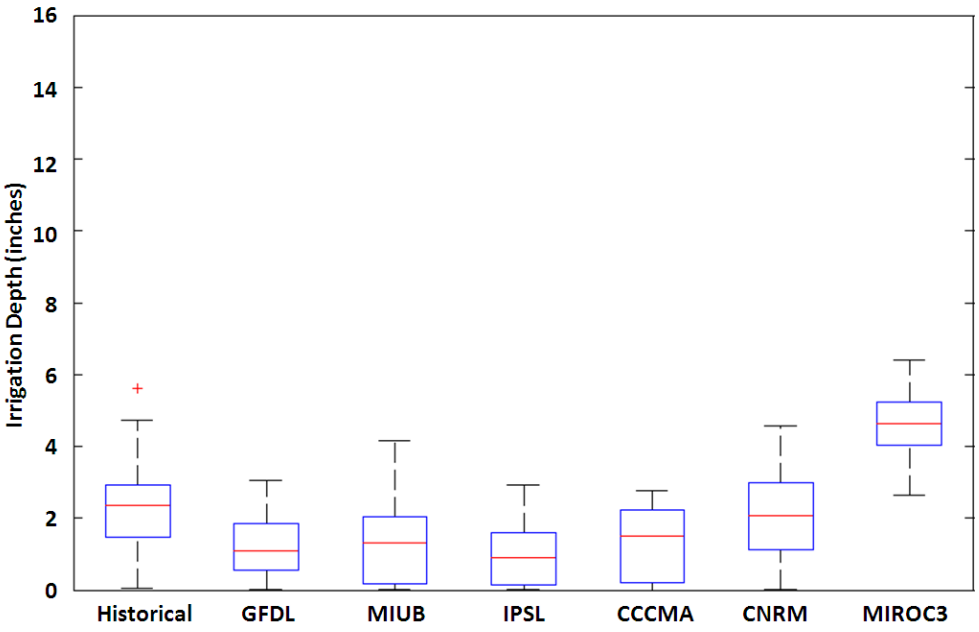

Figure A.95. Sept. demand in Iron City under A2 emissions scenario (2081-2100).

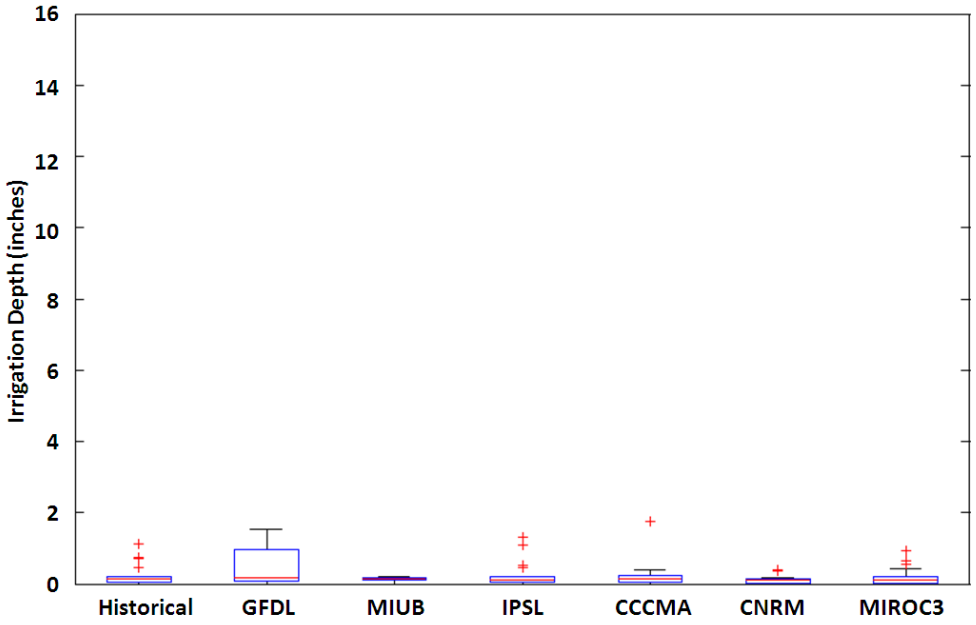

Figure A.96. May demand in Milford under A1B emissions scenario (2046-2065).

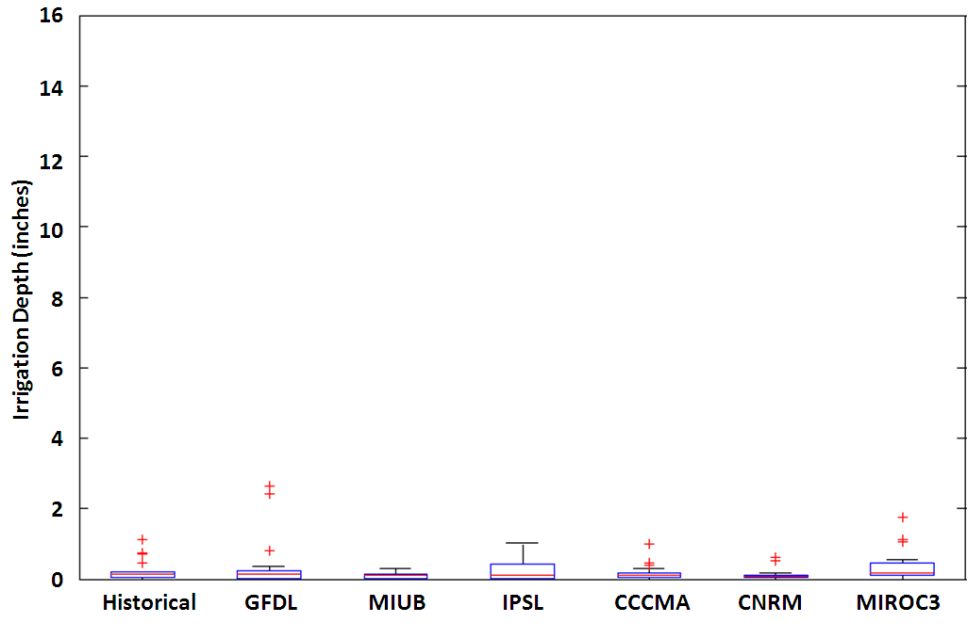

Figure A.97. May demand in Milford under A1B emissions scenario (2081-2100).

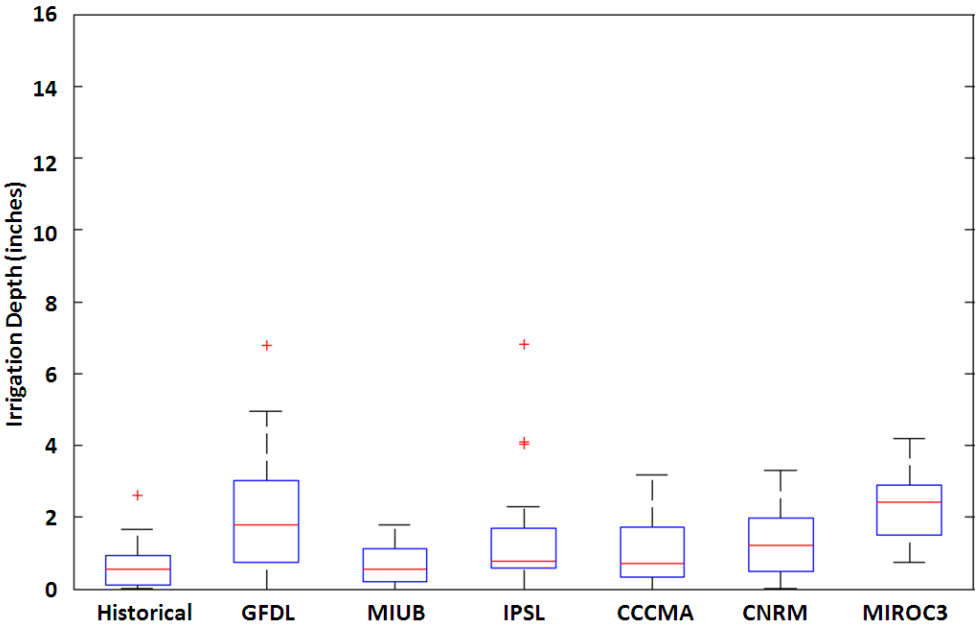

Figure 5.98. June demand in Milford under A1B emissions scenario (2046-2065).

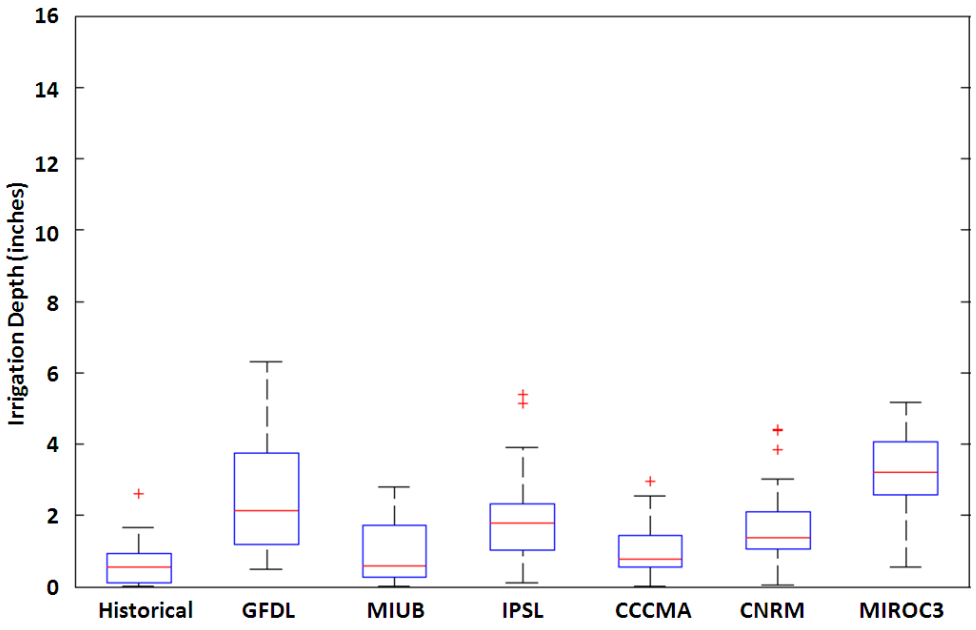

Figure A.99. June demand in Milford under A1B emissions scenario (2081-2100).

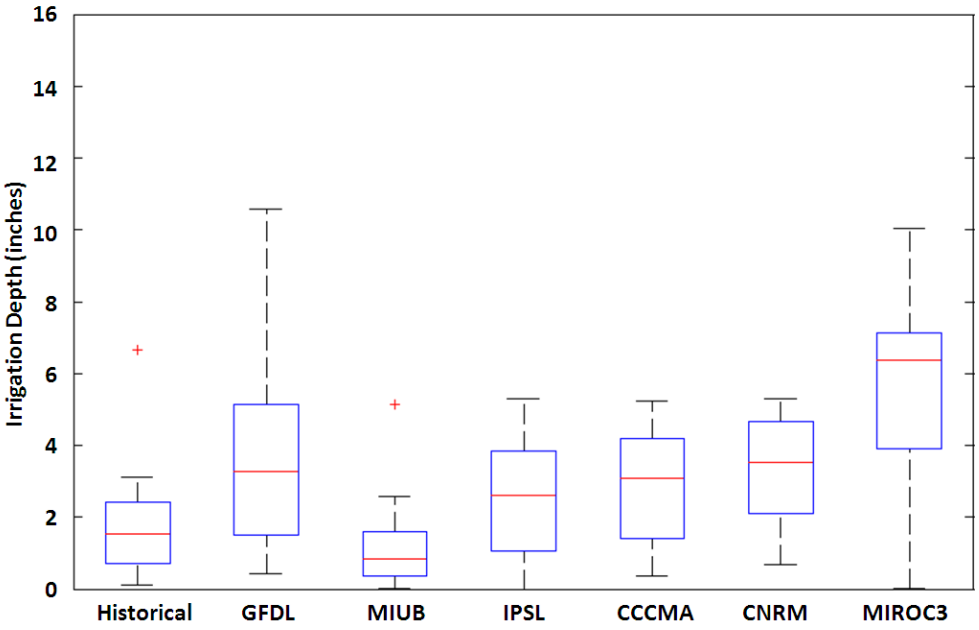

Figure A.100. July demand in Milford under A1B emissions scenario (2046-2065).

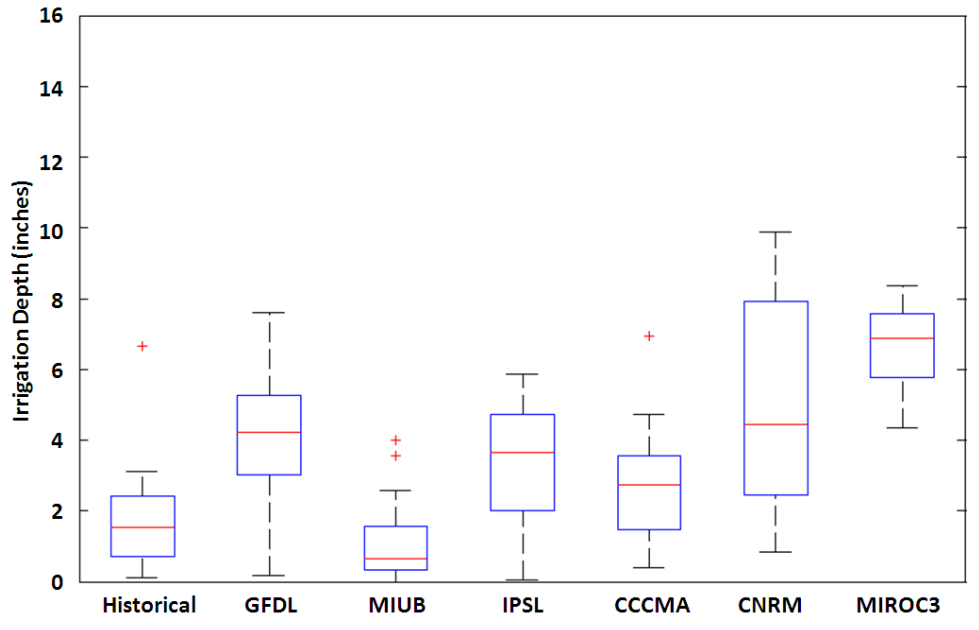

Figure A.101. July demand in Milford under A1B emissions scenario (2081-2100).

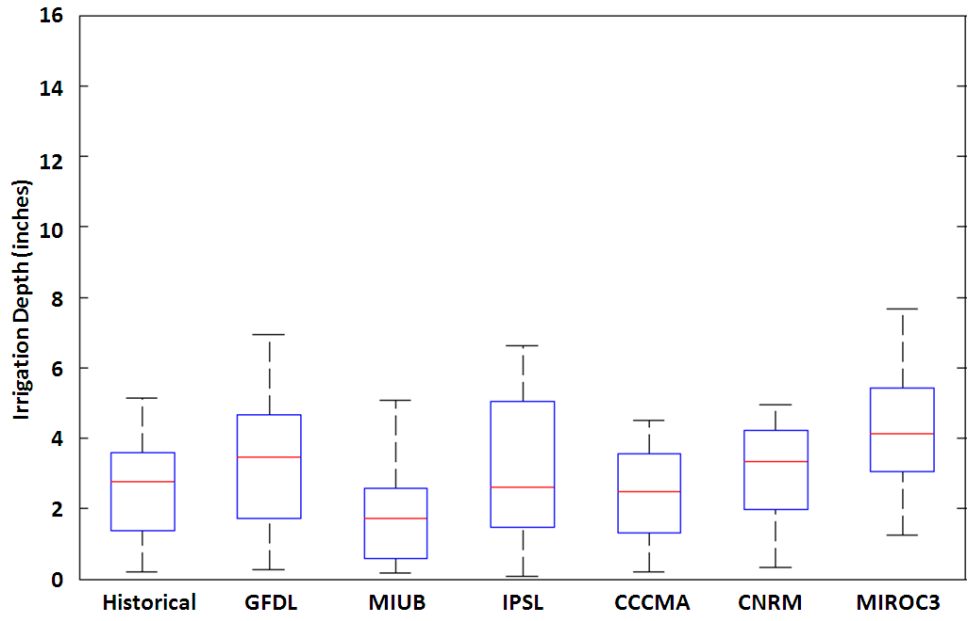

Figure A.102. August demand in Milford under A1B emissions scenario (2046-2065).

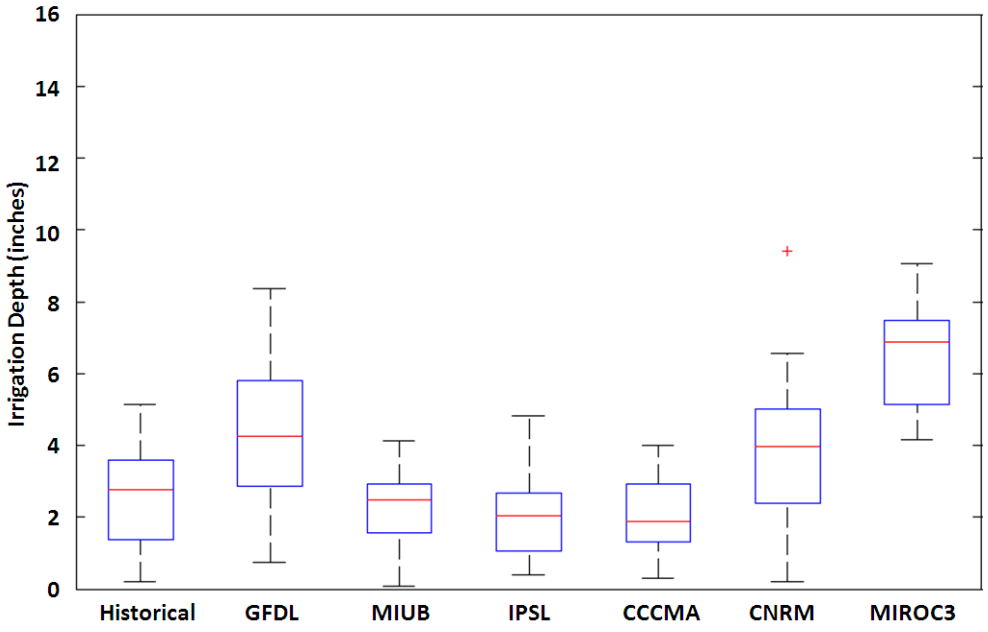

Figure A.103. August demand in Milford under A1B emissions scenario (2081-2100).

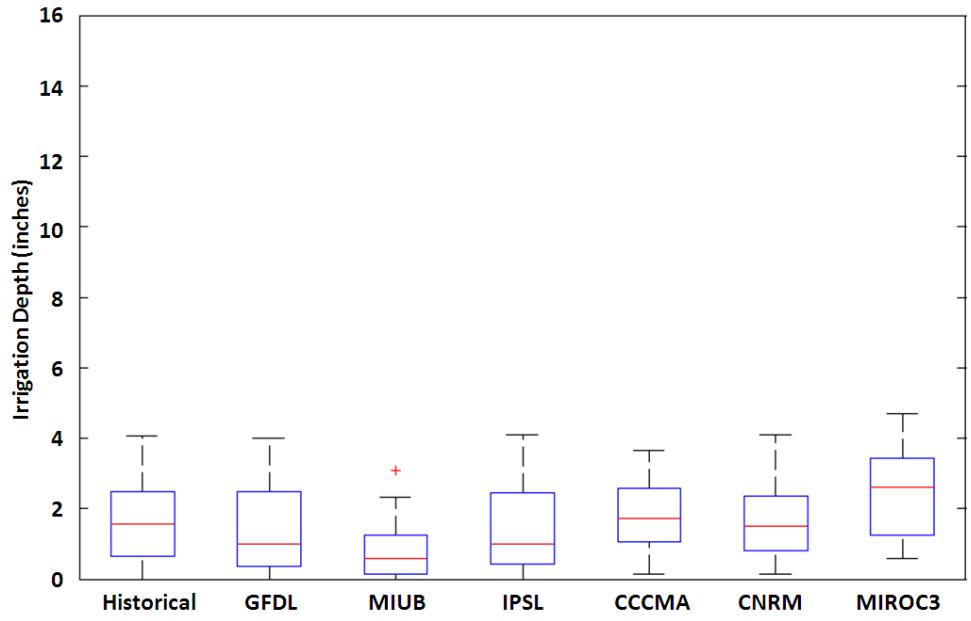

Figure A.104. Sept. demand in Milford under A1B emissions scenario (2046-2065).

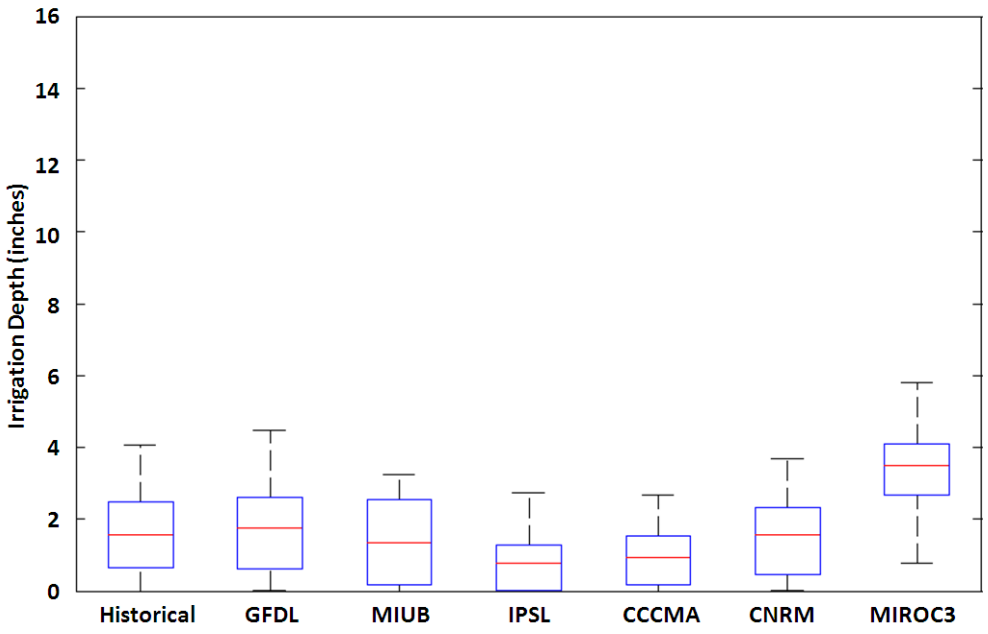

Figure A.105. Sept. demand in Milford under A1B emissions scenario (2081-2100).

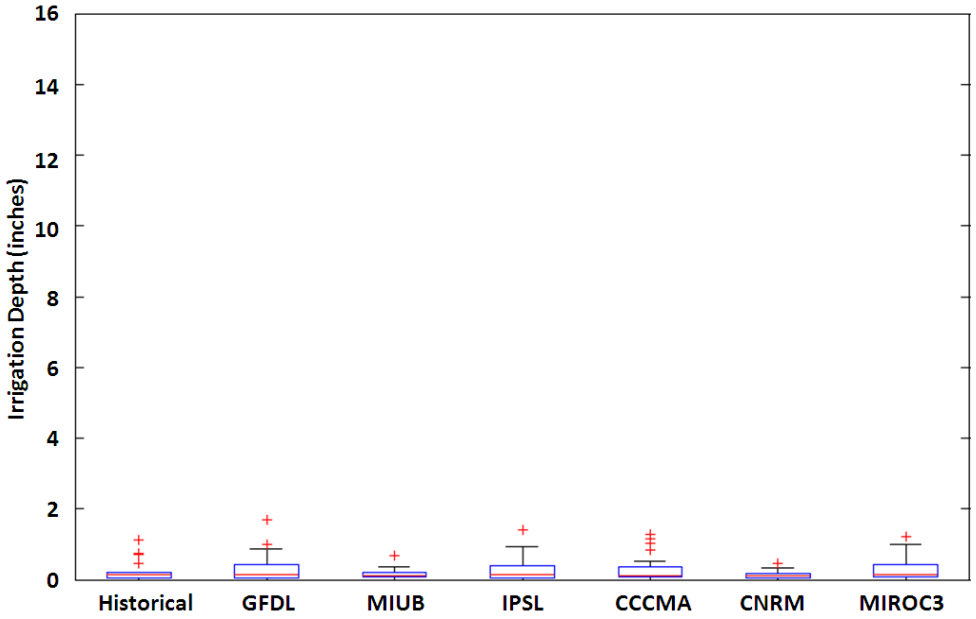

Figure A.106. May demand in Milford under A2 emissions scenario (2046-2065).

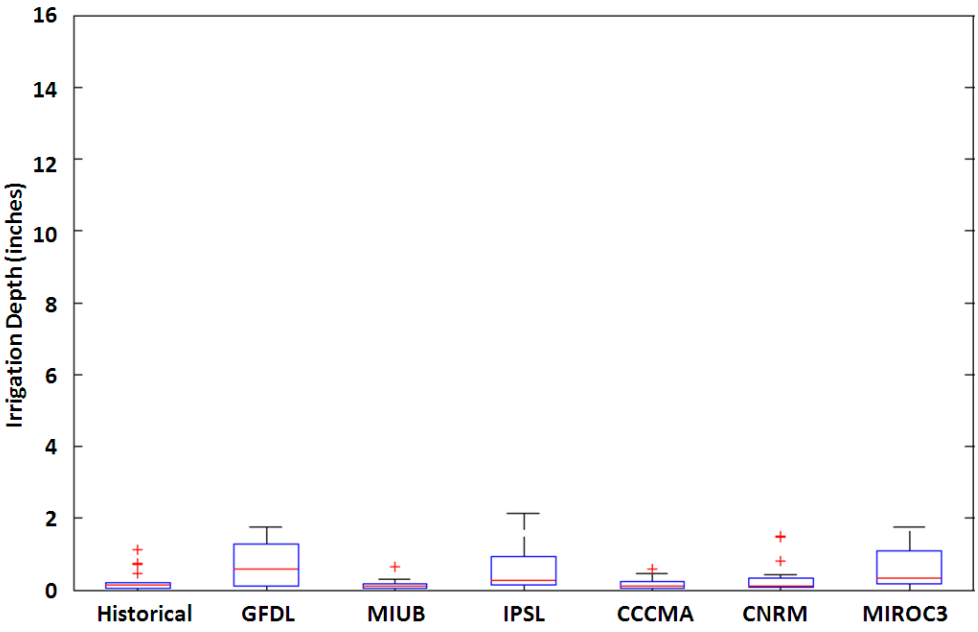

Figure A.107. May demand in Milford under A2 emissions scenario (2081-2100).

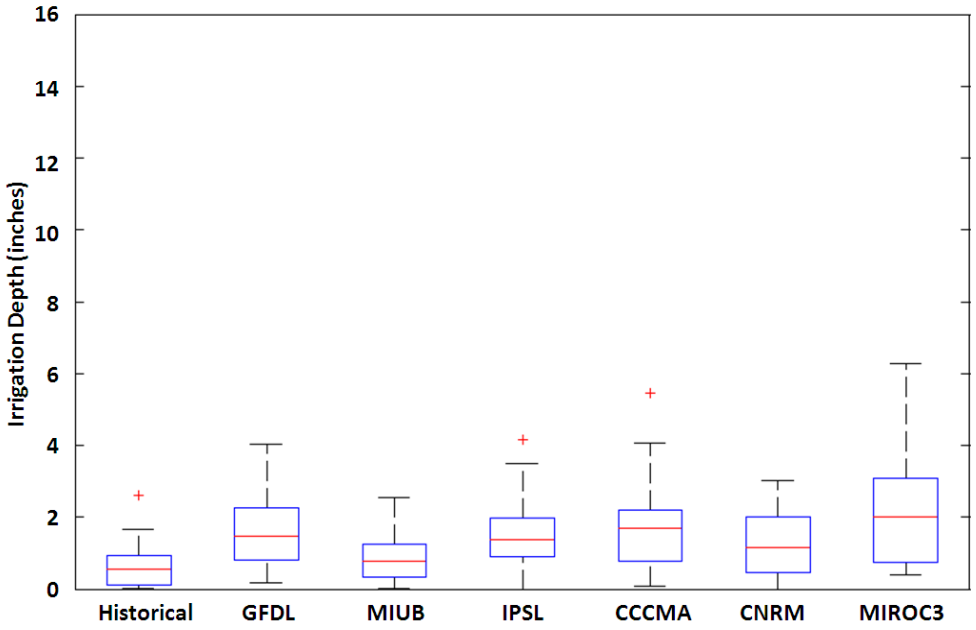

Figure A.108. June demand in Milford under A2 emissions scenario (2046-2065).

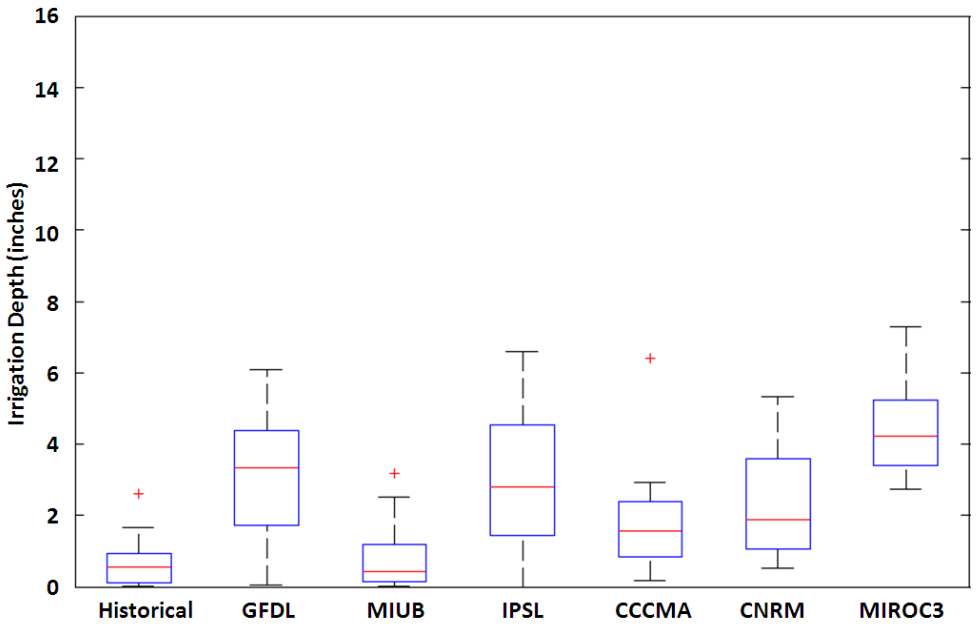

Figure A.109. June demand in Milford under A2 emissions scenario (2081-2100).

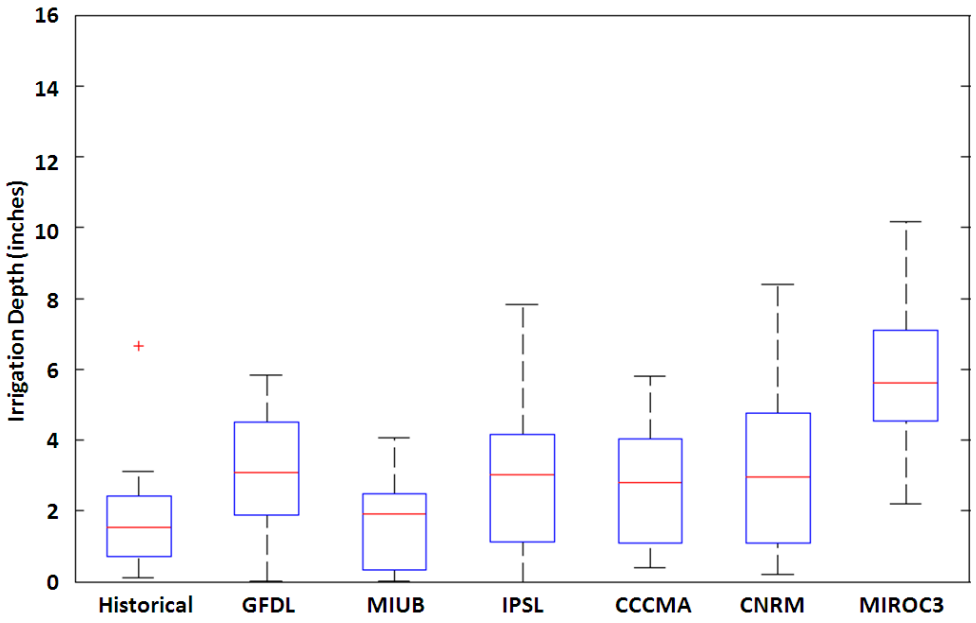

Figure A.110. July demand in Milford under A2 emissions scenario (2046-2065).

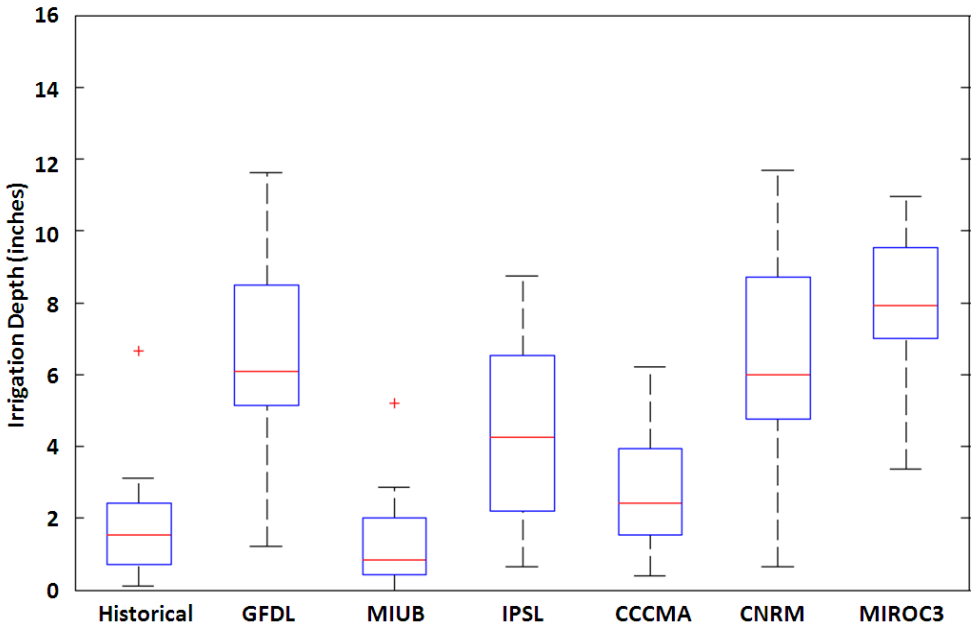

Figure A.111. July demand in Milford under A2 emissions scenario (2081-2100).

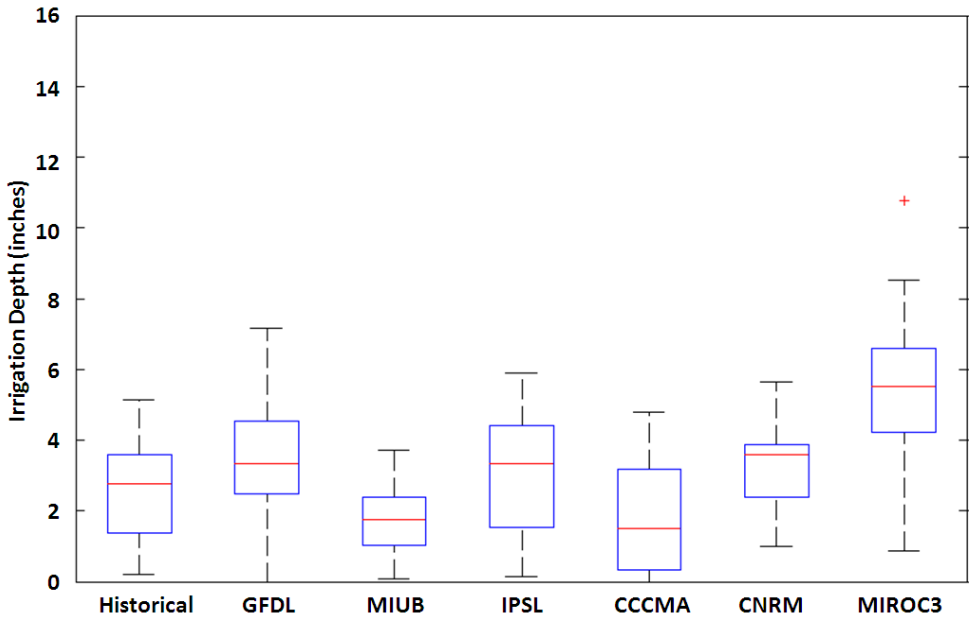

Figure A.112. August demand in Milford under A2 emissions scenario (2046-2065).

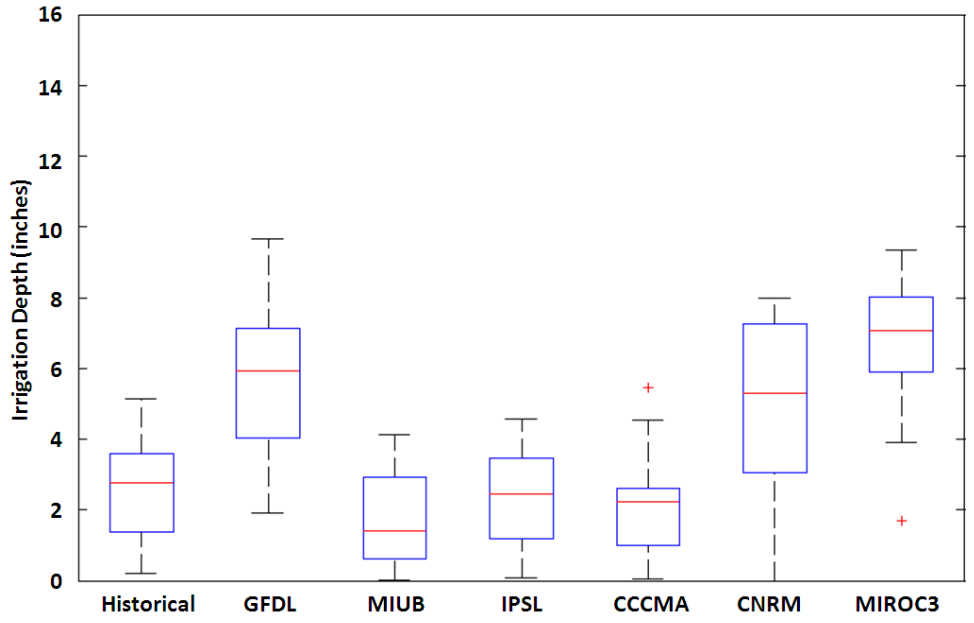

Figure A.113. August demand in Milford under A2 emissions scenario (2081-2100).

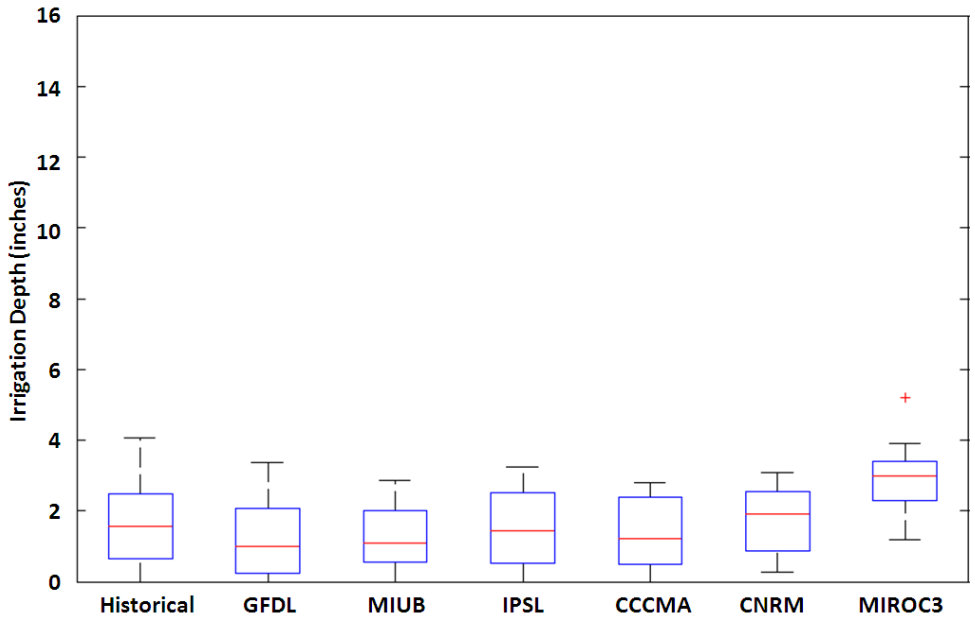

Figure A.114. Sept. demand in Milford under A2 emissions scenario (2046-2065).

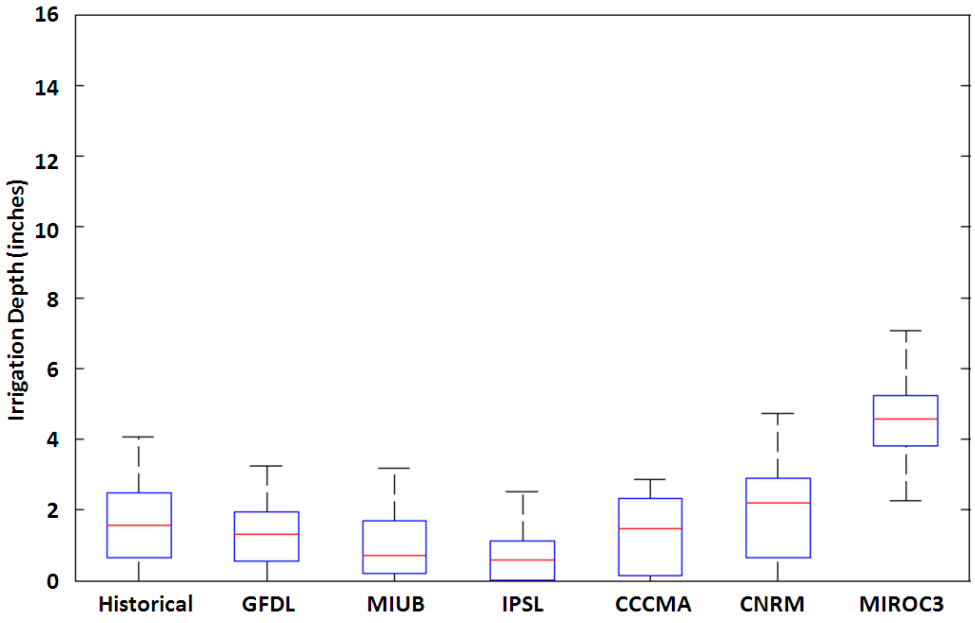

Figure A.115. Sept. demand in Milford under A2 emissions scenario (2081-2100).

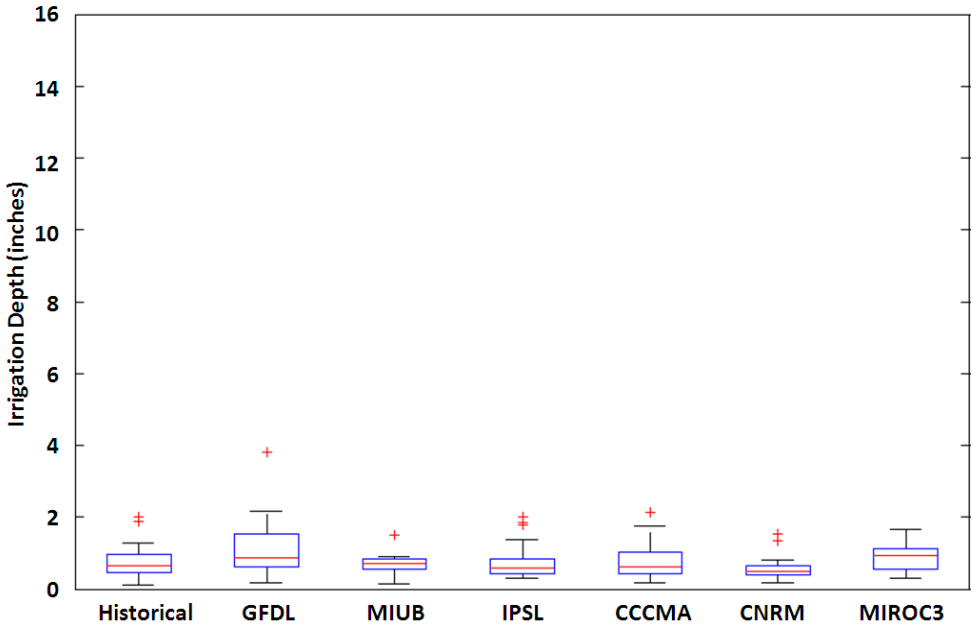

Figure A.116. May demand in Newton under A1B emissions scenario (2046-2065).

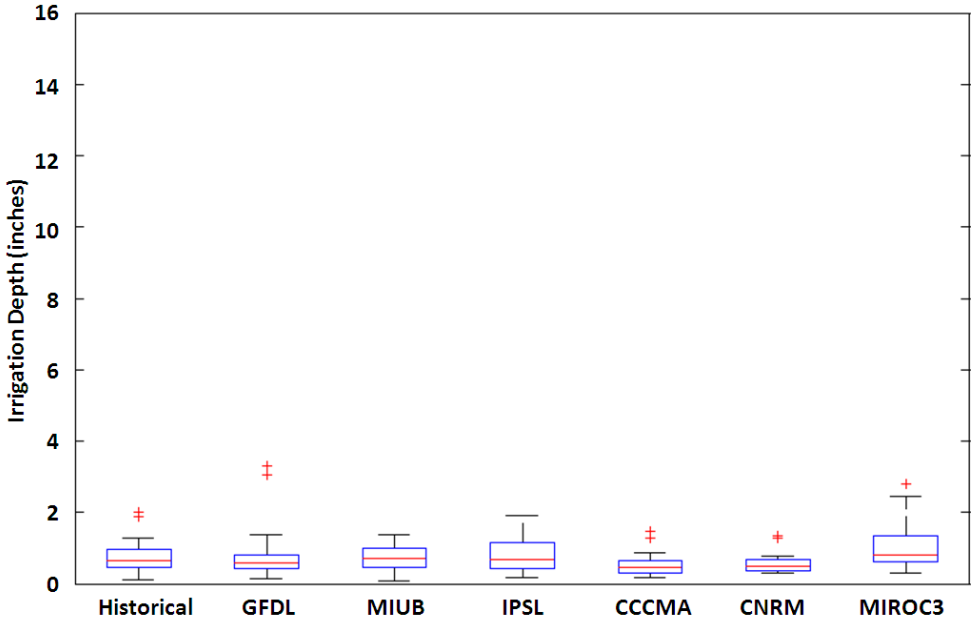

Figure A.117. May demand in Newton under A1B emissions scenario (2081-2100).

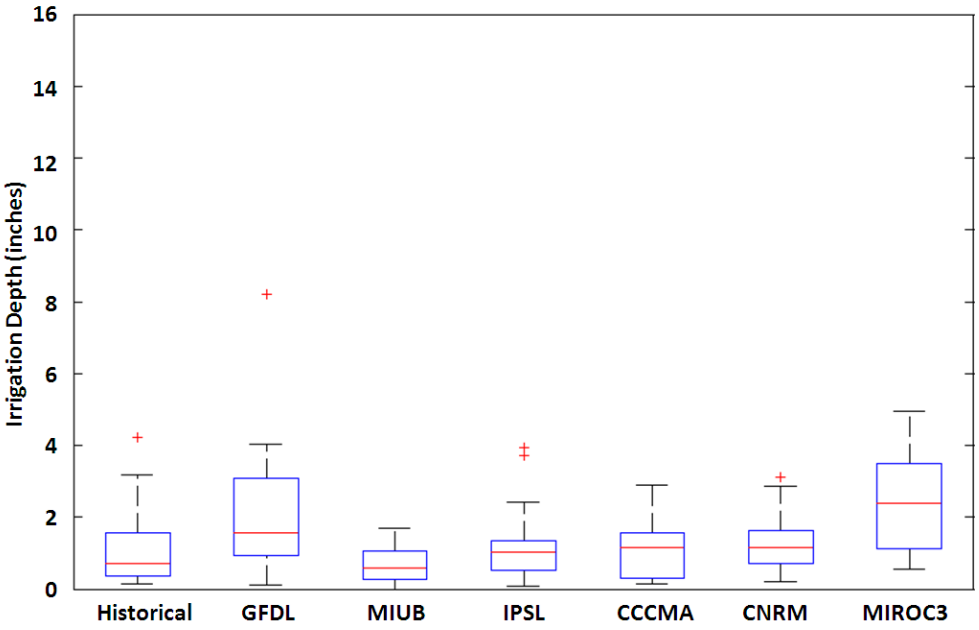

Figure A.118. June demand in Newton under A1B emissions scenario (2046-2065).

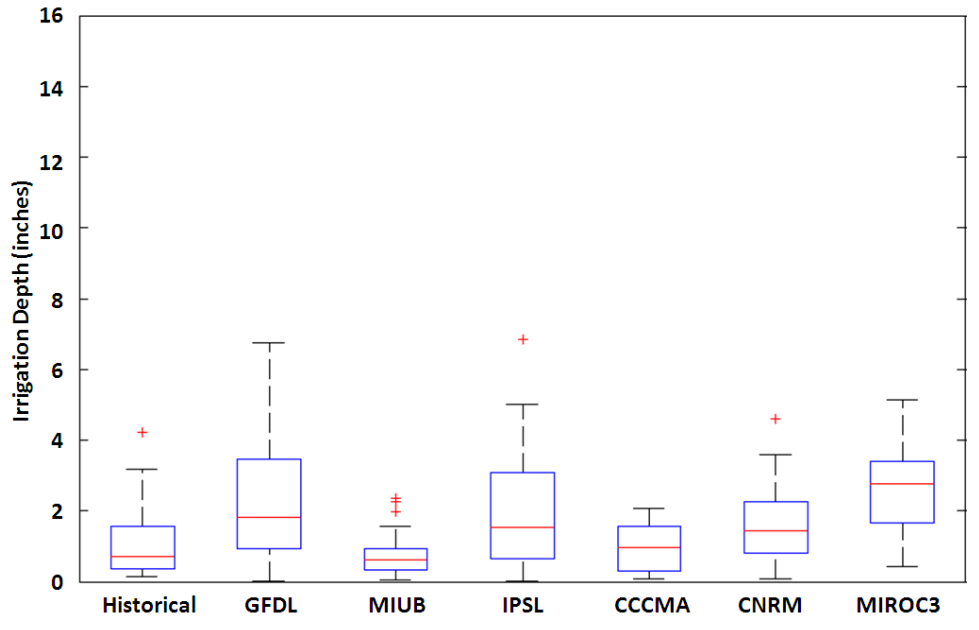

Figure A.119. June demand in Newton under A1B emissions scenario (2081-2100).

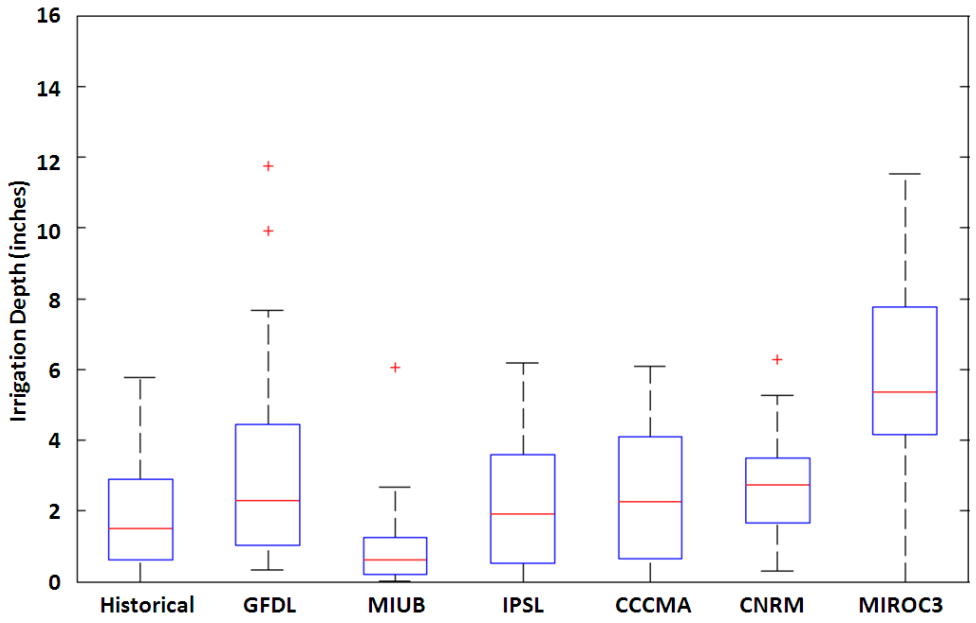

Figure A.120. July demand in Newton under A1B emissions scenario (2046-2065).

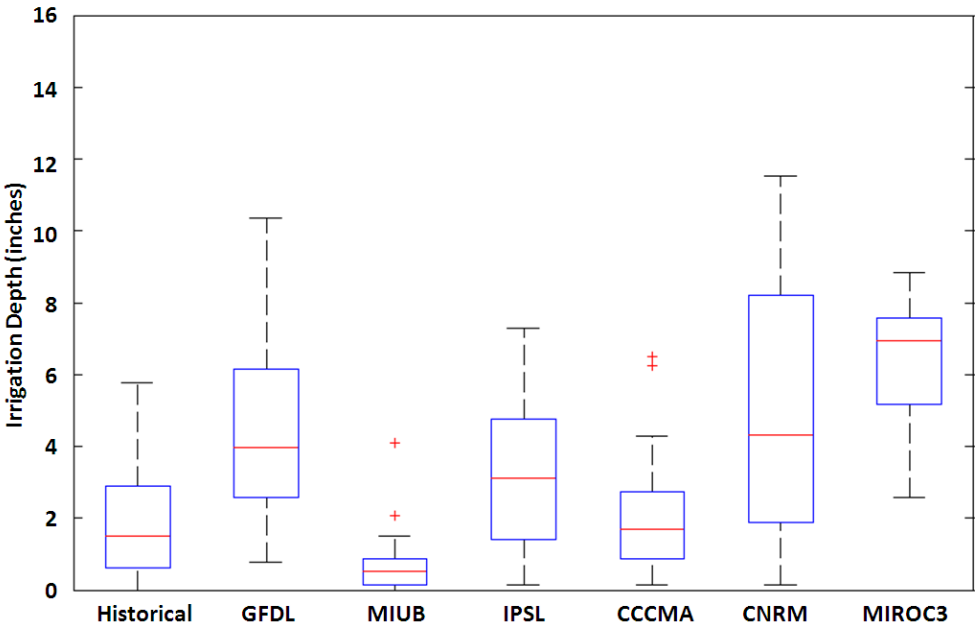

Figure A.121. July demand in Newton under A1B emissions scenario (2081-2100).

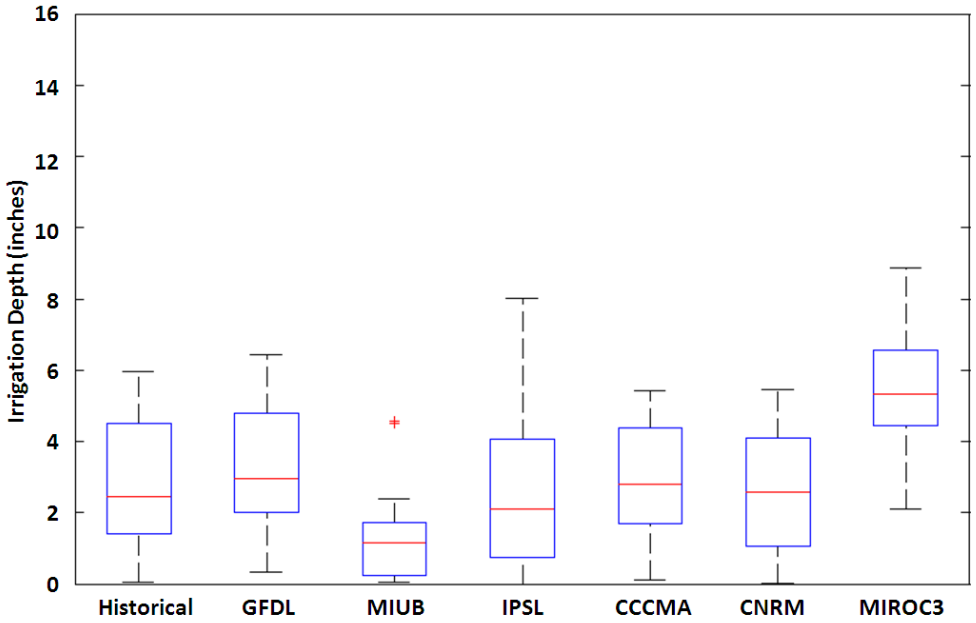

Figure A.122. August demand in Newton under A1B emissions scenario (2046-2065).

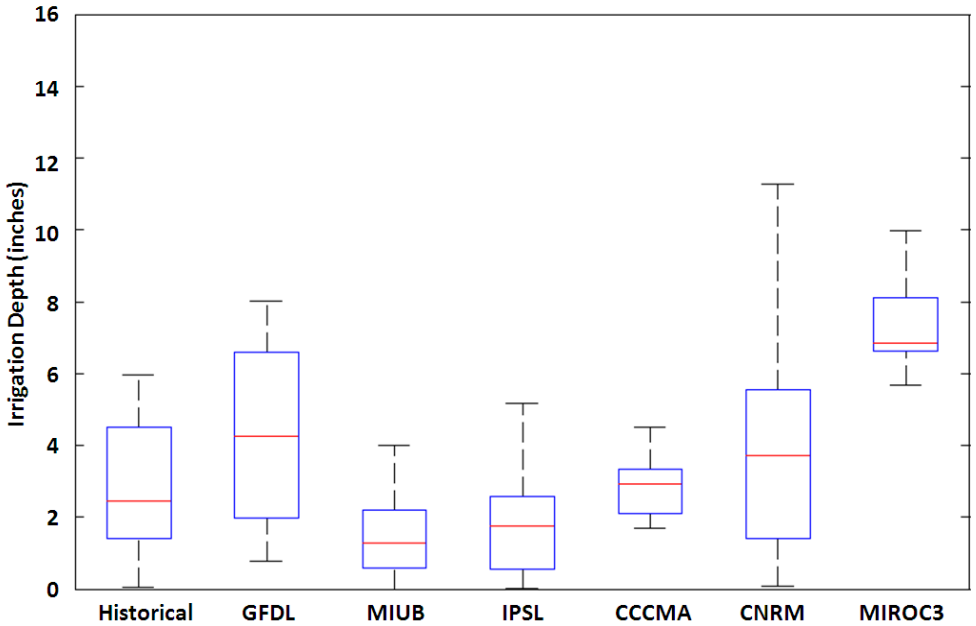

Figure A.123. August demand in Newton under A1B emissions scenario (2081-2100).

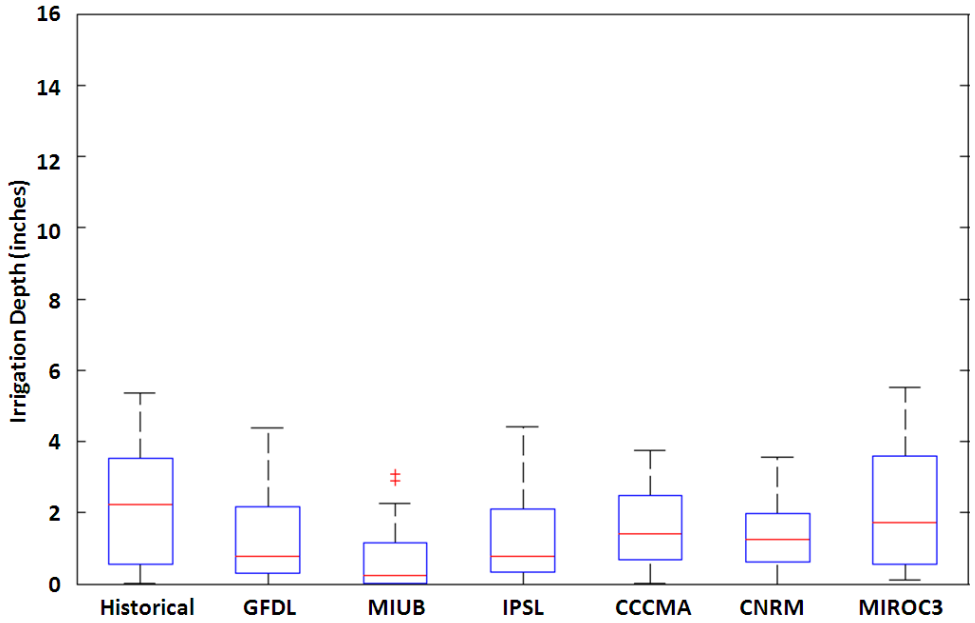

Figure A.124. Sept. demand in Newton under A1B emissions scenario (2046-2065).

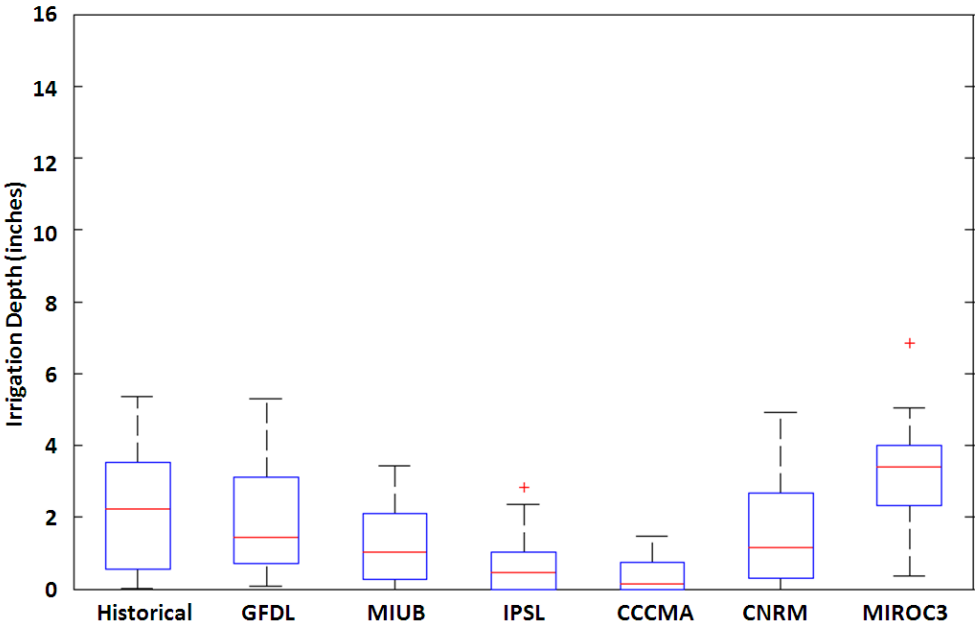

Figure A.125. Sept. demand in Newton under A1B emissions scenario (2081-2100).

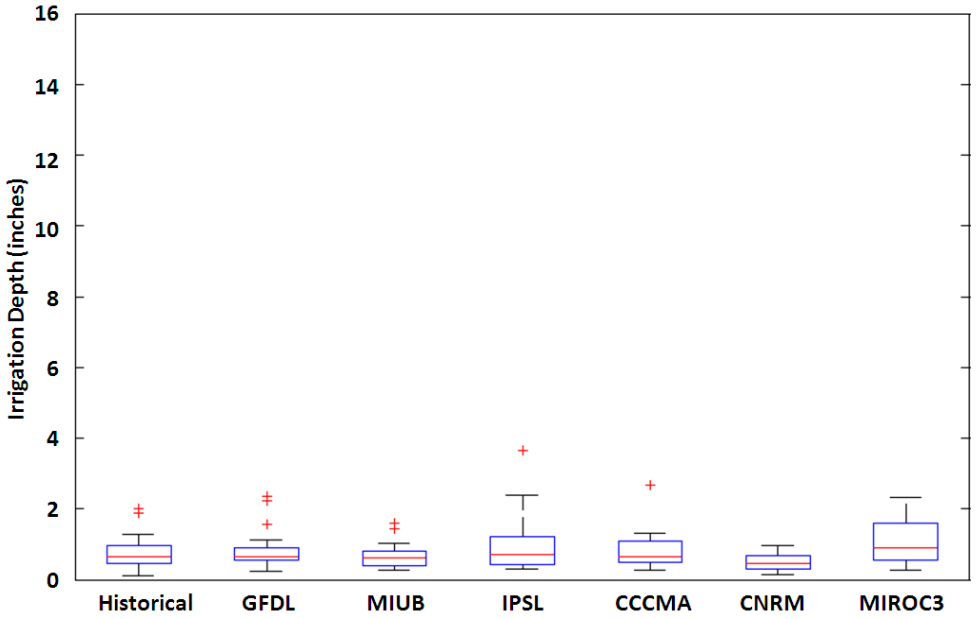

Figure A.126. May demand in Newton under A2 emissions scenario (2046-2065).

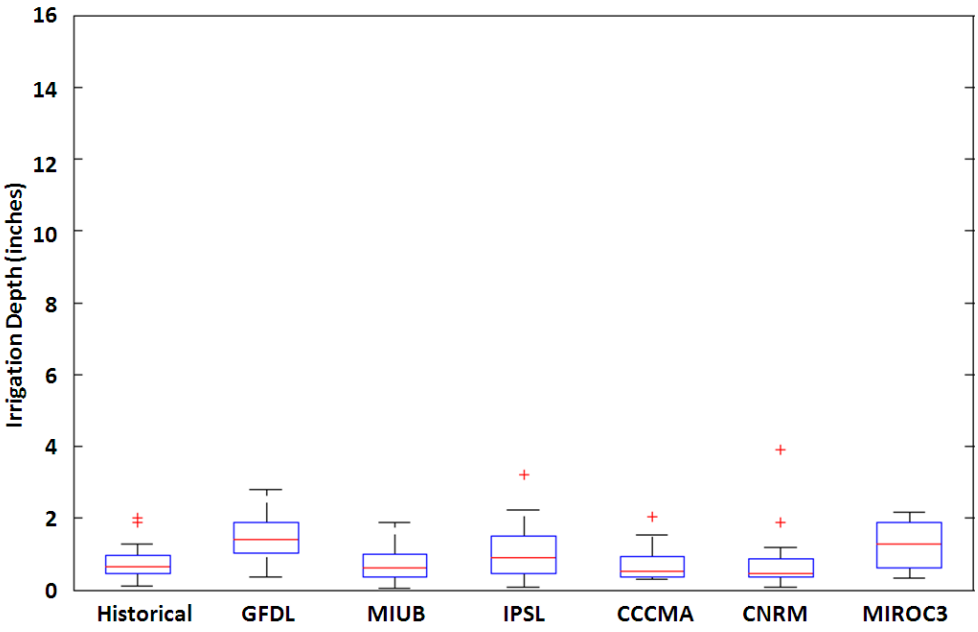

Figure A.127. May demand in Newton under A2 emissions scenario (2081-2100).

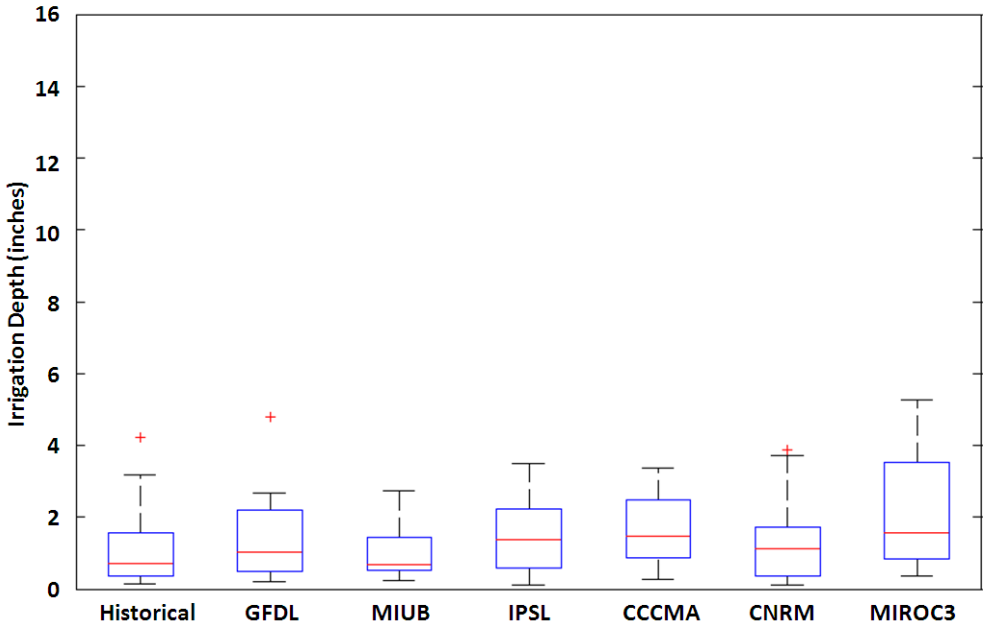

Figure A.128. June demand in Newton under A2 emissions scenario (2046-2065).

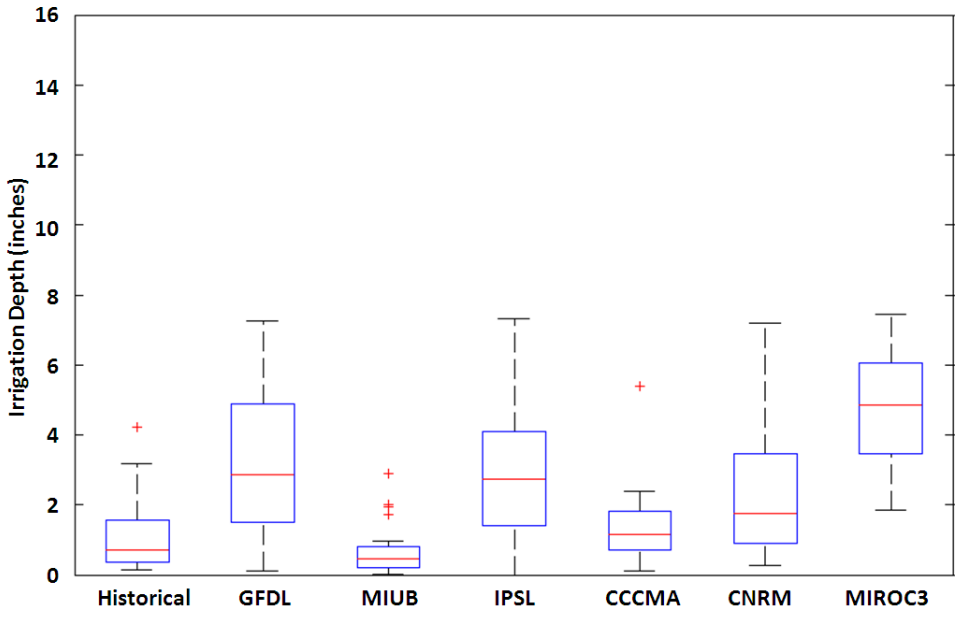

Figure A.129. June demand in Newton under A2 emissions scenario (2081-2100).

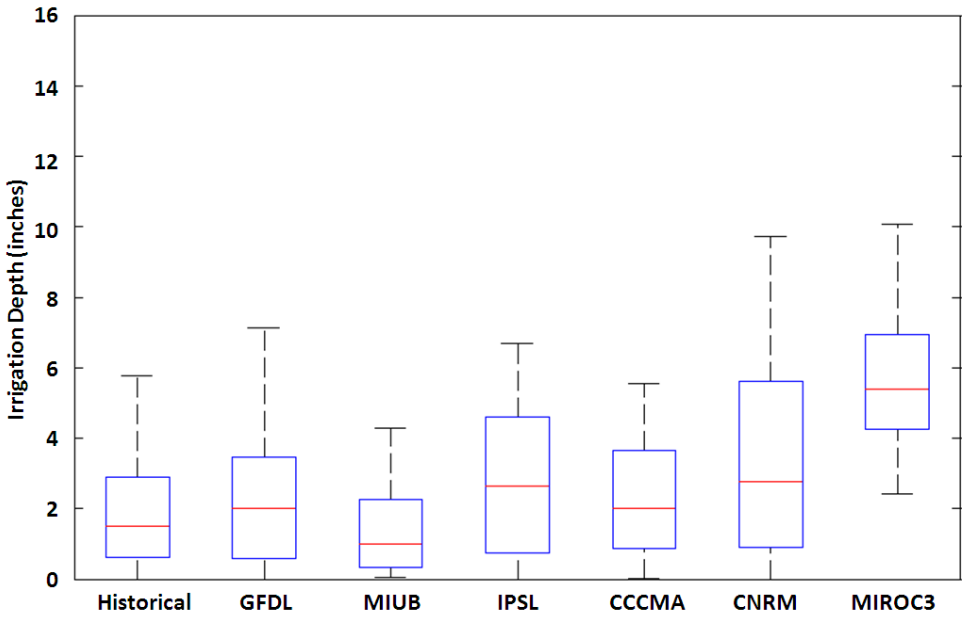

Figure A.130. July demand in Newton under A2 emissions scenario (2046-2065).

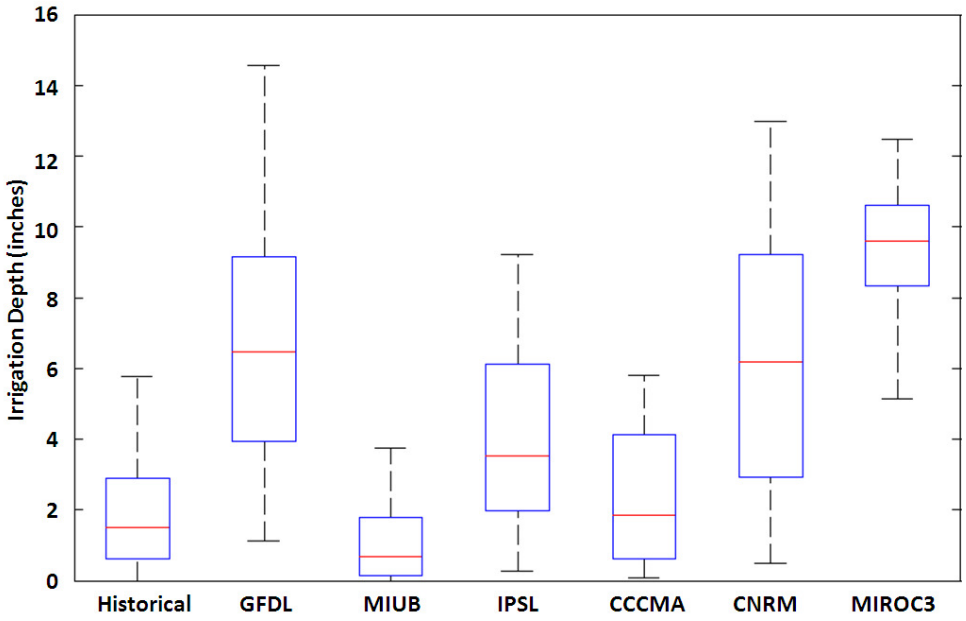

Figure A.131. July demand in Newton under A2 emissions scenario (2081-2100).

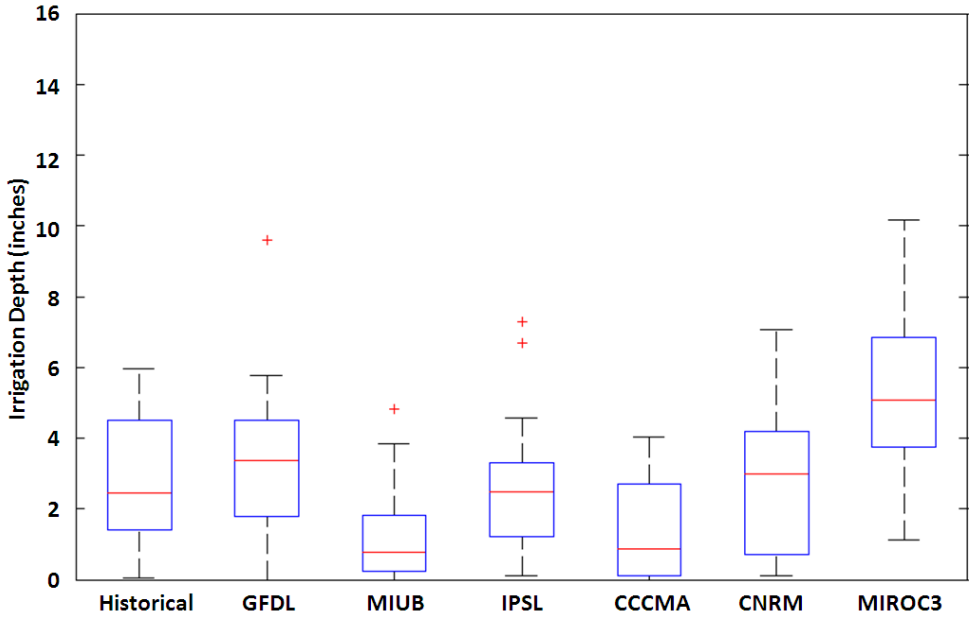

Figure A.132. August demand in Newton under A2 emissions scenario (2046-2065).

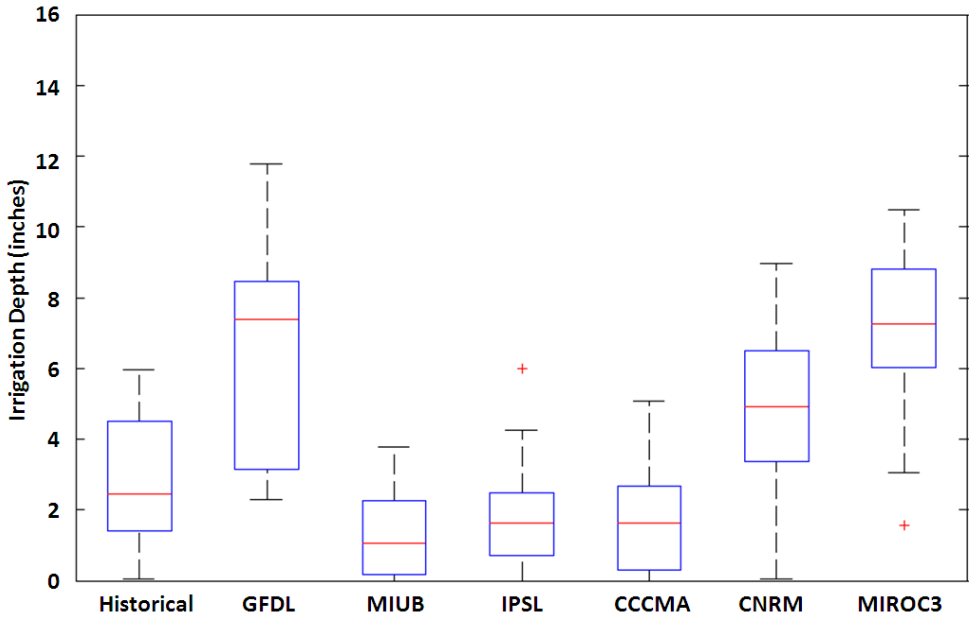

Figure A.133. August demand in Newton under A2 emissions scenario (2081-2100).

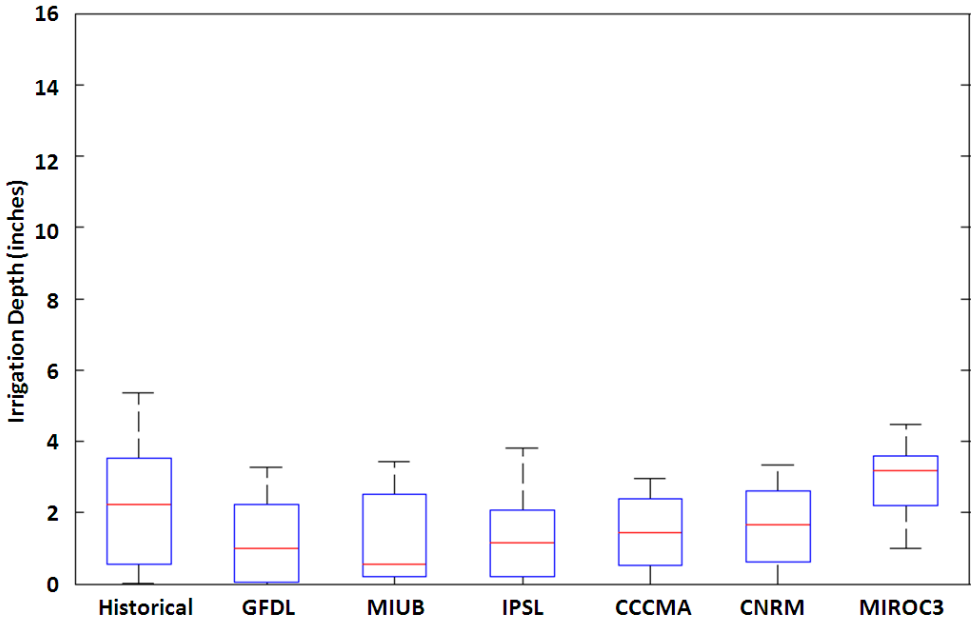

Figure A.134. Sept. demand in Newton under A2 emissions scenario (2046-2065).

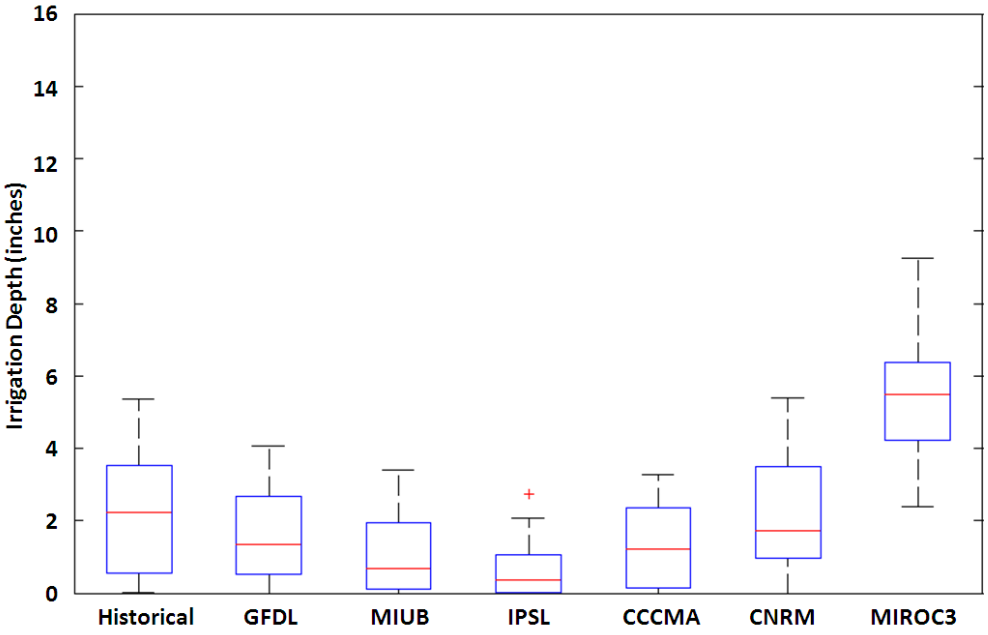

Figure A.135. Sept. demand in Newton under A2 emissions scenario (2081-2100).

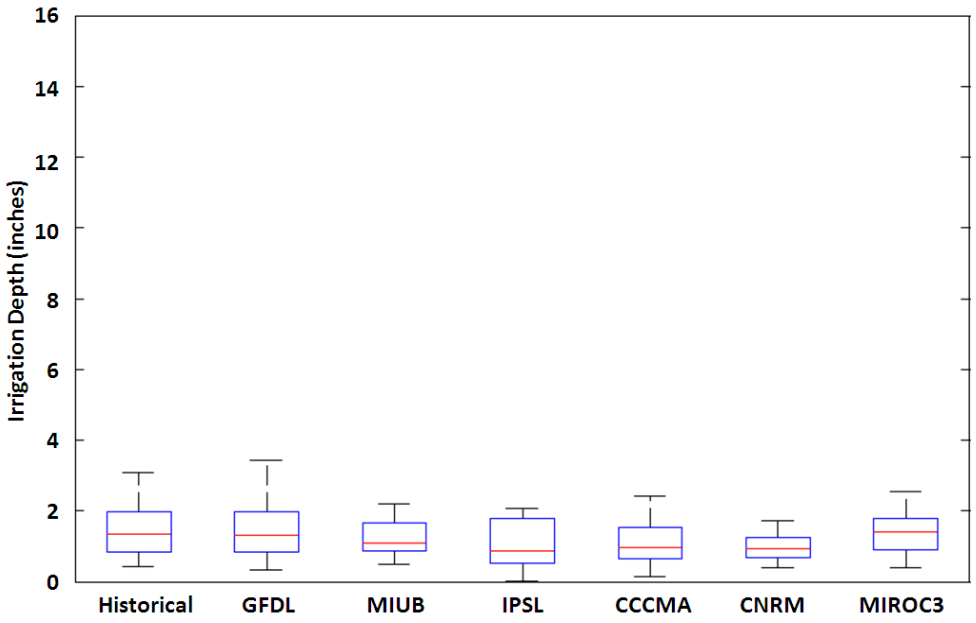

Figure A.136. May demand in Woodruff under A1B emissions scenario (2046-2065).

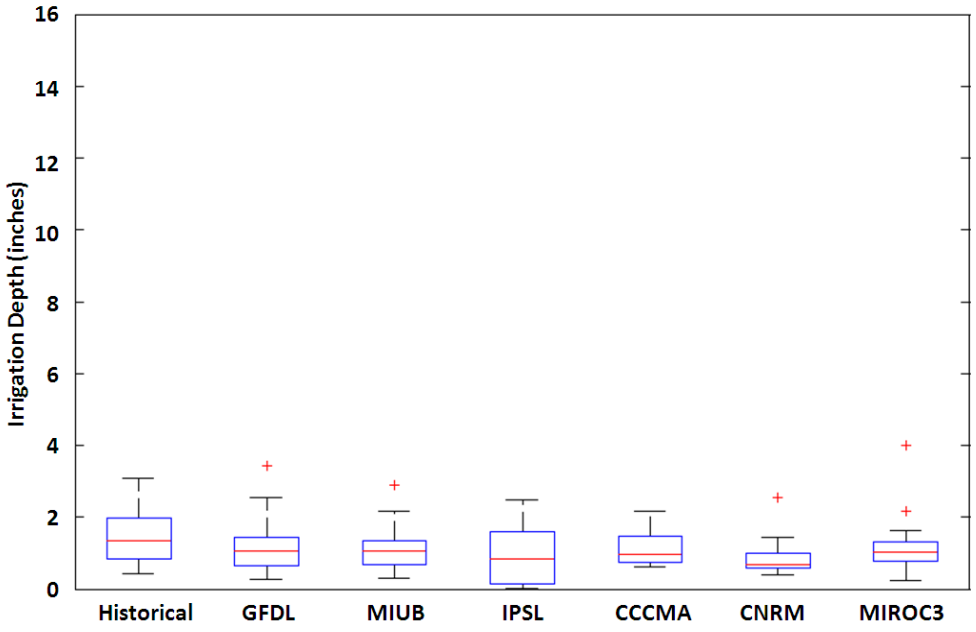

Figure A.137. May demand in Woodruff under A1B emissions scenario (2081-2100).

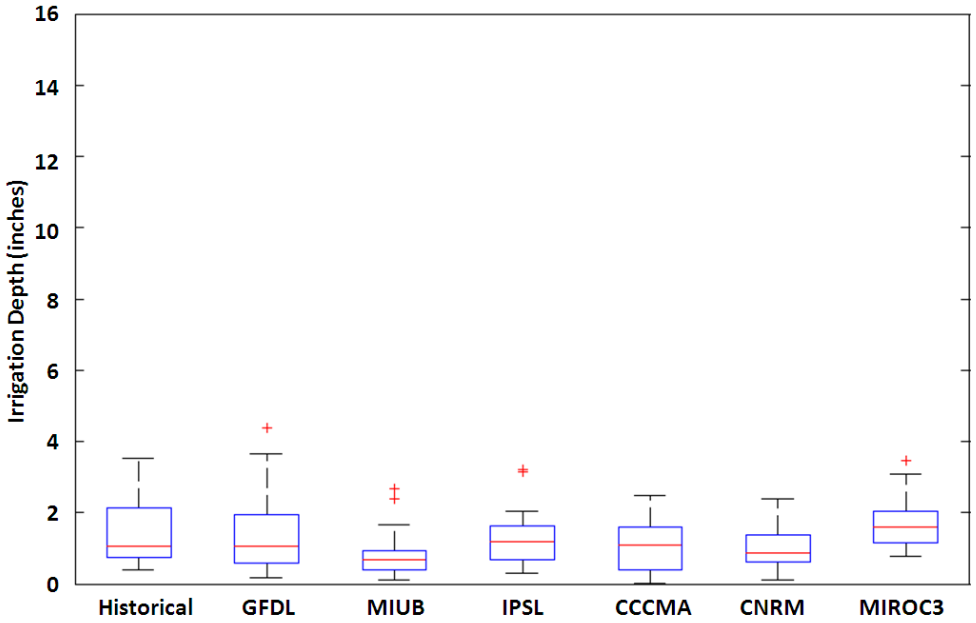

Figure A.138. June demand in Woodruff under A1B emissions scenario (2046-2065).

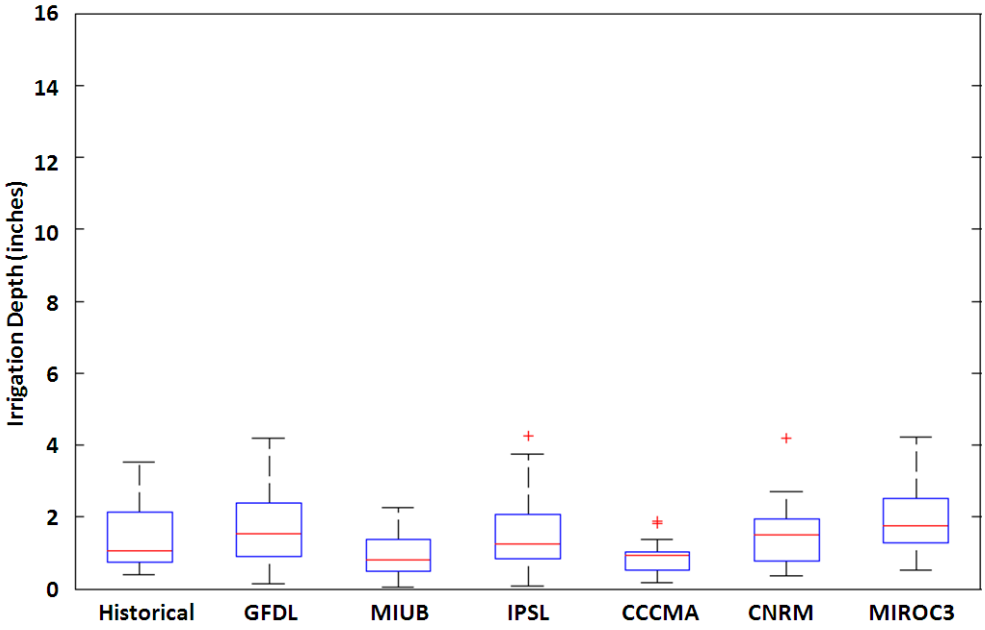

Figure A.139. June demand in Woodruff under A1B emissions scenario (2081-2100).

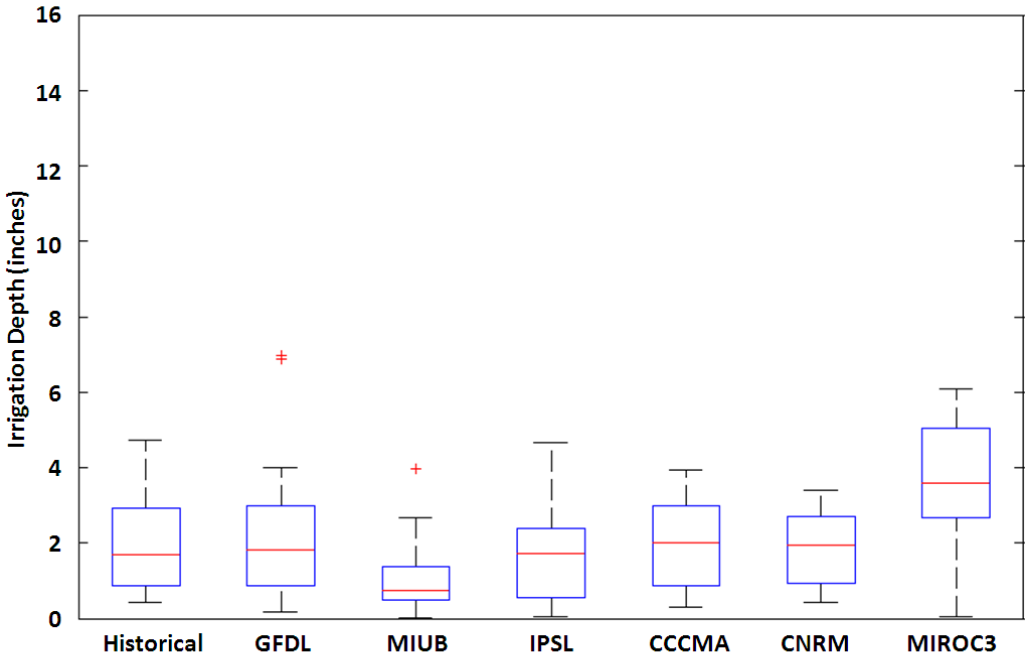

Figure A.140. July demand in Woodruff under A1B emissions scenario (2046-2065).

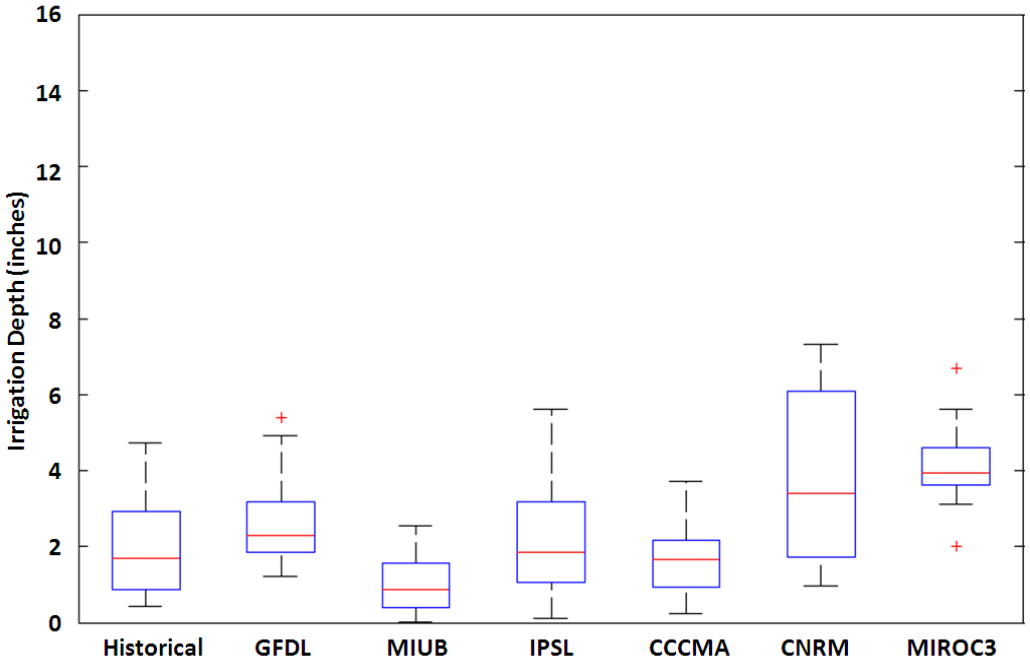

Figure A.141. July demand in Woodruff under A1B emissions scenario (2081-2100).

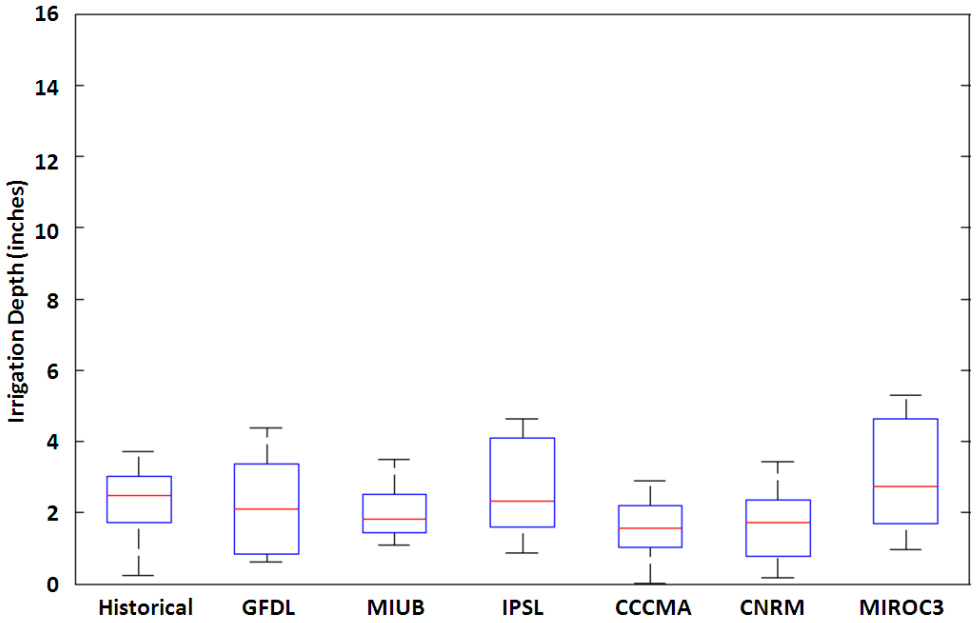

Figure A.142. August demand in Woodruff under A1B emissions scenario (2046-2065).

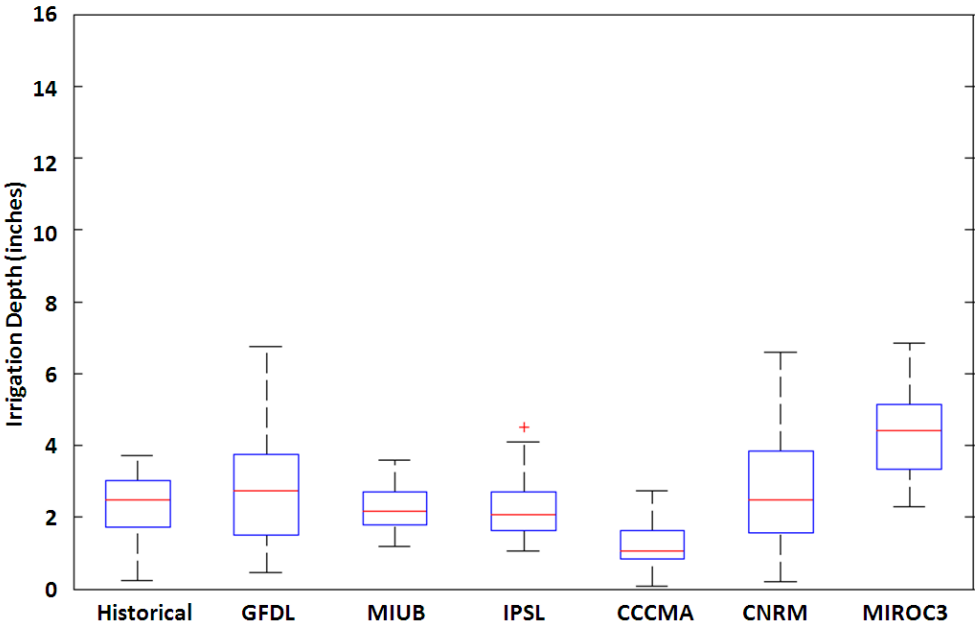

Figure A.143. August demand in Woodruff under A1B emissions scenario (2081-2100).

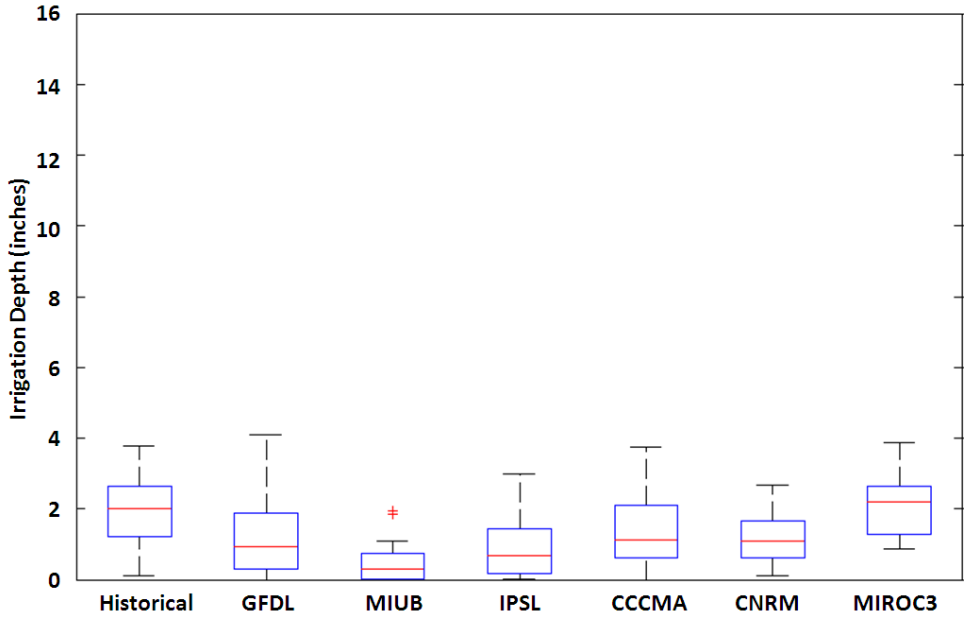

Figure A.144. Sept. demand in Woodruff under A1B emissions scenario (2046-2065).

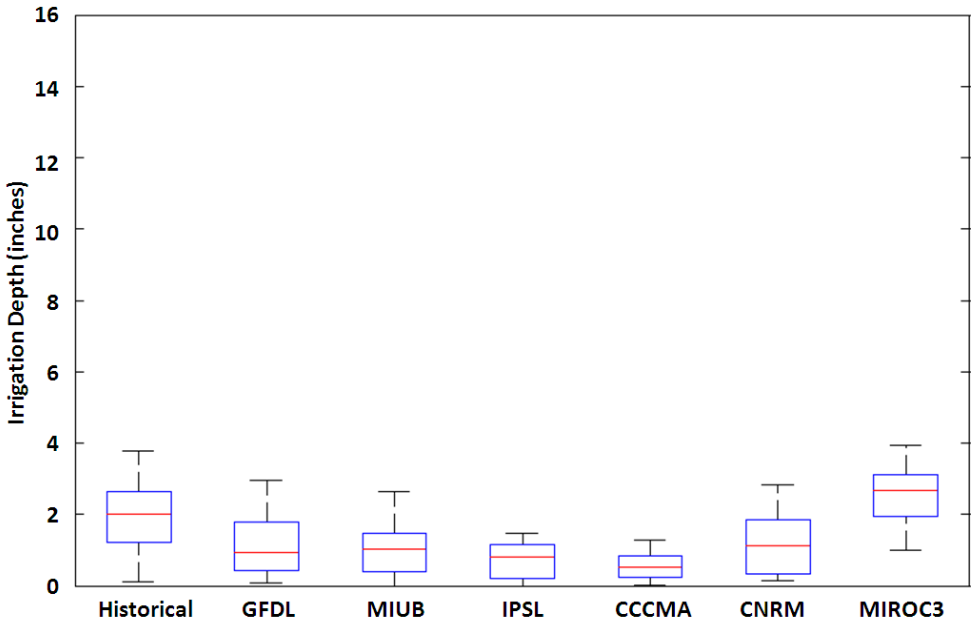

Figure A.145. Sept. demand in Woodruff under A1B emissions scenario (2081-2100).

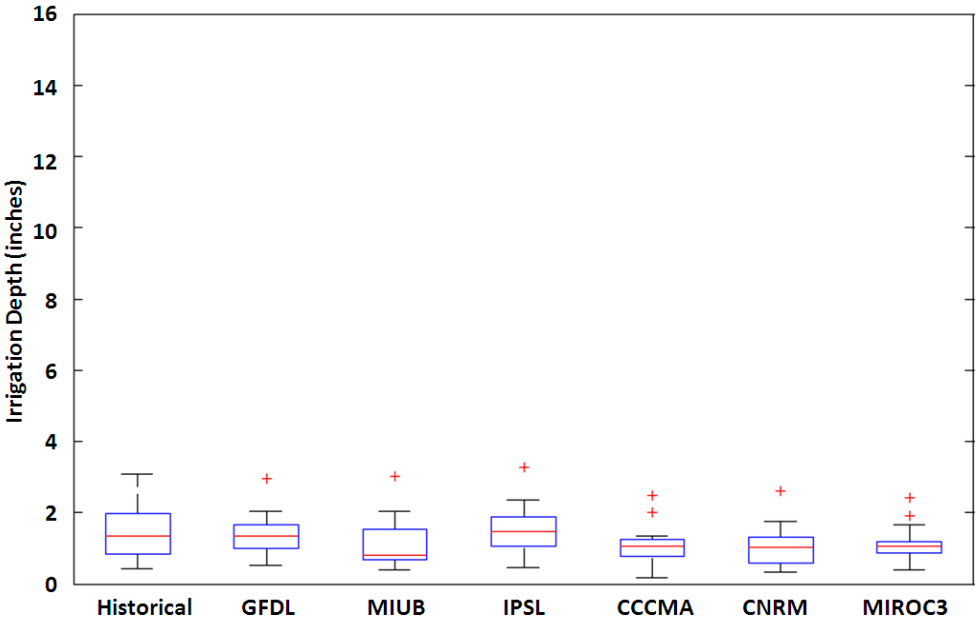

Figure A.146. May demand in Woodruff under A2 emissions scenario (2046-2065).

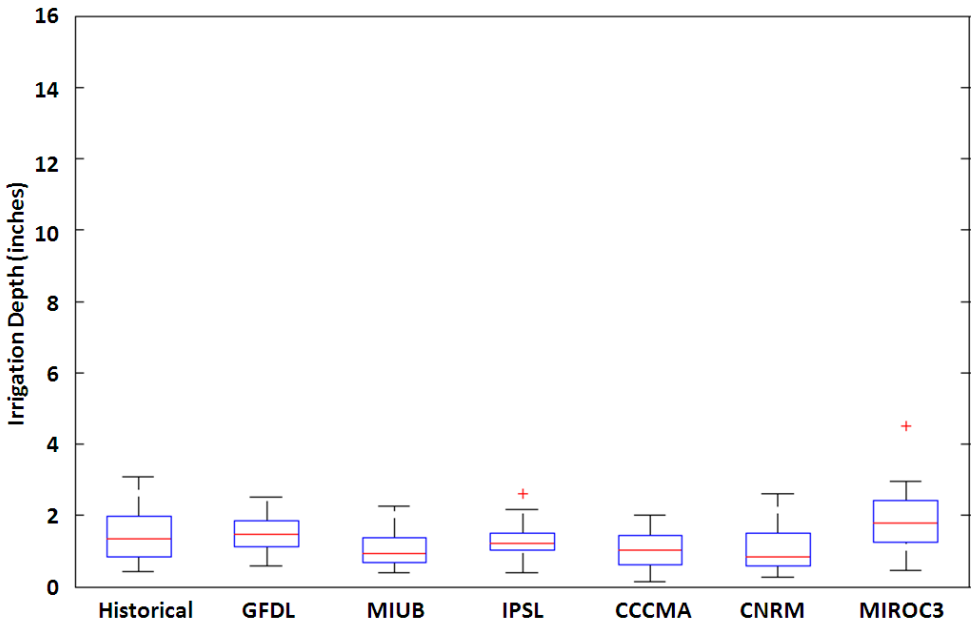

Figure A.147. May demand in Woodruff under A2 emissions scenario (2081-2100).

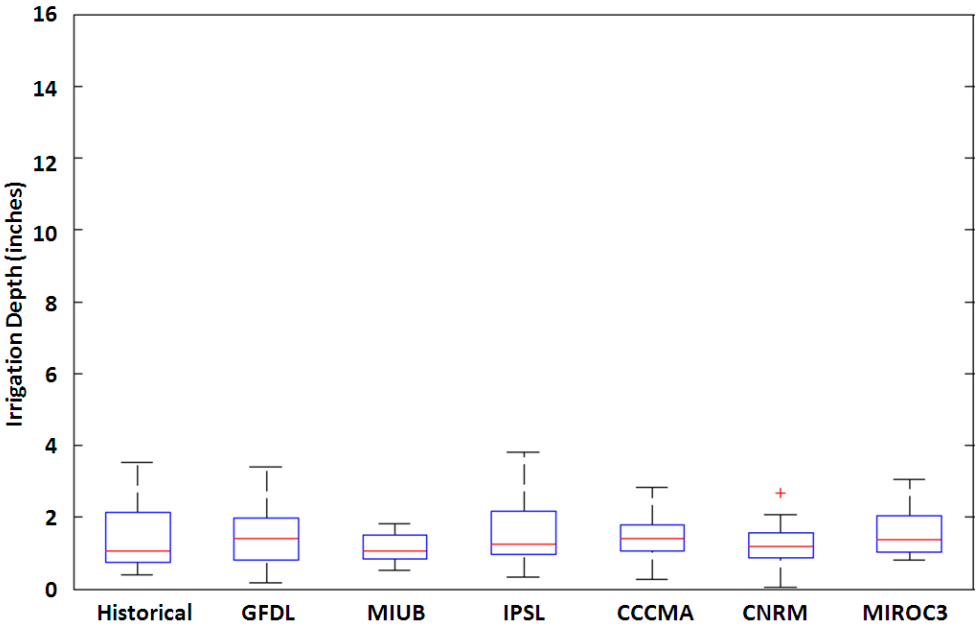

Figure A.148. June demand in Woodruff under A2 emissions scenario (2046-2065).

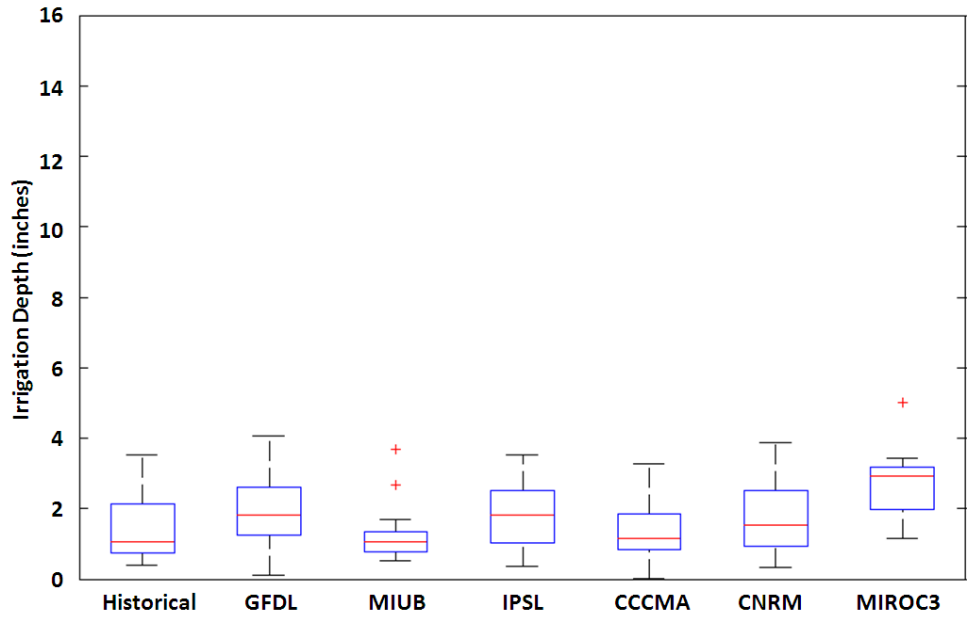

Figure A.149. June demand in Woodruff under A2 emissions scenario (2046-2065).

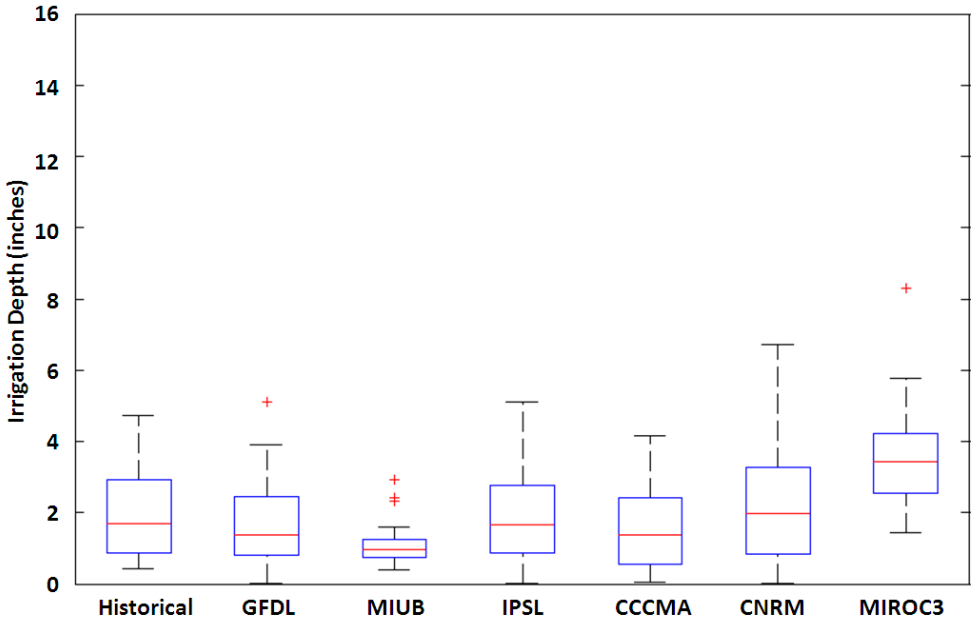

Figure A.150. July demand in Woodruff under A2 emissions scenario (2046-2065).

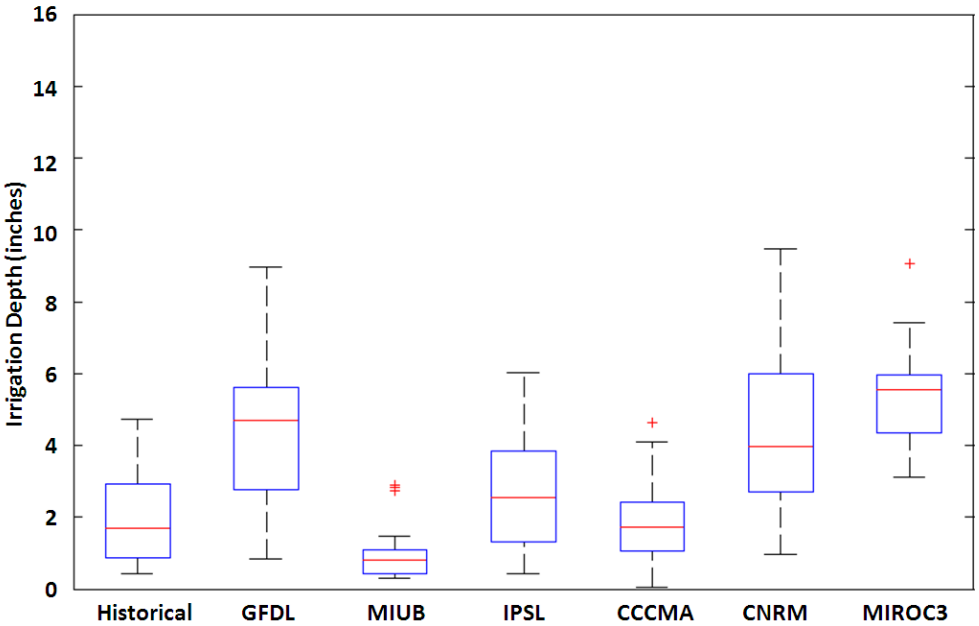

Figure A.151. July demand in Woodruff under A2 emissions scenario (2081-2100).

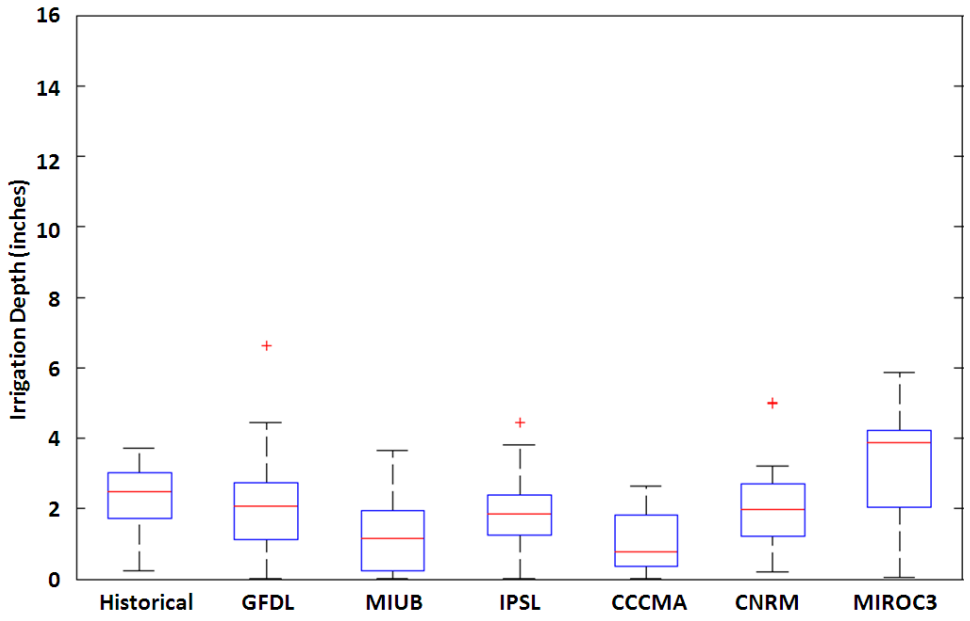

Figure A.152. August demand in Woodruff under A2 emissions scenario (2046-2065).

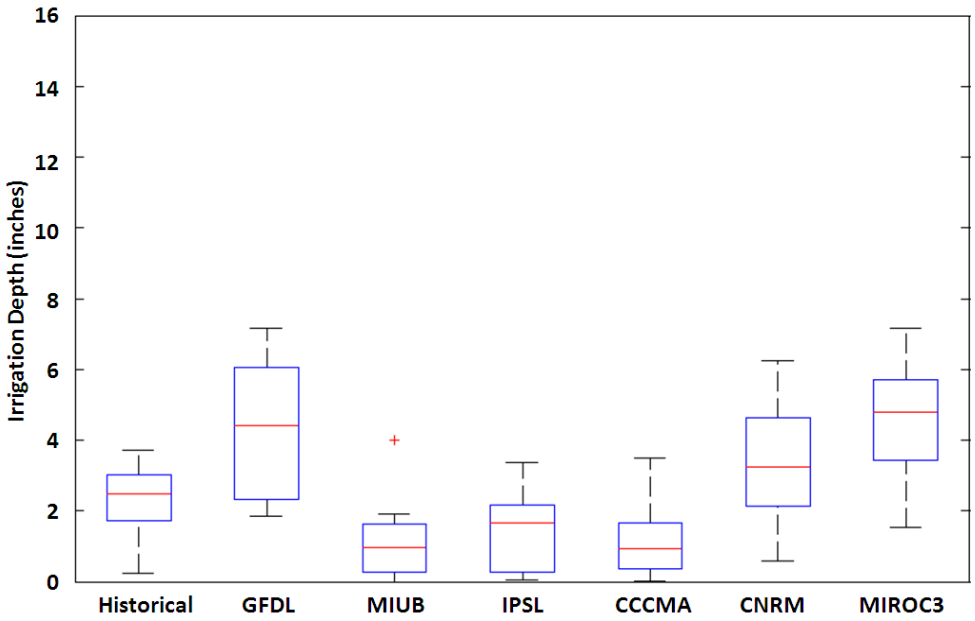

Figure A.153. August demand in Woodruff under A2 emissions scenario (2081-2100).

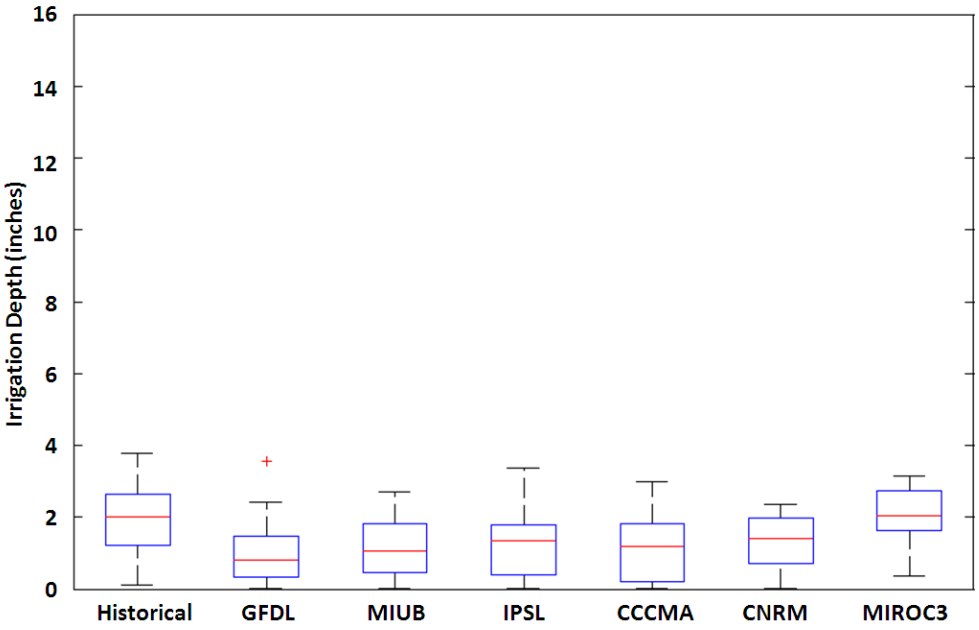

Figure A.154. Sept. demand in Woodruff under A2 emissions scenario (2046-2065).

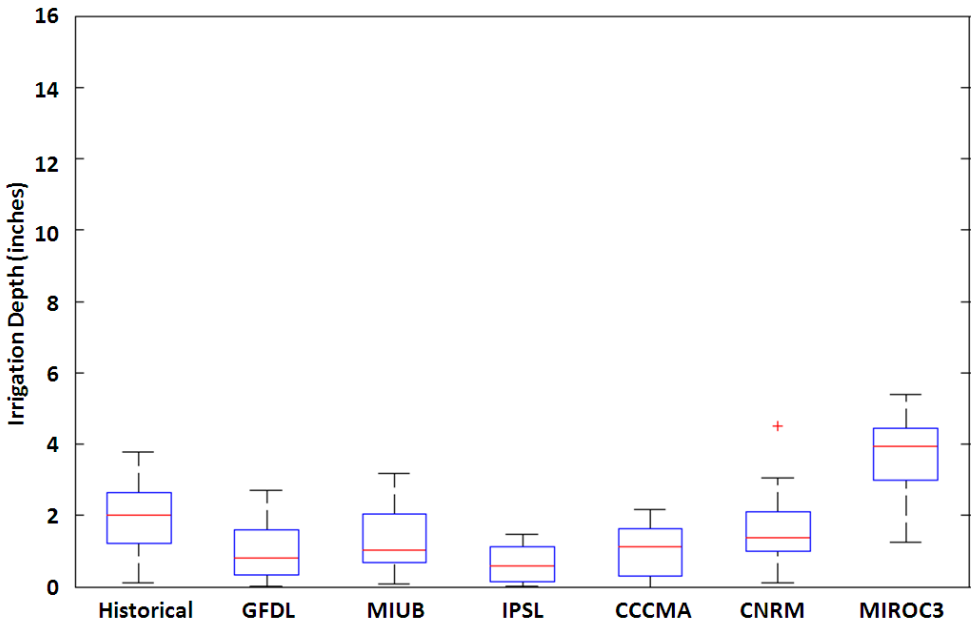

Figure A.155. Sept. demand in Woodruff under A2 emissions scenario (2081-2100).

REFERENCES

Aggarwal, P.K., 1995. Uncertainties in crop, soil and weather inputs used in growth models: Implications for simulated outputs and their applications. Agricultural Systems, 48(3): 361-384.

Allen, L.H., 1990. Plant Responses to Rising Carbon Dioxide and Potential Interactions with Air Pollutants. J. Environ. Qual., 19(1): 15-34.

Allen, R.G., Pereira, L.S., Raes, D. and Smith, M., 1998. Crop evapotranspiration: guidelines for computing crop water requirements.

Allen, R.G. and Pruitt, W.O., 1986. Rational Use of the Blaney-Criddle Formula. Journal of the Irrigation and Drainage Engineering Division, 112: 139-155.

Axel Garcia y, G. and Gerrit, H., 2005. Evaluation of an improved daily solar radiation generator for the southeastern USA. Climate Research, 29(2): 91-102.

Baigorria, G.A., Jones, J.W. and O'Brien, J.J., 2007. Understanding rainfall spatial variability in the Southeast USA. International Journal of Climatology: 749-760.

Banerjee, S., Tareen, I.Y., Gunter, L.F., Bramblett, J. and Wetzstein, M.E., 2007. Forecasting Irrigation Water Demand: A Case Study on the Flint River Basin in Georgia. Journal of Agricultural and Applied Economics, 39(3).

Baron, C. et al., 2005. From GCM grid cell to agricultural plot: scale issues affecting modelling of climate impact. Philos Trans R Soc B, 360.

Bell, M.A. and Fischer, R.A., 1994. Using yield prediction models to assess yield gains: a case study for wheat. Field Crops Research, 36: 161-166.

Bert, F.E., Laciana, C.E., Podestá, G.P., Satorre, E.H. and Menéndez, A.N., 2007. Sensitivity of CERES-Maize simulated yields to uncertainty in soil properties and daily solar radiation. Agricultural Systems, 94(2): 141-150.

Blaney, H. and Criddle, W., 1950. Determining Water Requirements in Irrigated Areas from Climatological and Irrigation Data. In: U.S.D.o.A. Soil Conservation Service (Editor).

Boote, K.J., Jones, J.W., Hoogenboom, G. and Pickering, N.B., 1998. The CROPGRO model for grain legumes. In: G. Tsuji, G. Hoogenboom and P. Thornton (Editors), Understanding Options for Agricultural Production. Systems Approaches for Sustainable Agricultural Development. Springer Netherlands, pp. 99-128.

Boote, K.J., Jones, J.W. and Pickering, N.B., 1996. Potential Uses and Limitations of Crop Models. Agron. J., 88(5): 704-716.

Boote, K.J. and Sinclair, T.R., 2006. Crop Physiology. Crop Sci., 46(5): 2270-2277.

Bouman, B.A.M., van Keulen, H., van Laar, H.H. and Rabbinge, R., 1996. The `School of de Wit' crop growth simulation models: A pedigree and historical overview. Agricultural Systems, 52(2-3): 171-198.

Boyer, J.S., 1969. Measurement of the Water Status of Plants. Annual Review of Plant Physiology, 20(1): 351-364.

Bramblett, J.R., 1995. Agricultural Water Demand in the ACF and ACT River Basins, Georgia Water Resources Conference, UGA, Athens, GA.

Braneon, C.V. and Georgakakos, A.P., 2011. Climate Change Impacts on Georgia Agriculture and Irrigation Demand . Georgia Water Resources Conference, Athens, GA.

Bras, R., 1990. Hydrology: An Introduction to Hydrologic Science.

Brumbelow, K., 2001. Improved Methods for Agricultural and Water Resources Planning and Management, Georgia Institute of Technology, Atlanta.

Brumbelow, K., Bourne, S. and Georgakakos, A., 2003. Nile Decision Support Tool (Nile DST): Agricultural Planning, Georgia Water Resources Institute.

Brumbelow, K. and Georgakakos, A., 2007. Consideration of Climate Variability and Change in Agricultural Resources Planning. Journal of Water Resources Planning and Management, 133(2).

Cai, X., McKinney, D.C. and Lasdon, L.S., 2003. Integrated Hydrologic-Agronomic-Economic Model for River Basin Management. Journal of Water Resources Planning and Management, 129.

Cai, X., Wang, D. and Laurent, R., 2009. Impact of Climate Change on Crop Yield: A Case Study of Rainfed Corn in Central Illinois. Journal of Applied Meteorology and Climatology, 48(9): 1868-1881.

Challinor, A.J., Ewert, F., Arnold, S., Simelton, E. and Fraser, E., 2009. Crops and climate change: progress, trends, and challenges in simulating impacts and informing adaptation. Journal of Experimental Botany, 60(10): 2775-2789.

Chow, V.T., Maidment, D. and Mays, L., 1988. Applied Hydrology.

Cros, M., Garcia, F., Martin-Clouaire, R. and Rellier, J., 2003. Modeling Management Operations in Agricultural Production Simulators, Agricultural Engineering International.

Daly, C., Neilson, R.P. and Phillips, D.L., 1994. A Statistical-Topographic Model for Mapping Climatological Precipitation over Mountainous Terrain. Journal of Applied Meteorology, 33(2): 140-158.

Daniels, A.E. et al., 2012. Climate Projections FAQ, United States Department of Agriculture / Forest Service.

Dehghanisanij, H., Nakhjavani, M.M., Tahiri, A.Z. and Anyoji, H., 2009. Assessment of wheat and maize water productivities and production function for cropping system decisions in arid and semiarid regions. Irrigation and Drainage, 58(1): 105-115.

Delonge, M.S., 2007. Hydrologically-Influenced Feedbacks Between Phosphorus and Vegetation in Dry Tropical Forests, University of Virginia.

Dingman, S.L., 2002. Physical Hydrology.

Doorenbos, J. and Kassam, A.M., 1979. Yield Response to Water, FAO, Rome, Italy.

Doorenbos, J. and Pruitt, W.O., 1977. Guidlines for Predicting Crop Water Requirements, FAO, Rome, Italy.

Eash, N., Green, C., Rasvi, A. and Bennett, W., 2008. Soil Science Simplified.

Farahani, H.J., Izzi, G. and Oweis, T.Y., 2009. Parameterization and Evaluation of the AquaCrop Model for Full and Deficit Irrigated Cotton. Agron. J., 101(3): 469-476.

Fourcard, T., Zhang, X., Stokes, A., Lambers, H. and Korner, C., 2008. Plant Growth Modelling and Applications: The Increasing Importance of Plant Architecture in Growth Models. Annals of Botany, 101: 1053-1063.

Garcia, A., Hoogenbom, G., Guerra, L.C., Paz, J. and Fraisse, C.W., 2006. Analysis of the Inter-Annual Variation of Peanut Yield in Georgia Using a Dynamic Crop Simulation Model. Transactions of the ASABE.

Garcia y Garcia, A., Guerra, L.C. and Hoogenboom, G., 2008. Impact of generated solar radiation on simulated crop growth and yield. Ecological Modelling, 210(3): 312-326.

Gifford, R.M. and Evans, L.T., 1981. Photosynthesis, carbon partioning, and yield. Annual Review of Plant Physiology, 32.

Goovaerts, P., 2001. Geostatisitcal modelling of uncertainty in soil science. Geoderma: 3-26.

Guerra, L.C. et al., 2007. Irrigation water use estimates based on crop simulation models and kriging. Agricultural Water Management, 89(3): 199-207.

Hansen, J., Challinor, A., Ines, A., Wheeler, T. and Moron, V., 2006. Translating climate forecasts into agricultural terms: advances and challenges. Climate Research, 33: 27-41.

Hansen, J.W. and Indeje, M., 2004. Linking dynamic seasonal climate forecasts and crop simulation for maize yield preciction in semi-arid Kenya. Agricultural and Forest Meteorology, 125.

Hansen, J.W. and Ines, A.M.V., 2005. Stochastic disaggregation of monthly rainfall data for crop simulation studies. Agricultural and Forest Meteorology, 131.

Hansen, J.W. and Jones, J.W., 2000. Scaling-up crop models for climate variability applications. Agricultural Systems, 65(1): 43-72.

Hatch, U., Jagtap, S., Jones, J. and Lamb, M., 1999. Potential Effects of Climate Change on Agricultural Water Use in the Southeast U.S. JAWRA Journal of the American Water Resources Association, 35(6): 1551-1561.

Helton, J.C., Johnson, J.D. and Oberkampf, W.L., 2004. An exploration of alternative approaches to the representation of uncertainty in model predictions. Reliability Engineering & System Safety, 85(1–3): 39-71.

Hesketh, J.D., 1963. Limitations to photosynthesis responsible for differences among species. Crop Science, 3: 493-496.

Hesketh, J.D. and Moss, D.N., 1963. Variation in the response of photosynthesis to light. Crop Science, 3: 107-110.

Hidalgo, H.G., Dettinger, M.D. and Cayan, D.R., 2008. Downscaling with Constructed Analogues: Daily Precipitation and Temperature Fields Over the United States, PIER Energy-Related Environmental Research, California Energy Commission, Sacramento, CA.

Hodges, T., French, V. and LeDuc, S.K., 1985. Estimating solar radiation for plant simulation models.

Hodgson, S., 2006. Modern water rights, Theory and practice, FAO, Rome.

Hoogenboom, G., 2000. Contribution of agrometeorology to the simulation of crop production and its applications. Agricultural and Forest Meteorology, 103(1-2): 137-157.

Hoogenboom, G. et al., 2010. Decision Support System for Agrotechnology Transfer (DSSAT) Version 4.5, University of Hawaii, Honolulu, Hawaii, pp. [CD-ROM].

Hook, J.E., Blood, E.R., Thomas, D.L., Harrison, K.A. and Powell, R., 1999. Agricultural Water Consumption in the A.C.F. River Basin: Current Approaches for Quantifying Irrigation in Georgia. In: K.J. Hatcher (Editor), Georgia Water Resources Conference, UGA, Athens, GA.

Hook, J.E., Harrison, K.A., Hoogenboom, G. and Thomas, D.L., 2005. Ag Water Pumping, Georgia Geological Survey, Georgia Environmental Protection Division.

Hook, J.E. et al., 2010. Agricultural Irrigation Water Demand: Georgia's Major and Minor Crops, 2011 through 2050, Georgia Environmental Protection Division, Georgia Environmental Facilities Authorities.

Hook, J.E. et al., 2009. Assessing Agricultural Groundwater Needs for the Future: Identifying Irrigated Area and Sources, GWRC, UGA, Athens, GA.

Horton, R.M. et al., 2011. Climate Hazard Assessment for Stakeholder Adaptation Planning in New York City. Journal of Applied Meteorology and Climatology, 50(11): 2247-2266.

Howell, T.A., 2001. Enhancing Water Use Efficiency in Irrigated Agriculture Contrib. from the USDA-ARS, Southern Plains Area, Conserv. and Production Res. Lab., Bushland, TX 79012. Mention of trade or commercial names is made for information only and does not imply an endorsement, recommendation, or exclusion by USDA-ARS. Agron. J., 93(2): 281-289.

Hsiao, T.C., 1973. Plant Responses to Water Stress. Annual Review of Plant Physiology, 24(1): 519-570.

Hunt, L.A., White, J.W. and Hoogenboom, G., 2001. Agronomic data: advances in documentation and protocols for exchange and use. Agricultural Systems, 70(2-3): 477-492.

Ines, A. and Hansen, J., 2006. Bias correction of daily GCM outputs for crop simulation studies. Agricultural and Forest Meteorology, 138.

J.E.Pallas, Stansell, J.R. and Koske, T.J., 1979. Effects of Drought on Florunner Peanuts. Agrionomy Journal, 71.

Jagtap, S.S. and Jones, J.W., 2002. Adaptation and evaluation of the CROPGRO-soybean model to predict regional yield and production. Agriculture, Ecosystems & Environment, 93(1–3): 73-85.

Jiang, X. and Yang, Z.L., 2012. Projected changes of temperature and precipitation in Texas from downscaled global climate models. Climate Research, 53.

Jones, J.W. et al., 2003. The DSSAT cropping system model. European Journal of Agronomy, 18(3-4): 235-265.

Jones, J.W., Keating, B.A. and Porter, C.H., 2001. Approaches to modular model development. Agricultural Systems, 70(2-3): 421-443.

Jones, J.W. et al., 1998. Understanding Options for Agricultural Production. In: G.Y. Tsuji, G. Hoogenboom and P.K. Thornton (Editors), System Approaches for Sustainable Agricultural Development.

Kaboosi, K. and Kaveh, F., 2011. Sensitivity analysis of FAO 33 crop water production function. Irrigation Science: 1-12.

Katz, R.W., 2002. Techniques for estimating uncertainty in climate change scenarios and impact studies. Climate Research: 167-185.

Kersebaum, K., Hecker, J., Mirschel, W. and Wegenhenkel, M., 2007. A comparison of simulation models applied on common data sets. In: J.H. K. Kersebaum, W. Mirschel, M. Wegenhenkel (Editor), Modelling water and nutrient dynamics in soil-crop systems, Germany, pp. 1-17.

Kijne, J.W., Barker, R. and Molden, D. (Editors), 2003. Water productivity in agriculture: Limits and opportunities for improvement, Wallingford, UK.

Kimaite, F.M., 2011. A hydroeconomic model for water resources assessments with application to the Apalachicola Chattahoochee Flint River basin, Georgia Institute of Technology.

Kimball, B.A., 1983. Carbon Dioxide and Agricultural Yield: An Assemblage and Analysis of 430 Prior Observations1. Agron. J., 75(5): 779-788.

Kirda, C., 2002. Deficit Irrigation Scheduling Based on Plant Growth Stages Showing Drought Tolerance, FAO.

Kitanidis, P., 1997. Introduction to Geostatistics: Applications in Hydrogeology. Cambridge University Press.

Kittel, T.G.F., Rosenbloom, N.A., Royle, J.A., Daly, C. and others, 2004. VEMAP Phase 2 Bioclimatic Database. Climate Research, 27.

Leenhardt, D., Angevin, F., Biarnès, A., Colbach, N. and Mignolet, C., 2010. Describing and locating cropping systems on a regional scale. A review. Agronomy for Sustainable Development, 30(1): 131-138.

Leenhardt, D. et al., 2004. Estimating irrigation demand for water management on a regional scale. Agricultural Water Management, 68(207-232).

Li, H. and Wu, J., 2006. Uncertainty analysis in ecological studies: an overview. In: J. Wu, K.B. Jones, H. Li and O. Loucks (Editors), Scaling and uncertainty analysis in ecology: methods and applications. Springer, Dordrect, Netherlands.

Li, J. and Heap, A.D., 2011. A review of comparative studies of spatial interpolation methods in environmental sciences: Performance and impact factors. Ecological Informatics, 6(3–4): 228-241.

Liang, X., Lettenmaier, D.P., Wood, E.F. and Burges, S.J., 1994. A simple hydrologically based model of land surface water and energy fluxes for general circulation models. Journal of Geophysical Research: Atmospheres, 99(D7): 14415-14428.

Lichtfouse, E. et al., 2009. Spatialising Crop Models, Sustainable Agriculture. Springer Netherlands, pp. 687-705.

Lorite, I.J., Mateos, L. and Fereres, E., 2005. Impact of spatial and temporal aggregation of input parameters on the assessment of irrigation scheme performance. Journal of Hydrology, 300(1–4): 286-299.

Luxmoore, R.J., King, A.W. and Tharp, M.L., 1991. Approaches to scaling up physiologically based soil–plant models in space and time. Tree Physiology, 9(1-2): 281-292.

Maton, L., Leenhardt, D., Goulard, M. and Bergez, J.E., 2005. Assessing irrigation strategies over a wide geographical area from structural data about farming systems. Agricultural Systems, 86.

Maurer, E.P., Wood, A.W., Adam, J.C., Lettenmaier, D.P. and Nijssen, B., 2002. A Long-Term Hydrologically Based Dataset of Land Surface Fluxes and States for the Conterminous United States*. Journal of Climate, 15(22): 3237-3251.

McNider, R.T. et al., 2011. A Real-Time Gridded Crop Model for Assessing Spatial Drought Stress on Crops in the Southeastern United States. Journal of Applied Meteorology and Climatology, 50(7): 1459-1475.

Mearns, L., Rosenzweig, C. and Goldberg, R., 1997. Mean and Variance Change in Climate Scenarios: Methods, Agricultural Applications, and Measures of Uncertainty. Climatic Change, 35(4): 367-396.

Meehl, G.A. et al., 2007. The WCRP CMIP3 Multimodel Dataset: A New Era in Climate Change Research. Bulletin of the American Meteorological Society, 88(9): 1383-1394.

Merz, B. and Thieken, A.H., 2005. Separating natural and epistemic uncertainty in flood frequency analysis. Journal of Hydrology, 309(1–4): 114-132.

Minchenkov, A., 2009. USDA Study Finds 54.9 Million Acres of U.S. Farmland Now Irrigated. USDA.

Monteith, J.L., 1965. Evaporation and Environment, The State and Movement of Water in Living Organisms, XIX Symposium. Cambridge University Press, Swansea, England.

Monteith, J.L., 1980. The development and extension of Penman's evaporation formula. In: D. Hillel (Editor), Applications of Soil Physics.

Moutonnet, P., 2002. Yield Response Factors of Field Crops to Deficit Irrigation FAO.

Nour, M.H., Smit, D.W. and El-Din, M.G., 2006. Geostatistical mapping of precipitation: implications for rain gauge network design. Water Science & Technology, 53(10).

Overman, A. and Scholtz, R., 2002. Mathematical Models of Crop Growth and Yield.

Penman, H.L., 1948. Natural Evaporation from Open Water, Bare Soil, and Grass. Proceedings of the Royal Society of London, 193: 120-145.

Perkins, E.F., 1987. Characterization Data for Selected Georgia Soils, UGA.

Persson, T., Garcia, A., Paz, J., Jones, J. and Hoogenbom, G., 2008. Maize ethanol feedstock production and net energy value as affected by climate variability and crop management practices. Agricultural Systems.

Porter, C.H., Braga, R. and Jones, J.W., 1999. An Approach for Modular Crop Model Development, University of Florida, Gainesville.

Priestly, C.H.B. and R.J.Taylor, 1972. On the Assessment of Surface Heat Flux and Evaporation Using Large-Scale Parameters. Monthly Weather Review, 100: 81-92.

Rabbinge, R., 1993. The ecological background in food production, Crop protection and sustainable agriculture, pp. 2-29.

Rao, N.H., Sarma, P.B.S. and Chander, S., 1988. A simple dated water-production function for use in irrigated agriculture. Agricultural Water Management, 13(1): 25-32.

Rastetter, E.B. et al., 1992. Aggregating fine-scale ecological knowledge to model coarse-scale attributes of ecosystems. Ecological Applications.

Ritchie, J.T., 1972. Model for predicting evaporation from a row crop with incomplete cover. Water Resources Research: 1204-1213.

Ritchie, J.T., 1998. Soil Water Balance and Plant Water Stress. In: G. Tsuji Y., G. Hoogenboom and P.K. Thornton (Editors), Understanding Options for Agricultural Production. Kluwer Academic Publishers.

Rogers, H.H., Bingham, G.E., Cure, J.D., Smith, J.M. and Surano, K.A., 1983. Responses of Selected Plant Species to Elevated Carbon Dioxide in the Field1. J. Environ. Qual., 12(4): 569-574.

Rosenzweig, C. and Wilbanks, T., 2010. The state of climate change vulnerability, impacts, and adaptation research: strengthening knowledge base and community. Climatic Change, 100(1): 103-106.

Saarikko, R.A., 2000. Applying a site based crop model to estimate regional yields under current and changed climates. Ecological Modelling, 131.

Salazar, M.R. et al., 2012. Estimating irrigation water use for maize in the Southeastern USA: A modeling approach. Agricultural Water Management, 107(0): 104-111.

Schmidli, J., Frei, C. and Vidale, P.L., 2006. Downscaling from GCM precipitation: a benchmark for dynamical and statistical downscaling methods. International Journal of Climatology, 26.

Schulze, R., 2000. Transcending scales of space and time in impact studies of climate and climate change on agrohydrological responses. Agriculture, Ecosystems & Environment, 82(1–3): 185-212.

Semenov, M.A. and Porter, J.R., 1995. Climatic variability and the modelling of crop yields. Agricultural and Forest Meteorology, 73(3–4): 265-283.

Southworth, J. et al., 2002. The sensitivity of winter wheat yields in the Midwestern United States to future changes in climate, climate variability, and CO2 fertilization. Climate Research.

Steduto, P., Hsiao, T.C., Raes, D. and Fereres, E., 2009. AquaCrop:The FAO Crop Model to Simulate Yield Response to Water: I. Concepts and Underlying Principles. Agron. J., 101(3): 426-437.

Suleiman, A.A., Tojo Soler, C.M. and Hoogenboom, G., 2007. Evaluation of FAO-56 crop coefficient procedures for deficit irrigation management of cotton in a humid climate. Agricultural Water Management, 91(1–3): 33-42.

Torak, L.J. and Painter, J.A., 2011. Summary of the Georgia Agricultural Water Conservation and Metering Program and evaluation of methods used to collect

and analyze irrigation data in the middle and lower Chattahoochee and Flint River basins, 2004–2010, USGS.

Tsuji, G.Y., Hoogenboom, G. and Thornton, P.K. (Editors), 1998. Understanding Options for Agricultural Production. Systems Approaches for Sustainable Agricultural Development, 7.

USDA, 1970. Irrigation Water Requirements.

Van Bavel, C.H., 1966. Potential Evaporation: the combination concept and its experimental verification. Water Resources Research, 2: 455-467.

Walker, W.E. et al., 2003. Defining Uncertainty: A Conceptual Basis for Uncertainty Management in Model-Based Decision Support. Integrated Assessment, 4(1): 5-17.

Wallach, D., Makowski, D. and Jones, J.W. (Editors), 2006. Working with Dynamic Crop Models: Evaluation, Analysis, Parameterization, and Applications.

Willocquet, L., Savary, S., Fernandez, L., Elazegui, F. and Teng, P., 1998. Simulation of Yield Losses Caused by Rice Diseases, Insects, and Weeds in Tropical Asia. IRRI DISCUSSION PAPER SERIES.

Xu, C.Y. and Singh, V.P., 2004. Review on Regional Water Resources Assessment Models under Stationary and Changing Climate. Water Resources Management, 18(6): 591-612.

Zhang, F. and Georgakakos, A., 2011. Joint Variable Spatial Downscaling. Climatic Change.